

**Mechanistic study of physicochemical and biochemical processes affecting
intestinal absorption of the sesquiterpene lactone nobilin from
multi-component systems in the Caco-2 model.**

Inauguraldissertation

zur

Erlangung der Würde eines Doktors der Philosophie

vorgelegt der

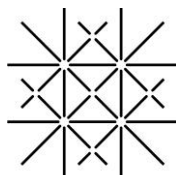
Philosophisch-Naturwissenschaftlichen Fakultät

der Universität Basel

von

URSULA STEPHANIE THORMANN

aus Bern (BE)



U N I
B A S E L

Basel, 2015

Originaldokument gespeichert auf dem Dokumentenserver der Universität Basel edoc.unibas.ch

Dieses Werk ist unter dem Vertrag „Creative Commons Namensnennung-Keine kommerzielle Nutzung-Keine Bearbeitung 3.0 Schweiz“ (CC BY-NC-ND 3.0 CH) lizenziert. Die vollständige Lizenz kann unter creativecommons.org/licenses/by-nc-nd/3.0/ch/ eingesehen werden.

Genehmigt von der Philosophisch-Naturwissenschaftlichen Fakultät
auf Antrag von

Prof. Dr. G. Imanidis

und

Prof. Dr. H. E. U. Meyer zu Schwabedissen

Basel, den 18. Februar 2014

Prof. Dr. J. Schibler



Namensnennung-Keine kommerzielle Nutzung-Keine Bearbeitung 3.0 Schweiz
(CC BY-NC-ND 3.0 CH)

Sie dürfen: Teilen — den Inhalt kopieren, verbreiten und zugänglich machen

Unter den folgenden Bedingungen:



Namensnennung — Sie müssen den Namen des Autors/Rechteinhabers in der von ihm festgelegten Weise nennen.



Keine kommerzielle Nutzung — Sie dürfen diesen Inhalt nicht für kommerzielle Zwecke nutzen.



Keine Bearbeitung erlaubt — Sie dürfen diesen Inhalt nicht bearbeiten, abwandeln oder in anderer Weise verändern.

Wobei gilt:

- **Verzichtserklärung** — Jede der vorgenannten Bedingungen kann **aufgehoben** werden, sofern Sie die ausdrückliche Einwilligung des Rechteinhabers dazu erhalten.
- **Public Domain (gemeinfreie oder nicht-schützbare Inhalte)** — Soweit das Werk, der Inhalt oder irgendein Teil davon zur Public Domain der jeweiligen Rechtsordnung gehört, wird dieser Status von der Lizenz in keiner Weise berührt.
- **Sonstige Rechte** — Die Lizenz hat keinerlei Einfluss auf die folgenden Rechte:
 - Die Rechte, die jedermann wegen der Schranken des Urheberrechts oder aufgrund gesetzlicher Erlaubnisse zustehen (in einigen Ländern als grundsätzliche Doktrin des **fair use** bekannt);
 - Die **Persönlichkeitsrechte** des Urhebers;
 - Rechte anderer Personen, entweder am Lizenzgegenstand selber oder bezüglich seiner Verwendung, zum Beispiel für **Werbung** oder Privatsphärenschutz.
- **Hinweis** — Bei jeder Nutzung oder Verbreitung müssen Sie anderen alle Lizenzbedingungen mitteilen, die für diesen Inhalt gelten. Am einfachsten ist es, an entsprechender Stelle einen Link auf diese Seite einzubinden.

Meiner Familie

Acknowledgements

This Ph.D. thesis was carried out at the Institute of Pharma Technology of the School of Life Sciences-FHNW and was sponsored by the Alpinia Laudanum Institute of Phytopharmaceutical Sciences AG.

I gratefully thank Prof. Dr. Georgios Imanidis for the excellent supervision of my Ph.D. work, especially, for his patience, for the long and fruitful discussions, for the profound explanations, for the long data fitting sessions, for the technical help with HPLC problems, and for encouraging me to explore new ways of reflecting a problem.

Furthermore, I would like to thank Alpinia Laudanum Institute of Phytopharmaceutical Sciences AG for its financial support of my work. I am particularly grateful to Dr. Matthias Kreuter for the lively discussions and his ideas and Peter Altmann for the isolation of Nobilin and other helpful contributions.

I would like to express my gratitude to Prof. Dr. Henriette E. Meyer zu Schwabedissen of the University of Basel (Division of Biopharmacy, Department of Pharmaceutical Sciences) for being the co-referee for this thesis.

A special thank deserves Dr. Maria de Mieri of the University of Basel (Division of Pharmaceutical Biology, Department of Pharmaceutical Sciences) for her excellent work of structure elucidation of the five degradation products of Nobilin and of suggesting a degradation mechanism. I am grateful to Dr. Markus Neuhauser of the University of Basel (Division of Inorganic Chemistry, Department of Chemistry) for the X-ray structure of the degradation product 1 and Dr. Claude Schärer of the HLS-FHNW (Institute of Chemistry und Bioanalytics) for his help with the isolation of the degradation products.

I thank the bachelor student Sheela Verjee from the HLS-FHNW and the master student Rahel Hänggi of the University of Basel for their great work in the laboratory and their contributions to my thesis.

Many thanks go to the people of the Institute of Pharma Technology. First of all I would like to thank Fabienne Thoenen who made me familiar with the cell culture and always provided great technical help in the laboratory. Additionally, I thank her, Dr. Michael Lanz, Martin Cavegn, and Dr. Cordula Stillhart for the amusing and reflecting discussions during break times and for their friendship and support. I also thank all other members of the Institute for having a great time with them.

Last but not least I sincerely thank my family, especially, my parents Regula and Georg Thormann and my sister Kathrin Thormann and Adrian Megert for their love and support in what I am doing.

Abstract

The overall aim of this work was to investigate the intestinal absorption of the sesquiterpene lactone nobiletin from the flowers of *Anthemis nobilis* L. (*Chamomillae romanae flos*) in the in vitro Caco-2 model and identify strategies for its improvement. The influence of physicochemical processes i.e., stability and solubility and biochemical processes i.e., bioconversion and membrane permeation by passive diffusion and carrier mediated transport on nobiletin absorption were elucidated to gain a basic mechanistic understanding of the absorption of the compound. Physiologically based multi-compartment kinetic modeling was employed to delineate the influence of simultaneously acting phenomena. Based on this understanding, possibilities were finally explored to improve absorption of nobiletin utilizing plant extract, formulation, and post-prandial application approaches. The thesis is divided into one theoretical part and three experimental studies, each addressing other aspects of physicochemical and biochemical processes affecting nobiletin absorption.

The first study focused on chemical degradation of nobiletin and its solubility under conditions of concurrent degradation and the effect of biorelevant media used in the in vitro measurement of intestinal absorption. Purely aqueous medium (aq-TM_{Caco}), fasted and fed state simulated intestinal fluid (FaSSIF-TM_{Caco} and FeSSIF-TM_{Caco}), and two liposomal formulations (Liposomes_{FaSSIF} and Liposomes_{FeSSIF}) with the same lipid concentration as FaSSIF-TM_{Caco} and FeSSIF-TM_{Caco} were used. Degradation products were identified by NMR and X-ray crystallography and the order of reaction kinetics was determined. Solubility was deduced with a mathematical model encompassing dissolution and degradation kinetics that took into account particle size distribution of the solid material. Degradation mechanism of nobiletin involved water catalyzed opening of the lactone ring and transannular cyclization resulting in five degradation products. Degradation followed first order kinetics in aq-TM_{Caco} and FaSSIF-TM_{Caco} and higher order kinetics in FeSSIF-TM_{Caco} and the two liposomal formulations while degradation in the latter media was reduced. Solubility of purified nobiletin increased in the order: aq-TM_{Caco} < FaSSIF-TM_{Caco} < Liposomes_{FaSSIF} < FeSSIF-TM_{Caco} < Liposomes_{FeSSIF}. Improvement of stability and solubility of nobiletin was consistent with incorporation of the molecule into colloidal lipid particles. The developed kinetic model is proposed to be a useful tool for deducing solubility of a highly unstable compound with a wide particle size distribution.

In the second study, the role of bioconversion and carrier mediated efflux of conjugation products in the absorption mechanism of nobiletin in the Caco-2 model and the impact of the extract of *Chamomillae romanae flos* and its ingredients on bioconversion and efflux was investigated. Permeation and bioconversion parameter values were deduced by means of kinetic multi-compartment modeling. Nobiletin exhibited high permeability, low absorption and fast bioconversion producing glucuronide, cysteine conjugate, and glutathione conjugate that were transported by P-gp (the first two), apical MRP2 and basal MRP3 and possibly MRP1 out of the cell. Inhibition of efflux resulted in diminished bioconversion and improved absorption. The extract increased the relative fraction absorbed primarily by directly inhibiting bioconversion but also by reducing efflux. This effect of the extract was only partly explained by its individual ingredients. The transport-bioconversion interplay is shown to be a possible mechanism for increasing absorption of a compound undergoing extensive bioconversion. Plant extracts may increase absorption by this mechanism in addition to metabolic enzyme inhibition.

The focus of the third study was the effect of biorelevant media and two lipid based formulations (SMEDSS1 and SMEDDS2) on in vitro absorption of nobiletin applied as a pure compound or as a full ethanolic extract of *Chamomillae romanae flos*. Permeation and bioconversion parameters were deduced by means of kinetic multi-compartment modeling. FaSSIF-TM_{Caco} reduced apical efflux of all conjugates but did not affect nobiletin absorption while FeSSIF-TM_{Caco} increased absorption which was attributed to the increased chemical stability in the medium and decreased bioconversion while permeability coefficient was also decreased. SMEDDS1 increased and SMEDDS2 decreased absorption due to a decrease and an increase of bioconversion, respectively, although both formulations improved chemical stability and decreased permeability coefficient. The effect of FeSSIF-TM_{Caco}, SMEDDS1, and SMEDDS2 is consistent with an incorporation of nobiletin into colloidal lipid particles while FeSSIF-TM_{Caco}, SMEDDS1 appeared to inhibit and SMEDDS2 to promote enzymatic reaction in the cell. In combination with the extract, no additional effect was observed. Formulation and transport media influence, therefore, in vitro absorption by changing bioconversion, chemical stability and permeation parameters.

This work gives an insight in the absorption mechanism of nobiletin and shows the effect of physicochemical and biochemical processes on absorption and possibilities to improve it. With multi-compartment modeling simultaneous processes which took place during absorption were unraveled and their contribution to absorption was elucidated. This technique allowed studying the effect of external factors such as inhibitors of transporters, plant extract, formulations, and biorelevant media on individual processes, on the interplay between these processes and further on the entire absorption mechanism. The work contributes towards raising the awareness that intestinal absorption is a complex puzzle of different processes which can be influenced by external factors and which bear a high potential for interaction.

Contents

Abstract	i
1 Introduction	1
1.1 BACKGROUND	1
1.2 OBJECTIVES	3
1.3 REFERENCES	5
2 Theoretical section: <i>An Overview</i>	10
2.1 ABSORPTION OF PHYTOPHARMAZEUTICALS	10
2.1.1 Bioavailability of phytopharmaceuticals	10
2.1.2 Absorption of phytopharmaceuticals in the Caco-2 model	12
2.1.2.1 <i>Absorption of single phytopharmaceutical compounds</i>	12
2.1.2.2 <i>Influence of plant extracts on absorption of phytopharmaceutical compounds</i>	13
2.1.2.3 <i>Influence of plant ingredients on absorption of phytopharmaceutical compounds</i>	16
2.1.2.4 <i>Advantages and difficulties in determining absorption of phytopharmaceuticals with the Caco-2 model</i>	19
2.2 CARRIER MEDIATED TRANSPORT AND METABOLISM IN THE CACO-2 MODEL	20
2.2.1 Carrier mediated transport in the Caco-2 model	20
2.2.1.1 <i>Human enterocytes vs. Caco-2 cells</i>	20
2.2.1.2 <i>Experimental approach to study carrier mediated transport</i>	22
2.2.1.3 <i>Reported transport studies</i>	24
2.2.2 Metabolism in the Caco-2 model	24
2.2.2.1 <i>Human enterocytes vs. Caco-2 cells</i>	24
2.2.2.2 <i>Reported studies</i>	28
2.2.3 Interplay between transporters and metabolizing enzymes	29
2.3 ANTHEMIS NOBILIS L.	31

2.3.1 Chamomillae romanae flos (PhEur 6)	31
2.3.1.1 Chemical composition of Chamomillae romanae flos	32
2.3.1.2 Use of Chamomillae romanae flos	32
2.3.2 Nobilin (CAS: 31824-11-0)	33
2.4 REFERENCES	35
3 Mechanism of chemical degradation and determination of solubility by kinetic modeling of the highly unstable sesquiterpene lactone nobilin in different media	53
3.1 ABSTRACT	53
3.2 INTRODUCTION	54
3.3 MATERIALS AND METHODS	55
3.3.1 Chemicals	55
3.3.2 Purified nobilin	55
3.3.3 Isolation of chemical degradation products	56
3.3.4 Vehicles	56
3.3.4.1 Media	56
3.3.4.2 Liposomal formulations	57
3.3.5 Particle size measurement	58
3.3.6 Structural elucidation of degradation products 1-5	58
3.3.7 Single crystal X-ray analysis of degradation product 1	58
3.3.8 Kinetics of chemical degradation	59
3.3.9 Solubility study	60
3.3.10 Model for the estimation of solubility	60
3.3.11 HPLC	62
3.4 RESULTS	63
3.4.1 Stability study	63
3.4.1.1 Structure elucidation of degradation products 1, 2, and 3	63
3.4.1.2 Structure elucidation of degradation product 4	65
3.4.1.3 Structure elucidation of degradation product 5	65
3.4.1.4 Kinetics of chemical degradation	67
3.4.2 Solubility study	71
3.5 DISCUSSION	72
3.6 CONCLUSION	76
3.7 REFERENCES	77

4	Transport of nobilin conjugation products and the use of the extract of <i>Chamomillae romanae</i> flos influence absorption of nobilin in the Caco-2 model	82
4.1	ABSTRACT.....	82
4.2	INTRODUCTION.....	83
4.3	MATERIALS AND METHODS.....	85
4.3.1	Chemicals.....	85
4.3.2	Cell culture.....	86
4.3.3	TEER.....	86
4.3.4	Permeation experiment.....	86
4.3.5	Cell extraction.....	87
4.3.6	HPLC.....	88
4.3.7	Kinetic modeling.....	89
4.4	RESULTS.....	95
4.4.1	Transport of nobilin and its conjugates.....	95
4.4.2	Influence of transporter inhibition on the transport of nobilin and its conjugates.....	99
4.4.3	Influence of the full extract and extract ingredients on the transport of nobilin and its conjugates.....	101
4.5	DISCUSSION.....	104
4.6	CONCLUSION.....	109
4.7	APPENDIX.....	110
4.8	REFERENCES.....	129
5	Influence of biorelevant media and lipid based formulations on the in vitro absorption and bioconversion of nobilin as pure compound and as plant extract in the Caco-2 model	135
5.1	ABSTRACT.....	135
5.2	INTRODUCTION.....	136
5.3	MATERIALS AND METHODS.....	138
5.3.1	Chemicals.....	138
5.3.2	Media.....	138
5.3.3	Liposomal formulations.....	139
5.3.4	Lipid based formulations.....	140
5.3.5	Particle size measurement.....	140
5.3.6	Kinetics of chemical degradation.....	140
5.3.7	Cell culture.....	141
5.3.8	TEER.....	141

5.3.9 Permeation experiment.....	141
5.3.10 Cell extraction.....	142
5.3.11 HPLC.....	143
5.3.12 Kinetic modeling.....	144
5.4 RESULTS.....	147
5.4.1 Stability study.....	147
5.4.2 Influence of media on the transport of nobilin and its conjugates.....	147
5.4.3 Influence of SMEDDS on the transport of nobilin and its conjugates.....	153
5.4.4 Influence of biorelevant media and SMEDDS on transport of nobilin and its conjugates in full extract.....	156
5.5 DISCUSSION.....	162
5.6 CONCLUSION.....	165
5.7 APPENDIX.....	166
5.8 REFERENCES.....	170
List of Abbreviations	175
List of Symbols	177
List of Figures	181
List of Schemes	187
List of Tables	188

Chapter 1

Introduction

1.1 BACKGROUND

Per oral administration is the most convenient way of systemic application of a pharmacologically active compound. To reach satisfactory bioavailability, good absorption in the small intestine is required.

Several factors may limit absorption such as chemical instability and poor solubility of the drug in the gastrointestinal tract, bioconversion by metabolizing enzymes, low permeation by diffusion and carrier mediated epithelial efflux transport at the plasma membrane of enterocytes.^{1,2}

Chemical stability and solubility in the gastrointestinal tract are influenced by the aqueous environment, the pH range of 1 to 8 and ingredients such as bile salts, phospholipids, digestive enzymes, food components, and digestion products.^{1,3} The biopharmaceutics classification system (BCS) classifies compounds with respect to intestinal absorption based on their intestinal permeability and their solubility⁴ whereas solubility of the largest dose strength in 250 mL or less of purely aqueous media over the pH range of 1 to 7.5 defines a highly soluble compound.⁵ Several drug compounds do not fulfill this requirement including danazol, mefenamic acid, ketoconazole, glyburide, troglitazone, atovaquone, sanfetrinem cilexetil, dantrolene, indinavir, saquinavir, sirolimus, albendazole, 9-nitrocamptothecin, and curcumin.⁶⁻²¹ Additionally, chemical instability in the gastrointestinal tract has been reported to compromise absorption such as for curcumin or sirolimus.^{14,15} Issues of poor stability of a compound are frequently accompanied by low solubility. Penicillins, for instance, show pH dependent degradation and solubility with a maximum stability and lowest solubility at pH 6-7.^{22,23}

In recent years, components of the gastrointestinal tract were considered in connection with food effect on absorption. The bioavailability of the poorly water-soluble drug danazol, for example, was found to be increased by food whereas its solubility was increased by micelles of bile salts, phospholipids, and lipolysis products.^{10,11,16,20} Food effect has become the subject of a guidance for the industry issued by the FDA.²⁴ Therefore, several attempts have been made to develop biorelevant media to simulate the conditions in the intestine in the fasted and fed state.^{1,6,7,16,25,26} An in vitro-in vivo correlation between in

vivo bioavailability and in vitro dissolution using these media was seen.^{7-9,16-18,25,27} Recently, biorelevant transport media for in vitro absorption studies with the Caco-2 cell model simulating intestinal fluid in the fasted and the fed state, FaSSIF-TM_{Caco} and FeSSIF-TM_{Caco}, respectively, were developed.¹² The influence of these media on solubility and stability is essential for their role in drug absorption.

Enterocytes, which constitute the barrier in the intestinal tract between the intestinal fluid and the blood circulation, show high level of apical and basal membrane transporters and metabolizing enzymes. Paclitaxel, digoxin, verapamil, and fexofenadine are some of the drugs that are transported apically out of the intestinal cell by the well characterized transporter protein P-gp (P-glycoprotein, ABCB1).²⁸⁻³⁰ Fexofenadine is in addition substrate of the apical MRP2 (multidrug resistance protein, ABCC2) and the basal MRP3 (ABCC3).^{28,30} Methotrexate, further, is substrate of the apical MRP2, and BCRP (breast cancer resistance protein, ABCG2) and the basal MRP3, and MRP1 (ABCC1).^{28,31} Fexofenadine is not only substrate of efflux carriers but also of the influx transporter protein OATP2B1 (organic anion transporting polypeptide, SLCO2B1) at the apical membrane.^{28,30}

Numerous drugs undergo phase I metabolism by different cytochrome P450 (CYP) enzymes in the enterocytes, e.g., verapamil and midazolam.^{29,32} Other drugs are substrates of phase II metabolizing enzymes such as the flavonoid apigenin which is glucuronidated by UDP-glucuronosyltransferase and sulfonated by sulfotransferase or busulfan which is conjugated by glutathione S-transferase to the glutathione conjugate.^{33,34} These metabolites are often substrates of the above mentioned efflux carriers. The metabolites of verapamil are transported by P-gp, apigenin glucuronide and sulfate are substrates of MRPs and/or BCRP and glutathione conjugates such as the endogenous leukotriene C4 are transported by MRPs.^{29,34-36} Furthermore, the influx carriers OATP transport steroid conjugates.²⁸

Interestingly, some cases of functional interplay between metabolizing enzymes and transporter proteins were observed in recent years. For instance, metabolism of K77 and sirolimus, which are substrates of cytochrome P450 and P-gp, was decreased by inhibition of the efflux transporter in the Caco-2 model whereas the inhibition did not reduce metabolism of the non P-gp substrates midazolam and felodipine.^{32,37} Also, interplay between phase II metabolism and transporters was suggested such as for the glucuronidation of apigenin and genistein with BCRP or glucuronidation and sulfonation of apigenin with MRPs.^{34,36,38,39}

In vitro study of intestinal absorption which can take into consideration these factors is routinely carried out using the Caco-2 cell culture model.⁴⁰⁻⁴³ This well-established and well characterized model shows a largely similar expression pattern of transporters and metabolizing enzymes as intestinal cells.⁴⁴⁻⁴⁶ In a study involving 10 different laboratories, Caco-2 cells were shown to well express the transporters P-gp, BCRP, MRP2, MRP3, MRP1, and OATP. In contrast to the intestine, phase I metabolizing enzyme CYP was

poorly expressed whereas the phase II conjugating enzymes glutathione S-transferase and UDP-glucuronosyltransferase were well expressed.⁴³

The above mentioned factors bear a high potential of interaction between different compounds affecting their absorption behavior. Interaction between synthetic drugs has been extensively studied whereas in recent years the interest in the absorption of compounds from phytopharmaceuticals being multi-component mixtures has risen. Increased absorption of a compound applied as full plant extract was reported for instance for paclitaxel from *Taxus yunnanensis*, aconitine, mesaconitine, and hyaconitine from *Aconitum* species, and rosmarinic acid from *Plectranthus barbatus*.⁴⁷⁻⁴⁹

The influence of formulation ingredients on absorption has been extensively discussed in recent years.⁵⁰⁻⁵² Lipid based formulations such as self-(micro)emulsifying drug delivery systems (S(M)EDDS) were shown to increase absorption of several poorly water soluble drugs including cyclosporine which is commercially available as a lipid based formulation (Neoral®)⁵³ and sirolimus whose stability and solubility was improved in the presence of D- α -tocopheryl polyethylene glycol succinate micelles or SMEDDS.^{14,54}

Nobilin, a sesquiterpene lactone of the germacranolide type is a marker compound isolated from the flowers of *Anthemis nobilis* L. called *Chamomillae romanae flos*.⁵⁵ No reports about the chemical stability and solubility of this compound in the intestinal tract exist in the literature. Also, nothing is known about bioavailability of nobilin and the effect of food, formulation, metabolism and cellular transport on absorption. Further, the role of the plant extract on the absorption of nobilin is unknown.

The increase of absorption frequently observed for plant extracts and mixtures of compounds consisting of food or pharmaceutical formulation ingredients is generally poorly understood. Also, the role of the interplay between metabolism and carrier mediated transport and its possible modulation by multi-component mixtures has not been fully elucidated. Finally, established methodology to determine dissolution of chemically instable material is not available.

1.2 OBJECTIVES

The overall aim of this work was to investigate the intestinal absorption of nobilin in vitro and identify strategies for its improvement. Factors determining nobilin absorption were investigated taking into account chemical stability, solubility, metabolism, and membrane permeation by passive diffusion and carrier mediated transport in order to gain a basic mechanistic understanding of the absorption process of the compound. Physiologically based multi-compartment kinetic modeling was employed to delineate the influence of simultaneously acting phenomena. Based on this understanding, possibilities are finally

explored to improve absorption of nobiletin utilizing plant extract, formulation, and post-prandial application approaches. The thesis is divided into four chapters.

Chapter 2 provides a review on one hand of the intestinal absorption of phytopharmaceutical drugs in the Caco-2 model and on the other hand of the present knowledge of transporters and metabolizing enzymes in Caco-2 studies. Additionally, it gives a short overview of the plant *Anthemis nobilis* L. and its sesquiterpene lactone nobiletin.

Chapter 3 focuses on chemical stability and solubility of nobiletin. The aim was to study mechanism and kinetics of degradation of purified nobiletin and identify its degradation products, and, further, to determine the solubility of nobiletin under conditions of concurrent rapid chemical degradation. To accomplish the latter goal, the use of a kinetic model is proposed. Moreover, the effect of media simulating the environment of the intestinal tract and of vehicles used in in vitro Caco-2 absorption studies on stability and solubility of purified nobiletin was investigated. The ultimate goal was to derive a basic understanding of the effect of the media on stability and solubility and its consequence for the bioavailability of nobiletin.

The objective of Chapter 4 is the investigation of the mechanism of intestinal absorption of nobiletin in the Caco-2 model. The first specific aim was to investigate the effect of bioconversion and of carrier mediated efflux of the ensuing conjugation products on nobiletin absorption and to ascertain a possible interplay between bioconversion and efflux. A kinetic model-based approach was employed to this end. The second aim was to elucidate the impact of the full extract of *Chamomillae romanae flos* and its ingredients, i.e., sesquiterpene lactones, essential oil and flavonoids⁵⁶ on metabolizing enzymes and transporter proteins that influence nobiletin absorption. By unraveling the interplay between bioconversion and efflux and the interaction between the plant extract and nobiletin or nobiletin bioconversion products with respect to these processes, biochemical principles for absorption improvement of nobiletin should be derived.

The focus of Chapter 5 is the effect of biorelevant media and lipid based formulations on nobiletin absorption taking into consideration chemical stability, bioconversion, and efflux of the conjugation products. The effect of the plant extract in combination with biorelevant media and lipid based formulations on nobiletin absorption is also studied. The objective of this part of the work was to first use stabilization as a physicochemical approach for absorption improvement that would then be investigated as a means to influence biochemical processes relevant for absorption.

1.3 REFERENCES

1. Dressman JB, Amidon GL, Reppas C, Shah VP 1998. Dissolution testing as a prognostic tool for oral drug absorption: Immediate release dosage forms. *Pharmaceutical Research* 15(1):11-22.
2. Custodio JM, Wu CY, Benet LZ 2008. Predicting drug disposition, absorption/elimination/transporter interplay and the role of food on drug absorption. *Advanced Drug Delivery Reviews* 60(6):717-733.
3. Diakidou A, Vertzoni M, Goumas K, Soderlind E, Abrahamsson B, Dressman J, Reppas C 2009. Characterization of the contents of ascending colon to which drugs are exposed after oral administration to healthy adults. *Pharmaceutical Research* 26(9):2141-2151.
4. Amidon GL, Lennernas H, Shah VP, Crison JR 1995. A theoretical basis for a biopharmaceutic drug classification - the correlation of in-vitro drug product dissolution and in-vivo bioavailability. *Pharmaceutical Research* 12(3):413-420.
5. FDA. 2000. Guidance for industry: Waiver of in vivo bioavailability and bioequivalence studies for immediate-release solid oral dosage forms based on a biopharmaceutics classification system. Rockville, MD, USA: Food and Drug Administration. <http://www.fda.gov/downloads/Drugs/.../Guidances/ucm070246.pdf>.
6. Galia E, Nicolaides E, Horter D, Lobenberg R, Reppas C, Dressman JB 1998. Evaluation of various dissolution media for predicting in vivo performance of class I and II drugs. *Pharmaceutical Research* 15(5):698-705.
7. Wei H, Lobenberg R 2006. Biorelevant dissolution media as a predictive tool for glyburide a class II drug. *European Journal of Pharmaceutical Sciences* 29(1):45-52.
8. Nicolaides E, Galia E, Efthymiopoulos C, Dressman JB, Reppas C 1999. Forecasting the in vivo performance of four low solubility drugs from their in vitro dissolution data. *Pharmaceutical Research* 16(12):1876-1882.
9. Kambayashi A, Dressman JB 2013. An in vitro-in silico-in vivo approach to predicting the oral pharmacokinetic profile of salts of weak acids: Case example dantrolene. *European Journal of Pharmaceutics and Biopharmaceutics* 84(1):200-207.
10. Vertzoni M, Markopoulos C, Symillides M, Goumas C, Imanidis G, Reppas C 2012. Luminal lipid phases after administration of a triglyceride solution of danazol in the fed state and their contribution to the flux of danazol across Caco-2 cell monolayers. *Molecular Pharmaceutics* 9(5):1189-1198.
11. Charman WN, Rogge MC, Boddy AW, Berger BM 1993. Effect of food and a monoglyceride emulsion formulation on danazol bioavailability. *Journal of Clinical Pharmacology* 33(4):381-386.
12. Markopoulos C, Thoenen F, Preisig D, Symillides M, Vertzoni M, Parrott N, Reppas C, Imanidis G 2013. Biorelevant media for transport experiments in the Caco-2 model to evaluate drug absorption in

the fasted and fed state and their usefulness. *European Journal of Pharmaceutics and Biopharmaceutics* <http://dx.doi.org/10.1016/j.ejpb.2013.10.017>.

13. Kapitza SB, Michel BR, van Hoogevest P, Leigh MLS, Imanidis G 2007. Absorption of poorly water soluble drugs subject to apical efflux using phospholipids as solubilizers in the Caco-2 cell model. *European Journal of Pharmaceutics and Biopharmaceutics* 66(1):146-158.
14. Sun MH, Si LQ, Zhai XZ, Fan ZZ, Ma YM, Zhang R, Yang XL 2011. The influence of co-solvents on the stability and bioavailability of rapamycin formulated in self-microemulsifying drug delivery systems. *Drug Development and Industrial Pharmacy* 37(8):986-994.
15. Mohanty C, Sahoo SK 2010. The in vitro stability and in vivo pharmacokinetics of curcumin prepared as an aqueous nanoparticulate formulation. *Biomaterials* 31(25):6597-6611.
16. Sunesen VH, Pedersen BL, Kristensen HG, Mullertz A 2005. In vivo in vitro correlations for a poorly soluble drug, danazol, using the flow-through dissolution method with biorelevant dissolution media. *European Journal of Pharmaceutical Sciences* 24(4):305-313.
17. Dressman JB, Reppas C 2000. In vitro-in vivo correlations for lipophilic, poorly water-soluble drugs. *European Journal of Pharmaceutical Sciences* 11:S73-S80.
18. Nicolaidis E, Symillides M, Dressman JB, Reppas C 2001. Biorelevant dissolution testing to predict the plasma profile of lipophilic drugs after oral administration. *Pharmaceutical Research* 18(3):380-388.
19. Saha SC, Patel D, Rahman S, Savva M 2013. Physicochemical characterization, solubilization, and stabilization of 9-nitrocamptothecin using pluronic block copolymers. *Journal of pharmaceutical sciences* 102(10):3653-3665.
20. Bakatselou V, Oppenheim RC, Dressman JB 1991. Solubilization and wetting effects of bile-salts on the dissolution of steroids. *Pharmaceutical Research* 8(12):1461-1469.
21. Lindenberg M, Kopp S, Dressman JB 2004. Classification of orally administered drugs on the World Health Organization model list of essential medicines according to the biopharmaceutics classification system. *European Journal of Pharmaceutics and Biopharmaceutics* 58(2):265-278.
22. Tsuji A, Nakashima E, Hamano S, Yamana T 1978. Physicochemical properties of amphoteric beta-lactam antibiotics I: Stability, solubility, and dissolution behavior of amino penicillins as a function of pH. *Journal of Pharmaceutical Sciences* 67(8):1059-1066.
23. Yamana T, Tsuji A, Mizukami Y 1974. Kinetic approach to development in beta-lactam antibiotics. I. comparative stability of semisynthetic penicillins and 6-aminopenicillanic acid in aqueous-solution. *Chemical & Pharmaceutical Bulletin* 22(5):1186-1197.
24. FDA. 2002. Guidance for industry: Food-effect bioavailability and fed bioequivalence studies. Rockville, MD, USA: Food and Drug Administration. [http://www.fda.gov/downloads/regulatory information/guidances/ucm126833.pdf](http://www.fda.gov/downloads/regulatory_information/guidances/ucm126833.pdf).

25. Parojcic J, Duric J, Jovanovic M, Ibric S, Jovanovic D 2004. Influence of dissolution media composition on drug release and in-vitro/in-vivo correlation for paracetamol matrix tablets prepared with novel carbomer polymers. *Journal of Pharmacy and Pharmacology* 56(6):735-741.
26. Vertzoni M, Fotaki N, Kostewicz E, Stippler E, Leuner C, Nicolaidis E, Dressman J, Reppas C 2004. Dissolution media simulating the intraluminal composition of the small intestine: Physiological issues and practical aspects. *Journal of Pharmacy and Pharmacology* 56(4):453-462.
27. Schamp K, Schreder SA, Dressman J 2006. Development of an in vitro/in vivo correlation for lipid formulations of EMD 50733, a poorly soluble, lipophilic drug substance. *European Journal of Pharmaceutics and Biopharmaceutics* 62(3):227-234.
28. Giacomini KM, Huang SM, Tweedie DJ, Benet LZ, Brouwer KLR, Chu XY, Dahlin A, Evers R, Fischer V, Hillgren KM, Hoffmaster KA, Ishikawa T, Keppler D, Kim RB, Lee CA, Niemi M, Polli JW, Sugiyama Y, Swaan PW, Ware JA, Wright SH, Yee SW, Zamek-Gliszczyński MJ, Zhang L, International T 2010. Membrane transporters in drug development. *Nature Reviews Drug Discovery* 9(3):215-236.
29. Pauli-Magnus C, von Richter O, Burk O, Ziegler A, Mettang T, Eichelbaum M, Fromm MF 2000. Characterization of the major metabolites of verapamil as substrates and inhibitors of P-glycoprotein. *Journal of Pharmacology and Experimental Therapeutics* 293(2):376-382.
30. Ming X, Knight BM, Thakker DR 2011. Vectorial transport of fexofenadine across Caco-2 cells: Involvement of apical uptake and basolateral efflux transporters. *Molecular Pharmaceutics* 8(5):1677-1686.
31. Estudante M, Morais JG, Soveral G, Benet LZ 2013. Intestinal drug transporters: An overview. *Advanced Drug Delivery Reviews* 64(10):1340-1356.
32. Cummins CL, Jacobsen W, Christians U, Benet LZ 2004. CYP3A4-transfected Caco-2 cells as a tool for understanding biochemical absorption barriers: Studies with sirolimus and midazolam. *Journal of Pharmacology and Experimental Therapeutics* 308(1):143-155.
33. Gibbs JP, Yang JS, Slattery JT 1998. Comparison of human liver and small intestinal glutathione S-transferase-catalyzed busulfan conjugation in vitro. *Drug Metabolism and Disposition* 26(1):52-55.
34. Hu M, Chen J, Lin HM 2003. Metabolism of flavonoids via enteric recycling: Mechanistic studies of disposition of apigenin in the Caco-2 cell culture model. *Journal of Pharmacology and Experimental Therapeutics* 307(1):314-321.
35. Zhou SF, Wang LL, Di YM, Xue CC, Duan W, Li CG, Li Y 2008. Substrates and inhibitors of human multidrug resistance associated proteins and the implications in drug development. *Current Medicinal Chemistry* 15(20):1981-2039.
36. Jiang W, Xu BB, Wu BJ, Yu R, Hu M 2012. UDP-glucuronosyltransferase (UGT) 1A9-overexpressing HeLa cells is an appropriate tool to delineate the kinetic interplay between breast cancer

resistance protein (BCRP) and UGT and to rapidly identify the glucuronide substrates of BCRP. *Drug Metabolism and Disposition* 40(2):336-345.

37. Cummins CL, Jacobsen W, Benet LZ 2002. Unmasking the dynamic interplay between intestinal P-glycoprotein and CYP3A4. *Journal of Pharmacology and Experimental Therapeutics* 300(3):1036-1045.
38. Siissalo S, Heikkinen AT 2013. In vitro methods to study the interplay of drug metabolism and efflux in the intestine. *Current Drug Metabolism* 14(1):102-111.
39. Jeong EJ, Liu X, Jia XB, Chen J, Hu M 2005. Coupling of conjugating enzymes and efflux transporters: Impact on bioavailability and drug interactions. *Current Drug Metabolism* 6(5):455-468.
40. Artursson P, Borchardt RT 1997. Intestinal drug absorption and metabolism in cell cultures: Caco-2 and beyond. *Pharmaceutical Research* 14(12):1655-1658.
41. Hubatsch I, Ragnarsson EGE, Artursson P 2007. Determination of drug permeability and prediction of drug absorption in Caco-2 monolayers. *Nature Protocols* 2(9):2111-2119.
42. Sugano K, Kansy M, Artursson P, Avdeef A, Bendels S, Di L, Ecker GF, Faller B, Fischer H, Gerebtzoff G, Lennernaes H, Senner F 2010. Coexistence of passive and carrier-mediated processes in drug transport. *Nature Reviews Drug Discovery* 9(8):597-614.
43. Hayeshi R, Hilgendorf C, Artursson P, Augustijns P, Brodin B, Dehertogh P, Fisher K, Fossati L, Hovenkamp E, Korjamo T, Masungi C, Maubon N, Mols R, Mullertz A, Monkkonen J, O'Driscoll C, Oppers-Tiemissen HM, Ragnarsson EGE, Rooseboom M, Ungell AL 2008. Comparison of drug transporter gene expression and functionality in Caco-2 cells from 10 different laboratories. *European Journal of Pharmaceutical Sciences* 35(5):383-396.
44. Hilgendorf C, Ahlin G, Seithel A, Artursson P, Ungell AL, Karlsson J 2007. Expression of thirty-six drug transporter genes in human intestine, liver, kidney, and organotypic cell lines. *Drug Metabolism and Disposition* 35(8):1333-1340.
45. Prueksaritanont T, Gorham LM, Hochman JH, Tran LO, Vyas KP 1996. Comparative studies of drug-metabolizing enzymes in dog, monkey, and human small intestines, and in Caco-2 cells. *Drug Metabolism and Disposition* 24(6):634-642.
46. Englund G, Rorsman F, Ronnblom A, Karlbom U, Lazorova L, Grasjo J, Kindmark A, Artursson P 2006. Regional levels of drug transporters along the human intestinal tract: Co-expression of ABC and SLC transporters and comparison with Caco-2 cells. *European Journal of Pharmaceutical Sciences* 29(3-4):269-277.
47. Jin J, Cai D, Bi H, Zhong G, Zeng H, Gu L, Huang Z, Huang M 2013. Comparative pharmacokinetics of paclitaxel after oral administration of *Taxus yunnanensis* extract and pure paclitaxel to rats. *Fitoterapia* 90:1-9.
48. Li N, Tsao R, Sui ZG, Ma JW, Liu ZQ, Liu ZY 2012. Intestinal transport of pure diester-type alkaloids from an aconite extract across the Caco-2 cell monolayer model. *Planta Medica* 78(7):692-697.

49. Fale PL, Ascensao L, Serralheiro MLM 2013. Effect of luteolin and apigenin on rosmarinic acid bioavailability in Caco-2 cell monolayers. *Food & Function* 4(3):426-431.
50. Humberstone AJ, Charman WN 1997. Lipid-based vehicles for the oral delivery of poorly water soluble drugs. *Advanced Drug Delivery Reviews* 25(1):103-128.
51. Gershanik T, Benita S 2000. Self-dispersing lipid formulations for improving oral absorption of lipophilic drugs. *European Journal of Pharmaceutics and Biopharmaceutics* 50(1):179-188.
52. Gursoy RN, Benita S 2004. Self-emulsifying drug delivery systems (SEDDS) for improved oral delivery of lipophilic drugs. *Biomedicine & Pharmacotherapy* 58(3):173-182.
53. Dunn CJ, Wagstaff AJ, Perry CM, Plosker GL, Goa KL 2001. Cyclosporin - An updated review of the pharmacokinetic properties, clinical efficacy and tolerability of a microemulsion-based formulation (Neoral®)¹ in organ transplantation. *Drugs* 61(13):1957-2016.
54. Kim MS, Kim JS, Cho WK, Hwang SJ 2013. Enhanced solubility and oral absorption of sirolimus using D-alpha-tocopheryl polyethylene glycol succinate micelles. *Artificial Cells Nanomedicine and Biotechnology* 41(2):85-91.
55. Holub M, Samek Z 1977. Terpenes. CLXX. Isolation and structure of 3-epinobilin, 1,10-epoxynobilin and 3-dehydronobilin - other sesquiterpenic lactones from flowers of *Anthemis nobilis* L. revision of structure of nobilin and eucannabinolide. *Collection of Czechoslovak Chemical Communications* 42(3):1053-1064.
56. Otto I. 2007. *Chamaemelum nobilie* (L.) ALL. In Blaschek W, Ebel S, Hackenthal E, Holzgrabe U, Keller K, Reichling J, Schulz V, editors. *Hagers Enzyklopädie der Arzneistoffe und Drogen*, 6 ed., Stuttgart: Wissenschaftliche Verlagsgesellschaft mbh Stuttgart. p 298-308.

Chapter 2

Theoretical section: *An overview*

2.1 ABSORPTION OF PHYTOPHARMACEUTICALS

2.1.1 Bioavailability of phytopharmaceuticals

The use of phytopharmaceuticals is as old as mankind. It is estimated that nowadays there are more than 11,000 species used and 300 of them frequently. Approximately one third of the adults in developed countries and more than 80% in developing countries use phytopharmaceuticals. In the last years the interest in pharmacokinetics of such drugs increased but still more investigations have to be done to bring light into this field.¹

Most phytopharmaceuticals are orally administered but little is known about bioavailability of the ingredients of such drugs. They are mixtures of different compounds which show often poor bioavailability due to physicochemical properties, to being substrate of transporter proteins, or to being extensively metabolized by phase I and phase II enzymes.¹

Curcumin from *Curcuma longa* and hypericin from *Hypericum perforatum*, for example, are active compounds of those plants. They are poorly water soluble and curcumin is further instable at neutral and basic pH which results in poor bioavailability.²⁻⁴ Furthermore, polyphenols which are often present in their glycosylated form show poor bioavailability because of their chemical structure compared to their aglycones. They are hydrolyzed in the small intestine either by the brush border membrane enzyme lactase phloridizin hydrolase (LPH) or they are transported into the enterocytes by SGLT1 (sodium-dependent glucose transporter, SLC5A1) where they are hydrolyzed by the cytosolic β -glucosidase. Later in the colon they are hydrolyzed by intestinal bacteria to the aglycone and further converted to phenolic acids which was reported for daidzein metabolized to equol.⁵

Reduced bioavailability of phenolics was also often observed in vivo due to extensive metabolism, as they are substrates of phase I and phase II metabolism. Curcumin, for example, is extensively metabolized in vivo by the phase I metabolizing enzymes reductases and also by the phase II UDP-glucuronosyltransferase and sulfotransferase.^{1,4} Quercetin, which is widely distributed in plants,

such as in *Hypericum perforatum*, is glucuronidated and methylated or the catechin epigallocatechin gallate (EGCG) present in green tea is methylated and other catechins are mainly glucuronidated or sulfonated.⁵⁻⁷ Alkaloids are also metabolized, for example, berberine from *Rhizoma coptidis* is extensively demethylated (phase I) followed by glucuronidation (phase II) in vivo.⁸

Berberine was further shown in vivo to be substrate of the efflux transporter protein P-gp (P-glycoprotein, ABCB1) and some flavonoids were reported to be transported by P-gp, BCRP (breast cancer resistance protein, ABCG2), and MRPs (multidrug resistance proteins, ABCC).^{9,10 11,12}

Considering all those mechanisms which influence bioavailability it is not surprising that interactions occur between the ingredients of a phytopharmaceutical that alter bioavailability. The aqueous solubility of hypericin for example was increased with pure dimeric procyanidin B2 and trimeric procyanidin C1.³ It was suggested that also other polyphenols of the plant extract have an influence on solubility.¹³ This mechanism was proposed to be the reason of increased bioavailability in rats by administering hypericin with proanthocyanidin or quercetin glycoside.¹⁴ Another example is the increased bioavailability of ascorbic acid in citrus fruits which is supposed to be due to flavonoids in the extract that increase absorption and stability of ascorbic acid. Bioavailability of Kavain was improved by a special extract from Kava-kava and also absorption of gitoxin in a fraction of *Digitalis purpurea* extract could be increased.¹⁵

This high potential of interaction of natural products was also recognized by administering them with commercial synthetic drugs. Probably the two best known examples of such natural products are grapefruit juice and *Hypericum perforatum*. Grapefruit juice inhibits cytochrome P450 3A4, the influx transporters OATPs (organic anion transporting polypeptide), and efflux carrier P-gp. Bioavailability of felodipine which undergoes first-pass metabolism by CYP 3A4 was increased with grapefruit juice. This interaction was extensively studied in the last years and many drugs were identified to interact with grapefruit juice.¹⁶ The inhibitory effect of grapefruit juice on P-gp using the substrate digoxin was not seen in vivo but the inhibition of the influx transporter increased bioavailability of talinolol.^{17,18}

Hypericum perforatum was reported to induce CYPs (mainly the subfamily 2C and 3A) and P-gp which resulted in a decreased bioavailability of CYP and P-gp substrates such as digoxin or simvastatin.¹⁹⁻²¹

Other plants for which herbal-drug interactions were reported are, for example, *Crataegus monogyna/osyacantha*, *Valeriana officinalis*, and *Silybum marianum*.^{20,22,23} As a consequence of herbal-drug interaction also herb-herb interaction can occur which is of great interest in traditional Chinese medicine.²⁴

2.1.2 Absorption of phytopharmaceuticals in the Caco-2 model

The Caco-2 cell monolayer is a well-established and well characterized in vitro intestinal absorption model to study routinely in vitro absorption of synthetic drugs.²⁵⁻²⁸ Therefore, it is also a useful tool to study absorption of phytopharmaceuticals.²⁹ A more detailed description of the Caco-2 cells regarding carriers and metabolizing enzymes is given below.

2.1.2.1 Absorption of single phytopharmaceutical compounds

The increased interest in elucidating absorption processes of phytopharmaceutical compounds is reflected in the increasing numbers of published Caco-2 studies with isolated compounds in the last decade. Transport processes by passive diffusion and carriers, and metabolism were elucidated with Caco-2 cells.

Numerous investigations were carried out with polyphenols which are widely spread in plants. In a study involving 36 different flavonoids only five were proposed to be substrate of efflux transporters and the rest was assumed to be absorbed by passive diffusion in the Caco-2 model.³⁰ Naringin, for example, is substrate of P-gp and morin of MRPs whereas apigenin crosses the monolayer by passive diffusion.³¹⁻³³ Furthermore, the well-known extensive metabolism of flavonoids was studied. Apigenin, for instance, is extensively metabolized to glucuronides and sulfates which are further substrates of MRP2 (multidrug resistance protein, ABCC2).³³ A similar observation was reported for emodin which is glucuronidated and the metabolites are transported by MRPs.³⁴ Also inhibitory and inductive properties of polyphenols on transporter proteins and metabolic enzymes were investigated. The efflux transport of 2-amino-1-methyl-6-phenylimidazol[3,4-b]pyridine (PhIP) by P-gp, BCRP, and MRP could be decreased in presence of flavonoids quercetin, apigenin, luteolin, naringenin, and myricetin.³⁵⁻³⁷ Luteolin further inhibited the apical efflux of benzo[a]pyrene by BCRP, quercetin the efflux of N-acetyl 5-aminosalicylic acid (Ac-5-ASA) by MRP2, and naringenin, quercetin, genistein, and xanthohumol reduced P-gp mediated transport of cimetidine.³⁸⁻⁴⁰ Also influx transporters such as MCT1 (monocarboxylic acid transporter 1, SLC16A1) were reported to be inhibited by flavonoids.⁴¹ Furthermore, inductive effects on transporter proteins such as P-gp, BCRP, and MRP and stimulated apical efflux were observed in the presence of polyphenols in Caco-2 cells.⁴²⁻⁴⁵

Inhibition of metabolizing enzymes such as sulfotransferases by epigallocatechine gallate and other polyphenols, CYPs by certain polyphenols of apple juice and luteolin, and esterase by grapefruit juice flavonoids kaempferol and naringenin was documented.^{38,46-49} Induction of UDP-glucuronosyltransferases was observed in presence of quercetin and induction of CYPs was seen with polyphenols of apple juice and flavone.^{45,48,50,51}

Besides polyphenols other phytopharmaceutical compounds were reported being investigated with Caco-2 cells with respect to their transport mechanism, metabolism, inhibitory and inductive activity. Examples include alkaloids such as berberine, sinomenine, different terpenoids and steroids involving carotenoids and ginsenosides, further phenolic compounds such as curcumin, furanocoumarin derivatives, or isothiocyanate like sulforaphane.^{10,50,52-57}

2.1.2.2 Influence of plant extracts on absorption of phytopharmaceutical compounds

Beside the rising interest in the absorption profile of single phytopharmaceutical compounds also the awareness of the effect of the full extract on absorption of those compounds has risen in the last years. This is shown by the increasing numbers of published Caco-2 studies on this topic even though their quantity is still quite small. Table 1 shows reported Caco-2 studies addressing the influence of one or two extracts on absorption of their phytopharmaceutical compounds.

Paclitaxel which is a potent anticancer drug of *Taxus yunnanensis* is poorly bioavailable in vivo due to being substrate of P-gp and CYP3A. The Caco-2 study showed that the extract increased absorption of paclitaxel and had a similar effect on P-gp as the commonly used inhibitor verapamil.⁵⁸ *Echinacea saguinea* and *Echinacea pallida* are used to prevent upper respiratory tract infections associated with a cold and influenza. Bauer alkalamide 8, 10, and 1, and ketone 24 were assumed to be active compounds of the extracts whereas alkalamide 8 and 10 showed poor bioavailability in vivo. They were absorbed in the Caco-2 model by passive diffusion and metabolized to glucuronides. The extract did not have an effect on the absorption of the compounds but stimulated glucuronidation and increased basal transfer, apart from alkalamide 11 glucuronide, which was proposed to be due to regulation of transporter proteins expression.⁵⁹ The three alkaloids aconitine, mesaconitine, and hypaconitine are active compounds of *Aconitum* species. Their absorption was increased by the plant extract which was assumed to be due to P-gp inhibition.⁶⁰ *Prunella vulgaris* and *Salvia officinalis* are traditionally used against inflammation in the mouth. Rosmarinic acid present in *Prunella vulgaris* and ursolic acid in *Salvia officinalis* were reported to be poorly absorbed in vivo in combination with other plant extracts. In the Caco-2 study both compounds crossed the monolayer by passive diffusion and were metabolized to glucuronides and sulfates. The extract of *Salvia officinalis* and *Prunella vulgaris* did not influence their absorption and metabolism.⁶¹ However, inhibition of the apical efflux of rosmarinic acid was suggested with the extract of *Plectranthus barbatus* in the Caco-2 model.⁶² *Artemisia afra* is used against respiratory illnesses and contains luteolin which showed an increased bioavailability in monkeys when administered as extract. It was proposed that luteolin was absorbed by passive diffusion and also influx and efflux transporters could be involved in Caco-2 cells. Luteolin was extensively metabolized in the cells to luteolin monoglucuronide, sulfate, monoglucuronide sulfate, and methylated luteolin sulfate which were substrates of MRPs. Additionally, the study suggested that glycosylated luteolin (luteolin-7-O-glucoside)

was transported by SGLT into the cell where it was either hydrolyzed to luteolin which was further metabolized to the four metabolites or it crossed the basal membrane by an unknown transport process. Interestingly, the extract increased the uptake of luteolin and luteolin-7-O-glucoside and the metabolism in the cell to luteolin monoglucuronide, sulfate, and monoglucuronide sulfate whereas no luteolin and luteolin-7-O-glucoside was found in the basal compartment. The same observation was made with an acid-hydrolyzed extract of *Artemisia afra* containing only luteolin.⁶³ Mulberry (*Morus alba* L.) contains 1-deoxynojirimycin which is an α -glucosidase inhibitor. It crossed the Caco-2 monolayer in its intact form whereas in presence of the extract a slower permeation was observed.⁶⁴ Red clover (*Trifolium pratense*) is used, for example, as menopausal hormone replacement therapy. Its ingredients formononetin and biochanin A are absorbed and metabolized to glucuronides and to a smaller amount to sulfates which were excreted to both compartments whereas more formononetin was detected in the basal compartment and to a similar amount in the apical compartment compared to biochanin A. In presence of the extract no formononetin conjugates were found, the apical excretion of biochanin A was increased, and no sulfates were formed but these observations did not have an effect on absorption.⁶⁵

Danggui Buxue Tang is a combination of *Astragali radix* and *Angelicae sinensis radix* in traditional Chinese medicine to treat menopausal symptoms. The absorption of formononetin and calycosin compounds of *Astragali radix* was not increased by the extract of this plant whereas in combination with *Angelicae sinensis radix* extract an improvement was observed which was proposed amongst other to be due to reduced efflux in the Caco-2 model.⁶⁶

Several commercial products of *Hypericum perforatum* are available to treat mild to moderate symptoms of depression. Rutin, hyperoside, and isoquercitrin are phenolic glycoside of *Hypericum perforatum* which are transported in the Caco-2 model mainly from the apical-to-basal (rutin and hyperoside) or basal-to-apical (isoquercitrin) direction. The commercial products increased the transport from rutin and hyperoside from basal-to-apical. This observation was attributed to an increased apical efflux by MRP2 due to ingredients of the products. Interestingly, the three used products alternated the transport differently which was probably a result of the different composition of ingredients.⁶⁷ A similar observation was made for daizein, genistein, formononetin, and biochanin A in 6 products of red clover (*Trifolium pratense*). The absorption rate of the four isoflavones, the glucuronidation of biochanin A, and the efflux of its metabolites was differently affected by the 6 products which was also supposed to be a result of the different compositions of the products.⁶⁸

Table 1: Influence of plant extracts on absorption of phytopharmaceutical compounds in the Caco-2 model.

Plant extracts	Compounds	Effects of the extract in Caco-2 model	Year published
One extract			
<i>Taxus yunnanensis</i>	paclitaxel	apical efflux ↓ absorption ↑	2013 ⁵⁸
<i>Echinacea saguinea</i>	Bauer alkamide 8 Bauer alkamide 10 Bauer alkamide 11 Bauer ketone 24	glucuronidation ↑ basal transfer of glucuronides ↑ (apart from alkamide 11 glucuronide) absorption =	2013 ⁵⁹
<i>Echinacea pallida</i>	Bauer alkamide 8 Bauer alkamide 10 Bauer alkamide 11 Bauer ketone 24	glucuronidation ↑ basal transfer of glucuronides ↑ (apart from alkamide 11 glucuronide) absorption =	2013 ⁵⁹
<i>Aconitum</i> species	aconitine mesaconitine hypoconitine	apical efflux ↓ absorption ↑	2012 ⁶⁰
<i>Prunella vulgaris</i>	rosmarinic acid	metabolism = absorption =	2011 ⁶¹
<i>Plectranthus barbatus</i>	rosmarinic acid	apical efflux ↓ absorption ↑	2012 ⁶²
<i>Salvia officinalis</i>	ursolic acid	metabolism = absorption =	2011 ⁶¹
<i>Artemisia afra</i>	luteolin	uptake into the cell ↑ metabolism ↑ absorption ↓	2010 ⁶³
<i>Morbus alba</i> L.	1-deoxynojirimycin	absorption ↓	2010 ⁶⁴
<i>Trifolium pratense</i> L.	formononetin biochanin A	glucuronidation ↓ (formononetin) apical excretion of glucuronides ↑ (biochanin A) sulfonation ↓ absorption =	2004 ⁶⁵
Two extracts			
<i>Astragalus membranaceus</i> var. <i>mongholicus</i> and <i>Angelicae sinensis</i>	formononetin calycosin	absorption ↑ (with <i>Angelicae sinensis</i>)	2012 ⁶⁶
Commercial products			
<i>Hypericum perforatum</i>	rutin hyperoside	apical efflux ↑ absorption ↓	2010 ⁶⁷
<i>Trifolium pratense</i> L.	daizein genistein formononetin biochanin A	absorption ↑ ↓	2008 ⁶⁸
↑: increasing effect, ↓: decreasing effect, = no effect			

2.1.2.3 Influence of plant ingredients on absorption of phytopharmaceutical compounds

There is a great interest in elucidating interactions between specific phytopharmaceutical compounds of one plant or two different plants which is supported by the large number of reported Caco-2 studies on this topic. Some examples are given in Table 2.

The first four examples, in Table 2, show the influence of one or more phytopharmaceutical compounds on the absorption of another compound of the same plant. The apical efflux of curcumin was inhibited by the combination of α -tumerone and aromatic tumerone. This effect was attributed to α -tumerone which inhibited P-gp and possibly also other efflux transporters.⁶⁹ Influence of 9 different flavonoids on hesperetin metabolism (glucuronidation, sulfonation) and efflux of its conjugates decreased metabolism in the cell and apical efflux of metabolites probably due to BCRP inhibition, and increased the basal transport of metabolites. Further, in combination with quercetin it was shown that the total amount of hesperetin was increased. It was suggested that by reduction of metabolism absorption of hesperetin could be increased.⁷⁰ Also the transport of rosmarinic acid was influenced by flavonoids. It was proposed that the combination of luteolin and apigenin reduced the apical uptake by MCT and the apical efflux of rosmarinic acid by ABC transporters in a concentration dependent manner of the flavonoid composition which resulted in an increased absorption.⁶² Involvement of apical efflux inhibition of hypericin of *Hypericum perforatum* by seven different polyphenolic compounds of *Hypericum perforatum* was also suggested for the increased absorption of hypericin.^{13,71}

The second group in Table 2 deals with the influence of mixtures of compounds of one plant on each other's absorption. Increased absorption was reported for all three flavones baicalein, wogonin, and oroxylin A by administering them as a mixture which was attributed to a metabolic competition (glucuronidation and sulfonation).⁷² The co-administration of the three alkaloids aconitine, mesaconitine, and hyaconitine resulted in the inhibition of their own apical efflux by P-gp and therefore showed an increased absorption. Interestingly, the effect was not as strong as with the extract.⁶⁰ Quercetin and isorhamnetin (3'-O-methylquercetin) are compounds of *Hippophae rhamnoides* or *Gingko biloba* whereas the latter is a metabolite of quercetin formed in plants and humans by catechol-O-methyltransferase (COMT). The combination of those compounds increased absorption of each other which was ascribed to inhibitory effects of them on efflux transporters such as P-gp whereas other transporters might be involved as well. Reduced methylation of quercetin in the presence of the metabolite isorhamnetin was also discussed and was assumed to play a negligible role.⁷³

Finally, the last group shows that a compound of one plant can influence absorption of a substance of another plant. The given examples indicate that this interaction is of great interest in the field of traditional Chinese medicine. Puerarin is an active compound of *Pueraria lobata* and is often prescribed as a drug pair with *Angelicae dahuricae* in traditional Chinese medicine. The combination of puerarin in

the extract with total coumarin and/or essential oil of *Angelicae dahuricae* increased absorption of puerarin which was probably due to decreased activity or expression of P-gp and/or MRP.⁷⁴ A similar effect of total coumarin and/or essential oil of *Angelicae dahuricae* was observed on the absorption of baicalin in *Radix scutellariae* extract. It was improved as an effect of opening tight junctions and inhibition of function and expression of MRP.⁷⁵ The absorption of formononetin and calycosin in the extract of *Astragalus membranaceus* var. *mongholicus* was described above to be improved by the extract of *Angelicae sinensis*. The combination of *Astragalus membranaceus* var. *mongholicus* extract with two compounds of *Angelicae sinensis* extract showed that ferulic acid increased absorption of formononetin and calycosin, and ligustilide decreased it. It was assumed that ferulic acid inhibited apical efflux transport and ligustilide induced it.⁶⁶ The transport of the saponins notoginsenoside R1, ginsenoside Rg1, and ginsenoside Re was increased in both directions by co-administering each of them with borneol. This effect was explained by loosening the tight junctions.⁷⁶ A reduced absorption of baicalein was observed in the presence of berberine. The apical-to-basal transport was reduced by berberine and decreased baicalein and baicalin (glucuronide of baicalein) concentrations were detected in the basal compartment which suggested inhibition of the uptake into the cell.⁷⁷

Table 2: Influence of plant ingredients on absorption of phytopharmaceutical compounds in the Caco-2 model.

One plant	Influenced compound	Influencing compound	Effects in Caco-2 model	year published
<i>Curcuma longa</i>	curcumin	α -tumerone ar-tumerone	apical efflux ↓ absorption ↑ (in combination and with α -tumerone)	2012 ⁶⁹
<i>Not mentioned</i>	hesperetin	9 flavonoids	apical efflux ↓ (of metabolites) metabolism ↓ total amount ↑	2010 ⁷⁰
<i>Plectranthus barbatus</i>	rosmarinic acid	luteolin apigenin	apical efflux/influx ↓ absorption ↑	2012 ⁶²
<i>Hypericum perforatum</i>	hypericin	7 phenolics	apical efflux ↓ absorption ↑	2006 ¹³ /2010 ⁷¹
Mixture of compounds				
<i>Scutellariae baicalensis</i>	baicalein wogonin oroxylin A		metabolism ↓ absorption ↑ (of every compound)	2012 ⁷²
<i>Aconitum species</i>	aconitine mesaconitine hypaconitine		apical efflux ↓ absorption ↑ (of every compound)	2012 ⁶⁰
<i>Hippophae rhamnoides</i> or <i>Gingko biloba</i>	quercetin isorhamentin (3'-O-methylquercetin)		apical efflux ↓ absorption ↑ (of both compounds)	2008 ⁷³
Two plants (plant 1 and plant 2)				
<i>Pueraria labota</i> and <i>Angelicae Dahurica</i>	puerarin (in extract)	coumarins essential oil	apical efflux ↓ absorption ↑ (in combination and with the single compounds)	2012 ⁷⁴
<i>Scutellariae baicalensis</i> and <i>Angelicae</i> <i>dahurica</i>	baicalin (in extract)	coumarins essential oil	apical efflux ↓ tight junctions ↓ absorption ↑ (in combination and with the single compounds)	2013 ⁷⁵
<i>Astragalus membranaceus</i> var. <i>mongholicus</i> and <i>Angelicae sinensis</i>	formononetin calycosin (in extract)	ligustilide ferulic acid	absorption ↓ (with ligustilide) absorption ↑ (with ferulic acid)	2012 ⁶⁶
<i>Panax notoginseng</i> and <i>Blumea martiniana</i>	notoginsenoside R1 ginsenoside Rg1 ginsenoside Re	borneol	tight junction ↓ absorption ↑	2013 ⁷⁶
<i>Scutellariae baicalensis</i> and <i>Coptis chinensis</i>	baicalein	berberine	absorption ↓	2009 ⁷⁷

↑: increasing effect, ↓: decreasing effect, = no effect

2.1.2.4 Advantages and difficulties in determining absorption of pharmaceuticals with the Caco-2 model

The above mentioned examples show that the extract has often an effect on absorption but it is very difficult to elucidate the mechanism and to determine the compounds which are responsible. There are mainly two reasons for this problem. Firstly, many compounds of the extract show a complex absorption behavior which is due to a complex transport mechanism by diffusion and carriers, metabolism, and being inhibitors and inductors of carriers and metabolizing enzymes. These properties bear a high potential of interaction with other compounds. The second problem is the extract itself. It is a mixture of many phytochemicals which are not all fully identified. Therefore, it is very difficult to discover the compounds which have an effect on absorption. Regularly single compounds, mixtures of substances like flavonoids, or ingredients such as essential oils are used to identify the compounds which affect absorption. Often these results give only a suggestion but do not fully explain the effect of the extract. Mostly the combination of all ingredients is proposed to elicit the effect of an extract. Additionally, it has to be noted that the phytochemical profile of one plant can differ, for example, between batches of this plant or different extraction techniques. Therefore it is not surprising that different extracts of one plant can have diverse effects on absorption as it was discussed above for *Hypericum perforatum*.

To predict intestinal absorption governed by several processes, a model which comprises these processes has to be used. Caco-2 cells fulfill this requirement by expressing similar metabolizing enzymes and carriers as the human intestine.⁷⁸⁻⁸⁰ However, it is difficult to distinguish between all those processes and how much they contribute to absorption with the Caco-2 model. Inhibitors, especially of transporters, can help to provide clarification, particularly in the elucidation of the absorption process of a single compound. It becomes more difficult in the presence of multi-component systems like the above mentioned extracts and mixtures of compounds or combinations of compounds especially if they show a complex absorption behavior. Often the underlying mechanisms are guessed or assumed due to multiple interaction possibilities and lack of knowledge of the composition of the extract. Nevertheless, the Caco-2 model reflects reality very well and is therefore one of the best in vitro model to detect and predict effects of extracts on absorption due to inter- and intra-herb interactions.

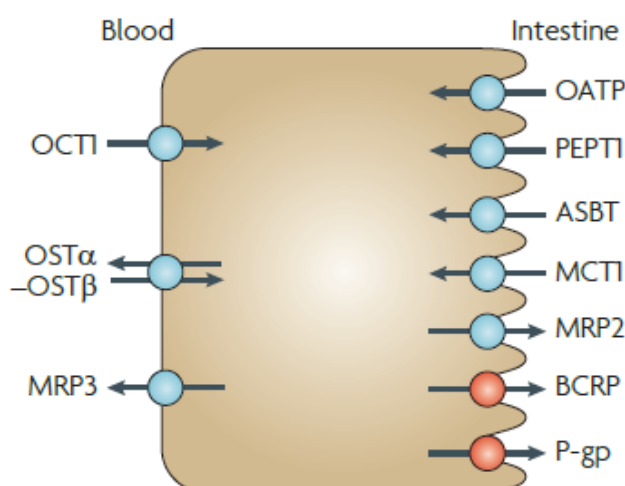
2.2 CARRIER MEDIATED TRANSPORT AND METABOLISM IN THE CACO-2 MODEL

2.2.1 Carrier mediated transport in the Caco-2 model

2.2.1.1 Human enterocytes vs. Caco-2 cells

Enterocytes

The enterocytes in the gastrointestinal tract express different efflux and influx transporter proteins which carry a drug in or out of the cells. They are asymmetrically located at the apical or basal membrane and divided into two superfamilies ATP-binding cassette (ABC) for efflux transporters and solute carrier (SLC) for influx transporters (Scheme 1). The transporters, which are considered as the clinically most important from the international consortium of transporters, are at the apical side P-gp (P-glycoprotein, MDR1, ABCB1), BCRP (breast cancer resistance protein, ABCG2), MRP2 (multidrug resistance protein 2, ABCC2) and at the basal side MRP3 (ABCC3). Influx transporters are at the apical membrane one or more members of the organic anion transporting polypeptide (OATP) family, PEPT1 (peptide transporter 1, SLC15A1), ASBT (ileal apical sodium/bile acid co-transporter, SLC10A2), and MCT1 (monocarboxylic acid transporter 1, SLC16A1) and at the basal membrane OCT1 (organic cation transporter 1, SLC22A1) and the heteromeric organic solute transporter (OST α -OST β).⁸¹ Interestingly, a recent study showed that OCT1 is localized at the apical membrane of Caco-2 cells and enterocytes and not at the basal membrane as assumed since 2001.⁸² This finding is important for the reason that different reviews and also the FDA guidance for the industry state that OCT1 is located at the basal membrane.⁸¹⁻⁸⁴



Scheme 1: Transporters of the intestinal epithelia are P-gp (P-glycoprotein, ABCB1), BCRP (breast cancer resistance protein, ABCG2), MRP2 (multidrug resistance protein, ABCC2), MRP3 (ABCC3), one or more members of the organic anion transporting polypeptide (OATP) family, PEPT1 (peptide transporter 1, SLC15A1), ASBT (ileal apical sodium/bile acid co-transporter, SLC10A2), MCT1 (monocarboxylic acid transporter 1, SLC16A1), OCT1 (organic cation transporter 1, SLC22A1), and the heteromeric organic solute transporter (OST α -OST β).⁸¹

These transporters show different but also overlapping substrate specificities. P-gp transports mainly hydrophobic molecules which are often cationic. BCRP is proposed to transport molecules with one amine bonded to one carbon of a heterocyclic ring, molecules with fused heterocyclic ring(s) and two substituents on a carbocyclic ring of the fused heterocyclic ring(s) such as protein kinase inhibitors, for example, imatinib or phytoestrogens like genistein, and phase II metabolites such as glucuronides, glutathione conjugates, and sulfates.^{81,85} MRPs were reported to transport hydrophilic compounds including phase II metabolites like glucuronides, glutathione conjugates, and sulfates.⁸⁵ OATPs show a wide substrate specificity of amphiphilic organic compounds such as glucuronides, bile acids, sulfates, and anionic peptides.⁸¹ PEPT1 transports small peptides and drugs with peptide like structures such as β -lactam antibiotics.⁸⁶ MCT transports monocarboxylates, for example, salicylic acid.^{87,88} ASBT is responsible for the uptake of bile acids and sterols and OST α -OST β for the efflux of them at the basal membrane.^{86,89} OCTs transport relatively hydrophilic cations with a low molecular mass like metformin.⁸¹

Caco-2 cells

Caco-2 cells show a similar expression pattern of transporters as the human intestinal cells.^{78,80,90-92}

Figure 1 illustrates that mainly the ABC transporters P-gp (MDR1), BCRP, MRP2, and MRP3 and the SLC transporters HPT1, PEPT1, MCT1, MCT5, OCTN2, IBAT (Ileal sodium/bile acid co-transporter, SLC10A2), and OATP2B1 (OATP-B) were expressed in Caco-2 cells. Compared to human jejunum the expression level especially of P-gp, MRP2, BCRP, and PEPT1 was lower and that of HPT1 (human peptide transporter 1, CDH17) and OATP2B1 increased.⁷⁸ In a study involving Caco-2 cells of 10 different laboratories it was shown that the important transporters represented in Scheme 1 were expressed in the following order: MRP2, OATP2B1, ASBT > P-gp, MRP3, BCRP, OST α , PEPT1, MCT1, > OST β , OCT. Furthermore, high levels of HPT1, GLUT3 (facilitated glucose transporter, SLC2A3), and GLUT5 (SLC2A5) were expressed.²⁸

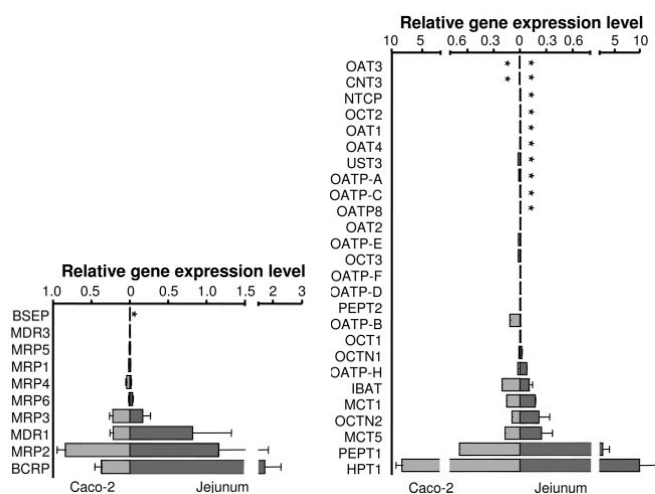
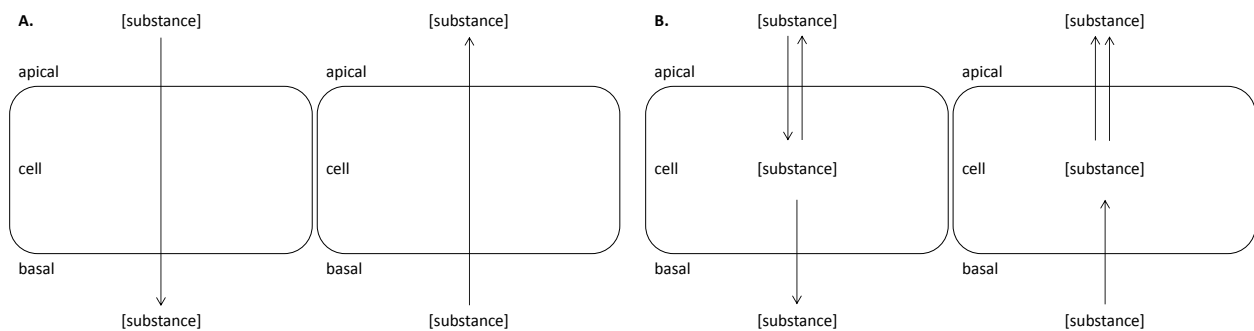


Figure 1: Relative transporter gene expression levels of ABC (left panel) and SLC (right panel) transporters in 16 day old Caco-2 cells (light grey bars), human tissues isolated from jejunum mucosa (dark grey bars). * absence of gene expression.⁷⁸

Transporter expression in Caco-2 cells depends on the culture time and passage number. An increase in P-gp, BCRP, MRP2, OATP2B1, and PEPT1 was observed during culture time which reached a plateau after 21 days post seeding.^{80,93} The effect of passage number was mainly investigated on nutrient transporters such as glucose transporter and only little is known about xenobiotic transporters. Cells which were treated with the P-gp inducer vinblastine showed that P-gp expression and function was reduced between passages 29 through 49.⁹⁴ Also BCRP was observed to be expressed in a lower level between passages 36 through 56.⁹⁵ Therefore, it was proposed to carry out transport experiments around 21 days post seeding with cells within 10 passage numbers.²⁶

2.2.1.2 Experimental approach to study carrier mediated transport

In vitro absorption studies with Caco-2 cells are carried out in transwell™ plates with polycarbonate membranes on which the cells grow. The substance of interest is either added to the apical or basal compartment corresponding to the transport direction from apical-to-basal (absorptive transport) or from basal-to-apical (secretory transport). The change of concentration in the compartments is observed as a function of time.⁹⁶



Scheme 2: A) Unidirectional single barrier model: Transport process is modeled as a unidirectional process from the apical to the basal or from the basal to the apical compartment across a single barrier (arrows indicate the transport direction). B) Compartment modeling: Transport process is modeled as a combination of different processes from the apical to the basal or from basal to the apical compartment whereas the monolayer is considered as a compartment (arrows indicate an example of different processes during both transport directions).⁹⁷

A common approach to analyze permeation data is the "unidirectional single barrier model" (Scheme 2).⁹⁷ The concentration of the drug is measured in the receiver compartment as a function of time and an apparent permeability coefficient P_{app} is calculated by the following equation which is based on the Fick's first law of diffusion.

$$P_{app} = \frac{J}{C_0} = \frac{dX/dt}{A \cdot C_0}$$

Equation 1

where, J is the flux, X is the measured mass, C_0 is the initial concentration, A is the surface area, and t is time. P_{app} values are typically calculated for both transport directions. The first indication of involved transporter proteins or metabolism might be indicated by a change of P_{app} values by using different initial concentrations. A common method to elucidate the contribution of transporters is by calculating the efflux ratio (ER).

$$ER = \frac{P_{app,BA}}{P_{app,AB}} \quad \text{Equation 2}$$

where, $P_{app,AB}$ is the permeability coefficient for the transport direction from apical-to-basal and $P_{app,BA}$ from basal-to-apical. A calculated ER of > 2 shows that a drug is substrate of an efflux transporter.^{26,96,97} To evaluate which transporters are involved and if a transport is increased or reduced in one direction inhibitors of specific transporters are used and the absorptive quotient (AQ) was proposed.

$$AQ = \frac{P_{PD,AB} - P_{app,AB}}{P_{PD,AB}} \quad \text{Equation 3}$$

where, $P_{PD,AB}$ is the permeability coefficient in presence of an inhibitor.⁹⁸ The AQ values reach from 0 through 1 which denotes no transport by efflux carriers up to complete transport by efflux transporters. A drug with AQ > 0.3 is suggested to be a substrate of an efflux transporter.⁹⁹

To elucidate different parallel processes, compartment modeling was introduced for analyzing permeation data of Caco-2 experiments several years ago which leads to a better mechanistic understanding of the absorption process (Scheme 2). Parameters of the different processes can be defined and values deduced which allow a quantitative evaluation of the involved mechanisms during absorption.⁹⁷ One of the first compartment model which was reported included passive diffusion and apical efflux by P-gp of digoxin and vinblastine across MDCK cell monolayer.¹⁰⁰ It considered three compartments and explained the data better than the "unidirectional single barrier model". Other models are similar or more complex including possible location and binding site, Michaelis-Menten type concentration-dependent function or distinguish between the binding, transport, and dissociation rate of the P-gp mediated carrier.¹⁰¹⁻¹⁰⁴ Furthermore, there are also models taking into account, for example, different transporters, metabolism, paracellular transport, intracellular compartments such as lysosomes, lipids, and mitochondria, adsorption to the plastic of the transwell™ plate, and different compositions of solutions in the apical and basal compartments.¹⁰⁵⁻¹¹⁴

2.2.1.3 Reported transport studies

Numerous substances were investigated in the Caco-2 model and found to be substrates of the important intestinal transporters shown in Scheme 1. Table 3 shows examples of elucidated transport processes. Most studies consider the well characterized P-gp. In recent years also other transporters were taken into account.

Table 3: Substrates of carrier mediated transport, investigated in the Caco-2 model.

Transporter	Substrate	Reference
P-gp	saquinavir, indinavir, nelfinavir, digoxin, verapamil, paclitaxel, talinolol, fexofenadine, atorvastatin, cyclosporin A, digoxin, doxorubicin, rhodamine 123, vinblastine, colchicine, grepofloxacin	58,98,111,115-118
BCRP	ochratoxin A, methotrexate, rosuvastatin, estrone-3-sulfate	95,119-121
MRP2	methotrexate, fexofenadine, grepofloxacin	95,116,118
MRP3	fexofenadine	116
OATPB	fexofenadine, estone-3-sulfate, salicylic acid	88,116,122
PEPT1	cephalexin, cefixime, levovirin produrgs, midodrine, amino acid ester produrgs of acyclovir and zidovudine	123-127
MCT1	atorvastatin, butyrate, salicylic acid	88,117,128
ASBT	taurocholic acid, ceftriaxone with an oral drug carrier derived from deoxycholic acid	121,129
OCT1	ranitidine, metformin, pentamidine	82,108,130
OST α -OST β	taurocholic acid, estrone-3-sulfate	121

2.2.2 Metabolism in the Caco-2 model

2.2.2.1 Human enterocytes vs. Caco-2 cells

Enterocytes

The human intestine plays an important role in the first-pass metabolism of a drug. Enterocytes comprise enzymes that mediate phase I and phase II reactions.¹³¹

Phase I

Phase I metabolizing enzymes catalyze redox reactions and hydrolysis.¹³²

Cytochrome P450 (CYP):

The most important metabolizing enzymes of phase I reactions are those of the cytochrome P450 (CYP) superfamily. They are haem proteins localized in the membrane of the endoplasmic reticulum and in the

inner membrane of mitochondria and catalyze mainly oxidation reactions of drugs. The subfamilies which are involved in drug metabolism are CYP1, CYP2, and CYP3. The CYP3A is the most abundant subfamily with 70-80% of total CYP content in the small intestine. Its major isoenzyme is CYP3A4 followed by CYP3A5. The second most abundant family is CYP2C with about 18% of the total CYP content in the intestine. Major isoenzymes are CYP2C9 and CYP2C19. Furthermore, the isoenzyme CYP2J2, CYP2D6, CYP1A1, and CYP2E1 are reported to be expressed in small amounts only and are thus not considered to play a significant role in the metabolism of drugs in the small intestine.¹³³

Other phase I metabolizing enzymes:

The intestine contains besides CYPs amine oxidases, xanthine oxidoreductase, peroxidases, dehydrogenases, reductases, and hydrolases such as carboxylesterases, β -glucuronidase, β -glucosidase, lactase phloridizin hydrolase (LPH).^{5,131,132,134-136}

One important hydrolase for drug metabolism especially for ester-containing drugs and prodrugs is the carboxylesterase (CES). CESs are localized in the endoplasmatic reticulum and catalyze ester cleavage using the co-reactant water. The CESs isozymes are classified into four groups CES1, CES2, CES3, and CES4 and several subgroups. The hCE-1 (CES1A1, HU1) is an isozyme of CES1 and hCE-2 (hiCE, HU3) one of CES2, which are the major groups of CES. hCE-2 is present in the small intestine whereas hCE-1 is expressed in low levels. Interestingly, hCE-1 can carry out also transesterification reactions beside hydrolysis of esters. Furthermore, they show different substrate specificities. hCE-1 prefers compounds with large acyl groups and small esterified alcohol groups whereas hCE-2 prefers small acyl groups and large alcohol groups.¹³⁴

Phase II

Phase II metabolizing enzymes conjugate parent drugs or their phase I metabolites with an endogenous substrate to form generally better water soluble compounds with an increased molecular weight.^{131,137}

The three major conjugation enzymes are UDP-glucuronosyltransferase, glutathione S-transferase, and sulfotransferases.

UDP-glucuronosyltransferase (UDP-glucuronyltransferase, UGT):

UDP-glucuronosyltransferase is beside glutathione S-transferase one of the most important conjugation enzyme which is indicated by its broad substrate specificity such as hydroxyl groups, amines, thiols, and enolic acids. It is a membrane bound enzyme localized in the smooth endoplasmatic reticulum and catalyzes glucuronidation which includes the transfer of glucuronic acid from the co-factor uridin-5'-diphospho- α -D-glucuronic acid (UDPGA) to the substrate. UDPGA is formed endogenously by oxidation of UDP- α -glucose and is present in (1 α)-conformation. Due to the reaction mechanism the products are β -glucuronides and depending on the site of glucuronidation termed as O-, N-, S-, and C-glucuronides.

Glucuronosyltransferases are low affinity enzymes compared to sulfotransferases which indicates that glucuronidation is slower at low substrate concentration than sulfonation.¹³⁷ Besides glucuronidation glucuronosyltransferases can also catalyze conjugation reactions with glucose and other hexoses.¹³⁷ There are four gene families UGT1, UGT2, UGT3, and UGT8 whereas UGT1 and UGT2 are involved in glucuronidation of drugs and showing numerous polymorphisms. UGT2 is further divided in two subfamilies UGT2A and UGT2B.^{138,139} Different UGT forms are expressed in the small intestine such as UGT1A1, 1A3, 1A4, 1A5, 1A6, 1A7, 1A8, 1A9, 1A10, 2B4, 2B7, 2B10, 2B11, 2B15, 2B17, and 2B28.¹³⁸⁻¹⁴⁰ The expression pattern of UGT in the small intestine is similar to that of the liver apart from the main difference that UGT1A7, 1A8, and 1A10 are absent in the liver.^{138,139}

Glutathione S-transferase (GST):

As mentioned above, glutathione S-transferase is beside UDP-glucuronosyltransferase one of the most important conjugation enzyme. It catalyzes the conjugation with the tripeptide glutathione (GSH) containing L-glutamic acid, L-cysteine, and glycine. There are two superfamilies of glutathione S-transferase the microsomal GST (MGST) which are homotrimers and the cytoplasmic GST (GST) which are mainly homodimers with a few heterodimers. The GST is the largest family and is divided into 8 classes: Alpha (GSTA), kappa (GSTK) (which is located in mitochondria and peroxisomes), mu (GSTM), omega (GSTO), pi (GSTP), sigma (GSTS), theta (GSTT), and zeta (GSTZ).¹³⁷ In the intestine mainly GSTA1, GSTA2, and GSTP1 are expressed and to a lower extent, also GSTM1 and GSTM3.^{141,142}

Sulfotransferase (SULT):

Sulfotransferase is a cytosolic enzyme which catalyzes sulfonation (commonly termed sulfatation) of a substrate with a sulfonate group ($-\text{SO}_3^-$) by the cofactor 3'-phosphoadenylyl sulfate (3'-phosphoadenosine 5'-phosphosulfate, PAPS) to sulfates (R-O-SO_3^-) or sulfamates ($\text{R-NR}'\text{-SO}_3^-$). Around 50 gene superfamilies of sulfotransferases are known whose products are classified into different families and subfamilies. The most important sulfotransferases in drug metabolism are the phenol sulfotransferases (SULT1), alcohol sulfotransferases (SULT2), and amine sulfotransferases (SULT3) that show also substrate overlaps.¹³⁷ The human intestine expresses the subfamilies SULT1B1 by 36% (thyroid hormone sulfotransferase), SULT1A3 by 31% (monoamine-sulfating phenol transferase), SULT1A1 by 19% (aryl sulfotransferase 1), SULT1E1 by 8% (estrogen sulfotransferase), and SULT2A1 by 6% (alcohol/hydrosteroid sulfotransferase) which are considered as the most important SULTs. SULT1A3 is not expressed and SULT1B1 is significantly lower expressed in the liver.¹⁴³⁻¹⁴⁵

Other phase II metabolizing enzymes:

In addition to the above mentioned enzymes methyltransferases and acetyltransferases (N- and O-acetyltransferases) are also found in the intestine.^{131,137}

Caco-2 cells

Caco-2 cells show a similar expression pattern of drug metabolizing enzymes as the intestinal cells with some exceptions.

Phase I

Cytochrome P450 (CYP):

Cytochrome P450 is poorly expressed in the Caco-2 model.^{28,79} A cross laboratory study showed that the major isoenzyme of the intestine CYP3A4 of the subfamily of CYP3A was not or only poorly expressed.²⁸ Also the isoenzyme CYP3A5 was only expressed in low levels.²⁸ CYP2C9 and CYP2C19 of the subfamily CYP2C showed low to moderate expression levels whereas CYP1A2 and CYP2D6 were not found.²⁸ Interestingly, the isoenzyme CYP2A6 was reported to be expressed at low level whereas it is absent or only faintly detected in the small intestine.^{28,133} Also the isoenzymes CYP1A1 and CYP2E1 were reported to be present in the Caco-2 cells.^{146,147}

The expression of CYP3A4 in the Caco-2 cells can be induced by vitamin D₃ (1 α ,25-dihydroxyvitamin D₃) or it can be expressed through transfection of the CYP3A4 gene which allows studies involving metabolism by this important intestinal enzyme.¹⁴⁸⁻¹⁵⁰

Other phase I metabolizing enzymes:

Caco-2 cells contain other enzymes such as different hydrolases, including carboxylesterases, β -glucuronidase, and lactase phloridizin hydrolase (LPH).^{50,151-154}

Interestingly, the cells express the hydrolases carboxylesterases hCE-1 and hCE-2 in significantly lower levels than the intestine. The hCE-1 is further higher expressed than hCE-2 which is exactly the opposite of the human intestine and similar to the expression pattern of the liver.^{134,155}

Phase II

UDP-glucuronosyltransferase (UGT):

UDP-glucuronosyltransferases activity in Caco-2 cells was found comparable to that in the intestine, particularly the colon.⁷⁹ The cells express UGT1A1, 1A3, 1A4, 1A5, 1A6, 1A7, 1A8, 1A9, 1A10, 2B4, 2B7, 2B10, 2B11, 2B15, 2B17, and 2B28, whereas the major UGTs are 1A6, 1A8, and 2B17.^{28,156-158}

Glutathione S-transferase (GST):

The activity of glutathione S-transferase is higher in the Caco-2 cells compared to the intestinal cells.⁷⁹ In differentiated Caco-2 cells mainly GSTPA1, A2, A3, A4 and GSTP1 and GSTO1 were detected in high levels whereas GSTM were not or marginally expressed.^{28,159,160}

Sulfotransferase (SULT):

The sulfotransferases which were found in the Caco-2 cells are SULT1A1, SULT1A2, SULT1A3, SULT1B1, SULT1C1, SULT1C2 and SULT2A1.^{28,161} The expression pattern is similar to that in the intestine, although, SULT1A1 and SULT1B1 were lower, SULT1C1 higher expressed, and SULT1E1 was absent in one report and found in another.^{161,162}

Other phase II metabolizing enzymes:

N-acetyltransferase activity for Caco-2 cells was reported to be in agreement with observations in the human small and large intestine.⁷⁹

It was discussed above that culture time and passage number influence expression of transporter proteins. This is also true for metabolizing enzymes. The UGTs expression in differentiated cells (21 days post seeding) was increased compared to undifferentiated cells.^{156,157,163} Interestingly, UGT1A6 was the only glucuronosyltransferase which was also found in high levels in undifferentiated cells.¹⁵⁶ Passage number affected UGT expression in differentiated cells and was increased at higher passages whereas the passage numbers varied between 43 and 130.^{156,164} Expression of glutathione S-transferase increased during culture time (between 14 and 32 days post seeding) especially of GSTAs whereas GSTO1 and GSTP1 remained the same.^{159,160} Also sulfotransferases were increasingly expressed during differentiation (20 days post seeding).¹⁶¹ No report describing the effect of passage number on GST and SULT expression could be found in the literature. As discussed above for carriers, these reported observations confirm that it is important to keep culture time and passage number constant for the experiment not only to assure a reproducible expression pattern of carriers but also of metabolizing enzymes.

2.2.2.2 Reported studies

Table 4 summarizes reported studies which were carried out with Caco-2 cells. They were either used as monolayer, for example, in a transport experiment or as cell homogenate, cell lysate, or microsomes made of Caco-2 cells to study the metabolism of a compound.

Table 4: Reported studies of metabolism in Caco-2 cells.

Enzymes	Substrate	Reference
Phase I		
CYP	sirolimus ^a , midazolam ^{a,b} , benzo[a]pyrene ^a , testosterone ^a , K77 ^a , felodipine ^{a,b} , carvedilol ^{a,b}	148-150,165-170
esterases	acetylsalicylic acid ^b , p-nitrophenol acetate ^b , temocapril ^{a,b} , carindacillin ^a , phenylmethyl sulfonylfluoride ^a , 2'-benzoyloxycinnamaldehyde ^a , praeruptorin A ^a , lovastatin ^a , enalapril ^a	49,79,171-174
Phase II		
UGT	1-naphthol ^{a,b} , raloxifene ^b , carvedilol ^a , scutellarein ^a , apigenin ^{a,b} , estradiol ^b , testosterone ^b , diclofenac ^b , indomethacin ^b , oxazepam ^b , propranolol ^b , zidovudine ^b , trifluoperazine ^b , propofol ^b , biochanin A ^a , formononetin ^a , emodin ^{a,b} , benzo[a]pyrene ^a	33,34,65,79,156,163,164,175-178
GST	curcumin ^a , benzo[a]pyrene ^a , 9-norbornyl-6-chloropurine ^a	179-181
SULT	1-naphthol ^a , apigenin ^{a,b} , benzo[a]pyrene ^a , 1-chloro-2,4-dinitrobenzene ^b , raloxifene ^{a,b}	33,46,79,165,175,178
acetyltransferase	sulfamethazine ^b	79

^a cell monolayer, ^b cell homogenate, lysate, microsomes of Caco-2 cells

2.2.3 Interplay between transporters and metabolizing enzymes

As mentioned above, the formed metabolites are often substrates of efflux transporter proteins.

Metabolites of verapamil are transported by P-gp, apigenin glucuronide and sulfates are substrates of MRPs and/or BCRP, and glutathione conjugates such as the endogenous leukotriene C4 are transported by MRPs.^{33,182-184} Interestingly, some cases of functional interplay between metabolizing enzymes and

transporter proteins were observed in recent years and can be divided into two different types

(Scheme 3).^{185,186} The first type can be termed parallel-metabolism interplay between transporter and

enzyme.¹⁸⁵ Transporter and enzyme have overlapping substrate specificity which was observed and

extensively discussed especially for P-gp and CYPs.^{185,187,188} This interplay results in a larger extent of

metabolism and a poor absorption of the substrate.^{185,186} Mechanistically the efflux transporter prevents

saturation of the metabolizing enzyme leading to a prolonged exposure to the enzyme by re-permeation

of the substrate into the cell. The second type of interplay can be termed concatenated interplay

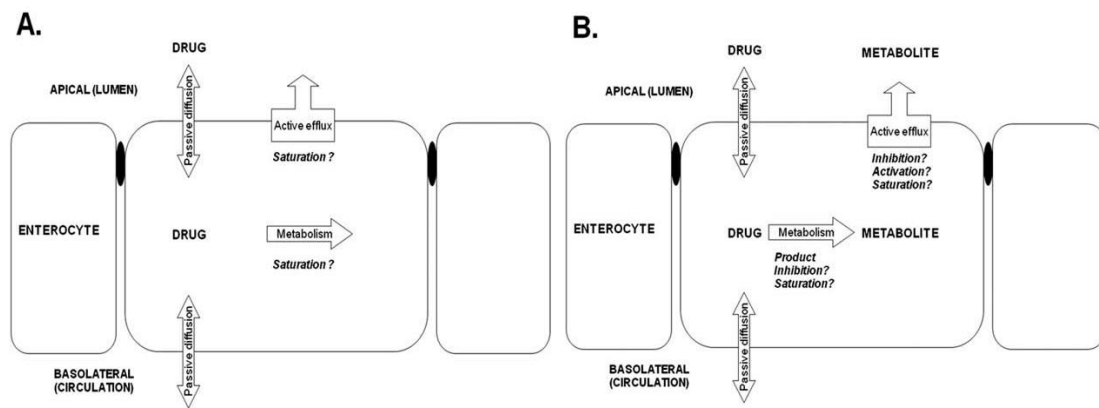
between transporter and enzyme.¹⁸⁵ In this interplay, the formed metabolite is substrate of the

transporter. The efflux transporter prevents the enzyme from substrate/product inhibition which also

results in a poor absorption of the substrate.^{185,186} These interplays show a new aspect in drug

absorption and might play an essential role whereas the impact of these interplays on in vivo intestinal

drug absorption and therefore on bioavailability is not known at the moment.^{185,186}



Scheme 3: A) Parallel interplay: The parent compound is substrate of both a metabolic enzyme and an efflux transporter. They both decrease the exposure to these proteins, which can prevent saturation. B) Concatenated interplay: Metabolite is an efflux transporter substrate and metabolism inhibitor. Efflux increases the contribution of metabolism by preventing the accumulation of the metabolite, thus reducing the product inhibition of metabolism.¹⁸⁵

The Caco-2 cells are a good model to study interplay between transporter and enzyme as they express both of them. For instance, metabolism of K77 and sirolimus, which are substrates of cytochrome P450 and P-gp, was decreased by inhibition of the efflux transporter in the Caco-2 model whereas the inhibition did not reduce metabolism of the non P-gp substrates midazolam and felodipine.^{166,167} Also, concatenated interplays between phase II metabolism and transporters was observed in Caco-2 cells such as for the glucuronidation of apigenin, raloxifene, emodin, biochanin A, formononetin, and sulfonation of apigenin, and raloxifene with MRPs.^{33,34,65,175,186}

2.3 ANTHEMIS NOBILIS L.

Synonym: *Anthemis chamomilla-romaona* CRANTZ, *Anthemis odorata* LAM., *Chamaemelum nobilie* (L.) All., *Chamaemelum odoratum* DOD., *Chamomilla nobilis* GOD., *Leucanthemum odoratum* EID. AP., *Lyonnetia abrotanifolia* WEBB., *Matricaria nobilis* BAILL., *Ormenis aurea* R. LOWE., *Ormenis nobilis* J. GAY.¹⁸⁹

Anthemis nobilis L. belongs to the family of Asteraceae. It is a low growing, of about 20 to 50 cm herb with 2-3 pinnately divided leaves. The wild form has similar flowers as *Chamomilla recutita* (L.) RAUSCHERT, however, the flowers are bigger. The cultivated double variety of *Chamaemelum nobile* (L.) All. (*Anthemis nobilis* (L.)), which is used in medicine, differs in its flowers which are up to 3 cm wide, consisting almost exclusively of white ligulate florets (Figure 2). It is cultivated in Belgium, France, England, Italy, Poland, Czech Republic, northern USA, and Argentina. It originates from southern and western Europe (England, Belgium, France, Germany, Italy, Spain) and northern Africa (Marocco, Algeria) and the Azores.^{189,190}



Figure 2: *Anthemis nobilis* L. (left picture) and dried flowers of *Anthemis nobilis* L. (*Chamomillae romanae flos*) (right picture).¹⁹⁰

2.3.1 Chamomillae romanae flos (PhEur 6)

The European pharmacopoeia describes *Chamomillae romanae flos* as "white or yellowish-grey, composed of solitary hemispherical capitula, made up of a solid conical receptacle bearing the florets, each subtended by a transparent small palea" (Figure 2). It has a "strong and characteristic odor" and should contain "minimum 7 ml/kg of essential oil (dried drug)".¹⁹¹

2.3.1.1 Chemical composition of *Chamomillae romanae flos*

The chemical composition of the flowers is summarized in Table 5. Normally *Chamomillae romanae flos* contains 0.6-2.5% *essential oil*. It is blue after distillation and becomes brown during storage.

Furthermore, it contains sesquiterpene lactones, organic peroxides, polyphenols, polyynes, terpenes, and steroids.¹⁸⁹

Table 5: Chemical composition of *Chamomillae romanae flos*.^{189,190}

Substances	Ingredients
essential oil	mainly esters of angelic acid, tiglic acid, methacryl- and isobutyric acid with aliphatic C ₃ -C ₆ alcohols like n-butanol, isobutanol, isoamylalcohol, and 3 methyl-pentan-1-ol terpenes such as α-pinen, β-pinen, α-caryophyllene β-caryophyllene, chamazulene, farnesene, bisabolene, cadinene, bisabolol
sesquiterpene lactones	sesquiterpene lactones of the germacranolide such as nobilin, 3-epinobilin, 1,10-epoxynobilin, 3-dehydronobilin
organic peroxides	1β-hydroperoxyisonobilin (germacranolide type sesquiterpene lactone), proazulene 4α-hydroperoxyromanolide (guaianolide type sesquiterpene lactone), allyl hydroperoxide
phenolics	flavonoides such as chamaemeloside and anthemside (acylglucoside derivatives of flavonoid-7-glucoside with 3-hydroxy-3-methylglutaric and 2,4-dihydroxycinnamic acid components, respectively), cosmosioside (apigenin-7-glucoside), luteolin-7-glucoside, and also aglycones, apiin (apigenin-7-apiosylglucoside), kaempferol, and several methylated flavonoid aglycones scopolin (scopoletin-7β-glucoside), scopoletin catechin glucose esters of caffeic acid
polyynes	<i>cis</i> -dehydro matricaria ester, <i>trans</i> -dehydro matricaria ester, two <i>cis-trans</i> -isomers of thiophen ester
terpenes and steroids	pentacyclic triterpenes β-amyrin and pseudo taraxasterol, β-sitosterol

2.3.1.2 Use of *Chamomillae romanae flos*

Chamomillae romanae flos is used in pharmacy as a herbal drug in tea mixtures especially as a decorative drug.¹⁸⁹ It is used in France, England, and Germany against menstrual disorders and as carminative.¹⁹⁰ Furthermore it is applied as aromatic bitter to stimulate appetite and digestion which was suggested to be attributed to sesquiterpenes.^{189,190} It can be also helpful against nervousness, hysteria and general weakness.¹⁸⁹ Externally, it is applied as wound and mouth rinse, or as a lotion for toothaches, headaches, and pains encountered during a flu.^{189,190}

A few pharmacological activities were found for *Chamomillae romanae flos*. The essential oil is active against gram-positive bacteria (*Enterococcus faecalis*, methicillin-resistant *Staphylococcus aureus*), gram-negative bacteria (*Escherichia coli*, *Pseudomonas aeruginosa*, *Porphyromonas gingivalis*), yeast (*Candida albicans*), and dermatophytes (*Trichophyton mentagrophytes*).^{189,192-195} Antimicrobial activities were also proposed for sesquiterpene lactones which are possibly also active against protozoa.¹⁸⁹ Furthermore, cytostatic effect of sesquiterpene lactones such as nobilin, 1,10-epoxynobilin, and 3-dehydronobilin on human HeLa (cervical carcinoma cells) and KB (nasopharynx carcinoma cells) were reported.¹⁹⁶⁻¹⁹⁹ Also an antiaggressive effect in aggressive mice, hypoglycemic activity which was attributed to the 3-hydroxy-3-methylglutaric acid containing flavonoids, an in vitro vasorelaxant effect of the aerial parts of *Anthemis nobilis* L., and preventive effects against sunburn and curative effects by regeneration of erythematous skin were observed.^{189,200-202}

The flowers are further used in the cosmetic industry such as to brighten of colored blond hair, as repellent against mosquitos and other insects, against weeds, plant pests, and plant pathogens, and as aroma in liqueur industry and cigarette industry.^{189,203-205}

2.3.2 Nobilin (CAS: 31824-11-0)²⁰⁶

Nobilin (C₂₀ H₂₆ O₅), a sesquiterpene lactone with M_r 346 and a calculated clogP of 2.572 (± 0.601)²⁰⁶ is a marker compound of the flowers of *Anthemis nobilis* L. as mentioned above. It was first isolated and mentioned 1964 and the chemical structure was revised 1970 and 1977.^{196,207,208} The absolute configuration of nobilin was elucidated 2013, in connection with this thesis, and the proposed configuration from 1977 was confirmed (Figure 3).

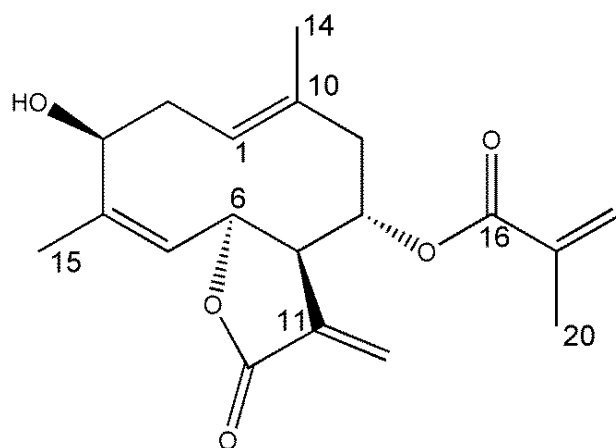


Figure 3: Chemical structure of nobilin with absolute configuration.¹⁹⁶

Only few studies were carried out with nobilin. Nobilin was reported 1977 to show cytostatic activity in HeLa and KB cells, as mentioned above.¹⁹⁶ Recently, it was shown that sesquiterpene lactones, also nobilin, inhibit the c-Myb-dependent gene expression. The c-Myb is a transcription factor that regulates

gene expressions which are involved in proliferation, cell survival, and differentiation. Deregulation of c-Myb expression results in tumors such as of leukemia, breast, and colon cancer.²⁰⁹ Another study reported that a mixture of six sesquiterpene lactones, one of them was nobilin, is a useful tool to diagnose Asteraceae allergic contact dermatitis.²¹⁰ Also the sensory property of nobilin was investigated by identifying nobilin as agonist of the bitter taste receptor hTAS2R46.²¹¹

2.4 REFERENCES

1. He SM, Li CG, Liu JP, Chan E, Duan W, Zhou SF 2010. Disposition pathways and pharmacokinetics of herbal medicines in humans. *Current Medicinal Chemistry* 17(33):4072-4113.
2. Mohanty C, Sahoo SK 2010. The in vitro stability and in vivo pharmacokinetics of curcumin prepared as an aqueous nanoparticulate formulation. *Biomaterials* 31(25):6597-6611.
3. Butterweck V, Peterleit F, Winterhoff H, Nahrstedt A 1998. Solubilized hypericin and pseudohypericin from *Hypericum perforatum* exert antidepressant activity in the forced swimming test. *Planta Medica* 64(4):291-294.
4. Metzler M, Pfeiffer E, Schulz SI, Dempe JS 2013. Curcumin uptake and metabolism. *Biofactors* 39(1):14-20.
5. D'Archivio M, Filesi C, Vari R, Scaccocchio B, Masella R 2010. Bioavailability of the polyphenols: Status and controversies. *International Journal of Molecular Sciences* 11(4):1321-1342.
6. Manach C, Williamson G, Morand C, Scalbert A, Remesy C 2005. Bioavailability and bioefficacy of polyphenols in humans. I. Review of 97 bioavailability studies. *American Journal of Clinical Nutrition* 81(1):230S-242S.
7. Wu BJ, Kulkarni K, Basu S, Zhang SX, Hu M 2011. First-pass metabolism via UDP-glucuronosyltransferase: A barrier to oral bioavailability of phenolics. *Journal of Pharmaceutical Sciences* 100(9):3655-3681.
8. Liu YT, Hao HP, Xie HG, Lai L, Wang QO, Liu CX, Wang GJ 2010. Extensive intestinal first-pass elimination and predominant hepatic distribution of berberine explain its low plasma levels in rats. *Drug Metabolism and Disposition* 38(10):1779-1784.
9. Nies AT, Herrmann E, Brom M, Keppler D 2008. Vectorial transport of the plant alkaloid berberine by double-transfected cells expressing the human organic cation transporter 1 (OCT1, SLC22A1) and the efflux pump MDR1 P-glycoprotein (ABCB1). *Naunyn-Schmiedeberg's Archives of Pharmacology* 376(6):449-461.
10. Pan GY, Wang GJ, Liu XD, Fawcett JP, Xie YY 2002. The involvement of P-glycoprotein in berberine absorption. *Pharmacology & Toxicology* 91(4):193-197.
11. Jiang W, Hu M 2012. Mutual interactions between flavonoids and enzymatic and transporter elements responsible for flavonoid disposition via phase II metabolic pathways. *Rsc Advances* 2(21):7948-7963.
12. Li Y, Paxton JW 2013. The effects of flavonoids on the ABC transporters: Consequences for the pharmacokinetics of substrate drugs. *Expert Opinion on Drug Metabolism & Toxicology* 9(3):267-285.
13. Sieger R, Nahrstedt A 2006. Effects of phenolic compounds from *Hypericum perforatum* L. on the solubility and permeation of hypericin in vitro. *Planta Medica* 72(11):1073-1073.

14. Butterweck V, Lieflander-Wulf U, Winterhoff H, Nahrstedt A 2003. Plasma levels of hypericin in presence of procyanidin B2 and hyperoside: A pharmacokinetic study in rats. *Planta Medica* 69(3):189-192.
15. Eder M, Mehnert W 2000. Plant excipients-valuable pharmaceutical aids or superfluous ballast? *Pharmazie in unserer Zeit* 29(6):377-384.
16. Bailey DG, Malcolm J, Arnold O, Spence JD 1998. Grapefruit juice-drug interactions. *British Journal of Clinical Pharmacology* 46(2):101-110.
17. Parker RB, Yates CR, Soberman JE, Laizure SC 2003. Effects of grapefruit juice on intestinal P-glycoprotein: Evaluation using digoxin in humans. *Pharmacotherapy* 23(8):979-987.
18. Schwarz UI, Seemann D, Oertel R, Miehlke S, Kuhlisch E, Fromm MF, Kim RB, Bailey DG, Kirch W 2005. Grapefruit juice ingestion significantly reduces talinolol bioavailability. *Clinical Pharmacology & Therapeutics* 77(4):291-301.
19. Madabushi R, Frank B, Drewelow B, Derendorf H, Butterweck V 2006. Hyperforin in St. John's wort drug interactions. *European Journal of Clinical Pharmacology* 62(3):225-233.
20. Unger M 2010. Pharmacokinetic drug interactions by herbal drugs: Critical evaluation and clinical relevance. *Wiener medizinische Wochenschrift (1946)* 160(21-22):571-577.
21. Rahimi R, Abdollahi M 2012. An update on the ability of St. John's wort to affect the metabolism of other drugs. *Expert Opinion on Drug Metabolism & Toxicology* 8(6):691-708.
22. Fugh-Berman A 2000. Herb-drug interactions. *Lancet* 355(9198):134-138.
23. Zhou SF, Lim LY, Chowbay B 2004. Herbal modulation of P-glycoprotein. *Drug Metabolism Reviews* 36(1):57-104.
24. Che CT, Wang ZJ, Chow MSS, Lam CWK 2013. Herb-herb combination for therapeutic enhancement and advancement: Theory, practice and future perspectives. *Molecules* 18(5):5125-5141.
25. Artursson P, Borchardt RT 1997. Intestinal drug absorption and metabolism in cell cultures: Caco-2 and beyond. *Pharmaceutical Research* 14(12):1655-1658.
26. Hubatsch I, Ragnarsson EGE, Artursson P 2007. Determination of drug permeability and prediction of drug absorption in Caco-2 monolayers. *Nature Protocols* 2(9):2111-2119.
27. Sugano K, Kansy M, Artursson P, Avdeef A, Bendels S, Di L, Ecker GF, Faller B, Fischer H, Gerebtzoff G, Lennernaes H, Senner F 2010. Coexistence of passive and carrier-mediated processes in drug transport. *Nature Reviews Drug Discovery* 9(8):597-614.
28. Hayeshi R, Hilgendorf C, Artursson P, Augustijns P, Brodin B, Dehertogh P, Fisher K, Fossati L, Hovenkamp E, Korjamo T, Masungi C, Maubon N, Mols R, Mullertz A, Monkkonen J, O'Driscoll C, Oppers-Tiëmissen HM, Ragnarsson EGE, Rooseboom M, Ungell AL 2008. Comparison of drug transporter gene expression and functionality in Caco-2 cells from 10 different laboratories. *European Journal of Pharmaceutical Sciences* 35(5):383-396.

29. Sumantran VN 2007. Experimental approaches for studying uptake and action of herbal medicines. *Phytotherapy Research* 21(3):210-214.
30. Tian XJ, Yang XW, Yang XD, Wang K 2009. Studies of intestinal permeability of 36 flavonoids using Caco-2 cell monolayer model. *International Journal of Pharmaceutics* 367(1-2):58-64.
31. Tourniaire F, Hassan M, Andre M, Ghiringhelli O, Alquier C, Amiot MJ 2005. Molecular mechanisms of the naringin low uptake by intestinal Caco-2 cells. *Molecular Nutrition & Food Research* 49(10):957-962.
32. Tian XJ, Yang XD, Wang K, Yang XW 2006. The efflux of flavonoids morin, isorhamnetin-3-O-rutinoside and diosmetin-7-O-beta-D-xylopyranosyl-(1-6)-beta-D-glucopyranoside in the human intestinal cell line Caco-2. *Pharmaceutical Research* 23(8):1721-1728.
33. Hu M, Chen J, Lin HM 2003. Metabolism of flavonoids via enteric recycling: Mechanistic studies of disposition of apigenin in the Caco-2 cell culture model. *Journal of Pharmacology and Experimental Therapeutics* 307(1):314-321.
34. Liu W, Feng Q, Li Y, Ye L, Hu M, Liu ZQ 2012. Coupling of UDP-glucuronosyltransferases and multidrug resistance-associated proteins is responsible for the intestinal disposition and poor bioavailability of emodin. *Toxicology and Applied Pharmacology* 265(3):316-324.
35. Schutte ME, Boersma MG, Verhallen DAM, Groten JP, Rietjens I 2008. Effects of flavonoid mixtures on the transport of 2-amino-1-methyl-6-phenylimidazo 4,5-b pyridine (PhIP) through Caco-2 monolayers: An in vitro and kinetic modeling approach to predict the combined effects on transporter inhibition. *Food and Chemical Toxicology* 46(2):557-566.
36. Schutte ME, van de Sandt JJM, Alink GM, Groten JP, Rietjens I 2006. Myricetin stimulates the absorption of the pro-carcinogen PhIP. *Cancer Letters* 231(1):36-42.
37. Schutte ME, Freidig AP, van de Sandt JJM, Alink GM, Rietjens I, Groten JP 2006. An in vitro and in silico study on the flavonoid-mediated modulation of the transport of 2-amino-1-methyl-6-phenylimidazo 4,5-b pyridine (PhIP) through Caco-2 monolayers. *Toxicology and Applied Pharmacology* 217(2):204-215.
38. Bothe H, Gotz C, Stobbe-Maicherski N, Fritsche E, Abel J, Haarmann-Stemmann T 2010. Luteolin enhances the bioavailability of benzo[a]pyrene in human colon carcinoma cells. *Archives of Biochemistry and Biophysics* 498(2):111-118.
39. Kamishikiryo J, Matsumura R, Takamori T, Sugihara N 2013. Effect of quercetin on the transport of N-acetyl 5-aminosalicylic acid. *Journal of Pharmacy and Pharmacology* 65(7):1037-1043.
40. Taur JS, Rodriguez-Proteau R 2008. Effects of dietary flavonoids on the transport of cimetidine via P-glycoprotein and cationic transporters in Caco-2 and LLC-PK1 cell models. *Xenobiotica* 38(12):1536-1550.

41. Shim CK, Cheon EP, Kang KW, Seo KS, Han HK 2007. Inhibition effect of flavonoids on monocarboxylate transporter 1 (MCT1) in Caco-2 cells. *Journal of Pharmacy and Pharmacology* 59(11):1515-1519.
42. Ebert B, Seidel A, Lampen A 2007. Phytochemicals induce breast cancer resistance protein in Caco-2 cells and enhance the transport of benzo[a]pyrene-3-sulfate. *Toxicological Sciences* 96(2):227-236.
43. Lies B, Martens S, Schmidt S, Boll M, Wenzel U 2012. Flavone potently stimulates an apical transporter for flavonoids in human intestinal Caco-2 cells. *Molecular Nutrition & Food Research* 56(11):1627-1635.
44. Lohner K, Schnabele K, Daniel H, Oesterle D, Rechkemmer G, Gottlicher M, Wenzel U 2007. Flavonoids alter P-gp expression in intestinal epithelial cells in vitro and in vivo. *Molecular Nutrition & Food Research* 51(3):293-300.
45. Bock KW, Eckle T, Ouzzine M, Fournel-Gigleux S 2000. Coordinate induction by antioxidants of UDP-glucuronosyltransferase UGT1A6 and the apical conjugate export pump MRP2 (multidrug resistance protein 2) in Caco-2 cells. *Biochemical Pharmacology* 59(5):467-470.
46. Isozaki T, Tamura H 2001. Epigallocatechin gallate (EGCG) inhibits the sulfation of 1-naphthol in a human colon carcinoma cell line, Caco-2. *Biological & Pharmaceutical Bulletin* 24(9):1076-1078.
47. Tamura H, Matsui M 2000. Inhibitory effects of green tea and grape juice on the phenol sulfotransferase activity of mouse intestines and human colon carcinoma cell line, Caco-2. *Biological & Pharmaceutical Bulletin* 23(6):695-699.
48. Pohl C, Will F, Dietrich H, Schrenk D 2006. Cytochrome p450 1A1 expression and activity in Caco-2 cells: Modulation by apple juice extract and certain apple polyphenols. *Journal of Agricultural and Food Chemistry* 54(26):10262-10268.
49. Li P, Callery PS, Gan LS, Balani SK 2007. Esterase inhibition by grapefruit juice flavonoids leading to a new drug interaction. *Drug Metabolism and Disposition* 35(7):1203-1208.
50. Petri N, Tannergren C, Holst B, Mellon FA, Bao YP, Plumb GW, Bacon J, O'Leary KA, Kroon PA, Knutson L, Forsell P, Eriksson T, Lennernas H, Williamson G 2003. Absorption/metabolism of sulforaphane and quercetin, and regulation of phase II enzymes, in human jejunum in vivo. *Drug Metabolism and Disposition* 31(6):805-813.
51. Ebert B, Seidel A, Lampen A 2005. Induction of phase-1 metabolizing enzymes by oltipraz, flavone and indole-3-carbinol enhance the formation and transport of benzo[a]pyrene sulfate conjugates in intestinal Caco-2 cells. *Toxicology Letters* 158(2):140-151.
52. Yoshida N, Koizumi M, Adachi I, Kawakami J 2006. Inhibition of P-glycoprotein-mediated transport by terpenoids contained in herbal medicines and natural products. *Food and Chemical Toxicology* 44(12):2033-2039.

53. Yang Z, Gao S, Wang JR, Yin TJ, Teng Y, Wu BJ, You M, Jiang ZH, Hu M 2011. Enhancement of oral bioavailability of 20(S)-ginsenoside Rh2 through improved understanding of its absorption and efflux mechanisms. *Drug Metabolism and Disposition* 39(10):1866-1872.
54. Zhang B, Zhu XM, Hu JN, Ye H, Luo T, Liu XR, Li HY, Li W, Zheng YN, Deng ZY 2012. Absorption mechanism of ginsenoside compound K and its butyl and octyl ester prodrugs in Caco-2 cells. *Journal of Agricultural and Food Chemistry* 60(41):10278-10284.
55. Eid SY, El-Readi MZ, Wink M 2012. Carotenoids reverse multidrug resistance in cancer cells by interfering with ABC-transporters. *Phytomedicine* 19(11):977-987.
56. Lu ZL, Chen WY, Viljoen A, Hamman JH 2010. Effect of sinomenine on the in vitro intestinal epithelial transport of selected compounds. *Phytotherapy Research* 24(2):211-218.
57. Ohnishi A, Matsuo H, Yamada S, Takanaga H, Morimoto S, Shoyama Y, Ohtani H, Sawada Y 2000. Effect of furanocoumarin derivatives in grapefruit juice on the uptake of vinblastine by Caco-2 cells and on the activity of cytochrome P450 3A4. *British Journal of Pharmacology* 130(6):1369-1377.
58. Jin J, Cai D, Bi H, Zhong G, Zeng H, Gu L, Huang Z, Huang M 2013. Comparative pharmacokinetics of paclitaxel after oral administration of *Taxus yunnanensis* extract and pure paclitaxel to rats. *Fitoterapia* 90:1-9.
59. Qiang ZY, Hauck C, McCoy JA, Widrlechner MP, Reddy MB, Murphy PA, Hendrich S 2013. Echinacea sanguinea and Echinacea pallida extracts stimulate glucuronidation and basolateral transfer of Bauer alkaloids 8 and 10 and ketone 24 and inhibit P-glycoprotein transporter in Caco-2 cells. *Planta Medica* 79(3-4):266-274.
60. Li N, Tsao R, Sui ZG, Ma JW, Liu ZQ, Liu ZY 2012. Intestinal transport of pure diester-type alkaloids from an aconite extract across the Caco-2 cell monolayer model. *Planta Medica* 78(7):692-697.
61. Qiang ZY, Ye Z, Hauck C, Murphy PA, McCoy JA, Widrlechner MP, Reddy MB, Hendrich S 2011. Permeability of rosmarinic acid in *Prunella vulgaris* and ursolic acid in *Salvia officinalis* extracts across Caco-2 cell monolayers. *Journal of Ethnopharmacology* 137(3):1107-1112.
62. Fale PL, Ascensao L, Serralheiro MLM 2013. Effect of luteolin and apigenin on rosmarinic acid bioavailability in Caco-2 cell monolayers. *Food & Function* 4(3):426-431.
63. Mukinda JT, Syce JA, Fisher D, Meyer M 2010. Effect of the plant matrix on the uptake of luteolin derivatives-containing *Artemisia afra* aqueous-extract in Caco-2 cells. *Journal of Ethnopharmacology* 130(3):439-449.
64. Kim JY, Kwon HJ, Jung JY, Kwon HY, Baek JG, Kim YS, Kwon O 2010. Comparison of absorption of 1-deoxynojirimycin from mulberry water extract in rats. *Journal of Agricultural and Food Chemistry* 58(11):6666-6671.

65. Jia XB, Chen J, Lin HM, Hu M 2004. Disposition of flavonoids via enteric recycling: Enzyme-transporter coupling affects metabolism of biochanin A and formononetin and excretion of their phase II conjugates. *Journal of Pharmacology and Experimental Therapeutics* 310(3):1103-1113.
66. Zheng KYZ, Choi RCY, Guo AJY, Bi CWC, Zhu KY, Du CYQ, Zhang ZX, Lau DTW, Dong TTX, Tsim KWK 2012. The membrane permeability of Astragali Radix-derived formononetin and calycosin is increased by Angelicae Sinensis Radix in Caco-2 cells: A synergistic action of an ancient herbal decoction Danggui Buxue Tang. *Journal of Pharmaceutical and Biomedical Analysis* 70:671-679.
67. Gao S, Jiang W, Yin TJ, Hu M 2010. Highly variable contents of phenolics in St. John's Wort products affect their transport in the human intestinal Caco-2 cell model: Pharmaceutical and biopharmaceutical rationale for product standardization. *Journal of Agricultural and Food Chemistry* 58(11):6650-6659.
68. Wang SWJ, Chen Y, Joseph T, Hu M 2008. Variable isoflavone content of red clover products affects intestinal disposition of biochanin A, formononetin, genistein, and daidzein. *Journal of Alternative and Complementary Medicine* 14(3):287-297.
69. Yue GGL, Cheng S-W, Yu H, Xu Z-S, Lee JKM, Hon P-M, Lee MYH, Kennelly EJ, Deng G, Yeung SK, Cassileth BR, Fung K-P, Leung P-C, Lau CBS 2012. The role of turmerones on curcumin transportation and P-glycoprotein activities in intestinal Caco-2 cells. *Journal of Medicinal Food* 15(3):242-252.
70. Brand W, Padilla B, van Bladeren PJ, Williamson G, Rietjens I 2010. The effect of co-administered flavonoids on the metabolism of hesperetin and the disposition of its metabolites in Caco-2 cell monolayers. *Molecular Nutrition & Food Research* 54(6):851-860.
71. Nahrstedt A, Butterweck V 2010. Lessons learned from herbal medicinal products: The example of St. John's Wort. *Journal of Natural Products* 73(5):1015-1021.
72. Li CR, Zhang L, Wo SK, Zhou LM, Lin G, Zuo Z 2012. Pharmacokinetic interactions among major bioactive components in Radix scutellariae via metabolic competition. *Biopharmaceutics & Drug Disposition* 33(9):487-500.
73. Lan K, He JL, Tian Y, Tan F, Jiang XH, Wang L, Ye LM 2008. Intra-herb pharmacokinetics interaction between quercetin and isorhamnetin. *Acta Pharmacologica Sinica* 29(11):1376-1382.
74. Liang XL, Zhao LJ, Liao ZG, Zhao GW, Zhang J, Chao YC, Yang M, Yin RL 2012. Transport properties of puerarin and effect of Radix angelicae dahuricae extract on the transport of puerarin in Caco-2 cell model. *Journal of Ethnopharmacology* 144(3):677-682.
75. Zhu ML, Liang XL, Zhao LJ, Liao ZG, Zhao GW, Cao YC, Zhang J, Luo Y 2013. Elucidation of the transport mechanism of baicalin and the influence of a Radix angelicae dahuricae extract on the absorption of baicalin in a Caco-2 cell monolayer model. *Journal of Ethnopharmacology* 150(2):553-559.

76. Wang S, Zang W, Zhao X, Feng W, Zhao M, He X, Liu Q, Zheng X 2013. Effects of borneol on pharmacokinetics and tissue distribution of notoginsenoside R1 and ginsenosides Rg1 and Re in *Panax notoginseng* in rabbits. *Journal of analytical methods in chemistry* 2013:706723.
77. Shi R, Zhou H, Liu ZM, Ma YM, Wang TM, Liu YY, Wang CH 2009. Influence of *Coptis chinensis* on pharmacokinetics of flavonoids after oral administration of *Radix scutellariae* in rats. *Biopharmaceutics & Drug Disposition* 30(7):398-410.
78. Hilgendorf C, Ahlin G, Seithel A, Artursson P, Ungell AL, Karlsson J 2007. Expression of thirty-six drug transporter genes in human intestine, liver, kidney, and organotypic cell lines. *Drug Metabolism and Disposition* 35(8):1333-1340.
79. Prueksaritanont T, Gorham LM, Hochman JH, Tran LO, Vyas KP 1996. Comparative studies of drug-metabolizing enzymes in dog, monkey, and human small intestines, and in Caco-2 cells. *Drug Metabolism and Disposition* 24(6):634-642.
80. Englund G, Rorsman F, Ronnblom A, Karlbom U, Lazorova L, Grasjo J, Kindmark A, Artursson P 2006. Regional levels of drug transporters along the human intestinal tract: Co-expression of ABC and SLC transporters and comparison with Caco-2 cells. *European Journal of Pharmaceutical Sciences* 29(3-4):269-277.
81. Giacomini KM, Huang SM, Tweedie DJ, Benet LZ, Brouwer KLR, Chu XY, Dahlin A, Evers R, Fischer V, Hillgren KM, Hoffmaster KA, Ishikawa T, Keppler D, Kim RB, Lee CA, Niemi M, Polli JW, Sugiyama Y, Swaan PW, Ware JA, Wright SH, Yee SW, Zamek-Gliszczynski MJ, Zhang L, International T 2010. Membrane transporters in drug development. *Nature Reviews Drug Discovery* 9(3):215-236.
82. Han T, Everett RS, Proctor WR, Ng CM, Costales CL, Brouwer KLR, Thakker DR 2013. Organic cation transporter 1 (OCT1/mOct1) is localized in the apical membrane of Caco-2 cell monolayers and enterocytes. *Molecular Pharmacology* 84(2):182-189.
83. FDA. 2012. Guidance for Industry: Drug interaction studies — study design, data analysis, implications for dosing, and labeling recommendations. Rockville, MD, USA: Food and Drug Administration. <http://www.fda.gov/downloads/Drugs/guidancecomplianceregulatoryinformation/guidances/ucm292362.pdf>.
84. Estudante M, Morais JG, Soveral G, Benet LZ 2013. Intestinal drug transporters: An overview. *Advanced Drug Delivery Reviews* 64(10):1340-1356.
85. Murakami T, Takano M 2008. Intestinal efflux transporters and drug absorption. *Expert Opinion on Drug Metabolism & Toxicology* 4(7):923-939.
86. Fricker G. 2009. Biological membranes and drug transporters. In Mannhold R, Kubinyi H, Folkers G, editors. *Transporters as drug carriers*, 1 ed., Weinheim: WILEY-VCH Verlag GmbH & Co. KGaA. p 215-262.

87. Neuhaus W, Noe C. 2009. Transport at the Blood-Brain Barrier. In Mannhold R, Kubinyi H, Folkers G, editors. *Transporters as drug carriers*, 1 ed., Weinheim: WILEY-VCH Verlag GmbH & Co. KGaA.
88. Koljonen M, Rousu K, Cierny J, Kaukonen AM, Hirvonen J 2008. Transport evaluation of salicylic acid and structurally related compounds across Caco-2 cell monolayers and artificial PAMPA membranes. *European Journal of Pharmaceutics and Biopharmaceutics* 70(2):531-538.
89. Dawson P. 2012. Bile formation and the enterohepatic circulation. In Johnson L, editor *Physiology of the gastrointestinal tract*, 5 ed., Amsterdam: Elsevier/Academic Press. p 1461-1484.
90. Taipalensuu J, Tornblom H, Lindberg G, Einarsson C, Sjoqvist F, Melhus H, Garberg P, Sjostrom B, Lundgren B, Artursson P 2001. Correlation of gene expression of ten drug efflux proteins of the ATP-binding cassette transporter family in normal human jejunum and in human intestinal epithelial Caco-2 cell monolayers. *Journal of Pharmacology and Experimental Therapeutics* 299(1):164-170.
91. Sun DX, Lennernas H, Welage LS, Barnett JL, Landowski CP, Foster D, Fleisher D, Lee KD, Amidon GL 2002. Comparison of human duodenum and Caco-2 gene expression profiles for 12,000 gene sequences tags and correlation with permeability of 26 drugs. *Pharmaceutical Research* 19(10):1400-1416.
92. Seithel A, Karlsson J, Hilgendorf C, Bjorquist A, Ungell AL 2006. Variability in mRNA expression of ABC- and SLC-transporters in human intestinal cells: Comparison between human segments and Caco-2 cells. *European Journal of Pharmaceutical Sciences* 28(4):291-299.
93. Behrens I, Kissel T 2003. Do cell culture conditions influence the carrier-mediated transport of peptides in Caco-2 cell monolayers? *European Journal of Pharmaceutical Sciences* 19(5):433-442.
94. Siissalo S, Laitinen L, Koljonen M, Vellonen KS, Kortejdrvi H, Urtti A, Hirvonen J, Kaukonen AM 2007. Effect of cell differentiation and passage number on the expression of efflux proteins in wild type and vinblastine-induced Caco-2 cell lines. *European Journal of Pharmaceutics and Biopharmaceutics* 67(2):548-554.
95. Xia CQ, Liu N, Yang D, Miwa G, Gan LS 2005. Expression, localization, and functional characteristics of breast cancer resistance protein in Caco-2 cells. *Drug Metabolism and Disposition* 33(5):637-643.
96. Proctor W, Ming X, Thakker R. 2010. In vitro techniques to study drug-drug interactions involving transport: Caco-2 model for study of p-glycoprotein and other transporters. In Pang K, Rodrigues A, Peter R, editors. *Enzyme- and transporter-based drug-drug interactions*, 1 ed., New York, Dordrecht, Heidelberg, London: Springer.
97. Heikkinen AT, Korjamo T, Monkkonen J 2010. Modelling of drug disposition kinetics in in vitro intestinal absorption cell models. *Basic & Clinical Pharmacology & Toxicology* 106(3):180-188.

98. Troutman MD, Thakker DR 2003. Novel experimental parameters to quantify the modulation of absorptive and secretory transport of compounds by P-glycoprotein in cell culture models of intestinal epithelium. *Pharmaceutical Research* 20(8):1210-1224.
99. Thiel-Demby VE, Tippin TK, Humphreys JE, Serabjit-Singh CJ, Polli JW 2004. In vitro absorption and secretory quotients: Practical criteria derived from a study of 331 compounds to assess for the impact of P-glycoprotein-mediated efflux on drug candidates. *Journal of Pharmaceutical Sciences* 93(10):2567-2572.
100. Ito S, Woodland C, Sarkadi B, Hockmann G, Walker SE, Koren G 1999. Modeling of P-glycoprotein-involved epithelial drug transport in MDCK cells. *American Journal of Physiology-Renal Physiology* 277(1):F84-F96.
101. Tran TT, Mittal A, Aldinger T, Polli JW, Ayrton A, Ellens H, Bentz J 2005. The elementary mass action rate constants of P-gp transport for a confluent monolayer of MDCKII-hMDR1 cells. *Biophysical Journal* 88(1):715-738.
102. Gonzalez-Alvarez I, Fernandez-Teruel C, Garrigues TM, Casabo VG, Ruiz-Garcia A, Bermejo M 2005. Kinetic modelling of passive transport and active efflux of a fluoroquinolone across Caco-2 cells using a compartmental approach in NONMEM. *Xenobiotica* 35(12):1067-1088.
103. Korjamo T, Kemilainen H, Heikkinen AT, Monkkonen J 2007. Decrease in intracellular concentration causes the shift in Km value of efflux pump substrates. *Drug Metabolism and Disposition* 35(9):1574-1579.
104. Kalvass JC, Pollack GM 2007. Kinetic considerations for the quantitative assessment of efflux activity and inhibition: Implications for understanding and predicting the effects of efflux inhibition. *Pharmaceutical Research* 24(2):265-276.
105. Sun HD, Pang KS 2008. Permeability, transport, and metabolism of solutes in Caco-2 cell monolayers: A theoretical study. *Drug Metabolism and Disposition* 36(1):102-123.
106. Tam D, Sun HD, Pang KS 2003. Influence of P-glycoprotein, transfer clearances, and drug binding on intestinal metabolism in Caco-2 cell monolayers or membrane preparations: A theoretical analysis. *Drug Metabolism and Disposition* 31(10):1214-1226.
107. Sun HD, Zhang L, Chow ECY, Lin G, Zuo Z, Pang KS 2008. A catenary model to study transport and conjugation of baicalein, a bioactive flavonoid, in the Caco-2 cell monolayer: Demonstration of substrate inhibition. *Journal of Pharmacology and Experimental Therapeutics* 326(1):117-126.
108. Bourdet DL, Pollack GM, Thakker DR 2006. Intestinal absorptive transport of the hydrophilic cation ranitidine: A kinetic modeling approach to elucidate the role of uptake and efflux transporters and paracellular vs. transcellular transport in Caco-2 cells. *Pharmaceutical Research* 23(6):1178-1187.

109. Heikkinen AT, Monkkonen J, Korjamo T 2009. Kinetics of cellular retention during Caco-2 permeation experiments: Role of lysosomal sequestration and impact on permeability estimates. *Journal of Pharmacology and Experimental Therapeutics* 328(3):882-892.
110. Zhang X, Shedden K, Rosania GR 2006. A cell-based molecular transport simulator for pharmacokinetic prediction and cheminformatic exploration. *Molecular pharmaceutics* 3(6):704-716.
111. Kapitza SB, Michel BR, van Hoogevest P, Leigh MLS, Imanidis G 2007. Absorption of poorly water soluble drugs subject to apical efflux using phospholipids as solubilizers in the Caco-2 cell model. *European Journal of Pharmaceutics and Biopharmaceutics* 66(1):146-158.
112. Markopoulos C, Thoenen F, Preisig D, Symillides M, Vertzoni M, Parrott N, Reppas C, Imanidis G 2013. Biorelevant media for transport experiments in the Caco-2 model to evaluate drug absorption in the fasted and fed state and their usefulness. *European Journal of Pharmaceutics and Biopharmaceutics* <http://dx.doi.org/10.1016/j.ejpb.2013.10.017>.
113. Vertzoni M, Markopoulos C, Symillides M, Goumas C, Imanidis G, Reppas C 2012. Luminal lipid phases after administration of a triglyceride solution of danazol in the fed state and their contribution to the flux of danazol across Caco-2 cell monolayers. *Molecular Pharmaceutics* 9(5):1189-1198.
114. Korzekwa K, Nagar S 2013. Compartmental models for apical efflux by P-glycoprotein: Part 2—A theoretical study on transporter kinetic parameters. *Pharmaceutical Research* DOI 10.1007/s11095-013-1163-8.
115. Kim RB, Fromm MF, Wandel C, Leake B, Wood AJJ, Roden DM, Wilkinson GR 1998. The drug transporter P-glycoprotein limits oral absorption and brain entry of HIV-1 protease inhibitors. *Journal of Clinical Investigation* 101(2):289-294.
116. Ming X, Knight BM, Thakker DR 2011. Vectorial transport of fexofenadine across Caco-2 cells: Involvement of apical uptake and basolateral efflux transporters. *Molecular Pharmaceutics* 8(5):1677-1686.
117. Wu XC, Whitfield LR, Stewart BH 2000. Atorvastatin transport in the Caco-2 cell model: Contributions of P-glycoprotein and the proton-monocarboxylic acid co-transporter. *Pharmaceutical Research* 17(2):209-215.
118. Lowes S, Simmons NL 2002. Multiple pathways for fluoroquinolone secretion by human intestinal epithelial (Caco-2) cells. *British Journal of Pharmacology* 135(5):1263-1275.
119. Schrickx J, Lektarau Y, Fink-Gremmels J 2006. Ochratoxin A secretion by ATP-dependent membrane transporters in Caco-2 cells. *Archives of Toxicology* 80(5):243-249.
120. Li JB, Wang Y, Zhang W, Huang YH, Hein K, Hidalgo IJ 2012. The role of a basolateral transporter in rosuvastatin transport and its interplay with apical breast cancer resistance protein in polarized cell monolayer systems. *Drug Metabolism and Disposition* 40(11):2102-2108.

121. Grandvuinet AS, Steffansen B 2011. Interactions between organic anions on multiple transporters in Caco-2 cells. *Journal of Pharmaceutical Sciences* 100(9):3817-3830.
122. Sai Y, Kaneko Y, Ito S, Mitsuoka K, Kato Y, Tamai I, Artursson P, Tsuji A 2006. Predominant contribution of organic anion transporting polypeptide OATP-B (OATP2B1) to apical uptake of estrone-3-sulfate by human intestinal Caco-2 cells. *Drug Metabolism and Disposition* 34(8):1423-1431.
123. Watanabe K, Jinriki T, Sato J 2004. Effects of progesterone and norethisterone on cephalixin uptake in the human intestinal cell line Caco-2. *Biological & Pharmaceutical Bulletin* 27(4):559-563.
124. Wenzel U, Kuntz S, Diestel S, Daniel H 2002. PEPT1-mediated cefixime uptake into human intestinal epithelial cells is increased by Ca²⁺ channel blockers. *Antimicrobial Agents and Chemotherapy* 46(5):1375-1380.
125. Li FJ, Hong L, Mau CI, Chan R, Hendricks T, Dvorak C, Yee C, Harris J, Alfredson T 2006. Transport of levovirin prodrugs in the human intestinal Caco-2 cell. *Journal of Pharmaceutical Sciences* 95(6):1318-1325.
126. Tsuda M, Terada T, Irie M, Katsura T, Niida A, Tomita K, Fujii N, Inui K 2006. Transport characteristics of a novel peptide transporter 1 substrate, antihypertensive drug midodrine, and its amino acid derivatives. *Journal of Pharmacology and Experimental Therapeutics* 318(1):455-460.
127. Han HK, Oh DM, Amidon GL 1998. Cellular uptake mechanism of amino acid ester prodrugs in Caco-2/hPEPT1 cells overexpressing a human peptide transporter. *Pharmaceutical Research* 15(9):1382-1386.
128. Hadjiagapiou C, Schmidt L, Dudeja PK, Layden TJ, Ramaswamy K 2000. Mechanism(s) of butyrate transport in Caco-2 cells: Role of monocarboxylate transporter 1. *American Journal of Physiology-Gastrointestinal and Liver Physiology* 279(4):G775-G780.
129. Jeon OC, Hwang SR, Al-Hilal TA, Park JW, Moon HT, Lee S, Park JH, Byun Y 2013. Oral delivery of ionic complex of ceftriaxone with bile acid derivative in non-human primates. *Pharmaceutical Research* 30(4):959-967.
130. Proctor WR, Bourdet DL, Thakker DR 2008. Mechanisms underlying saturable intestinal absorption of metformin. *Drug Metabolism and Disposition* 36(8):1650-1658.
131. Krishna DR, Klotz U 1994. Extrahepatic metabolism of drugs in humans. *Clinical Pharmacokinetics* 26(2):144-160.
132. Testa B, Krämer S. 2008. *The biochemistry of drug metabolism: Principles, redox reactions, hydrolyses.* 1 ed., Zürich, Weinheim: VHCA, WILEY-VCH.
133. Thelen K, Dressman JB 2009. Cytochrome P450-mediated metabolism in the human gut wall. *Journal of Pharmacy and Pharmacology* 61(5):541-558.
134. Imai T 2006. Human carboxylesterase isozymes: Catalytic properties and rational drug design. *Drug Metabolism and Pharmacokinetics* 21(3):173-185.

135. Chiang CP, Wu CW, Lee SP, Ho JL, Lee SL, Nieh S, Yin SJ 2012. Expression pattern, ethanol-metabolizing activities, and cellular localization of alcohol and aldehyde dehydrogenases in human small intestine. *Alcoholism-Clinical and Experimental Research* 36(12):2047-2058.
136. Kelner MJ, Bagnell RD, Montoya MA, Lanham KA 2000. Structural organization of the human gastrointestinal glutathione peroxidase (GPX2) promoter and 3'-nontranscribed region: Transcriptional response to exogenous redox agents. *Gene* 248(1-2):109-116.
137. Testa B, Krämer S. 2010. *The biochemistry of drug metabolism: Conjugations, consequences of metabolism, influencing factors*. 1 ed., Zürich, Weinheim: VHCA, WILEY-VCH.
138. Gregory PA, Lewinsky RH, Gardner-Stephen DA, Mackenzie PI 2004. Regulation of UDP glucuronosyltransferases in the gastrointestinal tract. *Toxicology and Applied Pharmacology* 199(3):354-363.
139. Rowland A, Miners JO, Mackenzie PI 2013. The UDP-glucuronosyltransferases: Their role in drug metabolism and detoxification. *International Journal of Biochemistry & Cell Biology* 45(6):1121-1132.
140. Kaminsky LS, Zhang QY 2003. The small intestine as a xenobiotic-metabolizing organ. *Drug Metabolism and Disposition* 31(12):1520-1525.
141. Coles BF, Chen GP, Kadlubar FF, Radomska-Pandya A 2002. Interindividual variation and organ-specific patterns of glutathione S-transferase alpha, mu, and pi expression in gastrointestinal tract mucosa of normal individuals. *Archives of Biochemistry and Biophysics* 403(2):270-276.
142. Pool-Zobel B, Veeriah S, Bohmer FD 2005. Modulation of xenobiotic metabolising enzymes by anticarcinogens - focus on glutathione S-transferases and their role as targets of dietary chemoprevention in colorectal carcinogenesis. *Mutation Research-Fundamental and Molecular Mechanisms of Mutagenesis* 591(1-2):74-92.
143. Riches Z, Stanley EL, Bloomer JC, Coughtrie MWH 2009. Quantitative evaluation of the expression and activity of five major sulfotransferases (SULTs) in human tissues: The SULT "Pie". *Drug Metabolism and Disposition* 37(11):2255-2261.
144. Teubner W, Meinel W, Florian S, Kretschmar M, Glatt H 2007. Identification and localization of soluble sulfotransferases in the human gastrointestinal tract. *Biochemical Journal* 404:207-215.
145. Chen GP, Zhang DQ, Jing N, Yin SH, Falany CN, Radomska-Pandya A 2003. Human gastrointestinal sulfotransferases: Identification and distribution. *Toxicology and Applied Pharmacology* 187(3):186-197.
146. Schreiber TD, Kohle C, Buckler F, Schmohl S, Braeuning A, Schmiechen A, Schwarz M, Munzel PA 2006. Regulation of CYP1A1 gene expression by the antioxidant tert-butylhydroquinone. *Drug Metabolism and Disposition* 34(7):1096-1101.

147. Lampen A, Bader A, Bestmann T, Winkler M, Witte L, Borlak JT 1998. Catalytic activities, protein- and mRNA-expression of cytochrome P450 isoenzymes in intestinal cell lines. *Xenobiotica* 28(5):429-441.
148. SchmedlinRen P, Thummel KE, Fisher JM, Paine MF, Lown KS, Watkins PB 1997. Expression of enzymatically active CYP3A4 by Caco-2 cells grown on extracellular matrix-coated permeable supports in the presence of 1 alpha,25-dihydroxyvitamin D-3. *Molecular Pharmacology* 51(5):741-754.
149. Engman HA, Lennernas H, Taipalensuu J, Otter C, Leidvik B, Artursson P 2001. CYP3A4, CYP3A5, and MDR1 in human small and large intestinal cell lines suitable for drug transport studies. *Journal of Pharmaceutical Sciences* 90(11):1736-1751.
150. Brimer C, Dalton JT, Zhu ZX, Schuetz J, Yasuda K, Vanin E, Relling MV, Lu Y, Schuetz EG 2000. Creation of polarized cells coexpressing CYP3A4, NADPH cytochrome P450 reductase and MDR1/P-glycoprotein. *Pharmaceutical Research* 17(7):803-810.
151. Shimoi K, Nakayama T. 2005. Glucuronidase deconjugation in inflammation. In Sies H, Parker L, editors. *Phase II conjugation enzymes and transport systems*, 1 ed., San Diego, New York, Berkeley, Boston, London, Sydney, Tokyo, Toronto: Academic Press. p 263-272.
152. Zhang Y, Wick DA, Haas AL, Seetharam B, Dahms NM 1995. Regulation of lysosomal and ubiquitin degradative pathways in differentiating human intestinal Caco-2 cells. *Biochimica Et Biophysica Acta-Molecular Cell Research* 1267(1):15-24.
153. Artursson P 1991. Cell - cultures as models for drug absorption across the intestinal - mucosa. *Critical Reviews in Therapeutic Drug Carrier Systems* 8(4):305-330.
154. Mizuma T, Fuseda N, Hayashi M 2005. Kinetic characterization of glycosidase activity from disaccharide conjugate to monosaccharide conjugate in Caco-2 cells. *Journal of Pharmacy and Pharmacology* 57(5):661-664.
155. Imai T, Imoto M, Sakamoto H, Hashimoto M 2005. Identification of esterases expressed in Caco-2 cells and effects of their hydrolyzing activity in predicting human intestinal absorption. *Drug Metabolism and Disposition* 33(8):1185-1190.
156. Siissalo S, Zhang HB, Stilgenbauer E, Kaukonen AM, Hirvonen J, Finel M 2008. The expression of most UDP-glucuronosyltransferases (UGTs) is increased significantly during Caco-2 cell differentiation, whereas UGT1A6 is highly expressed also in undifferentiated cells. *Drug Metabolism and Disposition* 36(11):2331-2336.
157. Sabolovic N, Magdalou J, Netter P, Abid A 2000. Nonsteroidal anti-inflammatory drugs and phenols glucuronidation in Caco-2 cells - Identification of the UDP-glucuronosyltransferases UGT1A6, 1A3 and 2B7. *Life Sciences* 67(2):185-196.
158. Jeong EJ, Liu Y, Lin HM, Hu M 2005. Species- and disposition model-dependent metabolism of raloxifene in gut and liver: Role of UGT1A10. *Drug Metabolism and Disposition* 33(6):785-794.

159. Scharmach E, Hessel S, Niemann B, Lampen A 2009. Glutathione S-transferase expression and isoenzyme composition during cell differentiation of Caco-2 cells. *Toxicology* 265(3):122-126.
160. Peters WHN, Roelofs HMJ 1989. Time-dependent activity and expression of glutathione S-transferases in the human-colon adenocarcinoma cell-line Caco-2. *Biochemical Journal* 264(2):613-616.
161. Meinel W, Ebert B, Glatt H, Lampen A 2008. Sulfotransferase forms expressed in human intestinal Caco-2 and TC7 cells at varying stages of differentiation and role in benzo[a]pyrene metabolism. *Drug Metabolism and Disposition* 36(2):276-283.
162. Tamura H, Taniguchi K, Hayashi E, Hiyoshi Y, Nagai F 2001. Expression profiling of sulfotransferases in human cell lines derived from extra-hepatic tissues. *Biological & Pharmaceutical Bulletin* 24(11):1258-1262.
163. Zhang HB, Tolonen A, Rousu T, Hirvonen J, Finel M 2011. Effects of cell differentiation and assay conditions on the UDP-glucuronosyltransferase activity in Caco-2 cells. *Drug Metabolism and Disposition* 39(3):456-464.
164. Mizuma T, Momota R, Haga M, Hayashi M 2004. Factors affecting glucuronidation activity in Caco-2 cells. *Drug metabolism and pharmacokinetics* 19(2):130-134.
165. Buesen R, Mock M, Seidel A, Jacob J, Lampen A 2002. Interaction between metabolism and transport of benzo[a]pyrene and its metabolites in enterocytes. *Toxicology and Applied Pharmacology* 183(3):168-178.
166. Cummins CL, Jacobsen W, Christians U, Benet LZ 2004. CYP3A4-transfected Caco-2 cells as a tool for understanding biochemical absorption barriers: Studies with sirolimus and midazolam. *Journal of Pharmacology and Experimental Therapeutics* 308(1):143-155.
167. Cummins CL, Jacobsen W, Benet LZ 2002. Unmasking the dynamic interplay between intestinal P-glycoprotein and CYP3A4. *Journal of Pharmacology and Experimental Therapeutics* 300(3):1036-1045.
168. Fisher JM, Wrighton SA, Watkins PB, Schmiedlin-Ren P, Calamia JC, Shen DD, Kunze KL, Thummel KE 1999. First-pass midazolam metabolism catalyzed by 1 alpha,25-dihydroxy vitamin D-3-modified Caco-2 cell monolayers. *Journal of Pharmacology and Experimental Therapeutics* 289(2):1134-1142.
169. Paine MF, Leung LY, Lim HK, Liao KC, Oganessian A, Zhang MY, Thummel KE, Watkins PB 2002. Identification of a novel route of extraction of sirolimus in human small intestine: Roles of metabolism and secretion. *Journal of Pharmacology and Experimental Therapeutics* 301(1):174-186.
170. Ishida K, Taguchi M, Akao T, Hashimoto Y 2009. Involvement of the CYP1A subfamily in stereoselective metabolism of carvedilol in beta-naphthoflavone-treated Caco-2 cells. *Biological & Pharmaceutical Bulletin* 32(3):513-516.
171. Li YH, Ito K, Tsuda Y, Kohda R, Yamada H, Itoh T 1999. Mechanism of intestinal absorption of an orally active beta-lactam prodrug: Uptake and transport of carindacillin in Caco-2 cells. *Journal of Pharmacology and Experimental Therapeutics* 290(3):958-964.

172. Tantishaiyakul V, Wiwattanawongsa K, Pinsuwan S, Kasiwong S, Phadoongsombut N, Kaewnopparat S, Kaewnopparat N, Rojanasakul Y 2002. Characterization of mefenamic acid-guaiacol ester: Stability and transport across Caco-2 cell monolayers. *Pharmaceutical Research* 19(7):1013-1018.
173. Lee K, Park SK, Kwon BM, Kim K, Yu HE, Ryu J, Oh SJ, Lee KS, Kang JS, Lee CW, Kwon MG, Kim HM 2009. Transport and metabolism of the antitumour drug candidate 2'-benzoyloxycinnamaldehyde in Caco-2 cells. *Xenobiotica* 39(12):881-888.
174. Jing WH, Song YL, Yan R, Bi HC, Li PT, Wang YT 2011. Transport and metabolism of (+/-)-praueruptorin A in Caco-2 cell monolayers. *Xenobiotica* 41(1):71-81.
175. Jeong EJ, Lin HM, Hu M 2004. Disposition mechanisms of raloxifene in the human intestinal Caco-2 model. *Journal of Pharmacology and Experimental Therapeutics* 310(1):376-385.
176. Ishida K, Honda M, Shimizu T, Taguchi M, Hashimoto Y 2007. Stereoselective metabolism of carvedilol by the beta-naphthoflavone-inducible enzyme in human intestinal epithelial Caco-2 cells. *Biological & Pharmaceutical Bulletin* 30(10):1930-1933.
177. Wang YZ, Ao HS, Qian ZM, Zheng Y 2011. Intestinal transport of scutellarein and scutellarin and first-pass metabolism by UDP-glucuronosyltransferase-mediated glucuronidation of scutellarein and hydrolysis of scutellarin. *Xenobiotica* 41(7):538-548.
178. Ebert B, Seidel A, Lampen A 2005. Identification of BCRP as transporter of benzo[a]pyrene conjugates metabolically formed in Caco-2 cells and its induction by Ah-receptor agonists. *Carcinogenesis* 26(10):1754-1763.
179. Usta M, Wortelboer HM, Vervoort J, Boersma MG, Rietjens I, van Bladeren PJ, Cnubben NHP 2007. Human glutathione S-transferase-mediated glutathione conjugation of curcumin and efflux of these conjugates in Caco-2 cells. *Chemical Research in Toxicology* 20(12):1895-1902.
180. Hessel S, John A, Seidel A, Lampen A 2013. Multidrug resistance-associated proteins are involved in the transport of the glutathione conjugates of the ultimate carcinogen of benzo[a]pyrene in human Caco-2 cells. *Archives of Toxicology* 87(2):269-280.
181. Plackova P, Rozumova N, Hrebabecky H, Sala M, Nencka R, Elbert T, Dvorakova A, Votruba I, Mertlikova-Kaiserova H 2013. 9-Norbornyl-6-chloropurine is a novel antileukemic compound interacting with cellular GSH. *Anticancer Research* 33(8):3163-3168.
182. Pauli-Magnus C, von Richter O, Burk O, Ziegler A, Mettang T, Eichelbaum M, Fromm MF 2000. Characterization of the major metabolites of verapamil as substrates and inhibitors of P-glycoprotein. *Journal of Pharmacology and Experimental Therapeutics* 293(2):376-382.
183. Zhou SF, Wang LL, Di YM, Xue CC, Duan W, Li CG, Li Y 2008. Substrates and inhibitors of human multidrug resistance associated proteins and the implications in drug development. *Current Medicinal Chemistry* 15(20):1981-2039.

184. Jiang W, Xu BB, Wu BJ, Yu R, Hu M 2012. UDP-glucuronosyltransferase (UGT) 1A9-overexpressing HeLa cells is an appropriate tool to delineate the kinetic interplay between breast cancer resistance protein (BCRP) and UGT and to rapidly identify the glucuronide substrates of BCRP. *Drug Metabolism and Disposition* 40(2):336-345.
185. Siissalo S, Heikkinen AT 2013. In vitro methods to study the interplay of drug metabolism and efflux in the intestine. *Current Drug Metabolism* 14(1):102-111.
186. Jeong EJ, Liu X, Jia XB, Chen J, Hu M 2005. Coupling of conjugating enzymes and efflux transporters: Impact on bioavailability and drug interactions. *Current Drug Metabolism* 6(5):455-468.
187. van Waterschoot RAB, Schinkel AH 2011. A critical analysis of the interplay between cytochrome P450 3A and P-glycoprotein: Recent insights from knockout and transgenic mice. *Pharmacological Reviews* 63(2):390-410.
188. Mudra DR, Desino KE, Desai PV 2011. In silico, in vitro and in situ models to assess interplay between CYP3A and P-gp. *Current Drug Metabolism* 12(8):750-773.
189. Otto I. 2007. *Chamaemelum nobilie* (L.) ALL. In Blaschek W, Ebel S, Hackenthal E, Holzgrabe U, Keller K, Reichling J, Schulz V, editors. *Hagers Enzyklopädie der Arzneistoffe und Drogen*, 6 ed., Stuttgart: Wissenschaftliche Verlagsgesellschaft mbh Stuttgart. p 298-308.
190. Willuhn G. 2004. *Chamomillae romanae flos*. In Wichtl M, editor *Herbal drugs and phytopharmaceuticals*, 3 ed., Stuttgart and Boca Raton, London, New York, Washington, D.C.: medpharm Scientific Publishers and CRC Press.
191. 2007. *Chamomillae romanae flos*. *European pharmacopoeia*, 6 ed., Strasbourg: Council of Europe. p 1487-1488.
192. Bail S, Buchbauer G, Jirovetz L, Denkova Z, Slavchev A, Stoyanova A, Schmidt E, Geissler M 2009. Antimicrobial activities of roman chamomile oil from France and its main compounds. *Journal of Essential Oil Research* 21(3):283-286.
193. Saderi H, Owlia P, Hosseini A, Semiyari H 2005. Antimicrobial effects of chamomile extract and essential oil on clinically isolated *Porphyromonas gingivalis* from periodontitis. *WOCMAP III: Traditional Medicine and Nutraceuticals* (680):145-146.
194. Chao S, Young G, Oberg C, Nakaoka K 2008. Inhibition of methicillin-resistant *Staphylococcus aureus* (MRSA) by essential oils. *Flavour and Fragrance Journal* 23(6):444-449.
195. Inouye S, Uchida K, Abe S 2006. Vapor activity of 72 essential oils against a Trichophyton mentagrophytes. *Journal of Infection and Chemotherapy* 12(4):210-216.
196. Holub M, Samek Z 1977. Terpenes. CLXX. Isolation and structure of 3-epinobilin, 1,10-epoxynobilin and 3-dehydronobilin - other sesquiterpenic lactones from flowers of *Anthemis nobilis* L. revision of structure of nobilin and eucannabinolide. *Collection of Czechoslovak Chemical Communications* 42(3):1053-1064.

197. Grabarczyk H, Drozd B, Hladon B, Wojciechowska J 1977. Sesquiterpene lactones. Part XV. New cytostatic active sesquiterpene lactone from herb of *Anthemis nobilis* L. *Polish Journal of Pharmacology and Pharmacy* 29(4):419-423.
198. Samek Z, M. H, Grabarczyk H, Herout V 1977. The structure of hydroxyisonobilin - a cytostatically active sesquiterpenic lactone form the leaves of *Anthemis nobilis* L. *Collection of Czechoslovak Chemical Communications* 42(3):1065-1067.
199. Fernandes MB, Scotti MT, Ferreira MJP, Emerenciano VP 2008. Use of self-organizing maps and molecular descriptors to predict the cytotoxic activity of sesquiterpene lactones. *European Journal of Medicinal Chemistry* 43(10):2197-2205.
200. König GM, Wright AD, Keller WJ, Judd RL, Bates S, Day C 1998. Hypoglycaemic activity of an HMG-containing flavonoid glucoside, chamaemeloside, from *Chamaemelum nobile*. *Planta Medica* 64(7):612-614.
201. Schrader A, Eckey H, Rohr E 1997. Die Prüfung der Wirksamkeit reizlindernder Stoffe an der menschlichen Haut am Beispiel verschiedener Kamillenextrakte. *SÖFW Journal* 123(1):3-11.
202. Zeggwagh NA, Michel JB, Eddouks M 2013. Vascular effects of aqueous extract of *Chamaemelum nobile*: In vitro pharmacological studies in rats. *Clinical and Experimental Hypertension* 35(3):200-206.
203. Feng W, Liu J, Xu S, Wei J, Yin G, Zhang H. 2012. *Chamaemelum nobile* extract for producing cigarette, is prepared by adding cleaned *Chamaemelum nobile* flowers with ethanol, digesting and filtering resultant product, collecting filtrate, adding ethanol and performing ethanol precipitation. A24B15/26 ed., China: YUNNAN TOBACCO SCI RES INST.
204. Gwinn KD, Green J, Hamilton S, Green JF. 2004. Bioactive herbage composition useful for controlling weeds, plant pests or plant pathogens, comprises herbage obtained from *Monarda*, *Chamaemelum*, *Matricaria* and/or *Chenopodium*. A01N65/00 ed.: UNIV TENNESSEE RES FOUNDATION [US], GWINN KIMBERLY D [US], GREEN JAMES E [US], HAMILTON SUSAN [US]. p 1-34.
205. Magro A, Carolino M, Bastos M, Mexia A 2006. Efficacy of plant extracts against stored products fungi. *Revista Iberoamericana de Micologia* 23(3):176-178.
206. Advanced Chemistry Development (ACD/Labs) Software V11.02 (© 1994-2012 ACD/Labs), <https://scifinder.cas.org>.
207. Benesova V, Herout V, Sorm F 1964. On terpenes. CLXX. Isolation and sturcture of nobilin sesquiterpenic lactone with 10-membered ring. *Collection of Czechoslovak Chemical Communications* 29(12):3096-3101.
208. Benesova V, Samek Z, Herout V, Sorm F 1970. Structure of nobilin. *Tetrahedron Letters* (57):5017-5020.

-
209. Schomburg C, Schuehly W, Da Costa FB, Klempnauer KH, Schmidt TJ 2013. Natural sesquiterpene lactones as inhibitors of Myb-dependent gene expression: Structure-activity relationships. *European Journal of Medicinal Chemistry* 63:313-320.
210. Jacob M, Brinkmann J, Schmidt TJ 2012. Sesquiterpene lactone mix as a diagnostic tool for Asteraceae allergic contact dermatitis: Chemical explanation for its poor performance and sesquiterpene lactone mix II as a proposed improvement. *Contact Dermatitis* 66(5):233-240.
211. Brockhoff A, Behrens M, Massarotti A, Appendino G, Meyerhof W 2007. Broad tuning of the human bitter taste receptor hTAS2R46 to various sesquiterpene lactones, clerodane and labdane diterpenoids, strychnine, and denatonium. *Journal of Agricultural and Food Chemistry* 55(15):6236-6243.

Chapter 3

Mechanism of chemical degradation and determination of solubility by kinetic modeling of the highly unstable sesquiterpene lactone nobiletin in different media

3.1 ABSTRACT

The objective of this work was firstly to investigate the chemical degradation of the sesquiterpene lactone nobiletin and determine its solubility under conditions of concurrent degradation; secondly, to study the effect of biorelevant media used in the in vitro measurement of intestinal absorption on degradation and solubility of nobiletin. Purely aqueous medium (aq-TM_{Caco}), fasted and fed state simulated intestinal fluid (FaSSIF-TM_{Caco} and FeSSIF-TM_{Caco}), and two liposomal formulations (Liposomes_{FaSSIF} and Liposomes_{FeSSIF}) with the same lipid concentration as FaSSIF-TM_{Caco} and FeSSIF-TM_{Caco} were used. Degradation products were identified by NMR and X-ray crystallography and the order of reaction kinetics was determined. Solubility was deduced with a mathematical model encompassing dissolution and degradation kinetics that took into account particle size distribution of the solid material. Degradation mechanism of nobiletin involved water catalyzed opening of the lactone ring and transannular cyclization resulting in five degradation products. Degradation followed first order kinetics in aq-TM_{Caco} and FaSSIF-TM_{Caco} and higher order kinetics in FeSSIF-TM_{Caco} and the two liposomal formulations, while degradation in the latter media was reduced. Solubility of purified nobiletin increased in the order: aq-TM_{Caco} < FaSSIF-TM_{Caco} < Liposomes_{FaSSIF} < FeSSIF-TM_{Caco} < Liposomes_{FeSSIF}. Improvement of stability and solubility of nobiletin was consistent with incorporation of the molecule into colloidal lipid particles. The developed kinetic model is proposed to be a useful tool for deducing solubility of a highly unstable compound with a wide particle size distribution.

Thormann U. et al. 2014. Mechanism of chemical degradation and determination of solubility by kinetic modeling of the highly unstable sesquiterpene lactone nobiletin in different media. Journal of Pharmaceutical Sciences, to be submitted

3.2 INTRODUCTION

Physicochemical properties such as stability and solubility play an important role in the absorption process of a drug. Therefore, these properties are integral part of drug profiling programs. Factors which potentially influence stability and solubility in the gastrointestinal tract are the aqueous environment, a pH range from 1 to 8 and ingredients such as bile salts, phospholipids, digestive enzymes, and lipolysis products.^{1,2} The biopharmaceutics classification system (BCS) classifies compounds with respect to intestinal absorption based on their intestinal permeability and their solubility³ whereas solubility of the largest dose strength in 250 mL or less of aqueous media over the pH range of 1 to 7.5 defines a highly soluble compound.⁴ Compounds which reportedly do not fulfill this requirement include danazol, mefenamic acid, ketoconazole, glyburide, troglitazone, atovaquone, sanfetrinem cilexetil, dantrolene, indinavir, saquinavir, sirolimus, albendazole, 9-nitrocamptothecin, and curcumin.⁵⁻²⁰ Additionally, chemical instability in the gastrointestinal tract has been reported to compromise absorption such as for curcumin or sirolimus.^{13,14} Furthermore, penicillins were shown to hydrolyze in aqueous solution. The half-life of penicillin G at pH 2, 35°C, and ionic strength of 0.5 is 7 min. It could be increased to 15-20 min with semisynthetic penicillins such as amoxicillin. Issues of poor stability of a compound are frequently accompanied by low solubility. All these penicillins, for instance, show pH dependent degradation and solubility with a maximum stability and lowest solubility at pH 6-7.^{21,22} Other examples of pH dependent stability and insufficient solubility are prodrugs of 9-β-D-arabinofuranosyladenine against herpes viruses, different HIV protease inhibitors such as 2',3'-dideoxypurine nucleosides, carbovir, or oxathiin carboxanilide.²³⁻²⁶

In recent years, further components of the gastrointestinal tract were considered in connection with studying food effect on absorption. The bioavailability of the poorly-water soluble drug danazol, for example, was found to be increased by food whereas its solubility was increased by micelles of bile salts, phospholipids, and lipolysis products.^{9,10,15,19} Food effect has become the subject of a guidance for the industry issued by the FDA.²⁷ Therefore, several attempts have been made to develop biorelevant media to simulate the conditions in the intestine in fasted and fed state.^{1,5,6,15,28,29} A quite good in vitro-in vivo correlation between in vivo bioavailability and in vitro dissolution was seen.^{6-8,15-17,28,30} Recently, biorelevant transport media for in vitro absorption studies with the Caco-2 cell model simulating intestinal fluid in the fasted and the fed state, FaSSIF-TM_{Caco} and FeSSIF-TM_{Caco}, respectively, were developed.¹¹ The influence of these media on solubility and stability is essential for their role in drug absorption.

Solubility is commonly determined experimentally by adding drug in excess to a medium and directly measuring drug concentration at equilibrium.³¹ This methodology has also been used in the literature for determining solubility of unstable compounds whereas sampling was performed typically at a

predefined time point.^{18,21,32-34} No method to determine solubility of an unstable compound taking into account chemical degradation has been reported to the best of the authors' knowledge.

Nobiletin, a sesquiterpene lactone of the germacranolide type which is a marker compound isolated from the flowers of *Anthemis nobilis* L. was used in this study.³⁵ No reports about the chemical stability or the solubility of this compound exist in the literature. The aim of the work was to study the mechanism and the kinetics of degradation of purified nobiletin and identify its degradation products and, further, to determine the solubility of nobiletin under conditions of concurrent rapid chemical degradation. To accomplish the latter goal, the use of a kinetic model is proposed. Moreover, the effect of media simulating the environment of the intestinal tract and of vehicles used in in vitro Caco-2 absorption studies on stability and solubility of purified nobiletin was investigated. The ultimate objective was to derive a basic understanding of the effect of the media on stability and solubility and its consequence for the bioavailability of nobiletin.

3.3 MATERIALS AND METHODS

3.3.1 Chemicals

D-glucose, L-glutamine, 4-(2-hydroxyethyl)piperazine-1-ethanesulfonic acid (HEPES), sodium chloride (NaCl), sodium hydroxide (NaOH), maleic acid, dimethyl sulfoxide (DMSO), Dulbecco's Modified Eagle's Medium (DMEM) base powder (without D-glucose, L-glutamine, phenol red, sodium pyruvate, and sodium bicarbonate),³⁶ and sodium oleate were purchased from SIGMA-Aldrich Chemie GmbH (Buchs, Switzerland). Lipoid E PC S and Lipoid S 100 were kindly provided by Lipoid GmbH (Ludwigshafen, Germany). Glycerol monooleate was purchased from Danisco (Copenhagen, Denmark). Sodium taurocholate was purchased from Prodotti Chimici e di Alimentari s. p. a. (Basaluzzo, Italy). Methanol (MeOH) and ethanol (EtOH) from J.T.Baker (Deventer, Nederland), sodium acetate and formic acid from SIGMA-Aldrich Chemie GmbH (Buchs, Switzerland) were of HPLC grade. Water was purified by reversed osmosis with the water purification system arium® 61215 from Sartorius (Goettingen, Germany). CD₃OD was purchased from Armar Chemicals (Döttingen, Switzerland).

3.3.2 Purified nobiletin

Purified nobiletin was kindly provided by Alpinia Laudanum Institute of Phytopharmaceutical Sciences AG (ALIPS) (Walenstadt, Switzerland). Nobiletin was purified from an ethanolic extract of *Chamomillae romanae flos* (Hänseler AG, Herisau, Switzerland). Fatty acids, phenols, and chlorophyll were precipitated with a 5% (w/v) lead(II)acetate solution, filtered over a Celite® 500 fine bed and ethanol was evaporated. The remaining water phase was extracted with dichloromethane, the organic phase

was dried with magnesium sulfate, filtered, and evaporated. The received precipitate was dissolved in ethanol, centrifuged (5810R, Eppendorf AG, Hamburg, Germany), and the supernatant was injected in a MPLC (Büchi equipped with a pump manager C-615, a pump module C-605, a variable wave length detector C-635, and a fraction collector C-660) operated under isocratic conditions (column: Büchi glass column C690 36 × 460 mm packed with silica Polygoprep 100-50 C18 (Macherey Nagel, Oensingen, Switzerland); mobile phase: methanol:water (60:40); flow rate: 40 mL/min; detection wave length: 218 nm). The nobilin-containing fractions were collected and combined, methanol was evaporated, water was lyophilized (Labconco, Freezone 2.5 liter, VWR, Switzerland), and purified nobilin was obtained as a yellowish white powder. Ethanol was purchased from Alcosuisse (Bern, Switzerland) and all other substances were obtained from SIGMA-Aldrich Chemie GmbH (Buchs, Switzerland). This method is based on the description of Fischer in *Methods of Plant Biochemistry*.³⁷

3.3.3 Isolation of chemical degradation products

For the isolation and structure elucidation of degradation products, the supplied purified nobilin underwent an additional purification step with a preparative HPLC-UV from Varian ProStar equipped with a 215 binary pump, a 410 autosampler, a variable wave length detector, a 701 fraction collector model, and a C-18 reversed phase column (Reprosil 100 C18, 7 µm, 250 mm × 20 mm ID, Dr. Maisch HPLC GmbH, Ammerbuch, Germany). The mobile phases were (A) water with 0.1% (v/v) formic acid and (B) MeOH with 0.1% (v/v) formic acid. The composition was varied in a gradient mode: 0 min 50:50 (A:B), 0-25 min linear change to 10:90 (A:B), 25-35 min 10:90 (A:B) with a flow rate of 25 mL/min and a runtime of 35 minutes. Nobilin and the degradation products were detected at 220 nm. The fractions were collected every 10 sec and the nobilin containing ones were pooled and lyophilized (Alpha 2-4 LD, Crist, Osterode am Harz, Germany). The obtained nobilin was dissolved in EtOH 1 mg/mL, added to water 0.05 mg/mL and stirred for 1 day at 37°C. A sample was taken and the advance of the degradation was checked by HPLC. The aqueous solution was lyophilized and a white powder was obtained. It was dissolved in MeOH:H₂O (70:30) and the five different degradation products were purified with preparative HPLC as described above.

3.3.4 Vehicles

3.3.4.1 Media

The three different TM_{Caco} (transport media) that are compatible with the Caco-2 cell line were described by Markopoulos et al.¹¹ The compositions are shown in Table 1 (purely aqueous medium [aq-TM_{Caco}], fasted state simulated intestinal fluid [FaSSIF-TM_{Caco}], and fed state simulated intestinal fluid

[FeSSIF-TM_{Caco}]). The media contained DMEM base powder, L-glutamine, and D-glucose to support the viability of the cells.

The DMEM base powder was dissolved in autoclaved water. It was supplemented with D-glucose, L-glutamine, NaCl (aq-TM_{Caco}), and HEPES (aq-TM_{Caco}) or maleic acid (FaSSIF-TM_{Caco} and FeSSIF-TM_{Caco}). After adjusting the pH with sodium hydroxide and sterile filtration (Supor-200, 0.2 µm pore size, Pall Corporation, Port Washington, NY, USA) under aseptic conditions FaSSIF-TM_{Caco} and FeSSIF-TM_{Caco} were supplemented with sodium taurocholate, lecithin, glycerol monooleate (only FeSSIF-TM_{Caco}), and sodium oleate (only FeSSIF-TM_{Caco}). Lecithin and glycerol monooleate were added to the media separately as dichloromethane solution and the organic solvent was evaporated with a rotary evaporator (RE 120, Büchi, Flawil, Switzerland) at 40°C and 100 mbar.

Table 1: Composition of the three transport media.

	aq-TM _{Caco}	FaSSIF-TM _{Caco}	FeSSIF-TM _{Caco}
DMEM base powder [g/L] ^a	8.3	8.3	8.3
D-glucose [mM]	25	25	25
L-glutamine [mM]	6	6	6
NaCl [mM]	34	-	-
HEPES [mM]	19.98	-	-
Maleic acid [mM]	-	19.12	55.02
NaOH	qs	qs	qs
Sodium taurocholate [mM]	-	3	6.8
Lecithin (Lipoid E PC S) [mM]	-	0.2	6.8
Glycerol monooleate [mM]	-	-	3.4
Sodium oleate [mM]	-	-	0.8
pH	7.4	6.5	5.8
Osmolality [mOsm/kg]	350	320	390

^a contains amino acids, vitamins, electrolytes, trace elements;³⁶ qs: sufficient

3.3.4.2 Liposomal formulations

Liposomes were prepared by the film method. Lipoid S 100 was dissolved in ethanol in a round bottomed flask and evaporated to dryness with a rotary evaporator at 40°C. The lipid film was suspended in tempered aq-TM_{Caco} (37°C) and extruded under nitrogen pressure of 8-9 bar through polycarbonate filters (Nucleopore track edge membrane filters, Whatman plc, Kent, UK) pore size 0.4 µm (3 times), 0.2 µm (5 times), and 0.1 µm (2 × 10 times).¹¹ The two liposomal formulations in

aq-TM_{Caco} had the same lipid concentrations as FaSSIF-TM_{Caco} (3.2 mM) and FeSSIF-TM_{Caco} (17.8 mM) and are termed Liposomes_{FaSSIF} and Liposomes_{FeSSIF}.

3.3.5 Particle size measurement

The particle size of the mixed micelles of FaSSIF-TM_{Caco} and FeSSIF-TM_{Caco} and the two liposomal formulations (Liposomes_{FaSSIF} and Liposomes_{FeSSIF}) were measured by dynamic light scattering using a Zetasizer (Nano ZS, Malvern Instruments, Worcestershire, UK). The solutions were equilibrated at least 30 min at 37°C before measurement. The particle size of the lyophilized purified nobilin was determined by laser diffractometry (Sympatec, Helios, Clausthal-Zellerfeld, Germany).

3.3.6 Structural elucidation of degradation products 1-5

The structures of the degradation products 1-5 were elucidated by means of LC-MS and extensive NMR studies. 1D and 2D NMR spectra were recorded on a Bruker AVANCE IIITM 500 MHz spectrometer operating at 500.13 (¹H) and 125.77 (¹³C) equipped with a 1 mm TXI microprobe. All the spectra were measured in CD₃OD with the residual solvent signal as internal reference. Standard pulse sequences from Topspin 3.0 software package were used.

3.3.7 Single crystal X-ray analysis of degradation product 1

Crystal data for degradation product 1: Formula C₂₀H₂₈O₆, M = 364.44, F(000) = 784, colorless needle, size 0.03 · 0.04 · 0.19 mm³, tetragonal, space group P 4₁, Z = 4, a = b = 10.2900(3) Å, c = 17.5267(8) Å, α = β = γ = 90°, V = 1855.80(11) Å³, D_{calc.} = 1.304 Mg · m⁻³. The crystal was measured on a Bruker Kappa Apex2 diffractometer at 123 K equipped with an Incoatec IμS with Cu-Anode (Cu K_α-radiation with λ = 1.54178 Å), Θ_{max} = 68.216°. Minimal/maximal transmission 0.97/0.98, μ = 0.785 mm⁻¹. The Apex2 suite (Bruker AXS Inc., Madison (2006)) was used for data collection and integration. From a total of 12,673 reflections, 3121 were independent (merging r = 0.039). From these, 2847 were considered as observed (I > 2.0σ(I)) and were used to refine 236 parameters. The structure was solved by charge flipping methods using the program Superflip.³⁸ Least-squares refinement against F was carried out on all non-hydrogen atoms using the program CRYSTALS.³⁹ R = 0.0352 (observed data), wR = 0.0369 (all data), GOF = 0.9815. Minimal/maximal residual electron density = -0.16/0.29 e Å⁻³. Sigma weights were used to complete the refinement. The Flack parameter was refined using weights derived from a leverage analysis as described by Parsons⁴⁰, and its value of 0.05(8) shows that the handedness of the current structural model is correct. Plots were produced using Mercury.⁴¹ Crystallographic data (excluding structure factors) for the structure in this paper have been deposited with the Cambridge Crystallographic Data Center, the deposition number is 981306. Copies of the data can be obtained, free

of charge, on application to the CCDC, 12 Union Road, Cambridge CB2 1EZ, UK [fax: +44-1223-336033 or e-mail: deposit@ccdc.cam.ac.uk].

3.3.8 Kinetics of chemical degradation

Purified nobilin was dissolved in DMSO at a concentration of 1 mg/mL and added either to purified water or to maleic acid / sodium maleate buffer (55.2 mM) with a pH from 4 to 7.5. The final nobilin concentration in purified water was 22.1 µg/mL and in maleate buffer around 50 µg/mL. DMSO solution of nobilin was added to all other vehicles except FeSSIF-TM_{CaCo} to a final concentration of about 3 µg/mL and additionally to aq-TM_{CaCo}, FaSSIF-TM_{CaCo}, and FeSSIF-TM_{CaCo} to a final concentration of around 50 µg/mL. The highest concentration of purified nobilin for stability studies was attained by adding an excess of solid nobilin to the vehicles, stirring at 37°C for 30 min, centrifuging at 37°C, and 16,100 g for 30 min (5415R, Eppendorf AG, Hamburg, Germany) and harvesting the supernatant. Degradation of nobilin was monitored in all preparations for 5-7 hours under magnetic stirring at 37°C.

The following relationship was used to describe the rate of decrease of nobilin concentration:

$$\frac{dC}{dt} = -k_d \cdot C^x \quad \text{Equation (1)}$$

where, C is concentrations, k_d is rate constant of degradation, x denotes the order of reaction kinetics and t is time.

The rate of nobilin degradation and the rate of formation of degradation products were described by the following system of differential equations:

$$\frac{dAN}{dt} = -k_d \cdot AN^x \quad \text{Equation (2)}$$

$$\frac{dA1}{dt} = k_1 \cdot AN^x \quad \text{Equation (3)}$$

$$\frac{dA2}{dt} = k_2 \cdot AN^x \quad \text{Equation (4)}$$

$$\frac{dA3}{dt} = k_3 \cdot AN^x \quad \text{Equation (5)}$$

$$\frac{dA4}{dt} = k_4 \cdot AN^x \quad \text{Equation (6)}$$

$$\frac{dA5}{dt} = k_5 \cdot AN^x \quad \text{Equation (7)}$$

$$\frac{dAr}{dt} = k_r \cdot AN^x \quad \text{Equation (8)}$$

where, AN is the area of the nobilin peak of the UV-chromatogram, A1 through A5 is peak area of degradation products 1 through 5, respectively, k_d is degradation rate constant of nobilin, k_1 through k_5 is rate constant of formation of degradation product 1 through 5, respectively, and x denotes the order of the reaction kinetics. Equation (8) was introduced to establish mass balance.

The rate constants fulfill Equation (9).

$$k_d = k_1 + k_2 + k_3 + k_4 + k_5 + k_r \quad \text{Equation (9)}$$

Equation (1) was employed to determine k_d of nobilin in purified water and aqueous maleate buffer by fitting to degradation data using $x = 1$. Equation (1) was further fitted simultaneously to degradation data of two or more starting nobilin concentrations in each vehicle to determine k_d and x . Equations (2) to (9) were fitted to data of nobilin and its degradation products at a single starting nobilin concentration to determine k_d and k_1 to k_5 . In this fitting, parameter x was kept constant at the value deduced by Equation (1). Estimation of parameter values was performed by least square regression analysis with the EASY-FIT® software.⁴²

3.3.9 Solubility study

An accurately weighted excess of purified nobilin was added to the vehicles and stirred at 37°C. The first sample was taken after 30 min, centrifuged at 37°C and 16,100 g for 30 min, diluted, and injected into the HPLC. The change in concentration of dissolved nobilin was monitored by repeating this procedure every 30 or 60 min for 7-7.5 hours.

3.3.10 Model for the estimation of solubility

To estimate solubility, a kinetic model was developed which included the dissolution rate and the degradation rate. The dissolution rate is typically expressed by:^{1,8,16,17,19}

$$\frac{dm}{dt} = \frac{D}{h} \cdot S \cdot (C_s - C) \quad \text{Equation (10)}$$

where, m is dissolved mass, D is diffusion coefficient, h is thickness of diffusion boundary layer, S is surface area, C is measured concentration in solution, C_s is solubility, and t is time.

The surface area is connected to the mass m_{solid} of a particulate solid consisting of equally sized spherical particles by:

$$S = \frac{6 \cdot m_{\text{solid}}}{\rho \cdot d} \quad \text{Equation (11)}$$

where, ρ is density, and d is particle diameter.

Therefore, dissolution rate can be expressed by inserting Equation (11) into Equation (10):

$$\frac{dm}{dt} = \frac{D}{h} \cdot \frac{\Gamma \cdot 6 \cdot (m_{\text{init}} - m)}{\rho \cdot d} \cdot (C_s - C) \quad \text{Equation (12)}$$

whereas, m_{init} is the initial mass of solid material and Γ is shape factor accounting for deviation from spherical shape.

For a solid material comprising a particle size distribution, the total dissolution rate is given by the sum of the contributions of the individual size fractions, i.e.,

$$\left(\frac{dm}{dt}\right)_{\text{total}} = \sum_{i=1}^n a \cdot \frac{m_{\text{init}}(i) - m(i)}{d(i)} \cdot (C_s - C) \quad \text{Equation (13)}$$

where, i denotes size fraction and all constant terms are collected in the coefficient a .

Taking into consideration that the dissolved nobilin is degraded, the rate of variation of measured concentration of intact compound in solution as a result of simultaneous dissolution and chemical degradation is given by:

$$\frac{dC}{dt} = \sum_{i=1}^n a \cdot \frac{m_{\text{init}}(i) - m(i) - m_{\text{degr}}(i)}{V \cdot d(i)} \cdot (C_s - C) - k_s \cdot C(i)^x \quad \text{Equation (14)}$$

where,

$$\frac{dm_{\text{degr}}(i)}{dt} = k_s \cdot V \cdot C(i)^x \quad \text{Equation (15)}$$

with m_{degr} being amount of degraded compound, $m(i) = C(i) \cdot V$, V is volume of the solution, and k_s is degradation rate constant. The initial mass of each size fraction was computed from the total weight of

the nobilin sample and the weight proportion of the fraction obtained from the particle size measurement; $n = 27$ fractions were used.

The system of Equations (14) and (15) was fitted to the measured concentration data with the EASY-FIT® software.⁴² The least square-based regression analysis provided an estimation of solubility. In this fitting, k_s was also treated as an adjustable parameter. The effect of sampling was neglected.

3.3.11 HPLC

Purified nobilin and the degradation products were analysed by a HPLC-UV-MS of Agilent series 1200 equipped with a degaser G1379B, a binary pump G1312A, an autosampler G1367B, a thermostat G1330B, a column oven G1316A (series 1100), a variable wave length detector G1314B, and a quadrupole LC/MS detector G6130A. A C-18 reversed phase column (Agilent Eclipse XBD-C18, 5 μm , 2 \times 125 mm) and mobile phases (A) water with 0.1% (v/v) formic acid and 0.05 mM sodium acetate and (B) methanol with 0.1% (v/v) formic acid and 0.05 mM sodium acetate were used. The composition was varied in a gradient mode: 0 min 50:50 (A:B), 0-18 min linear change to 10:90 (A:B), 18-22 min 10:90 (A:B), 22-23 min linear change to 50:50 (A:B), and 23-28 min 50:50 (A:B) with a flow rate of 0.25 mL/min, and a runtime of 28 minutes. The samples were cooled in the autosampler to 4°C and the column was heated to 40°C. The ions were generated by atmospheric pressure electrospray ionisation and MS detector was run in scan mode (m/z 100 - 1000) at positive polarity with capillary voltage 4000 V, fragmentor 160 V, drying gas flow 10 L/min, drying gas temperature 350°C, and nebuliser pressure 20 psig. Nobilin was detected at 218 nm in UV and at m/z 369 and 716 in MS corresponding to the sodium adduct of nobilin and the sodium adduct of the dimer of nobilin. The degradation products were analysed under the same conditions. The LOQ of nobilin for an injection volume of 100 μL was 0.02 $\mu\text{g}/\text{mL}$ in the UV. Linearity was fulfilled in UV for concentrations up to 100 $\mu\text{g}/\text{mL}$. Standard deviation of measured concentrations of the calibration curve in UV was at maximum 10%.

3.4 RESULTS

3.4.1 Stability study

Chromatograms of samples taken in the beginning and at the end of nobilin stability experiment in purified water (Figure 1) demonstrate that nobilin was degraded and five degradation products were formed. The measured m/z of the nobilin peak was 369.2 which corresponds to the adduct of nobilin with sodium. The ^1H and ^{13}C NMR data for degradation products 1-5 are listed in Table 2 and 3, respectively.

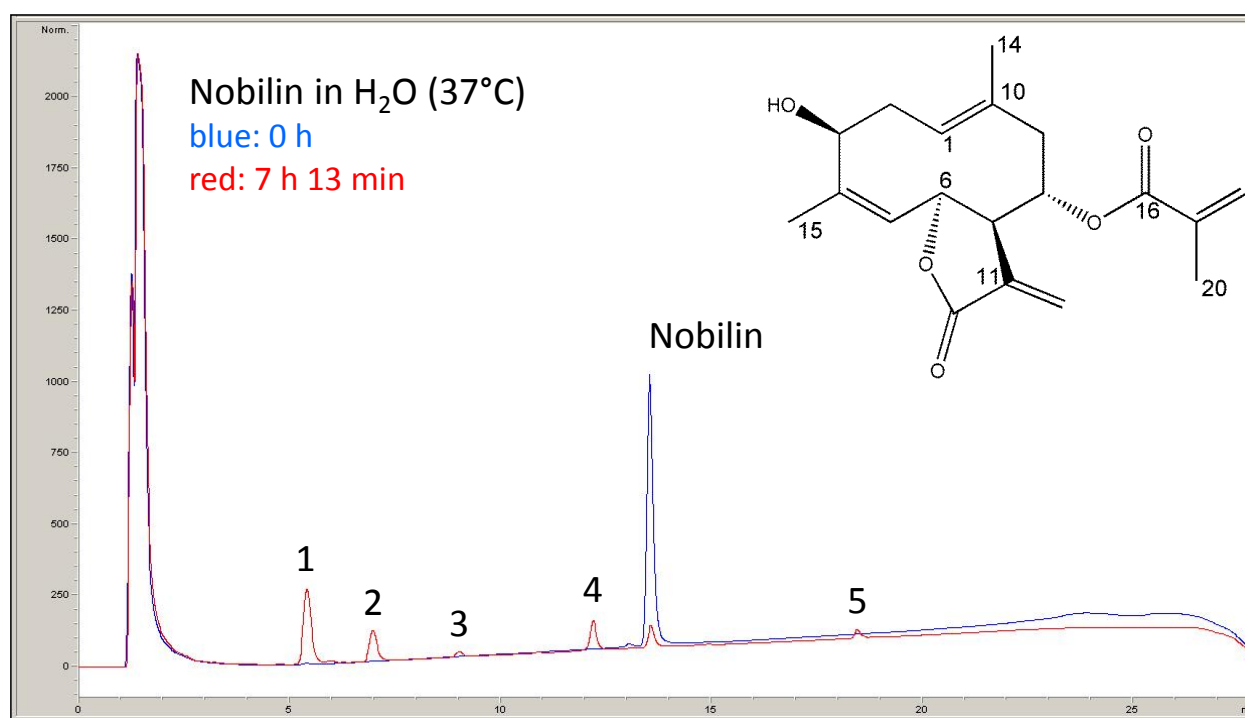


Figure 1: Chemical structure of nobilin and UV-chromatograms of nobilin and its degradation products at time zero and 7 h 13 min in purified water at 37°C.

3.4.1.1 Structure elucidation of degradation products 1, 2, and 3

Degradation products 1, 2, and 3 showed m/z of 387.2 $[\text{M}+\text{Na}]^+$ indicating the incorporation of a molecule of water in the structure of nobilin. Although, on the basis of the only MS data we could have only proposed that the hydrolysis of the lactone or the hydration of one double bond had occurred, a careful analysis of the NMR data of degradation products 1, 2, and 3 revealed that nobilin rearranged into different structures. The ^1H and ^{13}C spectroscopic data of degradation product 1, in comparison to the starting material, showed upfield resonances for H-1 ($\delta_{\text{H}} = 1.46$, $\delta_{\text{C}} = 50.0$ ppm in 1, $\delta_{\text{H}} = 5.37$, $\delta_{\text{C}} = 127.0$ ppm in nobilin) and CH_3 -14 ($\delta_{\text{H}} = 1.26$ ppm in 1, $\delta_{\text{H}} = 1.89$ ppm in nobilin) being the latter bounded to an oxygenated- sp^3 quaternary carbon C-10 ($\delta_{\text{C}} = 71.6$ ppm). Moreover, the methine at C-6 was significantly upfield shifted ($\delta_{\text{H}} = 2.40$, $\delta_{\text{C}} = 40.1$ ppm in 1, $\delta_{\text{H}} = 6.04$, $\delta_{\text{C}} = 79.5$ ppm in nobilin) thus

indicating that it was no more connected to the lactone moiety. The presence, in the COSY spectrum, of a strong correlation between methines H-1 and H-6, allowed us to conclude that C-1 and C-6 were connected through a single bond, thus leading to a decaline ring. The junction of the decaline system was deduced to be *trans* considering the coupling constants of H-1 who showed a dd, $J = 11.5$ and 11.5 Hz, indicative of diaxial interactions with H-2_{axial} and H-6. The absolute stereochemistry of the new cadinane structure was assigned by X-ray (Figure 2). A similar rearrangement was also revealed by the NMR data of compounds 2 and 3 that were diastereoisomers of 1. For compound 2 the *cis*-junction of the decaline system was established according to the value of the mutual coupling constant of the two angular methines $^3J_{H,H}$ H-1/H-6 ($J = 5.0$ Hz). The stereochemistry of the compound was then assigned on the basis of the NOESY correlations (H-8 β /H-6; H-1/H-6; H-1/CH₃-14) and it was consistent with that proposed previously for simpler cadinane-type structures.⁴³ Degradation product 3 is the 10-S epimer of 1, being the only remarkable difference between the NMR data of the 2 compounds the δ_c of CH₃-14 ($\delta_c = 21.6$ in 1, $\delta_c = 28.0$ in 3), thus suggesting its equatorial orientation in 3. This stereochemistry was corroborated by the diagnostic NOESY cross peak between H-2 α and CH₃-14.

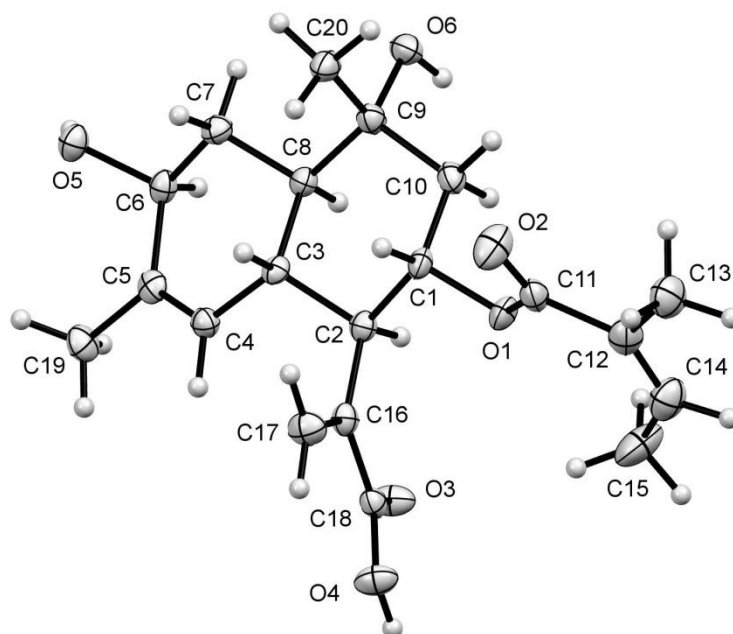


Figure 2: X-ray structure of degradation product 1.

3.4.1.2 Structure elucidation of degradation product 4

Degradation product 4 gave a m/z 369.2, i.e., the same as nobilin. Similarly to what was mentioned before, the lactone opening and the formation of the decaline moiety were deduced by the resonance of angular methine H-6 (br d, $J = 10.6$ Hz, $\delta_{\text{H}} = 3.14$, $\delta_{\text{C}} = 44.0$ ppm). 1D and 2D NMR data of 4 showed that the compound conserved the unsaturation at C1-C10 as in nobilin, although H-1 was replaced by a quaternary carbon ($\delta_{\text{C}} = 124.1$ ppm) due to the additional bond C-1/C-6. This structure assignment was corroborated by a $^3J_{\text{C,H}}$ HMBC correlation from H-2_{eq} ($\delta_{\text{H}} = 3.05$, $\delta_{\text{C}} = 37.3$ ppm) to C-6. The stereochemistry of C-6 was assigned to be β by the large value of $^3J_{\text{H,H}}$ H-6/H7 ($J = 10.6$ Hz) and was proved by the NOESY correlations H-8 β /H-6.

3.4.1.3 Structure elucidation of degradation product 5

Degradation product 5 showed a m/z value of 351.2 for the $[\text{M}+\text{Na}]^+$ that differed from that of nobilin by 18 mass units. The NMR spectra of 5 displayed two *ortho*-coupled aromatic protons at 7.17 ppm (d, $J = 8.0$ Hz) and 6.97 ppm (dd, $J = 8.0$ and 1.0 Hz) assigned to H-2 and H-3, respectively, by their HMBC correlations. Moreover, the ^1H spectrum of 5 lacked the resonances of H-1 and H-6, being C-1 and C-6 quaternary carbons ($\delta_{\text{C}} = 137.5$ ppm and $\delta_{\text{C}} = 138.7$ ppm respectively), thus corroborating the formation of the aromatic cadinanoate structure 5. The α -pseudo-equatorial orientation of CH₃-14 (d, 7.0 Hz, $\delta_{\text{H}} = 1.34$, $\delta_{\text{C}} = 22.3$ ppm) was deduced on the basis of $^3J_{\text{H,H}}$ H-9_{axial}/H-10 ($J = 10.3$ Hz) that suggested the pseudo-axial orientation of H-10.

Table 2: ¹H spectroscopic data (CD₃OD, 500.13 MHz) for degradation products 1-5.

Compound Position	1	2	3	4	5
1	1.46 dd, <i>J</i> = 11.5, 11.5 Hz	1.95 ddd, <i>J</i> = 12.9, 4.0, 5.0 Hz	1.35 dd, <i>J</i> = 11.0, 11.0 Hz	-	-
2_{axial}	1.26 ddd, <i>J</i> = 12.5, 11.5, 10.0 Hz	1.75 ^a m	1.45 ddd, <i>J</i> = 12.3, 11.0, 10.5 Hz	1.94 dd, <i>J</i> = 11.6, 11.6 Hz	7.17 d, <i>J</i> = 8.0 Hz
2_{equatorial}	2.38 ddd, <i>J</i> = 12.4, 6.0, 1.7 Hz	1.75 ^a m	2.23 ddd, <i>J</i> = 12.0, 6.0, 1.4 Hz	3.05 dd, <i>J</i> = 12.6, 5.5 Hz	-
3	4.12 t, <i>J</i> = 8.0 Hz	3.96 br s	4.14 t, <i>J</i> = 8.0 Hz	4.00 m, <i>W</i> _{1/2} = 9.0 Hz	6.97 dd, <i>J</i> = 8.0, 1.0 Hz
5	5.22 ^a br s	5.43 d, <i>J</i> = 2.5 Hz	5.22 br s	5.25 br s	6.82 br s
6	2.40-2.50 ^a m	2.70-2.87 ^a m	2.50-2.70 ^a m	3.14 br d, <i>J</i> = 10.6 Hz	-
7	2.40-2.50 ^a m	2.70-2.87 ^a m	2.50-2.70 ^a m	2.63 dd, <i>J</i> = 11.3, 10.5 Hz	4.02 d, <i>J</i> = 8.6 Hz
8	5.22 ^a m	5.36 ^a m	5.35 m	5.22 ddd, <i>J</i> = 11.2, 9.8, 5.7 Hz	5.53 ddd, <i>J</i> = 10.0, 8.6, 3.6 Hz
9_{axial}	1.57 dd, <i>J</i> = 11.5, 10.5 Hz	1.52 dd, <i>J</i> = 12.0, 11.3 Hz	1.57 dd, <i>J</i> = 12.6, 11.5 Hz	2.11 dd, <i>J</i> = 16.0, 9.8 Hz	1.61 ddd, <i>J</i> = 12.3, 10.3, 10.3 Hz
9_{equatorial}	2.17 dd, <i>J</i> = 11.8, 4.5 Hz	2.00 dd, <i>J</i> = 12.0, 4.0 Hz	2.14 dd, <i>J</i> = 12.8, 5.0 Hz	2.47 dd, <i>J</i> = 16.6, 5.7 Hz	2.26 ddd, <i>J</i> = 12.5, 5.5, 3.6 Hz
10	-	-	-	-	3.08 m, <i>W</i> _{1/2} = 18 Hz
13a	5.66 br s	5.78 br s	5.70 br s	5.71 br s	5.52 d, <i>J</i> = 1.3 Hz
13b	6.34 br s	6.34 br s	6.36 br s	6.38 br s	6.31 d, <i>J</i> = 1.3 Hz
14	1.26 s	1.26 s	1.27 s	1.72 s	1.34 d, <i>J</i> = 7.0 Hz
15	1.70 s	1.73 s	1.68 s	1.70 s	2.21 br s
18	6.00 qq, <i>J</i> = 7.3, 1.3 Hz	5.97 br q, <i>J</i> = 7.3 Hz	5.99 qq, <i>J</i> = 7.3, 1.3 Hz	6.02 qq, <i>J</i> = 7.3, 1.3 Hz	6.05 qq, <i>J</i> = 7.3, 1.3 Hz
19	1.88 dq, <i>J</i> = 7.3, 1.3 Hz	1.85 dq, <i>J</i> = 7.3, 1.3 Hz	1.86 dq, <i>J</i> = 7.3, 1.3 Hz	1.88 dq, <i>J</i> = 7.3, 1.3 Hz	1.90 dq, <i>J</i> = 7.3, 1.3 Hz
20	1.78 quint, <i>J</i> = 1.3 Hz	1.75 quint, <i>J</i> = 1.3 Hz	1.77 quint, <i>J</i> = 1.3 Hz	1.77 quint, <i>J</i> = 1.3 Hz	1.77 quint, <i>J</i> = 1.3 Hz

s, singlet; d, doublet; t, triplet; quint, quintet; m, multiplet; dd, doublet of doublets; ddd, doublet of doublets of doublets; qq, quartet of quartet; dq, doublet of quartet; br, broad.

^a Overlapped signals

Table 3: ^{13}C spectroscopic data (CD_3OD , hsqc/hmbc, 500.13 MHz) for degradation products 1-5.

Compound Position	1	2	3	4	5
1	50.0	40.4	48.9	124.1	137.5
2	33.50	31.0	33.6	37.3	127.5
3	68.7	68.7	72.0	71.2	128.2
4	139.4	136.5	138.6	138.9	136.6
5	126.2	128.1	126.8	126.2	129.5
6	40.1	37.0	39.7	44.0	138.7
7	51.6	45.1	49.5	49.3	51.2
8	71.9	74.8	73.6	73.9	74.2
9	48.1	40.9	46.7	39.1	37.9
10	71.6	74.2	72.3	129.3	32.5
11	140.0	140.3	140.1	141.8	144.2
12	169.9	170.2	170.3	170.3	170.5
13	129.2	127.5	126.8	126.1	129.0
14	21.6	28.9	28.0	19.2	22.3
15	19.6	20.7	19.5	18.3	21.0
16	168.6	169.4	168.6	168.9	168.9
17	129.2	129.3	129.4	128.9	129.4
18	138.6	138.2	138.1	138.6	138.6
19	16.0	16.0	15.9	16.0	16.0
20	20.7	21.5	19.5	20.7	20.8

3.4.1.4 Kinetics of chemical degradation

The decrease of nobiletin concentration in stability experiments in aqueous buffer solution at different pH values is shown in Figure 3. Similar concentration-time profiles were obtained at pH values ranging between 4 and 7.5. Values of the degradation rate constant k_d deduced from the fit of Equation (1) are given in Table 4. In this calculation, first order degradation kinetics was used by setting $x = 1$ which provided adequate description of the data ($r^2 = 0.9991-0.9995$). The use of first order kinetics is confirmed by the analysis of degradation kinetics in aq-TM_{Caco} discussed below.

The degradation of nobiletin in these purely aqueous solutions took place rather quickly with a half-life of approximately 2 hours. There was no difference of degradation rate between purified water and maleate buffer. Also, degradation was found to be independent of pH.

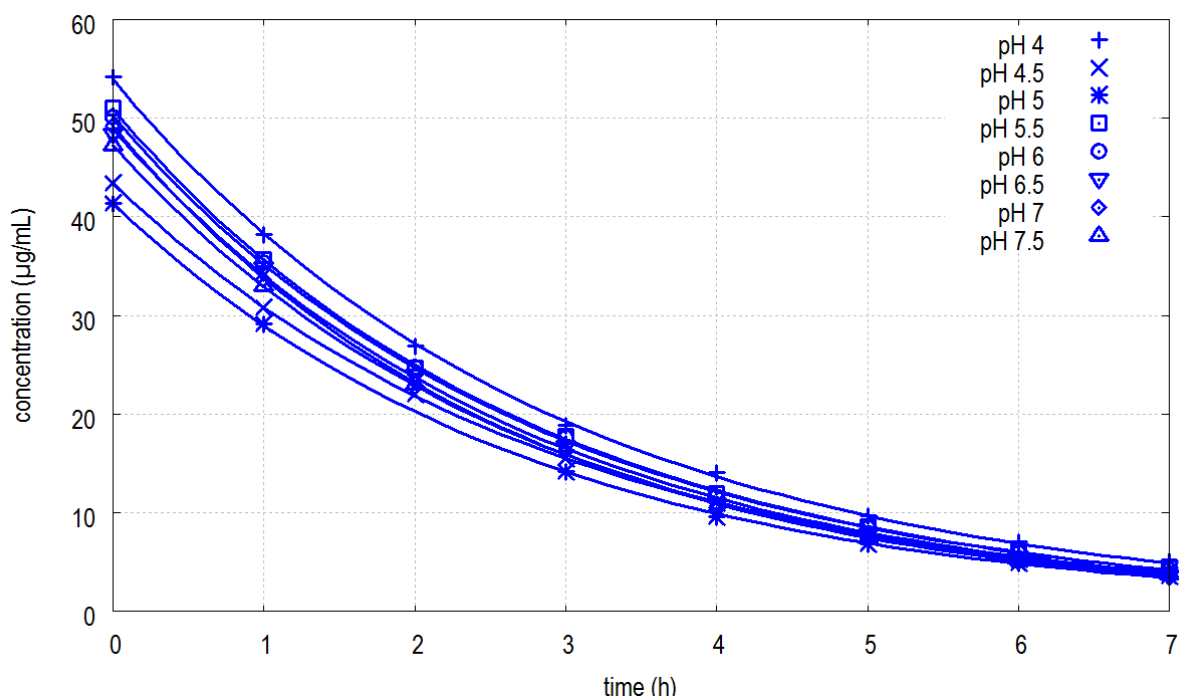


Figure 3: Measured concentrations of nobilin and fitted curves at different pH values as a function of time.

Table 4: Degradation rate constant and half-life of purified nobilin in water and maleate buffer.

Solvent	k_d [h^{-1}] ^a	$t_{1/2}$ [h]
purified water	0.3581 (3.10×10^{-3})	1.9
buffer pH 4	0.3436 (3.18×10^{-3})	2.0
buffer pH 4.5	0.3435 (3.18×10^{-3})	2.0
buffer pH 5	0.3579 (3.44×10^{-3})	1.9
buffer pH 5.5	0.3570 (3.28×10^{-3})	1.9
buffer pH 6	0.3553 (3.27×10^{-3})	2.0
buffer pH 6.5	0.3623 (3.32×10^{-3})	1.9
buffer pH 7	0.3771 (3.43×10^{-3})	1.8
buffer pH 7.5	0.3630 (4.09×10^{-3})	1.9

^a k_d are values deduced from regression analysis with standard error (in brackets), ^a x was set equal to one according to the results shown in Table 6.

Figure 4 illustrates the decrease of the nobilin peak area and the simultaneous increase of the peak of the different degradation products over time. The corresponding rate constants deduced by fitting Equations (2) through (9) to these data are given in Table 5. Degradation product 1 was most abundantly present accounting for 36.5% of total degradation followed by products 2 and 4 with 14.4% and 11.5%, respectively, while products 3 and 5 were more scarcely represented with 2.2% and 3.3%, respectively. Figure 4 further shows that the proportion of each degradation product remains constant in the course of the reaction.

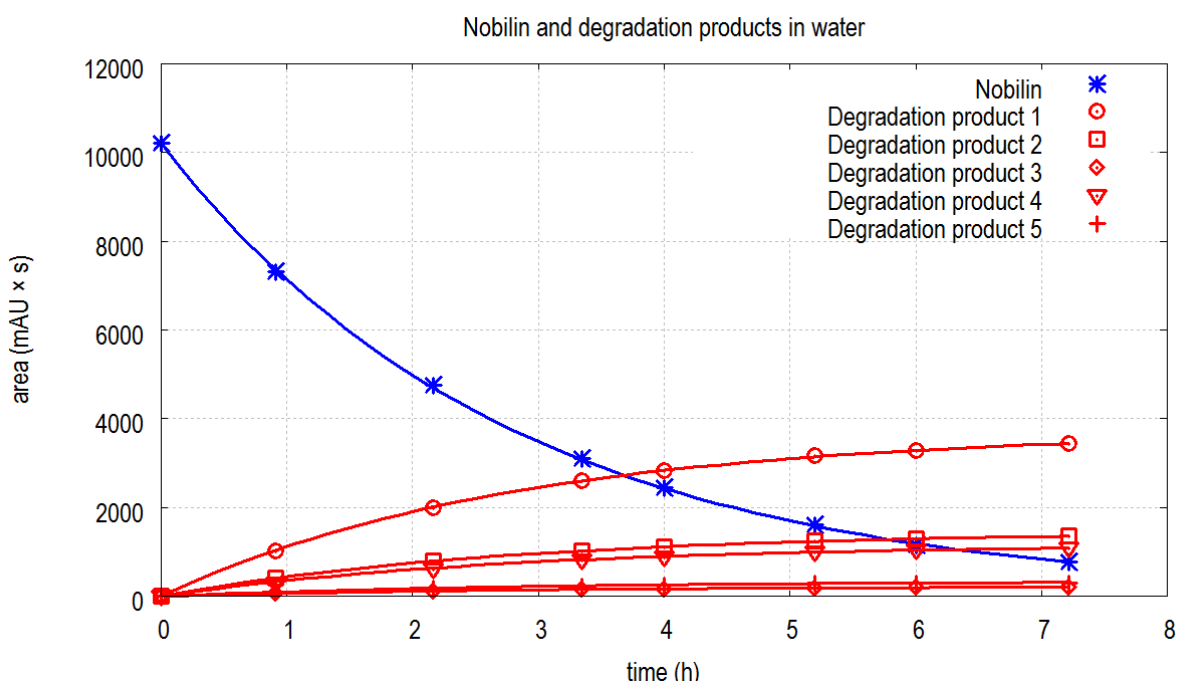


Figure 4: Peak area of UV chromatograms of nobilin and its degradation products in purified water as a function of time. Data points and fitted model curves of nobilin (*) in blue and its degradation products (other symbols) in red.

Table 5: Kinetic constants of nobilin degradation and formation of degradation products in purified water.

Substance	k_d [h^{-1}] ^a	k_{1-5} [h^{-1}] ^a	$(k_{1-5}/k_d) \times 100$ [%]
nobilin	0.3581 (3.10×10^{-3})	-	-
degradation product 1	-	0.1306 (9.98×10^{-4})	36.5
degradation product 2	-	0.0515 (3.93×10^{-4})	14.4
degradation product 3	-	0.0078 (5.99×10^{-5})	2.2
degradation product 4	-	0.0413 (3.16×10^{-4})	11.5
degradation product 5	-	0.0119 (9.11×10^{-5})	3.3

k_{1-5} and k_d are values with standard error (in brackets) deduced from regression analysis, ^a x was set equal to one according to the results shown in Table 6.

The degradation rate constants and the order of reaction kinetics in different vehicles obtained by fitting Equation (1) to degradation data with different initial nobilin concentrations are shown in Table 6. The degradation process of purified nobilin in aq-TM_{Caco} and FaSSIF-TM_{Caco} followed first order kinetics. For FeSSIF-TM_{Caco}, Liposomes_{FaSSIF}, and Liposomes_{FeSSIF} the exponent x acquired values 1.22, 1.19, and 1.11, respectively, these being greater than one. This suggests that in these colloidal systems the reaction rate had a somewhat stronger dependence on concentration compared to aq-TM_{Caco}. Also, a substantially slower degradation is evident for these vehicles compared to aq-TM_{Caco}.

Table 6: Degradation constant and order of reaction kinetics in different vehicles.

Vehicle	k_d [h^{-1} ($\mu g/mL$) ^{1-x}]	x	Total lipid conc. [mM]	Particle size [nm]
purified water	0.3581 (0.31×10^{-2})	1 ^a	-	-
aq-TM _{Caco}	0.4169 (0.29×10^{-2})	1.00 (0.31×10^{-2})	-	-
FaSSIF-TM _{Caco}	0.3297 (1.36×10^{-2})	0.97 (1.42×10^{-2})	3.2	83.2
FeSSIF-TM _{Caco}	0.0204 (0.44×10^{-2})	1.22 (3.95×10^{-2})	17.8	68.8
Liposomes _{FaSSIF}	0.0409 (0.28×10^{-2})	1.19 (1.45×10^{-2})	3.2	120.7
Liposomes _{FeSSIF}	0.0084 (0.12×10^{-2})	1.11 (2.36×10^{-2})	17.8	124.9

k_d and x are values with standard error (in brackets) deduced from regression analysis, ^a fixed to the value of aq-TM_{Caco}

The degradation products detected for these vehicles were the same as those found in the stability experiment with purified water shown in Figure 1. The relative amount of each of the five degradation products measured in the different vehicles was generally the same as the one found with purified water, when all five products were present at a detectable level (Table 7).

Table 7: Proportion of degradation products formed in different vehicles.

Vehicle	$(k_1/k_d) \times 100$ [%]	$(k_2/k_d) \times 100$ [%]	$(k_3/k_d) \times 100$ [%]	$(k_4/k_d) \times 100$ [%]	$(k_5/k_d) \times 100$ [%]
purified water	36.47	14.38	2.18	11.53	3.32
aq-TM _{Caco}	35.47	13.86	1.98	10.51	3.24
FaSSIF-TM _{Caco}	36.30	14.04	2.00	10.10	3.10
FeSSIF-TM _{Caco}	45.12	19.44	1.91	15.02	3.87
Liposomes _{FaSSIF}	39.27	16.95	nd	16.10	nd
Liposomes _{FeSSIF}	53.38	21.79	nd	24.82	nd

k_d , degradation rate constant of nobilin, k_1 through k_5 , rate constant of formation of degradation product 1 through 5, respectively, nd, not detectable

3.4.2 Solubility study

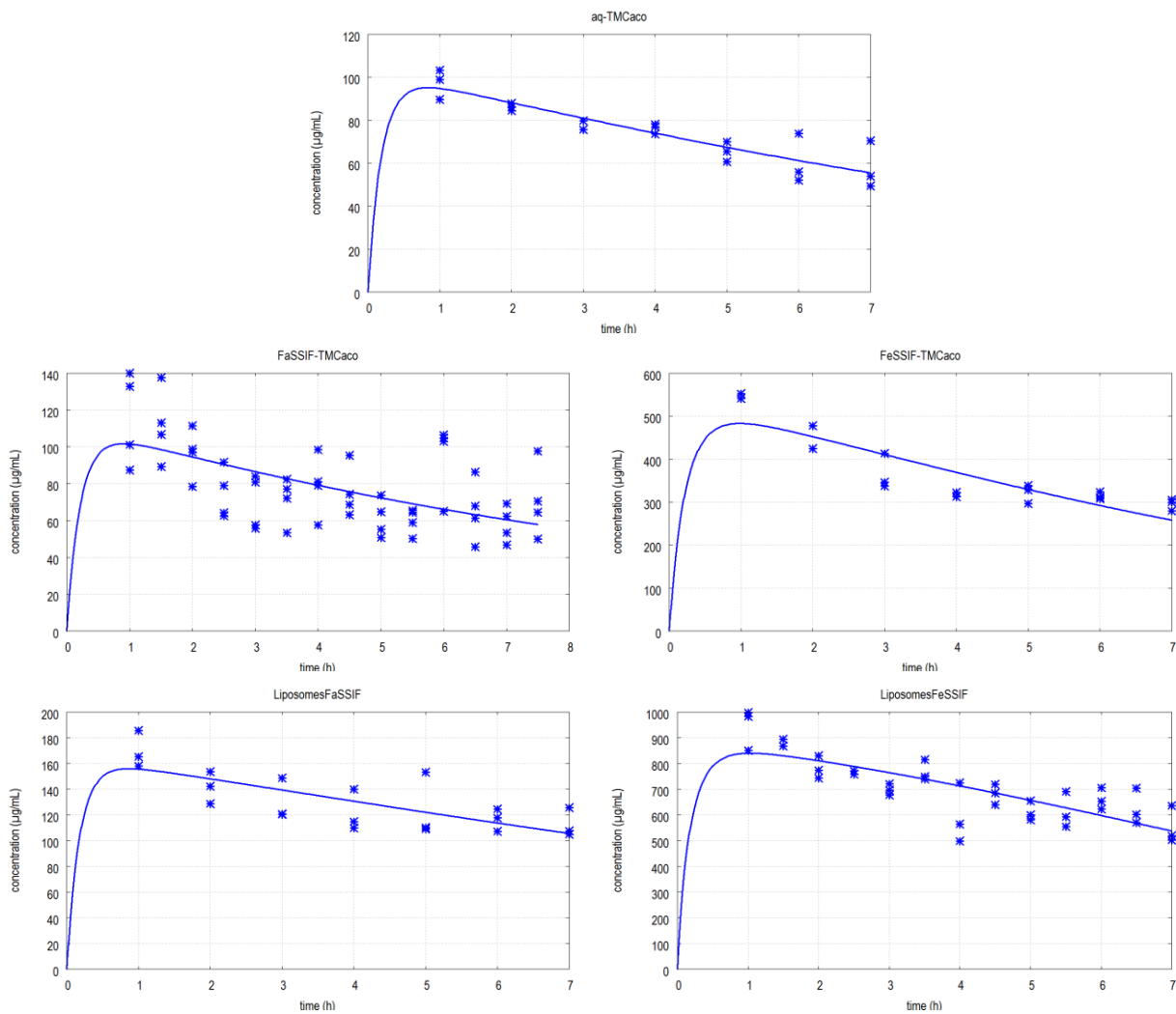


Figure 5: Concentration of dissolved nobiletin (*) as a function of time and fitted model curves in solubility measurements in different vehicles.

The data of the solubility experiments and the fitted curves of model Equation (14) are shown in Figure 5. A sharp increase of the dissolved nobiletin concentration is observed at first. Interestingly, this concentration did not stay constant but decreased as a function of time although an excess of solid material was available in the mixture. The calculated solubility and the degradation rate constant from Equation (14) are shown in Table 8. For this calculation, the relative mass frequency of each particle size fraction of purified nobiletin measured by laser diffractometry (Figure 6) was used. Purified nobiletin is very slightly soluble in aq-TM_{Caco} while solubility in FaSSiF-TM_{Caco}, FeSSiF-TM_{Caco}, Liposomes_{FaSSiF}, and Liposomes_{FeSSiF} was 1.3-, 4.7-, 1.5-, and 6.8-fold, respectively, larger compared to aq-TM_{Caco}. The coefficient a was between 0.5×10^{-6} and 1×10^{-6} cm⁴/(µg·h). The degradation rate constant, k_s , was comparable for aq-TM_{Caco} and FaSSiF-TM_{Caco} and was smaller for FeSSiF-TM_{Caco}, Liposomes_{FaSSiF}, and Liposomes_{FeSSiF} suggesting that degradation was slower in the last three vehicles. A similar result was

obtained in the stability experiments (Table 6). However, degradation rate constants determined in the solubility experiments were considerably larger in comparison to those determined in the same vehicles in the stability experiments. This difference was greater for the vehicles exhibiting slow degradation.

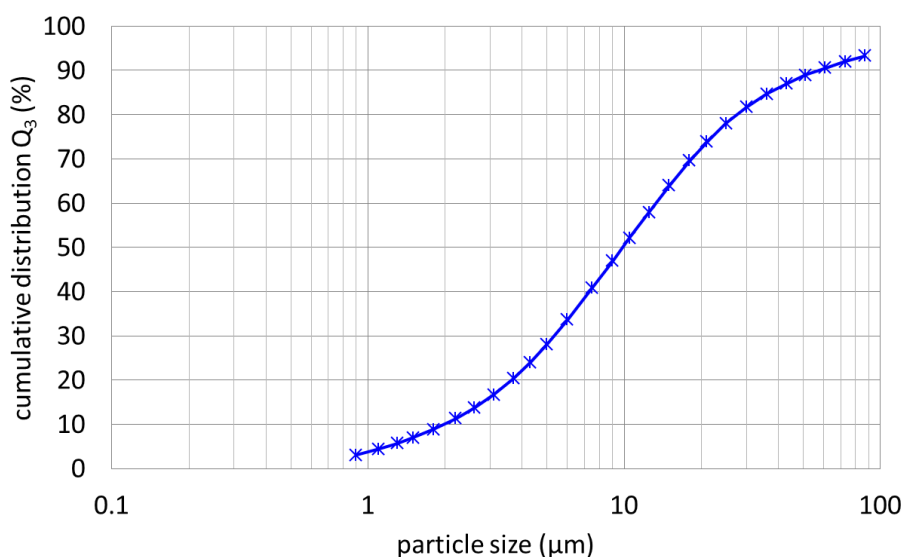


Figure 6: Particle size distribution of purified nobilin.

Table 8: Solubility of purified nobilin in different vehicles.

Vehicle	C_s [$\mu\text{g}/\text{mL}$]	α [$\text{cm}^4/(\mu\text{g}\cdot\text{h})$]	k_s [$\text{h}^{-1} (\mu\text{g}/\text{mL})^{1-x}$]
aq-TM _{Caco}	151.3	9.8×10^{-7}	1.7058
FaSSiF-TM _{Caco}	195.7	4.7×10^{-7}	2.0986
FeSSiF-TM _{Caco}	714.9	4.5×10^{-7}	0.4776
Liposomes _{FaSSiF}	225.7	7.2×10^{-7}	0.9690
Liposomes _{FeSSiF}	1032.4	5.5×10^{-7}	0.4053

C_s is solubility, α is a coefficient, k_s is degradation rate constant. Values are deduced from regression analysis.

3.5 DISCUSSION

The present work demonstrates that nobilin is a highly unstable compound in aqueous solution. Our findings are in agreement with the literature that documents the high susceptibility of germacranolides to undergo chemical transformations.⁴⁴ All the degradation products are acids with cadinane skeleton generated from nobilin through transannular cyclization of the *trans* 1(10) double bond and opening of the lactone. The reaction probably proceeds through a C-10 tertiary cation intermediate that can evolve in different ways, affording diastereoisomers 1, 2, and 3 after nucleophilic attack by water or product 4 if deprotonated. Further dehydration of the secondary alcohol bounded at C-3 gave aromatic product 5 (Figure 7). The kinetic of the reaction in aqueous medium did not show significant changes in a range of

pH between 4 and 7.5. The pathway involving addition of water appears to be the predominant pathway accounting for > 50% of nobilin degradation products (Table 5). Decay of nobilin concentration not accounted for by degradation products may be because of undetected HPLC peaks or variations in the UV absorption coefficient.

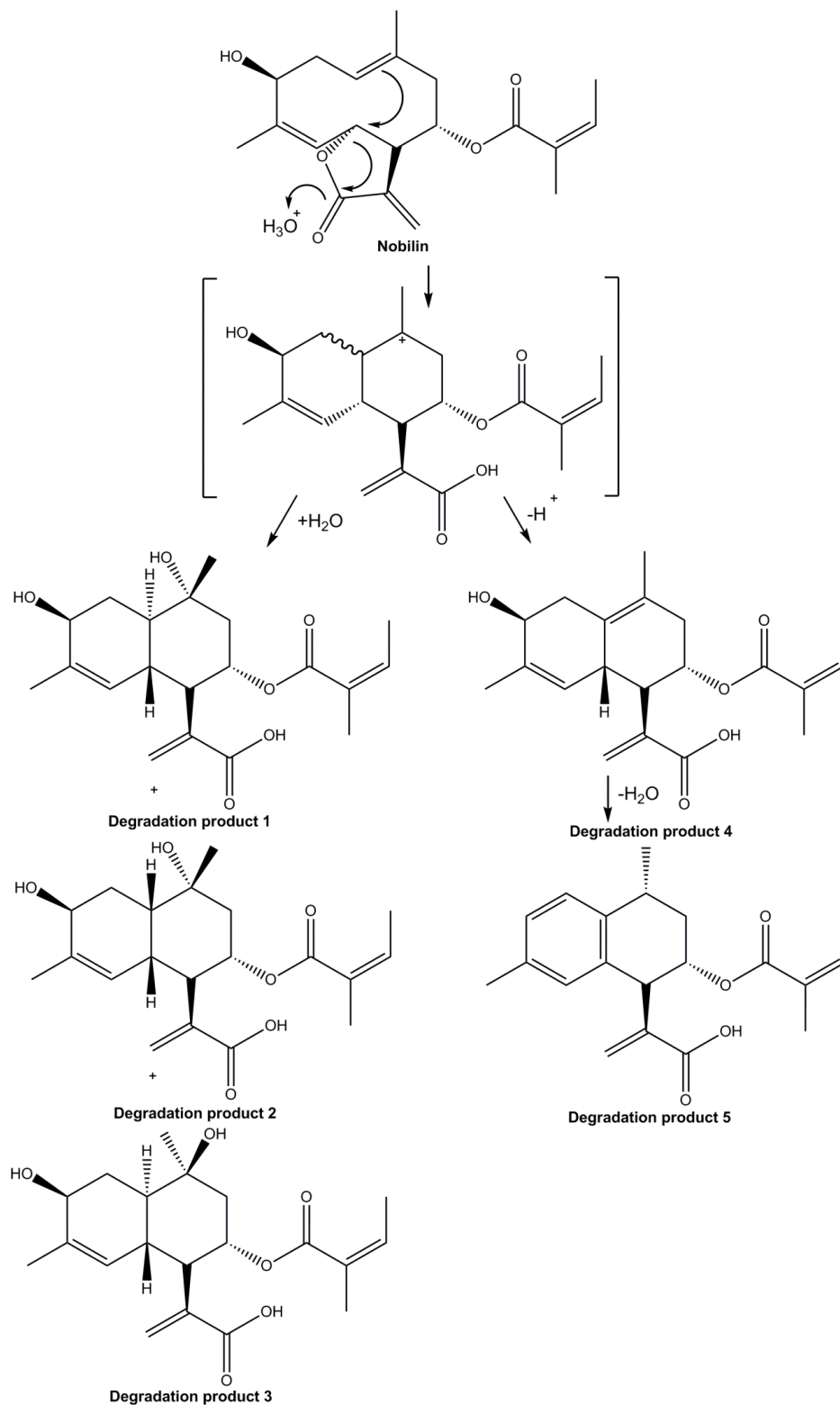


Figure 7: Proposed degradation mechanism of nobilin.

The degradation process follows first order kinetics in aq-TM_{Caco}. For FeSSIF-TM_{Caco}, Liposomes_{FaSSIF}, and Liposomes_{FeSSIF} on the other hand, a slightly higher order of reaction kinetics was found. This could explain the measured degradation rates at different initial nobiletin concentrations. The stronger dependence of the reaction rate on nobiletin concentration may be elicited by the colloidal lipid particles that are present in these media (Table 6). It may be suggested that reaction taking place at the surface of the colloidal particles has an impact on the kinetic order of the process. This effect was not observed for FaSSIF-TM_{Caco}, a fact that could be related to the small lipid content of this medium. It has been documented that the interface between two phases can affect the reaction process. Morales et al., for example, reported an increased reaction rate of the cyanide-catalyzed aerobic oxidation of the B₆ vitamers pyridoxal and pyridoxal-5'-phosphate in presence of cationic micelles and a change of the order of reaction kinetics at the surface of the micelles.⁴⁵ Sicilia et al. made a similar observation that the complexation kinetics of titanium(IV) with Pyrogallol Red and the oxidation of chromium(VI) by Pyrogallol Red was increased in presence of dodecyltrimethylammonium bromide micelles, this effect being due to the second order reaction at the interface.⁴⁶ Also, Ghosh et al. suggested the involvement of the surface of sodium dodecyl sulfate micelles in the oxidation of formaldehyde by Ce(IV).⁴⁷

Significantly, stability of purified nobiletin was considerably increased in the three vehicles FeSSIF-TM_{Caco}, Liposomes_{FaSSIF}, and Liposomes_{FeSSIF}. It appears therefore that the presence of lipid particles leads to a slower nobiletin degradation. This effect was stronger for the vehicles with high lipid content and may also depend on the nature of the lipid and/or the structure of the colloidal particle as indicated by comparing the liposomal vehicles to the mixed micellar FaSSIF-TM_{Caco} and FeSSIF-TM_{Caco} systems (Table 6). The degradation product profile in the vehicles did not change in comparison to that in water as long as all five degradation products were detectable suggesting that the mechanism of the chemical reaction was not affected by the used vehicles. Nobiletin is a rather lipophilic compound with a calculated clogP of 2.572 (± 0.601)⁴⁸ which suggests that it has the tendency to be incorporated in the colloidal lipid particles. This would shield nobiletin from the catalytic action of water discussed in the reaction mechanism (Figure 7) and may, therefore, explain its improved stability in these vehicles. A similar effect was reported for analogs of penicillin that were stabilized by cationic and nonionic micelles in acid solutions. It was proposed that this stabilization was because of the lipophilic character of the compounds leading to incorporation into the micelles that prevented acid-catalyzed degradation.⁴⁹ This effect also increased solubility of the drugs in the presence of nonionic micelles.⁴⁹

In the present study, the solubility of nobiletin was increased by the vehicles in the order: FaSSIF-TM_{Caco} < Liposomes_{FaSSIF} < FeSSIF-TM_{Caco} < Liposomes_{FeSSIF}. This may also be explained by the incorporation of the compound into colloidal lipid particles which is supported by its lipophilicity and was invoked in connection with its improved chemical stability in these vehicles. Solubility follows the same rank order

as the degree of stability improvement elicited by the vehicles. The increase of solubility is stronger for the vehicles with high lipid concentration whereas the liposomal vehicles seem to have a stronger effect than the mixed micelles. Saha et al. showed improved solubility and stability of 9-nitrocamptothecin in presence of pluronic micelles.¹⁸ The same was seen for the drug sirolimus which showed a higher solubility and stability in presence of D- α -tocopheryl polyethylene glycol succinate micelles or self-microemulsifying drug delivery systems.^{13,33} Solubility of the poorly water-soluble drug danazol was increased by micelles of bile salts, phospholipids, and lipolytic products.^{9,10,15,19}

For determining solubility, a model was developed that took into account simultaneous dissolution and degradation of the compound. This was necessary since no equilibrium concentration was reached in the solubility experiments. Instead, nobiletin concentration reached rapidly a peak and subsequently declined steadily in the presence of excess amount of solid material. This suggests that dissolution of nobiletin took place at a sharply decreasing rate in the course of the solubility experiment to the effect that dissolution rate was overwhelmed by degradation rate at later time points. The high initial dissolution rate can be due to the fine particles of the solid material exhibiting a large specific surface area which are quickly consumed while the remaining large particles dissolve at a much lower rate because of their comparatively small specific surface area. This time dependent decline of the dissolution rate is expected to become more pronounced for solid material with a wide particle size distribution.

The developed model accounts for this pattern of dissolution rate by considering dissolution of individual size fractions of the solid material accompanied by chemical degradation. This population balance approach is new for this application in the literature. The developed model provided adequate fits of the experimental concentration data ($GOF > 0.999$) and allowed the estimation of nobiletin solubility. Moreover, the good approximation afforded by the model substantiates the assumed mechanism of simultaneous dissolution and chemical degradation of a highly unstable compound.

The coefficient a seemed to be lowered somewhat by the used vehicles (Table 8). This is not surprising since incorporation in vesicles or micelles may alter the apparent diffusivity of the compound. Modeling of the degradation rate was based on the kinetic equation with the same order used in the stability study, whereas the rate constant was treated as adjustable parameter. Interestingly, the deduced degradation rate constants of purified nobiletin from the solubility study, k_s , were larger compared to k_d that was obtained in the stability experiments. This may be attributed to degradation reaction taking place at the surface of solid particles, in analogy to the effect of the surface of colloidal particles on degradation reaction kinetics discussed above. This is compatible with the observation that the difference between k_d and k_s is larger for the vehicles exhibiting slow degradation in the stability

experiment as the protective effect due to incorporation of nobilin in colloidal particles is partially alleviated by reaction at the solid surface.

The developed model for calculating drug solubility with concurrent rapid chemical degradation can be a useful tool in drug development for estimating solubility of an unstable compound. Typically, solubility in these cases has been estimated at reduced degradation rate by selecting appropriate conditions, for example, of pH or temperature.²⁴⁻²⁶ In other reports, solubility was determined after addition of an excess of solid drug, vigorous agitation and sampling at one time point or at equilibrium.^{18,21,32-34,49} The present study demonstrates that these practices are not universally applicable for determining solubility of highly unstable compounds. It is also noteworthy, that rate constants of degradation determined with drug solutions in colloidal systems can not be a priori transferred to drug suspensions in these systems. Rather, drug solubility in suspensions should be estimated by taking simultaneously into consideration the degradation rate in the system.

Chemical stability and solubility are properties affecting drug bioavailability that are part of routine drug profiling programs. Based on the high instability and poor solubility of nobilin in water, a low bioavailability of the compound after per-oral administration may be predicted. The presence of lipid constituents in the form of colloidal particles markedly improved stability, which is in accord with the identified degradation reaction mechanism of the drug, while increasing its solubility in aqueous environment. The investigated vehicles constitute biorelevant media simulating the fasted and the fed state in the intestinal tract as well as a prototype lipid-based formulation of liposomes. The strong effect of FeSSIF-TM_{Caco} suggests that intestinal absorption of nobilin might be improved in the fed state, while a lipid formulation-based approach could also have a promising effect on absorption.⁵⁰ These questions are explored in a subsequent study using the Caco-2 model.

3.6 CONCLUSION

Nobilin degrades quickly in aqueous solution into five main degradation products by a mechanism involving water catalyzed opening of the lactone ring and transannular cyclization followed by water addition or proton elimination. Stability can be improved by incorporation of the compound in colloidal lipid particles. Degradation reaction is accelerated in the presence of solid nobilin suspension and the order of reaction kinetics is altered by colloidal lipids. Water solubility of nobilin is low and is considerably increased in mixed micellar biorelevant media and by phospholipid vesicles.

Determination of solubility of a highly unstable compound requires kinetic modeling of simultaneous dissolution and degradation processes taking into account particle size distribution of solid material.

3.7 REFERENCES

1. Dressman JB, Amidon GL, Reppas C, Shah VP 1998. Dissolution testing as a prognostic tool for oral drug absorption: Immediate release dosage forms. *Pharmaceutical Research* 15(1):11-22.
2. Diakidou A, Vertzoni M, Goumas K, Soderlind E, Abrahamsson B, Dressman J, Reppas C 2009. Characterization of the contents of ascending colon to which drugs are exposed after oral administration to healthy adults. *Pharmaceutical Research* 26(9):2141-2151.
3. Amidon GL, Lennernas H, Shah VP, Crison JR 1995. A theoretical basis for a biopharmaceutic drug classification - the correlation of in-vitro drug product dissolution and in-vivo bioavailability. *Pharmaceutical Research* 12(3):413-420.
4. FDA. 2000. Guidance for industry: Waiver of in vivo bioavailability and bioequivalence studies for immediate-release solid oral dosage forms based on a biopharmaceutics classification system. Rockville, MD, USA: Food and Drug Administration. <http://www.fda.gov/downloads/Drugs/.../Guidances/ucm070246.pdf>.
5. Galia E, Nicolaidis E, Horter D, Lobenberg R, Reppas C, Dressman JB 1998. Evaluation of various dissolution media for predicting in vivo performance of class I and II drugs. *Pharmaceutical Research* 15(5):698-705.
6. Wei H, Lobenberg R 2006. Biorelevant dissolution media as a predictive tool for glyburide a class II drug. *European Journal of Pharmaceutical Sciences* 29(1):45-52.
7. Nicolaidis E, Galia E, Efthymiopoulos C, Dressman JB, Reppas C 1999. Forecasting the in vivo performance of four low solubility drugs from their in vitro dissolution data. *Pharmaceutical Research* 16(12):1876-1882.
8. Kambayashi A, Dressman JB 2013. An in vitro-in silico-in vivo approach to predicting the oral pharmacokinetic profile of salts of weak acids: Case example dantrolene. *European Journal of Pharmaceutics and Biopharmaceutics* 84(1):200-207.
9. Vertzoni M, Markopoulos C, Symillides M, Goumas C, Imanidis G, Reppas C 2012. Luminal lipid phases after administration of a triglyceride solution of danazol in the fed state and their contribution to the flux of danazol across Caco-2 cell monolayers. *Molecular Pharmaceutics* 9(5):1189-1198.
10. Charman WN, Rogge MC, Boddy AW, Berger BM 1993. Effect of food and a monoglyceride emulsion formulation on danazol bioavailability. *Journal of Clinical Pharmacology* 33(4):381-386.
11. Markopoulos C, Thoenen F, Preisig D, Symillides M, Vertzoni M, Parrott N, Reppas C, Imanidis G 2013. Biorelevant media for transport experiments in the Caco-2 model to evaluate drug absorption in the fasted and fed state and their usefulness. *European Journal of Pharmaceutics and Biopharmaceutics* <http://dx.doi.org/10.1016/j.ejpb.2013.10.017>.

12. Kapitza SB, Michel BR, van Hoogevest P, Leigh MLS, Imanidis G 2007. Absorption of poorly water soluble drugs subject to apical efflux using phospholipids as solubilizers in the Caco-2 cell model. *European Journal of Pharmaceutics and Biopharmaceutics* 66(1):146-158.
13. Sun MH, Si LQ, Zhai XZ, Fan ZZ, Ma YM, Zhang R, Yang XL 2011. The influence of co-solvents on the stability and bioavailability of rapamycin formulated in self-microemulsifying drug delivery systems. *Drug Development and Industrial Pharmacy* 37(8):986-994.
14. Mohanty C, Sahoo SK 2010. The in vitro stability and in vivo pharmacokinetics of curcumin prepared as an aqueous nanoparticulate formulation. *Biomaterials* 31(25):6597-6611.
15. Sunesen VH, Pedersen BL, Kristensen HG, Mullertz A 2005. In vivo in vitro correlations for a poorly soluble drug, danazol, using the flow-through dissolution method with biorelevant dissolution media. *European Journal of Pharmaceutical Sciences* 24(4):305-313.
16. Dressman JB, Reppas C 2000. In vitro-in vivo correlations for lipophilic, poorly water-soluble drugs. *European Journal of Pharmaceutical Sciences* 11:73-80.
17. Nicolaides E, Symillides M, Dressman JB, Reppas C 2001. Biorelevant dissolution testing to predict the plasma profile of lipophilic drugs after oral administration. *Pharmaceutical Research* 18(3):380-388.
18. Saha SC, Patel D, Rahman S, Savva M 2013. Physicochemical characterization, solubilization, and stabilization of 9-nitrocamptothecin using pluronic block copolymers. *Journal of pharmaceutical sciences* 102(10):3653-3665.
19. Bakatselou V, Oppenheim RC, Dressman JB 1991. Solubilization and wetting effects of bile-salts on the dissolution of steroids. *Pharmaceutical Research* 8(12):1461-1469.
20. Lindenberg M, Kopp S, Dressman JB 2004. Classification of orally administered drugs on the World Health Organization model list of essential medicines according to the biopharmaceutics classification system. *European Journal of Pharmaceutics and Biopharmaceutics* 58(2):265-278.
21. Tsuji A, Nakashima E, Hamano S, Yamana T 1978. Physicochemical properties of amphoteric beta-lactam antibiotics I: Stability, solubility, and dissolution behavior of amino penicillins as a function of pH. *Journal of Pharmaceutical Sciences* 67(8):1059-1066.
22. Yamana T, Tsuji A, Mizukami Y 1974. Kinetic approach to development in beta-lactam antibiotics. I. comparative stability of semisynthetic penicillins and 6-aminopenicillanic acid in aqueous-solution. *Chemical & Pharmaceutical Bulletin* 22(5):1186-1197.
23. Anderson BD, Fung MC, Kumar SD, Baker DC 1985. Hydrolysis and solvent-dependent 2'-5' and 3'-5' acyl migration in prodrugs of 9-beta-D-arabinofuranosyladenine. *Journal of Pharmaceutical Sciences* 74(8):825-830.

24. Anderson BD, Wygant MB, Xiang TX, Waugh WA, Stella VJ 1988. Preformulation solubility and kinetic-studies of 2',3'-dideoxypurine nucleosides - potential anti-aids agents. *International Journal of Pharmaceutics* 45(1-2):27-37.
25. Oh I, Chi SC, Vishnuvajjala BR, Anderson BD 1991. Stability and solubilization of oxathiin carboxanilide, a novel anti-hiv agent. *International Journal of Pharmaceutics* 73(1):23-31.
26. Anderson BD, Chiang CY 1990. Physicochemical properties of carbovir, a potential anti-hiv agent. *Journal of Pharmaceutical Sciences* 79(9):787-790.
27. FDA. 2002. Guidance for industry: Food-effect bioavailability and fed bioequivalence studies. Rockville, MD, USA: Food and Drug Administration. http://www.fda.gov/downloads/regulatory_information/guidances/ucm126833.pdf.
28. Parojcic J, Duric J, Jovanovic M, Ibric S, Jovanovic D 2004. Influence of dissolution media composition on drug release and in-vitro/in-vivo correlation for paracetamol matrix tablets prepared with novel carbomer polymers. *Journal of Pharmacy and Pharmacology* 56(6):735-741.
29. Vertzoni M, Fotaki N, Kostewicz E, Stippler E, Leuner C, Nicolaides E, Dressman J, Reppas C 2004. Dissolution media simulating the intraluminal composition of the small intestine: Physiological issues and practical aspects. *Journal of Pharmacy and Pharmacology* 56(4):453-462.
30. Schamp K, Schreder SA, Dressman J 2006. Development of an in vitro/in vivo correlation for lipid formulations of EMD 50733, a poorly soluble, lipophilic drug substance. *European Journal of Pharmaceutics and Biopharmaceutics* 62(3):227-234.
31. Murdande SB, Pikal MJ, Shanker RM, Bogner RH 2011. Aqueous solubility of crystalline and amorphous drugs: Challenges in measurement. *Pharmaceutical Development and Technology* 16(3):187-200.
32. Hou JP, Poole JW 1969. Amino acid nature of ampicillin and related penicillins. *Journal of Pharmaceutical Sciences* 58(12):1510-1515.
33. Kim MS, Kim JS, Cho WK, Hwang SJ 2013. Enhanced solubility and oral absorption of sirolimus using D-alpha-tocopheryl polyethylene glycol succinate micelles. *Artificial Cells Nanomedicine and Biotechnology* 41(2):85-91.
34. Kim MS, Kim JS, Park HJ, Cho WK, Cha KH, Hwang SJ 2011. Enhanced bioavailability of sirolimus via preparation of solid dispersion nanoparticles using a supercritical antisolvent process. *International Journal of Nanomedicine* 6:2997-3009.
35. Holub M, Samek Z 1977. Terpenes. CLXX. Isolation and structure of 3-epinobilin, 1,10-epoxynobilin and 3-dehydronobilin - other sesquiterpenic lactones from flowers of *Anthemis nobilis* L. revision of structure of nobilin and eucannabinolide. *Collection of Czechoslovak Chemical Communications* 42(3):1053-1064.

36. http://www.sigmaaldrich.com/etc/medialib/docs/Sigma/Product_Information_Sheet/1/d5030pis.Par.0001.File.tmp/d5030pis.pdf. (accessed on 2nd October 2013)
37. Fischer N. 1991. Sesquiterpenoid lactones. In Charlwood B, Banthorpe D, editors. *Methods in plant biochemistry*, 1 ed., London, San Diego, New York, Boston, Sydney, Tokyo, Toronto: Academic Press, Harcourt Brace Jovanovich. p 187-211.
38. Palatinus L, Chapuis G 2007. SUPERFLIP - a computer program for the solution of crystal structures by charge flipping in arbitrary dimensions. *Journal of Applied Crystallography* 40:786-790.
39. Betteridge PW, Carruthers JR, Cooper RI, Prout K, Watkin DJ 2003. CRYSTALS version 12: Software for guided crystal structure analysis. *Journal of Applied Crystallography* 36:1487-1487.
40. Parsons S, Wagner T, Presly O, Wood PA, Cooper RI 2012. Applications of leverage analysis in structure refinement. *Journal of Applied Crystallography* 45:417-429.
41. Macrae CF, Bruno IJ, Chisholm JA, Edgington PR, McCabe P, Pidcock E, Rodriguez-Monge L, Taylor R, van de Streek J, Wood PA 2008. Mercury CSD 2.0 - New features for the visualization and investigation of crystal structures. *Journal of Applied Crystallography* 41:466-470.
42. Schittkowski K. 2003. Numerical data fitting in dynamical systems - A practical introduction with applications and software. 1 ed., Dordrecht, Boston: Kluwer Academic Publisher.
43. Teresa JD, Valle MAM, Gonzalez MS, Bellido IS 1984. Sesquiterpenic acid from *leucanthemopsis-pulverulenta*. *Tetrahedron* 40(11):2189-2195.
44. Adio AM 2009. Germacrenes A-E and related compounds: Thermal, photochemical and acid induced transannular cyclizations. *Tetrahedron* 65(8):1533-1552.
45. Morales F, Sicilia D, Rubio S, PerezBendito D 1997. Application of micellar effects to the simultaneous kinetic determination of pyridoxal and pyridoxal-5'-phosphate. *Analytica Chimica Acta* 345(1-3):87-98.
46. Sicilia D, Rubio S, Perezbendito D 1994. Micellar effects on reaction-kinetics part II. study of the action of dedecyltrimethylammonium bromide on the reactions between pyrogallol red and chromium(VI), vanadium(V) and titanium(IV). *Analytica Chimica Acta* 297(3):453-464.
47. Ghosh A, Saha R, Sar P, Saha B 2013. Rate enhancement via micelle encapsulation for room temperature metal catalyzed Ce(IV) oxidation of formaldehyde to formic acid in aqueous medium at atmospheric pressure: A kinetic approach. *Journal of Molecular Liquids* 186:122-130.
48. Advanced Chemistry Development (ACD/Labs) Software V11.02 (© 1994-2012 ACD/Labs), <https://scifinder.cas.org>.
49. Tsuji A, Miyamoto E, Matsuda M, Nishimura K, Yamana T 1982. Effects of surfactants on the aqueous stability and solubility of beta-lactam antibiotics. *Journal of Pharmaceutical Sciences* 71(12):1313-1318.

50. Porter CJH, Pouton CW, Cuine JF, Charman WN 2008. Enhancing intestinal drug solubilisation using lipid-based delivery systems. *Advanced Drug Delivery Reviews* 60(6):673-691.

Chapter 4

Transport of nobiletin conjugation products and the use of the extract of *Chamomillae romanae flos* influence absorption of nobiletin in the Caco-2 model

4.1 ABSTRACT

Purpose: The objective of the present study was to investigate the role of bioconversion and carrier mediated efflux of conjugation products in the absorption mechanism of nobiletin in the Caco-2 model in vitro and to elucidate the impact of the extract of *Chamomillae romanae flos* and its ingredients on bioconversion and efflux.

Methods: Inhibitors of P-gp, BCRP, and MRPs were used to detect efflux and its connection to bioconversion and the effect of different ingredients of the extract on absorption processes was determined. Permeation and bioconversion parameter values were deduced by means of kinetic multi-compartment modeling.

Results: Nobiletin exhibited high permeability, low absorption and fast bioconversion producing glucuronide, cysteine conjugate, and glutathione conjugate that were transported by P-gp (first two), apical MRP2 and basal MRP3 and possibly MRP1 out of the cell. Inhibition of efflux resulted in diminished bioconversion and improved absorption. The extract increased the relative fraction absorbed primarily by directly inhibiting bioconversion but also by reducing efflux. This was only partly explained by the individual ingredients.

Conclusion: The transport-bioconversion interplay is shown to be a possible mechanism for increasing absorption of a compound undergoing extensive bioconversion. Plant extracts may increase absorption by this mechanism in addition to metabolic enzyme inhibition.

Thormann U. et al. 2014. Transport of nobiletin conjugation products and the use of the extract of *Chamomillae romanae flos* influence absorption of nobiletin in the Caco-2 model. Pharmaceutical research, to be submitted

4.2 INTRODUCTION

Bioconversion by metabolizing enzymes and membrane permeation by efflux and influx transporter proteins influence intestinal drug absorption. Absorption can be increased or decreased by the interplay between metabolizing enzymes and transporters or by the interaction between co-administered compounds; this can be due to inhibition or induction of metabolizing enzymes or transporters.^{1,2} Interaction between synthetic drugs has been extensively studied whereas in recent years the interest in the absorption of compounds from multi-component mixtures such as phytopharmaceuticals has risen. Increased absorption of a compound applied as full plant extract was reported for instance for paclitaxel from *Taxus yunnanensis*, aconitine, mesaconitine, and hypaconitine from *Aconitum* species, and rosmarinic acid from *Plectranthus barbatus*.³⁻⁵ Further, presence of *Angelicae sinensis* extract increased the absorption of formononetin and calycosin from *Astragalus membranaceus* var. *mongholicus* extract.⁶

Several drugs are documented to be substrates of apical and basal efflux and influx carriers. Paclitaxel, digoxin, verapamil, and fexofenadine, for example, are transported apically out of the enterocytes by the well characterized transporter protein P-gp (P-glycoprotein, ABCB1).⁷⁻⁹ Fexofenadine is in addition substrate of the apical MRP2 (multidrug resistance protein, ABCC2) and the basal MRP3 (ABCC3).^{7,9} Methotrexate, further, is substrate of MRP2, MRP3, and the basal MRP1 (ABCC1) transporter and is additionally transported apically out of the cell by BCRP (breast cancer resistance protein, ABCG2).^{7,10} Fexofenadine is not only transported by efflux carriers but also by the influx transporter protein OATP2B1 (organic anion transporting polypeptide, SLCO2B1) at the apical membrane.^{7,9} Further relevant influx transporter proteins are PEPT1 (peptide transporter 1, SLC15A1), MCT1 (monocarboxylic acid transporter 1, SLC16A1), ASBT (ileal apical sodium bile acid co-transporter) at the apical membrane and OCT1 (organic cation transporter 1, SLC22A1) and the heteromeric organic solute transporter (OST α -OST β) at the basal membrane.⁷

Drugs undergo phase I metabolism by different cytochrome P450 enzymes in the enterocytes, e.g., verapamil.⁸ Other substances are substrates of phase II enzymes for example the flavonoid apigenin which is glucuronidated by UDP-glucuronosyltransferase and sulfated by sulfotransferase or busulfan which is conjugated by glutathione S-transferase to the glutathione conjugate.^{11,12} These metabolites are often substrates of the above mentioned efflux transporter proteins. The metabolites of verapamil are transported by P-gp, apigenin glucuronide and sulfate are substrates of MRPs and/or BCRP and glutathione conjugates such as the endogenous leukotriene C4 are transported by MRPs.^{8,12-14} Furthermore, the influx carriers OATP transport steroid conjugates.⁷

Interestingly, some cases of functional interplay between metabolizing enzymes and transporter proteins were observed in recent years. For instance, metabolism of K77 and sirolimus, which are

substrates of cytochrome P450 and P-gp, was decreased by inhibition of the efflux transporter in the Caco-2 model whereas the inhibition did not reduce metabolism of the non P-gp substrates midazolam and felodipine.^{15,16} Also, interplay between phase II metabolism and transporters was suggested such as for the glucuronidation of apigenin and genistein with BCRP or glucuronidation and sulfonation of apigenin with MRPs.^{12,14,17,18}

The in vitro study of intestinal absorption taking into consideration transporter proteins and metabolizing enzymes is routinely carried out using the Caco-2 cell culture model.¹⁹⁻²² This is a well-established and well characterized model that shows a largely similar expression pattern of transporters and metabolizing enzymes as intestinal cells.²³⁻²⁵ In a study involving 10 different laboratories, Caco-2 cells were shown to well express the transporters P-gp, BCRP, MRP2, MRP3, MRP1, and OATP. In contrast to the intestine, phase I metabolizing enzyme CYP was poorly expressed whereas the phase II conjugating enzymes glutathione S-transferase and UDP-glucuronosyltransferase were well expressed.²²

The objective of the present study was to investigate the mechanism of intestinal absorption of nobilin in the Caco-2 model. Nobilin is a sesquiterpene lactone of the germacranolide type which is a marker compound isolated from *Chamomillae romanae flos*, the flowers of *Anthemis nobilis* L.²⁶ No reports about the bioavailability of nobilin exist in the literature. The first specific aim of the study was to investigate the effect of bioconversion and of carrier mediated efflux of the ensuing conjugation products on nobilin absorption and to ascertain a possible interplay between bioconversion and efflux. A kinetic model-based approach was employed to this end. The second aim was to elucidate the impact of the full extract of *Chamomillae romanae flos* and its ingredients, i.e., sesquiterpene lactones, essential oil, and flavonoids²⁷ on metabolizing enzymes and transporter proteins that influence nobilin absorption. By unraveling the interplay between bioconversion and efflux and the interaction between the plant extract and nobilin or nobilin bioconversion products with respect to these processes, possibilities to improve the absorption of nobilin should be elaborated.

4.3 MATERIALS AND METHODS

4.3.1 Chemicals

The human colon adenocarcinoma cell line Caco-2 was a gift of Prof. H. P. Hauri, Biocenter, University of Basel, and originated from the American Type Culture Collection (ATCC, Rockville, MD, USA). The Dulbecco's modified Eagle's medium (DMEM) (with L-glutamine, 4500 mg/L D-glucose, without sodium pyruvate), MEM non-essential amino acids solution (100×, without L-glutamine), L-glutamine 200 mM (100×), fetal bovine serum (FBS), Trypsin 0.5%-EDTA (10×) liquid, Dulbecco's phosphate buffered saline (with and without Ca^{2+} , Mg^{2+}) were all purchased from Gibco® Invitrogen corporation (Paisley, UK). The cell culture medium was supplemented with 10% (v/v) FBS, 1.8 mM L-glutamine, and 1% (v/v) MEM. The absorption studies were carried out in aq-TM_{Caco} (aqueous transport medium) containing Dulbecco's modified Eagle's medium (DMEM) base powder (without D-glucose, L-glutamine, phenol red, sodium pyruvate, and sodium bicarbonate) (8.6 g/L)²⁸ supplemented with D-glucose (25 mM), L-glutamine (6 mM), sodium chloride (34 mM) and HEPES (19.98 mM) was dissolved in purified water. The medium was adjusted to a pH 7.4 and sterile filtered (Supor-200, 0.2 µm pore size, Pall Corporation, Port Washington, NY, USA).²⁹ The substances were purchased from SIGMA-Aldrich Chemie GmbH (Buchs, Switzerland). Petri dishes (56.7 cm²) were purchased from Nunc A/S (Roskilde, Denmark), Petri dishes (21 cm²) and 6-well polycarbonate membrane transwell™ plates with an insert area of 4.7 cm² and 0.4 µm pore size were ordered from Costar (Corning Incorporated, Corning, NY, USA). Nobilin, a sesquiterpene lactone with M_r 346 was kindly provided by Alpinia Laudanum Institute of Phytopharmaceutical Sciences AG (ALIPS) (Walenstadt, Switzerland). Nobilin was purified from *Chamomillae romanae flos* (PhEur) as described before.³⁰ The inhibitors verapamil, Ko143, MK-571, and leukotriene C₄, the solvent dimethyl sulfoxide (DMSO), the detergent Triton® X-100 and the flavonoid apigenin were bought from SIGMA-Aldrich Chemie GmbH (Buchs, Switzerland). Luteolin was purchased from Extrasynthese (Genay Cedex, France), and essential oil of *Chamomillae romanae flos* from Essencia (Winterthur, Switzerland). Ethanolic extract and the sesquiterpene lactone fraction of *Chamomillae romanae flos* (PhEur) were provided by ALIPS. The sesquiterpene lactone fraction was obtained from 3 L of ethanolic extract of *Chamomillae romanae flos*. The extract was concentrated to a volume of approximately 300 mL by rotary evaporation. Fatty acids, phenols, and chlorophyll were precipitated with a 5% (w/v) lead(II)acetate solution and filtered over a Celite® 500 fine bed. The yellowish solution was applied on an Amberlite® XAD16 column (30 × 360 mm). The column was washed with 1 L of EtOH:water (50:50) and the lipophilic compounds were eluted with EtOH. Fractions of 100 mL were collected and the sesquiterpene lactone containing fractions were combined. EtOH was evaporated and the yellowish oily residue was collected. Ethanol was purchased from Alcosuisse (Bern, Switzerland) and all other substances were obtained from SIGMA-Aldrich Chemie GmbH (Buchs, Switzerland).

Methanol and ethanol from J.T.Baker (Deventer, Nederland), sodium acetate and formic acid from SIGMA-Aldrich Chemie GmbH (Buchs, Switzerland) were of HPLC grade. Water was purified by reversed osmosis with the water purification system arium® 61215 of Sartorius (Goettingen, Germany).

4.3.2 Cell culture

Caco-2 cells were cultivated in Petri dishes (56.7 cm²) using culture medium at 37°C in a water saturated atmosphere of 8% CO₂ (Sorvall Heraeus, Heracell, Kendro Laboratory Products, Zürich, Switzerland). The cells were passaged by treatment with a solution of 0.25% trypsin and 2.63 mM EDTA with a splitting ratio of 1:5-1:10 when the cell monolayer reached 70-90% confluence. Cells of passage numbers 60-65 were seeded at a density of 1.14×10^5 cells/cm² in 6-well transwell™ plates and incubated for 19-21 days. The medium was changed every other day.

4.3.3 TEER

The integrity of the Caco-2 cell monolayer in the transwell™ plates was ensured with TEER measurement before every permeation experiment. The monolayer was washed with pre-warmed (37°C) D-PBS (with Ca²⁺, Mg²⁺) (apical 3 mL and basal 4 mL). 1.6 mL of tempered aq-TM_{Caco} was added to the apical and 2.8 mL aq-TM_{Caco} to the basal compartment. The transwell™ plate was equilibrated for 60 min in the cell culture incubator and TEER was measured with an EVOM resistance meter (World Precision Instruments, Sarasota, FL, USA) equipped with an EndOhm-24SNAP chamber (World Precision Instruments, Sarasota, FL, USA) which was tempered at 37°C with 4.6 mL aq-TM_{Caco}. Caco-2 monolayers with TEER values above 470 Ω cm² were used for permeation experiments.

4.3.4 Permeation experiment

After the TEER measurement, the aq-TM_{Caco} was removed and the tempered nobiletin containing aq-TM_{Caco} was added. Nobiletin was dissolved in DMSO (1 mg/mL) and added to aq-TM_{Caco} (final DMSO concentration 0.3%) to a starting concentration of around 7 μM. To investigate the permeation in the apical-to-basal direction, 1.6 mL of the nobiletin solution was added to the apical compartment and 2.8 mL of blank aq-TM_{Caco} to the basal compartment. For the basal-to-apical direction, 1.6 mL of blank aq-TM_{Caco} was added to the apical and 2.8 mL of the nobiletin solution to the basal compartment. One plate was used for each direction.

Stock solutions of the inhibitors Ko143 in DMSO (4 mg/mL), MK-571 in aq-TM_{Caco} (5mg/mL) and leukotriene C4 in EtOH (26.5 μg/mL) were prepared. Leukotriene C4 was delivered dissolved in methanol which was replaced with EtOH. The final concentration of the inhibitors in aq-TM_{Caco} was for verapamil 100 μM³¹, Ko143 10 μM³², MK-571 50 μM³³, and leukotriene C4 0.035 μM. A combination of verapamil, Ko143 and MK-571 at the same concentrations was also used. Nobiletin from a stock solution of 1 mg/mL

or 2 mg/mL in DMSO was added to a final concentration of 6 to 14 μM . The final DMSO concentration was always < 1% (v/v). The inhibitors were added to both compartments.

The ethanolic extract was diluted 1:200 (v/v) with aq-TM_{Caco} yielding a nobilin concentration of approximately 2.5 μM . Stock solutions of the ingredients of the extract were prepared at the following concentrations: Essential oil in EtOH (4.1 mg/mL), sesquiterpene lactone fraction in EtOH (2.21 mg/mL), apigenin in EtOH (1.1 mg/mL) and in DMSO (1.94 mg/mL), luteolin in DMSO (2.2 mg/mL). The stock solutions were added to aq-TM_{Caco} to final concentrations of essential oil 5.56 $\mu\text{g/mL}$, sesquiterpene lactone fraction 7.83 $\mu\text{g/mL}$, apigenin 2.29 μM from EtOH stock solution (apigenin 1) and 10 μM from DMSO stock solution (apigenin 2), luteolin 10 μM , and apigenin 2 plus luteolin each 10 μM . Nobilin was added from stock solutions in EtOH or in DMSO to match the solvent of the ingredients of the extract to a final concentration of 2 to 12 μM . The final EtOH content was adjusted to 0.5% and that of DMSO was < 1% (v/v). The components of the extract were added only to the compartment containing nobilin. The transwell™ plate was shaken on an orbital shaker at 37°C in a water saturated atmosphere under an incubator hood with a stirring rate of 120 rpm (KS15, Edmund Bühler GmbH, Tübingen & Hechingen, Germany). Permeation of nobilin across the cell monolayer was monitored by drawing samples of 100 μL from both compartments after 10 min, 35 min, 1 h, 1.5 h, 2 h, and 2.5 h. One hundred μL of methanol was added and the samples were stored at 4°C. Under these conditions nobilin was chemically stable. At each time point one insert was removed and used for cell extraction.

4.3.5 Cell extraction

Both sides of the transwell™ were washed with 4°C cold D-PBS (without Ca^{2+} and Mg^{2+}), the insert was transferred to a Petri dish (21 cm^2), 750 μL of a 1% Triton X-100® solution in aq-TM_{Caco} was added and the dish was shaken at 120 rpm on an orbital shaker for 15 min at 37°C under an incubator hood. The cells were scraped of the polycarbonate membrane using a cell scraper (BD Falcon, BD Biosciences Discovery Labware, Bedford, USA), transferred into a 1.5 mL tube (Eppendorf AG, Hamburg, Germany), and frozen at -80°C.

The sample was thawed within 3 min at 37°C under shaking with 1400 rpm (Thermomixer comfort, Eppendorf AG, Hamburg, Germany), 750 μL MeOH was added, and kept on ice bath for 20 min. After shaking for 10 min at 37°C with 1400 rpm, the sample was centrifuged for 3 min at 16,100 g and 25°C (5415R, Eppendorf AG, Hamburg, Germany). The supernatant was transferred to a tube and stored at 4°C. The pellet was disintegrated in 750 μL methanol with 6 pulses of an ultrasonic disintegrator (Branson Sonifier 250, Model 101-063-197, Branson Ultrasonics Corporation, Danbury, CT, USA, instrument settings: output control 2, duty cycle 30%), shaken for 5 min on the thermomixer (37°C and 1400 rpm), and centrifuged at 16,100 g and 25°C for 3 min. After repeating the pellet disintegration once, the methanolic supernatants were united, and the methanol was evaporated under nitrogen flow.

The residue was taken up with the methanol-water supernatant of the first extraction. The sample was shaken on the thermomixer at 1400 rpm and 37°C for 3 min and centrifuged for 25 min at 16,100 g and 25°C before HPLC analysis.

4.3.6 HPLC

Nobilin and its conjugates were analysed by HPLC-UV-MS of Agilent series 1200 equipped with a degaser G1379B, a binary pump G1312A, an autosampler G1367B, a thermostat G1330B, a column oven G1316A, a variable wavelength detector G1314B, and a single quadrupole MS detector G6130A. A C-18 reversed phase column (Agilent Eclipse XBD-C18, 5 μ m, 2 \times 125 mm) and mobile phase consisting of (A) water with 0.1% (v/v) formic acid and 0.05 mM sodium acetate and (B) methanol with 0.1% (v/v) formic acid and 0.05 mM sodium acetate were used. The composition of the mobile phase was varied in a gradient mode: 0 min A:B 50:50, 0-18 min linear change to A:B 10:90, 18-22 min A:B 10:90, 22-23 min linear change to A:B 50:50, and 23-28 min A:B 50:50 with a flow rate of 0.25 mL/min and a runtime of 28 minutes. The samples were cooled in the autosampler to 4°C and the column was heated to 40°C. The ions were generated by atmospheric pressure electrospray ionisation and the MS detector was run in scan mode (m/z 100 - 1000, for all samples) and SIM mode (for samples of the cell extraction) at positive polarity with capillary voltage 4000 V, fragmentor 160 V, drying gas flow 10 L/min, drying gas temperature 350°C and nebulizer pressure 20 psig. Nobilin was detected at 218 nm in UV and at m/z 369, and 716 in MS corresponding to the sodium adduct of nobilin and the sodium adduct of the dimer of nobilin, respectively. The glucuronide was detected at m/z 525, the glutathione conjugate at m/z 654, and the cysteine conjugate at m/z 468 corresponding to their protonated forms. The conjugates were quantified with the calibration curve of nobilin. The LOQ of nobilin for an injection volume of 100 μ L was 0.02 μ g/mL in the UV and 0.004 and 0.0001 μ g/mL in MS scan and SIM mode, respectively. Linearity was fulfilled in UV for concentrations up to 4 μ g/mL and in MS (scan and SIM mode) up to 1 μ g/mL. Standard deviation of measured concentrations of the calibration curve in UV and MS (scan and SIM mode) was at maximum 10%.

4.3.7 Kinetic modeling

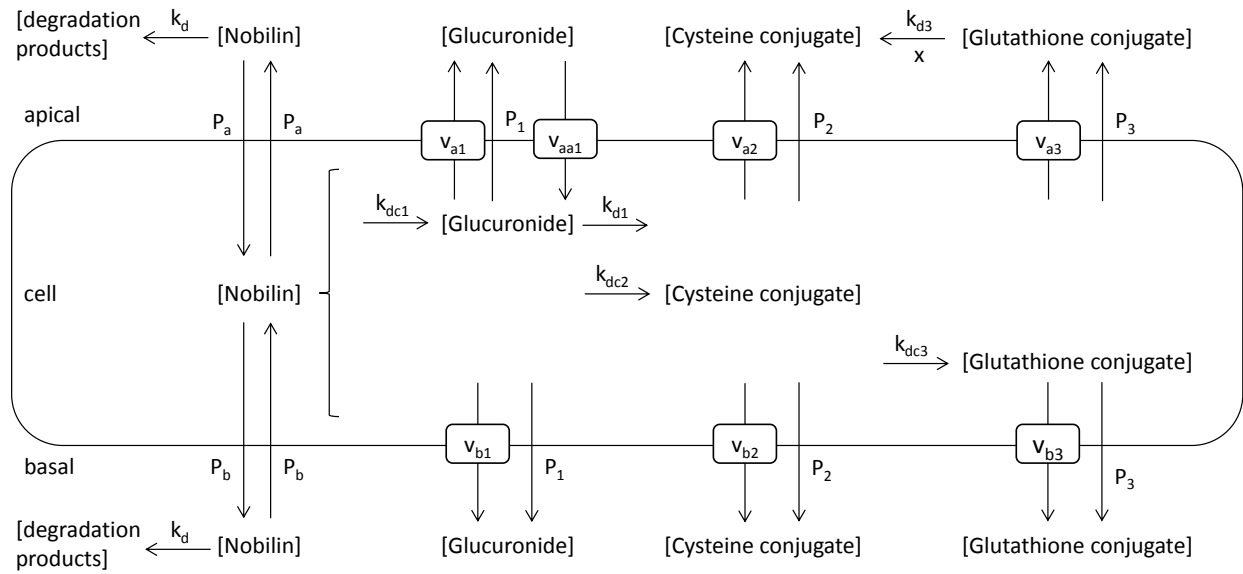
To describe the processes taking place in the course of nobilin absorption in the Caco-2 model and comprising diffusional and carrier mediated membrane permeation, intra- and extra-cellular bioconversion, and chemical degradation, a kinetic model was developed taking into account that:

1. Nobilin permeates the cell membrane by diffusion.
2. Nobilin is chemically degraded in aqueous solution following first order kinetics.³⁰
3. Three conjugation products of nobilin, i.e., glucuronide, cysteine conjugate, and glutathione conjugate are formed in the cells.
4. These conjugation products are transported out of the cells in an asymmetric fashion.

For the proposed model the following assumptions were made:

1. The conjugation products of nobilin cross the cell membrane by diffusion and by the action of the efflux transporters localized in the apical membrane (e.g., P-gp, BCRP, and MRP2) and transporters localized in the basal membrane (e.g., MRP1 and MRP3).^{7,10,22}
2. Glucuronide is transported apically into the cell (e.g. by OATP) and hydrolyzed in the cell by the action of β -glucuronidase.^{7,34,35}
3. The glutathione conjugate is hydrolyzed by the brush border membrane enzymes γ -glutamyltranspeptidase and dipeptidase yielding in part cysteine conjugate.³⁶
4. Conjugation reactions and the hydrolysis of glucuronide and glutathione conjugates obey first order kinetics.
5. Transporter mediated membrane permeation can be described by first order kinetics and the entire amount of substance in the compartment of origin, typically the cellular compartment, is substrate for the transporter. No back-transport occurs.^{29,37}
6. Permeability coefficient (diffusional) of nobilin is different for the apical and the basal membrane because of the difference between the two membranes whereas for glucuronide, cysteine conjugate, and glutathione conjugate the same permeability value applies to both membranes.

Scheme 1 illustrates the diffusional and carrier mediated membrane permeation, the intra- and extra-cellular bioconversion of nobilin and its conjugation products, and the chemical degradation of nobilin. The noted parameters are used in the equations of the model.



Scheme 1: Transport of nobilin and its conjugates.

A system of differential equations was established describing the change of concentration of nobilin and its three conjugation products as a function of time in the apical, the cellular, and the basolateral compartments for apical-to-basal and basal-to-apical transport taking into consideration the processes shown in Scheme 1. Similar but simpler models were described by this group previously.^{29,38,39}

The system of equations is given below:

Nobilin

apical-to-basal (index ab):

$$\frac{dCA_{ab}}{dt} = -P_a \cdot (CA_{ab} - K_{a/c} \cdot CC_{ab}) \cdot \frac{S}{VA} - k_d \cdot CA_{ab} \quad \text{Equation (1)}$$

$$\frac{dCB_{ab}}{dt} = P_b \cdot (K_{a/c} \cdot CC_{ab} - CB_{ab}) \cdot \frac{S}{VB} - k_d \cdot CB_{ab} \quad \text{Equation (2)}$$

$$\frac{dCC_{ab}}{dt} = P_a \cdot (CA_{ab} - K_{a/c} \cdot CC_{ab}) \cdot \frac{S}{VC} - P_b \cdot (K_{a/c} \cdot CC_{ab} - CB_{ab}) \cdot \frac{S}{VC} - k_{dc} \cdot CC_{ab} \quad \text{Equation (3)}$$

basal-to-apical (index ba):

$$\frac{dCA_{ba}}{dt} = P_a \cdot (K_{a/c} \cdot CC_{ba} - CA_{ba}) \cdot \frac{S}{VA} - k_d \cdot CA_{ba} \quad \text{Equation (4)}$$

$$\frac{dCB_{ba}}{dt} = -P_b \cdot (CB_{ba} - K_{a/c} \cdot CC_{ba}) \cdot \frac{S}{VB} - k_d \cdot CB_{ba} \quad \text{Equation (5)}$$

$$\frac{dCC_{ba}}{dt} = -P_a \cdot (K_{a/c} \cdot CC_{ba} - CA_{ba}) \cdot \frac{S}{VC} + P_b \cdot (CB_{ba} - K_{a/c} \cdot CC_{ba}) \cdot \frac{S}{VC} - k_{dc} \cdot CC_{ba} \quad \text{Equation (6)}$$

where, CA, CB, and CC are concentration in the apical, basal, and cellular compartments, respectively, P_a and P_b are permeability coefficient of the apical and the basal membranes, respectively, $K_{a/c}$ is the

partition coefficient between apical and cellular compartment, k_d is the chemical degradation rate constant in aq-TM_{Caco}, k_{dc} is the total conjugation rate constant in the cell, V_A , V_B , and V_C are volume of the apical, basal, and cellular compartments, respectively, S is the surface area (4.7 cm²), and t is time. The cellular volume was 0.0094 mL calculated with a monolayer thickness of 20 μm and k_d was determined previously to be $1.17 \times 10^{-4} \text{ s}^{-1}$ for nobilin and $1.08 \times 10^{-4} \text{ s}^{-1}$ for nobilin as plant extract.⁴⁰

A combined permeability coefficient, P , applying to both membranes was calculated from P_a and P_b by Equation (7) and the standard error with Equation (8).

$$P = \frac{2P_a P_b}{P_a + P_b} \quad \text{Equation (7)}$$

$$SE = \sqrt{\frac{4}{(P_a + P_b)^4} \cdot (P_b^4 \cdot (SE)_a^2 + P_a^4 \cdot (SE)_b^2)} \quad \text{Equation (8)}$$

The extent of in vitro absorption was introduced to quantify the maximal amount of intact nobilin appearing in the basal compartment and was expressed as the relative fraction absorbed given by Equation (9). The denominator of Equation (9) gives the amount of nobilin in the basal compartment at equilibrium when neither chemical degradation nor bioconversion takes place and was defined as 100% in vitro absorption.

$$F_a = \frac{\int_0^{t_{max}} P_b \cdot (K_{a/c} \cdot CC_{ab} - CB_{ab}) \cdot S \, dt}{\int_0^{t_{max}^o} P_b \cdot (K_{a/c} \cdot CC_{ab}^o - CB_{ab}^o) \cdot S \, dt} \quad \text{Equation (9)}$$

where, F_a is the relative fraction absorbed, CB_{ab}^o and CC_{ab}^o is concentration in the basal and cellular compartment, respectively, when neither chemical degradation nor bioconversion take place, and t_{max} and t_{max}^o is the time at which maximum absorption is observed. CB_{ab}^o and CC_{ab}^o were simulated using the determined values of P_b and $K_{a/c}$.

Glucuronide (conjugate 1)

apical-to-basal (index ab):

$$\begin{aligned} \frac{dMA1_{ab}}{dt} = & P_1 \cdot (MC1_{ab} - MA1_{ab}) \cdot \frac{S}{VA} + v_{a1} \cdot (MC1_{ab} \cdot VC) \cdot \frac{S}{VA} \\ & - v_{aa1} \cdot (MA1_{ab} \cdot VA) \cdot \frac{S}{VA} \end{aligned} \quad \text{Equation (10)}$$

$$\frac{dMB1_{ab}}{dt} = P_1 \cdot (MC1_{ab} - MB1_{ab}) \cdot \frac{S}{VB} + v_{b1} \cdot (MC1_{ab} \cdot VC) \cdot \frac{S}{VB} \quad \text{Equation (11)}$$

$$\begin{aligned} \frac{dMC1_{ab}}{dt} = & k_{dc1} \cdot CC_{ab} - P_1 \cdot (MC1_{ab} - MA1_{ab}) \cdot \frac{S}{VC} - P_1 \cdot (MC1_{ab} - MB1_{ab}) \cdot \frac{S}{VC} \\ & - v_{a1} \cdot (MC1_{ab} \cdot VC) \cdot \frac{S}{VC} + v_{aa1} \cdot (MA1_{ab} \cdot VA) \cdot \frac{S}{VC} \\ & - v_{b1} \cdot (MC1_{ab} \cdot VC) \cdot \frac{S}{VC} - k_{d1} \cdot MC1_{ab} \end{aligned} \quad \text{Equation (12)}$$

basal-to-apical (index ba):

$$\begin{aligned} \frac{dMA1_{ba}}{dt} = & P_1 \cdot (MC1_{ba} - MA1_{ba}) \cdot \frac{S}{VA} + v_{a1} \cdot (MC1_{ba} \cdot VC) \cdot \frac{S}{VA} \\ & - v_{aa1} \cdot (MA1_{ba} \cdot VA) \cdot \frac{S}{VA} \end{aligned} \quad \text{Equation (13)}$$

$$\frac{dMB1_{ba}}{dt} = P_1 \cdot (MC1_{ba} - MB1_{ba}) \cdot \frac{S}{VB} + v_{b1} \cdot (MC1_{ba} \cdot VC) \cdot \frac{S}{VB} \quad \text{Equation (14)}$$

$$\begin{aligned} \frac{dMC1_{ba}}{dt} = & k_{dc1} \cdot CC_{ba} - P_1 \cdot (MC1_{ba} - MA1_{ba}) \cdot \frac{S}{VC} - P_1 \cdot (MC1_{ba} - MB1_{ba}) \cdot \frac{S}{VC} \\ & - v_{a1} \cdot (MC1_{ba} \cdot VC) \cdot \frac{S}{VC} + v_{aa1} \cdot (MA1_{ba} \cdot VA) \cdot \frac{S}{VC} \\ & - v_{b1} \cdot (MC1_{ba} \cdot VC) \cdot \frac{S}{VC} - k_{d1} \cdot MC1_{ba} \end{aligned} \quad \text{Equation (15)}$$

Cysteine conjugate (conjugate 2)

apical-to-basal (index ab):

$$\frac{dMA2_{ab}}{dt} = P_2 \cdot (MC2_{ab} - MA2_{ab}) \cdot \frac{S}{VA} + v_{a2} \cdot (MC2_{ab} \cdot VC) \cdot \frac{S}{VA} + \frac{k_{d3} \cdot MA3_{ab}}{x} \quad \text{Equation (16)}$$

$$\frac{dMB2_{ab}}{dt} = P_2 \cdot (MC2_{ab} - MB2_{ab}) \cdot \frac{S}{VB} + v_{b2} \cdot (MC2_{ab} \cdot VC) \cdot \frac{S}{VB} \quad \text{Equation (17)}$$

$$\begin{aligned} \frac{dMC2_{ab}}{dt} = & k_{dc2} \cdot CC_{ab} - P_2 \cdot (MC2_{ab} - MA2_{ab}) \cdot \frac{S}{VC} - P_2 \cdot (MC2_{ab} - MB2_{ab}) \cdot \frac{S}{VC} \\ & - v_{a2} \cdot (MC2_{ab} \cdot VC) \cdot \frac{S}{VC} - v_{b2} \cdot (MC2_{ab} \cdot VC) \cdot \frac{S}{VC} \end{aligned} \quad \text{Equation (18)}$$

basal-to-apical (index ba):

$$\frac{dMA2_{ba}}{dt} = P_2 \cdot (MC2_{ba} - MA2_{ba}) \cdot \frac{S}{VA} + v_{a2} \cdot (MC2_{ba} \cdot VC) \cdot \frac{S}{VA} + \frac{k_{d3} \cdot MA3_{ba}}{x} \quad \text{Equation (19)}$$

$$\frac{dMB2_{ba}}{dt} = P_2 \cdot (MC2_{ba} - MB2_{ba}) \cdot \frac{S}{VB} + v_{b2} \cdot (MC2_{ba} \cdot VC) \cdot \frac{S}{VB} \quad \text{Equation (20)}$$

$$\begin{aligned} \frac{dMC2_{ba}}{dt} = & k_{dc2} \cdot CC_{ba} - P_2 \cdot (MC2_{ba} - MA2_{ba}) \cdot \frac{S}{VC} - P_2 \cdot (MC2_{ba} - MB2_{ba}) \cdot \frac{S}{VC} \\ & - v_{a2} \cdot (MC2_{ba} \cdot VC) \cdot \frac{S}{VC} - v_{b2} \cdot (MC2_{ba} \cdot VC) \cdot \frac{S}{VC} \end{aligned} \quad \text{Equation (21)}$$

Glutathione conjugate (conjugate 3)

apical-to-basal (index ab):

$$\frac{dMA3_{ab}}{dt} = P_3 \cdot (MC3_{ab} - MA3_{ab}) \cdot \frac{S}{VA} + v_{a3} \cdot (MC3_{ab} \cdot VC) \cdot \frac{S}{VA} - (k_{d3} \cdot MA3_{ab}) \quad \text{Equation (22)}$$

$$\frac{dMB3_{ab}}{dt} = P_3 \cdot (MC3_{ab} - MB3_{ab}) \cdot \frac{S}{VB} + v_{b3} \cdot (MC3_{ab} \cdot VC) \cdot \frac{S}{VB} \quad \text{Equation (23)}$$

$$\begin{aligned} \frac{dMC3_{ab}}{dt} = & k_{dc3} \cdot CC_{ab} - P_3 \cdot (MC3_{ab} - MA3_{ab}) \cdot \frac{S}{VC} - P_3 \cdot (MC3_{ab} - MB3_{ab}) \cdot \frac{S}{VC} \\ & - v_{a3} \cdot (MC3_{ab} \cdot VC) \cdot \frac{S}{VC} - v_{b3} \cdot (MC3_{ab} \cdot VC) \cdot \frac{S}{VC} \end{aligned} \quad \text{Equation (24)}$$

basal-to-apical (index ba):

$$\frac{dMA3_{ba}}{dt} = P_3 \cdot (MC3_{ba} - MA3_{ba}) \cdot \frac{S}{VA} + v_{a3} \cdot (MC3_{ba} \cdot VC) \cdot \frac{S}{VA} - (k_{d3} \cdot MA3_{ba}) \quad \text{Equation (25)}$$

$$\frac{dMB3_{ba}}{dt} = P_3 \cdot (MC3_{ba} - MB3_{ba}) \cdot \frac{S}{VB} + v_{b3} \cdot (MC3_{ba} \cdot VC) \cdot \frac{S}{VB} \quad \text{Equation (26)}$$

$$\begin{aligned} \frac{dMC3_{ba}}{dt} = & k_{dc3} \cdot CC_{ba} - P_3 \cdot (MC3_{ba} - MA3_{ba}) \cdot \frac{S}{VC} - P_3 \cdot (MC3_{ba} - MB3_{ba}) \cdot \frac{S}{VC} \\ & - v_{a3} \cdot (MC3_{ba} \cdot VC) \cdot \frac{S}{VC} - v_{b3} \cdot (MC3_{ba} \cdot VC) \cdot \frac{S}{VC} \end{aligned} \quad \text{Equation (27)}$$

where, MA, MB, and MC are concentration of the conjugate in the apical, basal, and cellular compartments, respectively, the digit 1, 2, and 3 in the name of the variable or as index denotes glucuronide, cysteine conjugate, and glutathione conjugate, respectively, k_{dc} is conjugation rate constant, k_{d1} is the hydrolysis rate constant of glucuronide in the cell, k_{d3} is hydrolysis rate constant of glutathione conjugate at the apical membrane, x is the inverse fraction of glutathione conjugate that is metabolized to cysteine conjugate, v is carrier mediated transport rate constant whereas indices a, aa, and b indicate apical efflux, apical influx, and basal efflux, respectively, and all other symbols were defined above.

The total conjugation rate constant in the cell, k_{dc} , was set equal to the sum of the individual rate constants k_{dc1} , k_{dc2} , k_{dc3} , and k_{dcr} .

$$k_{dc} = k_{dc1} + k_{dc2} + k_{dc3} + k_{dcr} \quad \text{Equation (28)}$$

Because conjugation products were quantified using nobilin as a standard and a possible chemical degradation of the conjugates or a further metabolite of nobilin were not detected, the parameter k_{dcr} was introduced to establish mass balance in the equations.

The system of differential equations was numerically solved and simultaneously fitted to experimental concentration or mass data of nobilin and its three conjugation products in all three compartments in both transport directions with Equation (28) as a constraint using the EASY-FIT® software.⁴¹ From the least square regression analysis, values of the permeability coefficients, carrier mediated transport rate constants, and bioconversion constants which were treated as adjustable parameters were deduced. Equation (1) to (6) were first fitted only to the nobilin data to deduce k_{dc} and then the system of Equation (1) through (6) and (10) through (27) was fitted to all data keeping the k_{dc} value fixed.

The reduction of the volume in the apical and basal compartment because of sampling was described by the following empirical equations.

$$VA = 1.6241 - 0.341t + 0.0821t^2 - 0.0148t^3 \quad \text{Equation (29)}$$

$$VB = 2.8241 - 0.341t + 0.0821t^2 - 0.0148t^3 \quad \text{Equation (30)}$$

Significance test was carried out based on the incidence of overlap of the confidence intervals at the $p = 0.01$ level of two estimated values of a parameter from different experimental sets. In addition, the relation

$$F = \frac{(\text{value}(\alpha) - \text{value}(\beta))^2}{(SE)_{\alpha}^2 + (SE)_{\beta}^2} \quad \text{Equation (31)}$$

was used where, $\text{value}(\alpha)$ and $\text{value}(\beta)$ are two values of a parameter and $(SE)_{\alpha}$ and $(SE)_{\beta}$ are the corresponding standard errors of the estimates. Significance was determined by comparing F with the critical value $F_{0.01[1,df]}$, where df is degrees of freedom of residuals for which $df = 8$ was used. An agreement between the two tests was required for declaring statistical significance of the difference between two values of a parameter; this agreement was observed in the vast majority of cases.

4.4 RESULTS

4.4.1 Transport of nobilin and its conjugates

Typical chromatograms of samples of the apical and basal compartments for both transport directions of the permeation experiment at 10 min and 2.5 h are shown in Figure 1. Nobilin was detected at m/z 369.2 and three additional peaks were detected with m/z 525, 468, and 654. Nobilin is present in the donor compartment at 10 min while marked peaks of the three further substances are evident in the apical and the basal solutions at 2.5 h. The m/z 525 peak was attributed to a conjugate of nobilin with glucuronic acid and addition of two hydrogen atoms detected as $[M+H]^+$. The m/z 468 peak indicated the formation of a conjugate of nobilin with cysteine and the m/z 654 peak a conjugation with glutathione, both detected as $[M+H]^+$.

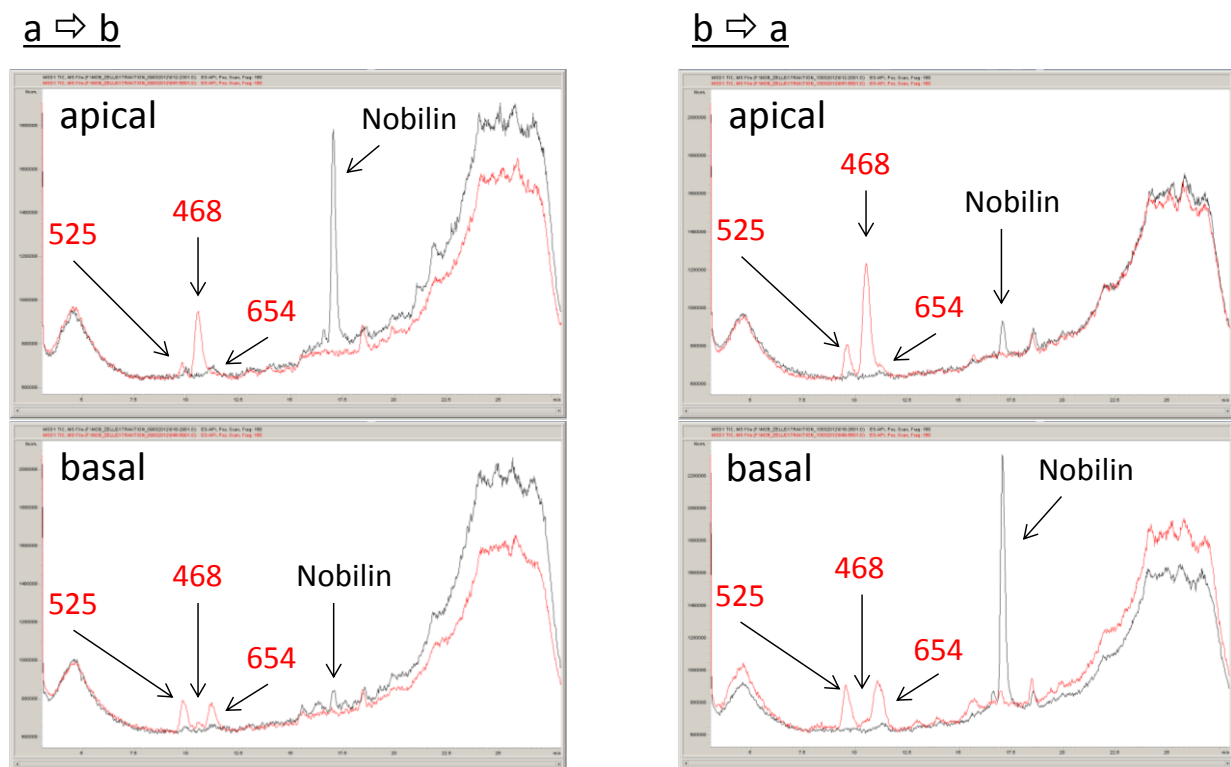


Figure 1: MS-chromatograms of the apical and basal compartment for the transport direction apical-to-basal ($a \Rightarrow b$) and basal-to-apical ($b \Rightarrow a$). Chromatograms in dark color with the nobilin peak represent the time point 10 min and the chromatograms in red (light) color with m/z 525, 468, and 654 represent the time point 2.5 h.

Figure 2 shows results of nobilin and Figure 3 results of the three conjugation products of nobilin in the Caco-2 permeation experiment. Drawn lines were obtained by simultaneous fitting of the model to all experimental data. A rapid permeation of nobilin from the donor into the cells and onward in the receiver compartment is observed. Nobilin concentration decreased quickly in all three compartments and reached near zero concentrations after 2.5 hours. Fitted curves are in good agreement with the data.

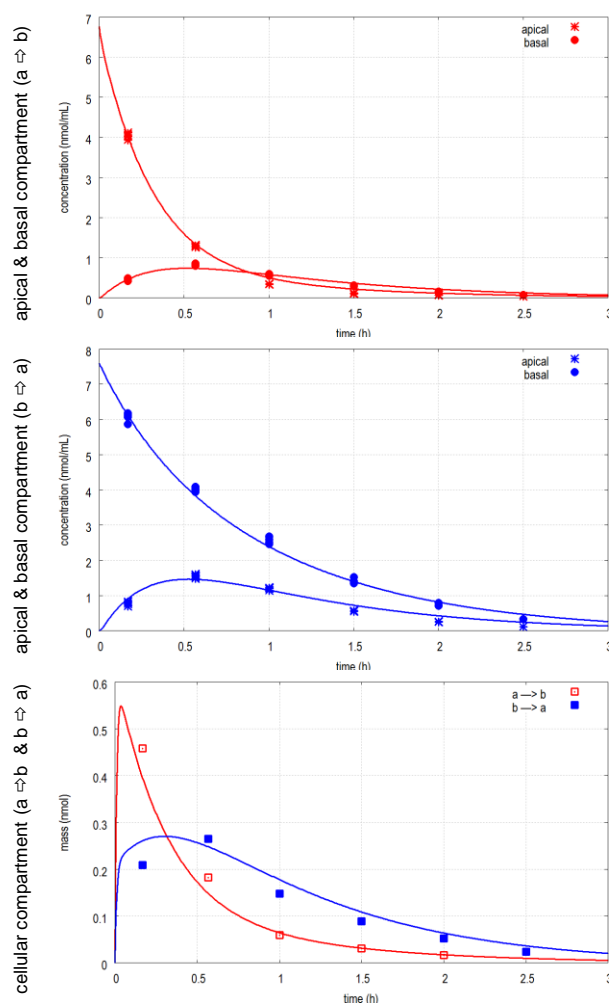


Figure 2: Nobilin concentration in the apical-to-basal (top panel, red) and the basal-to-apical (middle panel, blue) transport direction in both compartments and nobilin mass in the cellular compartment (bottom panel) in both transport directions as a function of time. (*) apical concentration, (●) basal concentration, (□) mass in apical-to-basal transport direction (red), (■) mass in basal-to-apical transport direction (blue). Symbols represent measured data and lines fitted model curves.

Rather large concentrations / amounts of all three conjugation products were detected. The concentration of glucuronide in the apical solution increased in the beginning and later decreased while concentration in the basal solution steadily increased over time. As a result, apical concentration was at early time points greater and at later times lower than the basal concentration. This was true for both transport directions. The concentration-time profiles of the cysteine conjugate were different. Apical and basal concentrations increased constantly with time but the former was considerably greater than the latter throughout the experiment in both transport directions. Glutathione conjugate concentration pattern, finally, was similar to that of glucuronide, apical concentrations, however, briefly increased and then rapidly declined while basal concentrations steadily increased reaching a large difference to the apical ones. The amount of all conjugates in the cell increased at first and then decreased to very low levels over time in both transport directions. These results demonstrate that transport of the conjugates out of the cell was highly asymmetric. Model curves generally described the data adequately.

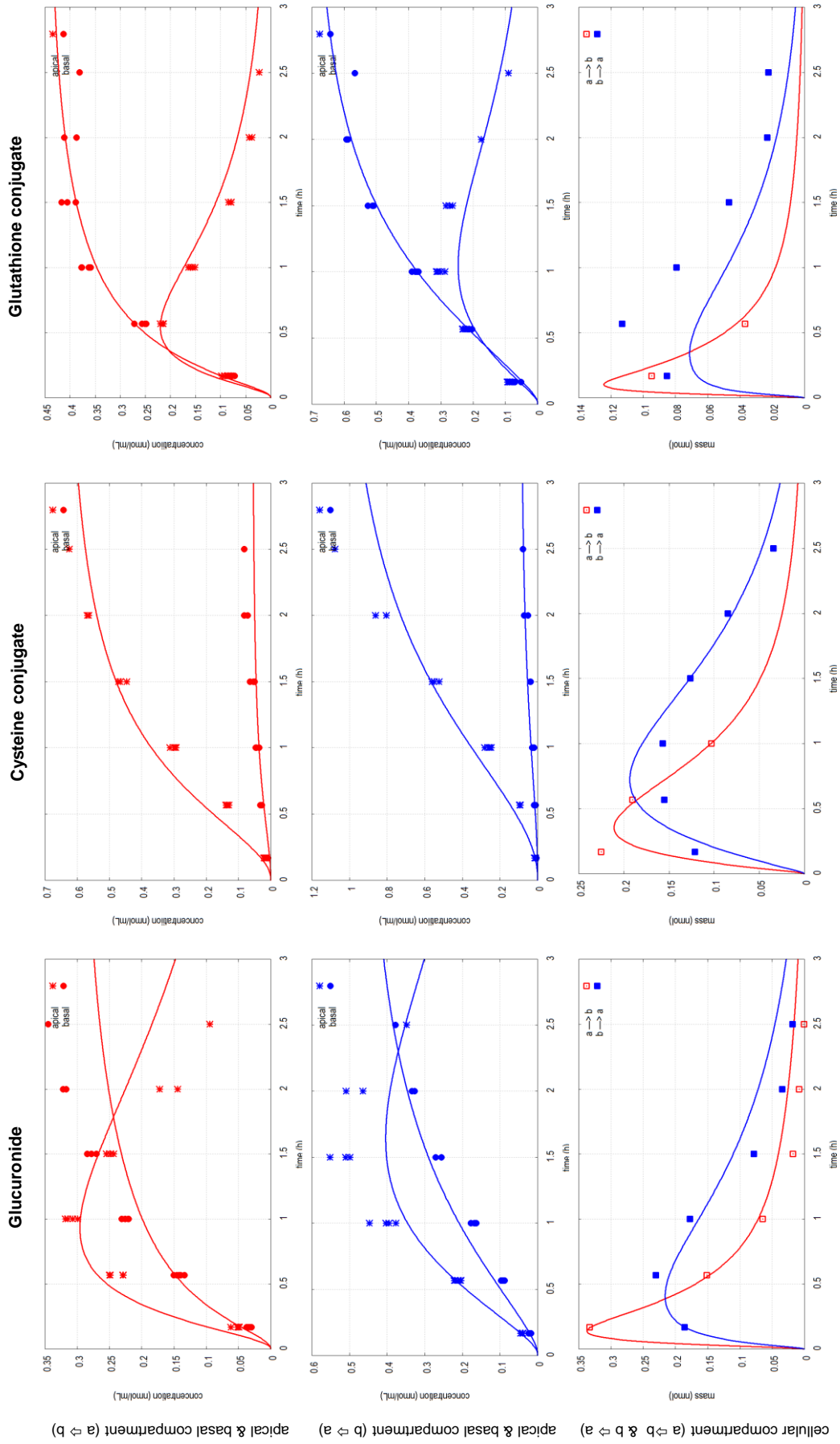


Figure 3: Concentration of (left to right) glucuronide, cysteine conjugate, and glutathione conjugate in the apical-to-basal (top panels, red) and the basal-to-apical (middle panels, blue) transport direction in both compartments and mass of (left to right) glucuronide, cysteine conjugate, and glutathione conjugate in the cellular compartment (bottom panels) in both transport directions as a function of time. (●) apical concentration, (●) basal concentration, (□) mass in apical-to-basal transport direction (red), (■) mass in basal-to-apical transport direction (blue). Symbols represent measured data and lines fitted model curves.

The parameter values deduced by fitting Equation (1) to (6) and (10) to (27) to the data are given in Table 1. Nobilin had a quite large permeability coefficient (2.75×10^{-4} cm/s) and a small partition coefficient $K_{a/c} = 0.058$. Bioconversion rate constant in the cell was much larger than the degradation rate constant in solution ($k_d = 1.17 \times 10^{-4} \text{ s}^{-1}$ versus $k_{dc} = 7.64 \times 10^{-3} \text{ s}^{-1}$).⁴⁰ The relative fraction absorbed was 38%.

Conversion of nobilin to glucuronide in the cell took place at the highest rate followed in decreasing order by the formation of the glutathione conjugate and the cysteine conjugate. Formation of glucuronide, glutathione conjugate, and cysteine conjugate accounted for 51%, 28%, and 10%, respectively, of total bioconversion. The introduced correction rate constant k_{dcr} accounted for less than 11% of total conversion.

Transport of the conjugation products out of the cell was considered to take place by diffusion and carrier mediated efflux. The permeability coefficients of the glucuronide (5.24×10^{-8} cm/s), the cysteine conjugate (3.68×10^{-8} cm/s), and the glutathione conjugate (1.24×10^{-7} cm/s) were estimated from the experiment with the combination of the inhibitors verapamil, Ko143, and MK-571 by omitting the terms of carrier mediated transport. The obtained values were used as fixed parameters in all experiments for the estimation of the other parameter values. The permeability coefficients of the conjugation products were 2000- to 20,000-fold smaller compared to that of nobilin. The estimated carrier mediated transport rate constants differed between the conjugates and also between apical and basal efflux and apical influx, where applicable. The glutathione conjugate showed the largest carrier mediated transport rate constant for the apical and basal membrane compared to glucuronide (3.4- and 5.5-fold difference) and cysteine conjugate (4.9- and 29-fold difference). The glucuronide, in turn, exhibited a slightly larger apical and a higher basal efflux rate constant than the cysteine conjugate. Apical efflux rates were higher than basal rates for glucuronide and cysteine conjugate while the opposite was true for the glutathione conjugate. The apical influx rate constant of glucuronide was marked lower than the efflux constants of this conjugate. The hydrolysis rate constant of glucuronide in the cell was found to be almost as large as the conjugation rate constant of glucuronidation. The hydrolysis rate constant of the glutathione conjugate in the apical compartment was 4-fold smaller than the rate constant of glutathione conjugation. Approximately one third of the glutathione conjugate yielded cysteine conjugate after hydrolysis.

Table 1: Kinetic parameter values of nobilin and its conjugates.^a

Parameter	Nobilin	Glucuronide	Cysteine conjugate	Glutathione conjugate
P [cm/s]	2.75×10^{-4} (1.18×10^{-5})	5.24×10^{-8}	3.68×10^{-8}	1.24×10^{-7}
K_{a/c}	0.058 (0.0025)	-	-	-
F_a	38%	-	-	-
v_a [s⁻¹cm⁻²]	-	0.79 (0.069)	0.54 (0.063)	2.65 (0.20)
v_{aa} [s⁻¹cm⁻²]	-	0.16 (0.027)	-	-
v_b [s⁻¹cm⁻²]	-	0.62 (0.031)	0.12 (0.0064)	3.44 (0.17)
k_{dc} [s⁻¹]	7.64×10^{-3} (3.00×10^{-4})	-	-	-
k_{dc1,2,3} [s⁻¹]	-	3.88×10^{-3} (7.25×10^{-4})	7.77×10^{-4} (6.67×10^{-5})	2.13×10^{-3} (1.03×10^{-4})
k_{d1} [s⁻¹]	-	3.10×10^{-3} (8.89×10^{-4})	-	-
k_{d3} [s⁻¹]	-	-	-	4.97×10^{-4} (5.00×10^{-5})
x	-	-	3.5 (1.35)	-

^a Deduced values from model fitting and standard error (in brackets).

P is permeability coefficient, K_{a/c} is partition coefficient between the apical and the cellular compartment, F_a is the relative fraction absorbed, v is the carrier mediated transport rate constant (index a, aa, and b denote apical efflux, apical influx, and basal efflux, respectively), k_{dc} is the total conjugation rate constant of nobilin, k_{dc1,2,3} is conjugation rate constant (index 1, 2, and 3 refers to the conjugates), k_{d1} is hydrolysis rate constant of glucuronide, k_{d3} is hydrolysis rate constant of glutathione conjugate, x is the inverse fraction of glutathione conjugate that is metabolized to cysteine conjugate.

4.4.2 Influence of transporter inhibition on the transport of nobilin and its conjugates

The estimated parameter values of nobilin in the presence of inhibitors of membrane carriers are shown in Figure 4. Concentration profiles of nobilin from the permeation experiments with the inhibitors are not shown (see appendix). The added inhibitors had generally no influence on the permeability coefficient or the partition coefficient K_{a/c}. Ko143 and MK-571 caused a significant reduction of the total conjugation rate constant of 1.5- and 15-fold, respectively. The inhibitor combination verapamil/Ko143/MK-571 yielded a k_{dc} value that was not statistically different from zero. Verapamil had no effect on k_{dc} while leukotriene C4 caused a rise of this parameter value. The reduction of the total conjugation rate constant was accompanied by an increase of the relative fraction absorbed from 38% with no inhibitor to 52%, 74%, and 81% for Ko143, MK-571, and the combination verapamil/Ko143/MK-571, respectively. The reported value of k_{dc} for the inhibitor combination verapamil/Ko143/MK-571 corresponds to three fold the standard error of the estimate because the estimated value of the parameter was within the error margin of the calculation.

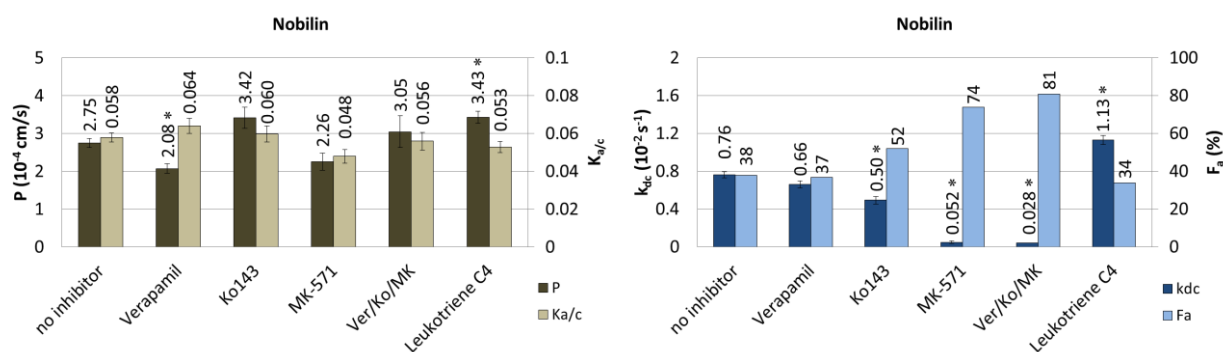


Figure 4: Deduced values (columns) and standard errors (bars) of permeability coefficient P , partition coefficient $K_{a/c}$ (dark and light columns, respectively, on left panel), total conjugation rate constant k_{dc} , and relative fraction absorbed F_a (dark and light columns, respectively, on right panel) of nobilin from model fitting in the presence of inhibitors. * $p < 0.01$.

The effect of the transport inhibitors on the estimated parameter values of the conjugates is shown in Figure 5. The apical and the basal efflux rate constants of glucuronide were reduced by 2- to 3-fold by verapamil and 20- to 170-fold by MK-571, respectively. The inhibitor combination did not further suppress efflux. The apical influx of glucuronide was not affected by verapamil while for MK-571 and the inhibitor combination no independent estimation was possible and the value was fixed to the average of the other experiments. The apical and the basal efflux rate constants of the cysteine conjugate were reduced 4.5- and 6.3-fold, respectively, by verapamil and MK-571 reduced the apical constant 16.9-fold and completely abolished basal efflux. Ko143, additionally, diminished basal efflux of the cysteine conjugate, and the inhibitor combination had a comparable effect as MK-571. The apical and the basal efflux rate constant of the glutathione conjugate was reduced only by MK-571 13.9- and 61-fold, respectively. Ko143 had no effect on the transport of glucuronide and glutathione conjugate and verapamil and leukotriene C4 had no effect on the transport of glutathione conjugate. Finally, for the basal efflux of glucuronide and cysteine conjugate an increase of the rate constant by leukotriene C4 was observed.

The rate constant of formation of glucuronide was significantly diminished in the presence of Ko143, MK-571, and the inhibitor combination. The formation rate constant of cysteine conjugate was reduced in the presence of MK-571, the inhibitor combination, and leukotriene C4. Finally, formation of the glutathione conjugate was diminished in the presence of all used inhibitors. The hydrolysis rate constant of glucuronide in the cell, k_{d1} , was reduced only by the inhibitor combination and the apical hydrolysis of the glutathione conjugate was not affected by the used inhibitors. The fraction of glutathione conjugate metabolized to cysteine conjugate was not affected by the inhibitors and varied between 0.21 and 1.

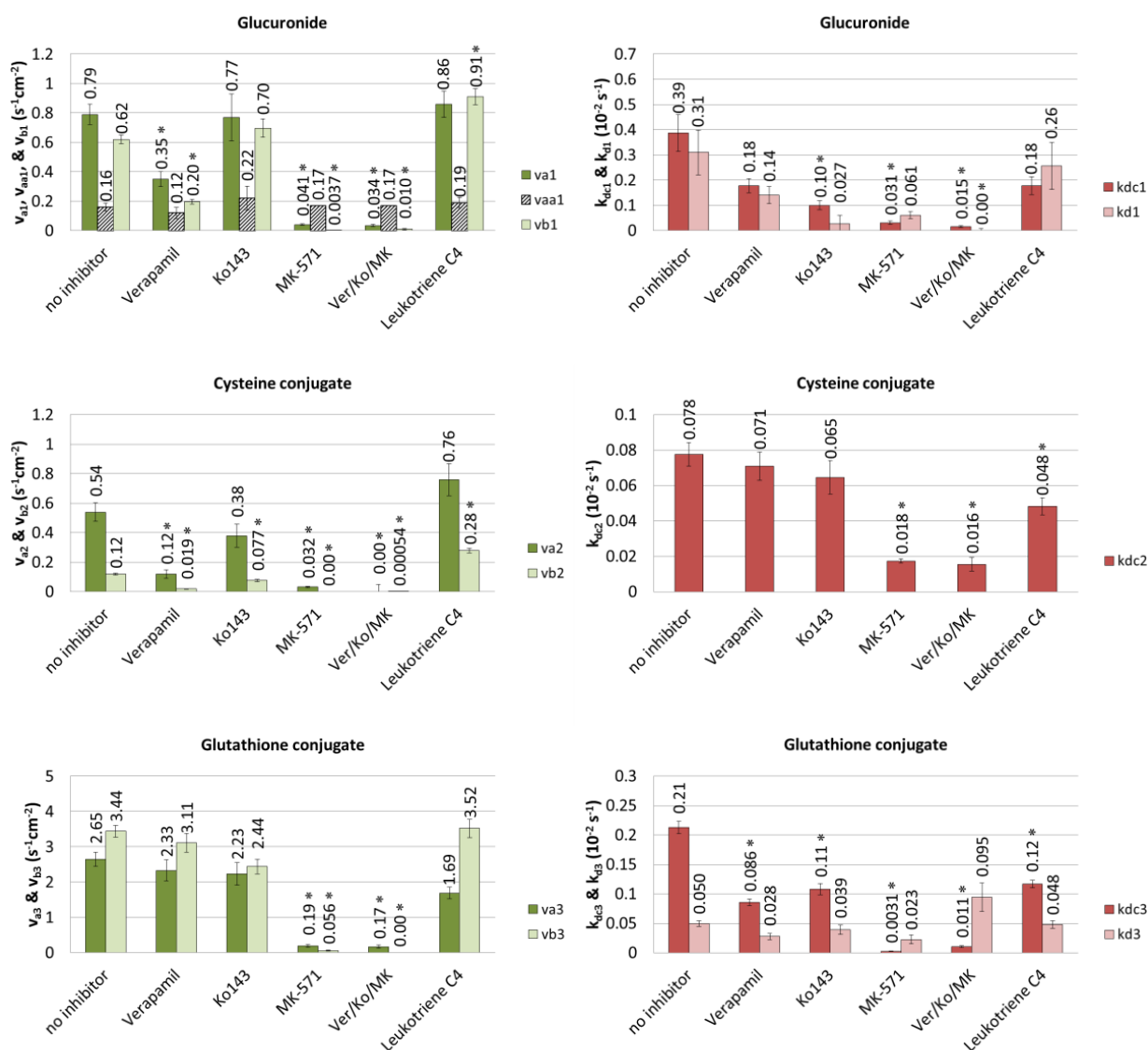


Figure 5: Deduced values (columns) and standard errors (bars) of carrier mediated apical efflux rate v_a , carrier mediated apical influx rate v_{aa} , carrier mediated basal efflux rate v_b (dark, diagonally hatched, and light columns, respectively, on left panel), conjugation rate constant k_{dc} , and hydrolysis rate constant of glucuronide and glutathione conjugate k_d (dark and light columns, respectively, on right panel) of the three conjugates (index 1, 2, and 3 refers to the conjugates) from model fitting in the presence of inhibitors. * $p < 0.01$.

4.4.3 Influence of the full extract and extract ingredients on the transport of nobilin and its conjugates

The estimated parameter values of nobilin applied as plant extract and nobilin in the presence of different extract ingredients are shown in Figure 6. Concentration profiles of nobilin are not shown (see appendix) for these permeation experiments. The full extract and the extract ingredients had no effect on the permeability coefficient while the extract, EtOH, and apigenin 2 reduced the partition coefficient $K_{a/c}$. The total conjugation rate constant was significantly reduced in the presence of the extract, EtOH, sesquiterpene lactone fraction, essential oil, luteolin, and the combination of apigenin 2 and luteolin,

whereas the full extract exhibited the strongest effect. The relative fraction absorbed was increased markedly only for the full extract from 38%, for the pure compound, to 71%.

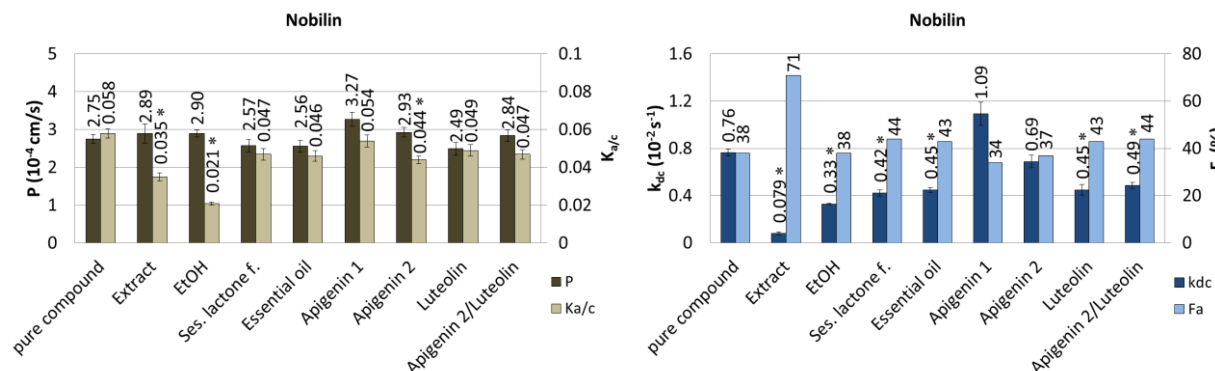


Figure 6: Deduced values (columns) and standard errors (bars) of permeability coefficient P , partition coefficient $K_{a/c}$ (dark and light columns, respectively, on left panel), total conjugation rate constant k_{dc} and relative fraction absorbed F_a (dark and light columns, respectively, on right panel) of nobilin from model fitting in the presence of full extract and ingredients of the extract. * $p < 0.01$.

The impact of extract and extract ingredients on the estimated parameter values of the conjugates is shown in Figure 7. Application of nobilin as plant extract caused a reduction of the apical efflux rate constant of glucuronide, cysteine conjugate, and glutathione conjugate by 2.7-, 2.6-, and 6-fold, respectively. The basal efflux rate constant of cysteine conjugate and glutathione conjugate was decreased by the extract 2- and 2.7-fold, respectively. Additionally, the extract decreased the conjugation constant of glucuronide, cysteine conjugate, and glutathione conjugate in the cell 14-, 4-, and 6-fold, respectively.

The apical efflux rate constant of glucuronide was significantly decreased only by the sesquiterpene lactone fraction whereas the basal efflux was reduced by the combination of apigenin 2 and luteolin. The apical efflux rate constant of cysteine conjugate was diminished by the sesquiterpene lactone fraction, essential oil, and apigenin 1 2.8-, 2.2-, and 6.2-fold, respectively and its basal efflux rate constant was 2.4-, 4.3-, and 2.2-fold smaller in the presence of the sesquiterpene lactone fraction, apigenin 1, and the combination of apigenin 2 and luteolin, respectively. The apical and the basal carrier mediated rate constant of the glutathione conjugate were decreased by the sesquiterpene lactone fraction, essential oil, apigenin 1, and the combination apigenin 2 and luteolin between 1.4- and 7.2-fold.

The apical efflux rate constant of glucuronide was larger in the presence of apigenin 2 and the basal efflux rate constant was increased by EtOH, essential oil, and apigenin 2. The basal efflux of the cysteine conjugate was also increased in the presence of apigenin 2.

The conjugation rate constant of glucuronide was diminished by EtOH, sesquiterpene lactone fraction, apigenin 1, apigenin 2, and luteolin. A decrease of the conjugation rate constant of cysteine and glutathione conjugate was observed in the presence of all ingredients of the extract except for apigenin 1. The fraction which was metabolized from glutathione conjugate to cysteine conjugate was between 0.35 and 1.

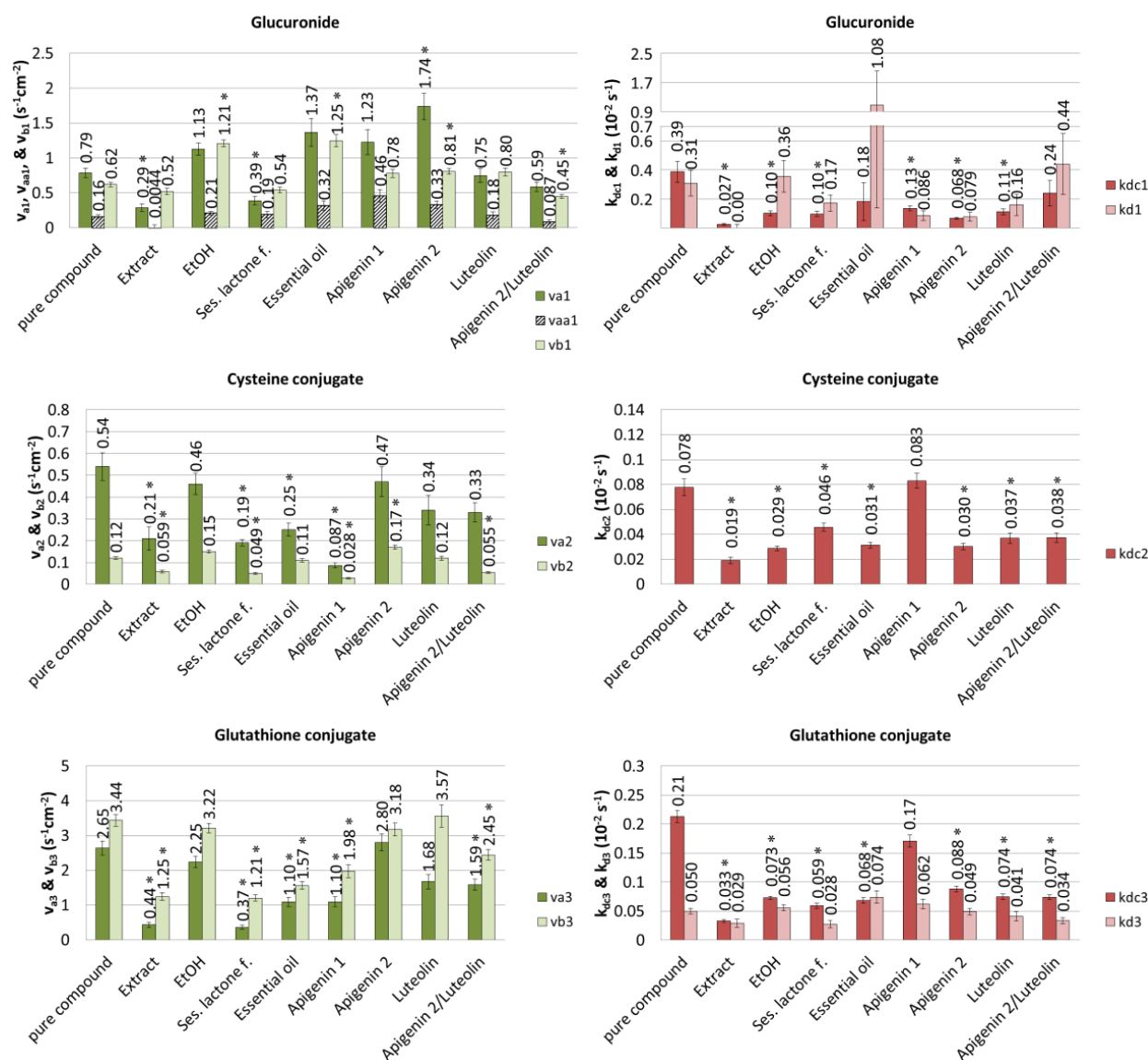


Figure 7: Deduced values (columns) and standard errors (bars) of carrier mediated apical efflux rate v_a , carrier mediated apical influx rate v_{aa} , carrier mediated basal efflux rate v_b (dark, diagonally hatched, and light columns, respectively, on left panel), conjugation rate constant k_{dc} , and hydrolysis rate constant of glucuronide and glutathione conjugate k_d (dark and light columns, respectively, on right panel) of the three conjugates (index 1, 2 and 3 refers to the conjugates) from model fitting in the presence of the full extract and ingredients of the extract. * $p < 0.01$.

4.5 DISCUSSION

Nobilin has moderate lipophilicity ($\text{clog}K_{O/W} 2.572 \pm 0.601$)⁴² and a molecular weight of less than 500 g/mol which are characteristics of a compound with good intestinal permeation.⁴³ The permeability coefficient of 2.75×10^{-4} cm/s determined in this study further confirms that according to the biopharmaceutics classification scheme a large extent of absorption should be expected.⁴⁴ Also, the determined partition coefficient between aqueous solution and cell interior ($K_{a/c} = 0.058$) indicates a high affinity of the molecule for the biological tissue which supports good permeation. However, an in vitro absorption of only 38% was found in the Caco-2 model while there are no reports about the in vivo bioavailability of nobilin. Little is known about the absorption of sesquiterpene lactones in general. The few studies with Caco-2 cells in the literature showed that sesquiterpene lactones are well absorbed by passive diffusion.⁴⁵⁻⁴⁷

In the present Caco-2 experiment, nobilin concentration decreased rapidly in all three compartments. This and the observed low relative absorption were in part due to the chemical instability of nobilin. The degradation kinetics and degradation products of nobilin in aqueous solution were reported elsewhere.³⁰ In addition, the present study shows an extensive bioconversion of nobilin taking place in the Caco-2 cells resulting in the formation of three conjugation products of nobilin, i.e., with glucuronic acid, cysteine, and glutathione. Glucuronidation of nobilin can take place through the action of UDP-glucuronosyltransferase most likely at the hydroxyl group at position 3 (Figure 8).⁴⁸ This enzyme was previously reported to be present in Caco-2 cells.²² The conjugation with cysteine is assumed to take place by non-enzymatic reaction at position 13 or 18 of the molecule (Figure 8). The α -methylene γ -lactone functionality and other $\alpha\beta$ -unsaturated carbonyl structures of sesquiterpene lactones were reported to react by Michaelis addition with cysteine and glutathione in connection with the cytotoxicity of sesquiterpene lactones.^{49,50} The glutathione conjugate was probably formed enzymatically by glutathione S-transferase and by non-enzymatic conjugation at position 13 or 18 (Figure 8).^{22,48} No metabolites were detected in previous absorption studies with sesquiterpene lactones in Caco-2 cells even though those compounds had similar functional groups as nobilin.^{45,46}

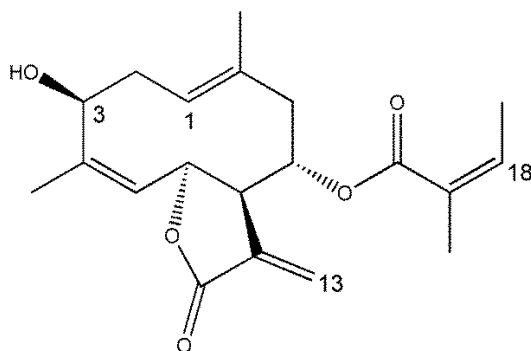


Figure 8: Chemical structure of nobilin with absolute configuration.^{26,30}

The three conjugation products exhibited asymmetric efflux from the cells. To describe the concentration-time profiles of the three conjugates and that of nobilin in a quantitative fashion and evaluate the underlying bioconversion and transport processes, a kinetic model was developed. This model included apical and basal efflux of the conjugates by carrier mediated transport potentially involving P-gp, BCRP, MRP1, MRP2, and MRP3. These transporters are known to be responsible for the efflux of conjugation products of drugs from the cell and were reported to be present in wild type Caco-2 cells in a cross-laboratory study.^{7,10,22} An asymmetric distribution of drug conjugates was also observed in earlier studies with Caco-2 cells.^{12,36} Furthermore, the model considered carrier mediated influx of glucuronide by OATPs in order to account for the decrease of the concentration of glucuronide in the apical compartment. Glucuronic acid conjugates are substrates of OATPs which were reported to be expressed at high levels in Caco-2 cells.^{7,22,25} Glucuronide was further assumed to be hydrolyzed in the cells by β -glucuronidase which was found in Caco-2 cells.^{34,35} Finally, to account for the decrease of glutathione conjugate concentration in the apical compartment, hydrolysis of this conjugate by the brush border enzymes γ -glutamyltranspeptidase and dipeptidase was included in the model. A process concerning carrier mediated transport of S-(pentachlorobutadienyl)glutathione out of Caco-2 cells and metabolism in the apical compartment to the cysteine conjugate was described before.³⁶

The conjugation rate constant followed the rank order glucuronide > glutathione conjugate > cysteine conjugate (Table 1). The enzymatic formation of conjugates seems, therefore, to proceed faster than the non-enzymatic one. The faster formation of glucuronide compared to glutathione conjugate is congruent with the finding that UDP-glucuronosyltransferase is higher expressed than glutathione S-transferase.²² The total bioconversion was considerably more extensive than the chemical degradation in solution as inferred from the larger rate constant and the higher nobilin concentration in the cell than in solution, indicating that bioconversion was the main reason for the low absorption of nobilin. The permeability coefficient of the conjugates was a lot smaller than that of nobilin which is because of the increased hydrophilicity and larger molecular size of the conjugates. Carrier mediated transport is the predominant process by which the conjugates exit the cells. The determined permeability coefficient of glucuronide, for example, corresponds to a clearance value of $2.4 \times 10^{-7} \text{ cm}^3/\text{s}$ which is a lot smaller than the clearance value ($3 \times 10^{-2} \text{ cm}^3/\text{s}$) roughly corresponding to the efflux rate constants of this conjugate. This comparison is also valid for the other conjugates.

The reduction of efflux rate constants by the employed inhibitors provides evidence about the role of the different transporters for the efflux of the conjugates (Figure 5). Apical efflux of glucuronide is shown to take place by P-gp and MRP2 as indicated by the inhibition of this efflux by verapamil and MK-571, respectively. The basal efflux of glucuronide took place by MRP3 and possibly MRP1 as indicated by the effect of MK-571. The effect of verapamil on basal efflux may be due to inhibition of

MRP1 in accordance to observations that verapamil may not be selective and also inhibit MRP1.^{51,52} Apical efflux of cysteine conjugate is suggested to take place by P-gp and MRP2 based on the inhibition of this efflux by verapamil and MK-571, respectively. The basal efflux of cysteine conjugate appeared to take place by MRP3 and possibly MRP1 as indicated by the effect of MK-571. Concerning the effect of verapamil on basal efflux, the explanation discussed for glucuronide may apply also to the cysteine conjugate, whereas the cause of the effect of Ko143 on basal efflux is presently not clear. Apical and basal efflux of the glutathione conjugate is suggested to be mediated by MRP2, and MRP3 (and possibly MRP1), respectively, due to the effect of MK-571. Ko143 did not inhibit apical efflux of any of the conjugates suggesting that BCRP was not involved in their transport out of the cell.

The conjugation rate constant of glucuronide was diminished by MK-571 and Ko143 but not affected by verapamil (Figure 5). For MK-571, this is most likely related to the inhibition of efflux resulting in an accumulation of glucuronide in the cell, which leads to an apparent net slowdown of its formation reaction. A considerable accumulation of glucuronide was found in the cells (not shown, see appendix). The susceptibility of phase II enzymes to product inhibition¹⁷ and a transporter-enzyme interplay between MRPs and UDP-glucuronosyltransferase in Caco-2 studies was also proposed before.^{12,53,54} Furthermore, the possibility of direct inhibition of UDP-glucuronosyltransferase by MK-571 was reported.¹² Although the latter can not be excluded in the present study, the cell accumulation of glucuronide strongly indicates that the reduction of glucuronide formation was due to efflux inhibition. Ko143 seemed to inhibit directly the glucuronidation but not the efflux and caused no accumulation of glucuronide in the cells (not shown, see appendix). This was in contrast to other studies which suggested an interplay also between BCRP and the enzyme.¹⁴ The formation rate constant of cysteine conjugate was decreased by MK-571. This was probably because of the reduced efflux which led to a cellular accumulation of the conjugate (not shown, see appendix) and an apparent net retardation of the conjugation reaction in accordance with the law of mass action. The inhibition of efflux of the cysteine conjugate by verapamil produced a buildup in the cells which apparently was not sufficient to reduce the net formation of this conjugate. The formation of the glutathione conjugate was hindered by MK-571, verapamil, and Ko143. For MK-571, this may be coupled to the inhibition of efflux and also be due to a direct effect on the metabolic enzyme as discussed above for glucuronide. Verapamil and Ko143 seem to have a direct effect on the conjugation reaction or on glutathione S-transferase. An increased efflux of glutathione from the cells elicited by verapamil might also be involved in this effect.^{52,55}

In the experiment with leukotriene C₄, the sum of the individual conjugation constants of glucuronide, cysteine conjugate, and glutathione conjugate accounted for roughly 30% of the total bioconversion constant of nobilin. The reason for this disparity and for the observed increase of the total

bioconversion rate constant while the formation of the cysteine and the glutathione conjugate diminished is currently not understood, neither is the increase of the basal efflux of the glucuronide and the cysteine conjugate elicited by leukotriene C₄, although a similar phenomenon was previously discussed.¹²

The overall reduction of conjugation rate constant comprising the sum of glucuronide, cysteine conjugate, and glutathione conjugate formation was larger for MK-571 than for Ko143 while not being statistically significant for verapamil (Figure 4). The combination of the three inhibitors showed an additive effect and the largest reduction of the conjugation rate constant. The decreasing conjugation had as a result an increase of the relative fraction absorbed of nobiletin in vitro. This positive effect on absorption appeared to be not only because of an inhibition of the bioconversion reaction but, significantly, also because of the inhibition of efflux of the conjugation products from the cell. The possible role of the interplay between conjugation and efflux for drug bioavailability was discussed theoretically before.¹⁸ However, an absorption enhancement based on this interplay has rarely been demonstrated experimentally to the best of the authors' knowledge so far. This study, therefore, provides evidence of a mechanism of absorption regulation based on efflux inhibition of bioconversion products from the cell. This mechanism represents an interesting possibility for improving the absorption of drugs exhibiting extensive conjugation type bioconversion in the intestine.

Interestingly, the full extract increased the relative fraction absorbed of nobiletin from 38% to 71% (Figure 6). This was related to the nearly 10-fold reduction of the total conjugation rate constant. The apical efflux and the conjugation to glucuronide were diminished by the full extract. Also, the apical and basal efflux and the formation of the cysteine conjugate and the glutathione conjugate were reduced by the full extract. A possible reason for the reduction of the formation of the cysteine conjugate by the extract may be the accumulation of this conjugate occurring in the cell (not shown, see appendix) as a result of the inhibition of efflux. This was analogous to the effect of MK-571 discussed above. For the glucuronide and the glutathione conjugate, the extract may have an inhibitory effect on both, the efflux and the conjugation reaction as no notable accumulation of these conjugates was observed in the cell (not shown, see appendix). This is different that the results obtained with MK-571 for which an interplay between the efflux and the conjugation reaction was proposed. Hence, the increased absorption of nobiletin elicited by the extract appears to be because of the direct impeding effect on the enzymatic conjugation reaction and, to a lesser extent, because of efflux inhibition of conjugates.

Of the different ingredients of the ethanolic extract of *Chamomillae romanae flos* all except of apigenin were found to decrease the conjugation of nobiletin. The sesquiterpene lactone fraction had the same effect on efflux and conjugation for all three conjugation products as the full extract. *Chamomillae romanae flos* contains besides nobiletin further sesquiterpene lactones which are structurally similar to

nobilin²⁶ and could form conjugation products and therefore competitively inhibit the conjugation reaction of nobilin and the efflux transporters. No influence of the sesquiterpene lactone fraction on apical influx of glucuronide was detected while a diminishing effect of the full extract on this influx narrowly missed significance. Such an effect could be due to inhibition of OATP by flavonoids as reported before.⁵⁶⁻⁵⁸ The essential oil of *Chamomillae romanae flos* reduced efflux and formation of cysteine and glutathione conjugates but not of glucuronide. Little is known about the effect of essential oil on these processes except perhaps that essential oils and terpenoids that are ingredients of essential oils were reported to be inhibitors of P-gp and/or MRPs^{59,60} and that essential oils, albeit of a different plant, can inhibit glutathione S-transferase in the rat.⁶¹ Ethanol used at the same concentration as in the full extract, the sesquiterpene lactone fraction and the essential oil caused a reduction of the formation of all three conjugates but did not affect efflux transporters. This is consistent with reports that organic solvents including EtOH can inhibit UDP-glucuronosyltransferase⁶² and glutathione S-transferase.⁶³

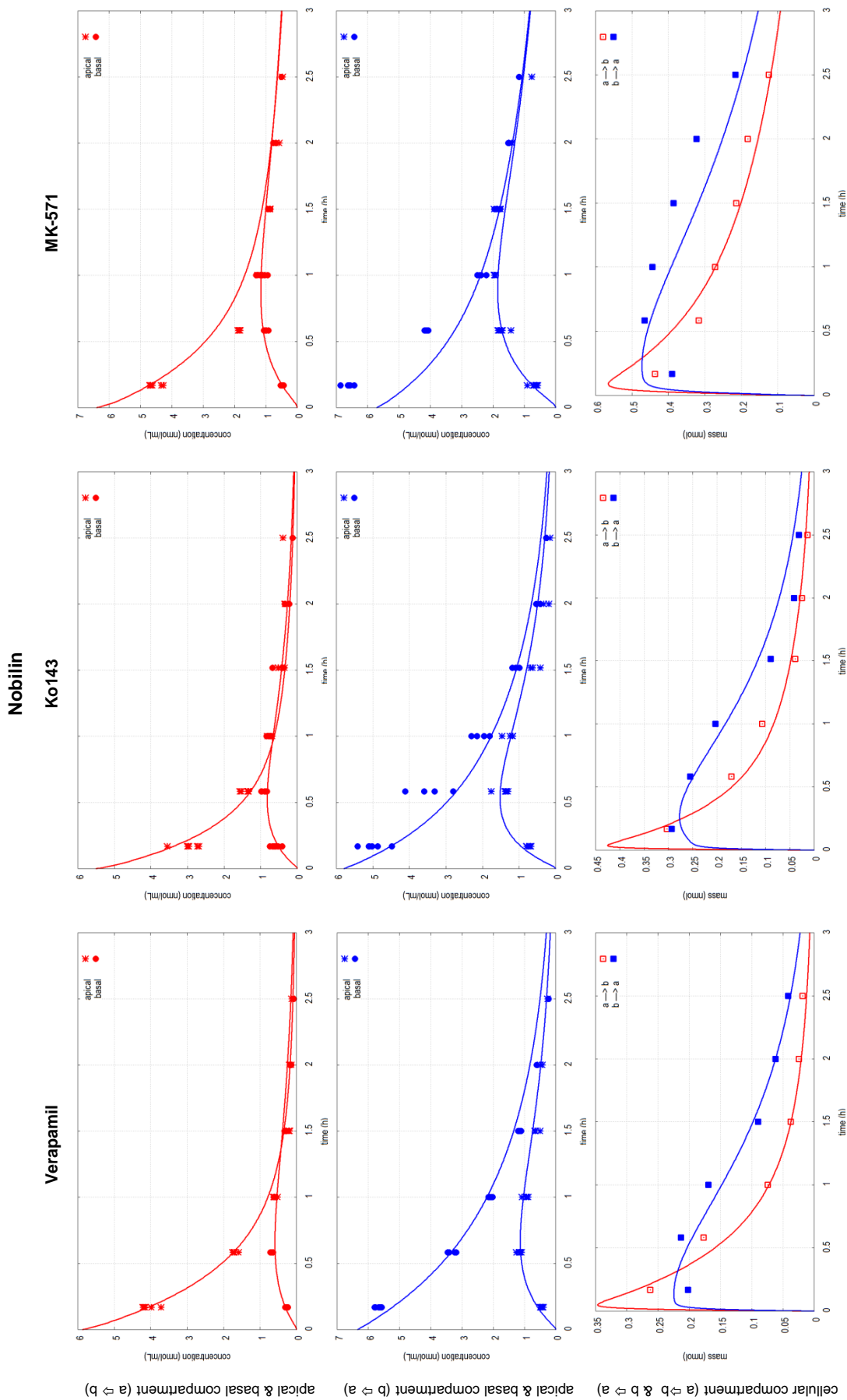
Apigenin and luteolin are representative flavonoids contained in *Chamomillae romanae flos*. Flavonoids and their conjugation products were reported to be substrates and inhibitors of efflux transporters such as P-gp and MRPs.^{58,64} Also, flavonoids were found to be substrates and potential inhibitors of UDP-glucuronosyltransferase⁵⁸ and inhibitors of glutathione S-transferase.⁶⁵ Moreover, flavonoids were reported to stimulate glutathione efflux just like verapamil,⁵⁵ and P-gp mediated transport.^{58,66} Although individual results of the present study appear to agree with these reports, no overall consistent picture is obtained. Apigenin and luteolin generally reduced the formation of the three conjugates and, in combination, possibly the efflux of the cysteine and the glutathione conjugate, this effect, however, may have been concentration dependent and, additionally for apigenin, the three conjugates accounted only for about 30% of the total bioconversion of nobilin. Hence the results with the flavonoids do not seem to be conclusive and their role as ingredients of the *Chamomillae romanae flos* extract for the absorption of nobilin requires further investigation.

Taken together, several of the investigated ingredients of the ethanolic extract are shown to contribute to the reduction of the total conjugation of nobilin in the cell. The effect of the individual ingredients on the relative fraction absorbed was, however, marginal. The full extract, on the other hand, elicited the largest reduction of conjugation and a marked increase of the relative fraction absorbed. These results confirm, therefore, that the combination of the ingredients of the extract is necessary for achieving a positive effect on absorption. The use of full extract further appears to offer a good possibility for improving absorption of compounds undergoing strong enteral bioconversion by inhibiting on one hand enzymatic reaction and on the other efflux of conjugation products.

4.6 CONCLUSION

Nobilin shows good permeability by diffusion of the cell membrane of the Caco-2 monolayer but a poor absorption because of extensive bioconversion in the cell yielding conjugation products with glucuronic acid, cysteine, and glutathione. All three conjugates were substrates of the apical and basal efflux transporters MRP2, MRP3, and possibly MRP1 while the glucuronide and the cysteine conjugate were also substrates of P-gp. Inhibition of efflux led to reduced bioconversion and increased absorption. This transport-bioconversion interplay is proposed to offer a good possibility to increase absorption in case of conjugation in the intestine. The full extract of *Chamomillae romanae flos* directly reduced conjugation and inhibited, in part, efflux leading to increased absorption of nobilin. The effect of the plant extract appears, therefore, to be due to a combination of mechanisms. This effect could not be attributed to a single ingredient; rather, the combination of ingredients of the extract was responsible.

4.7 APPENDIX

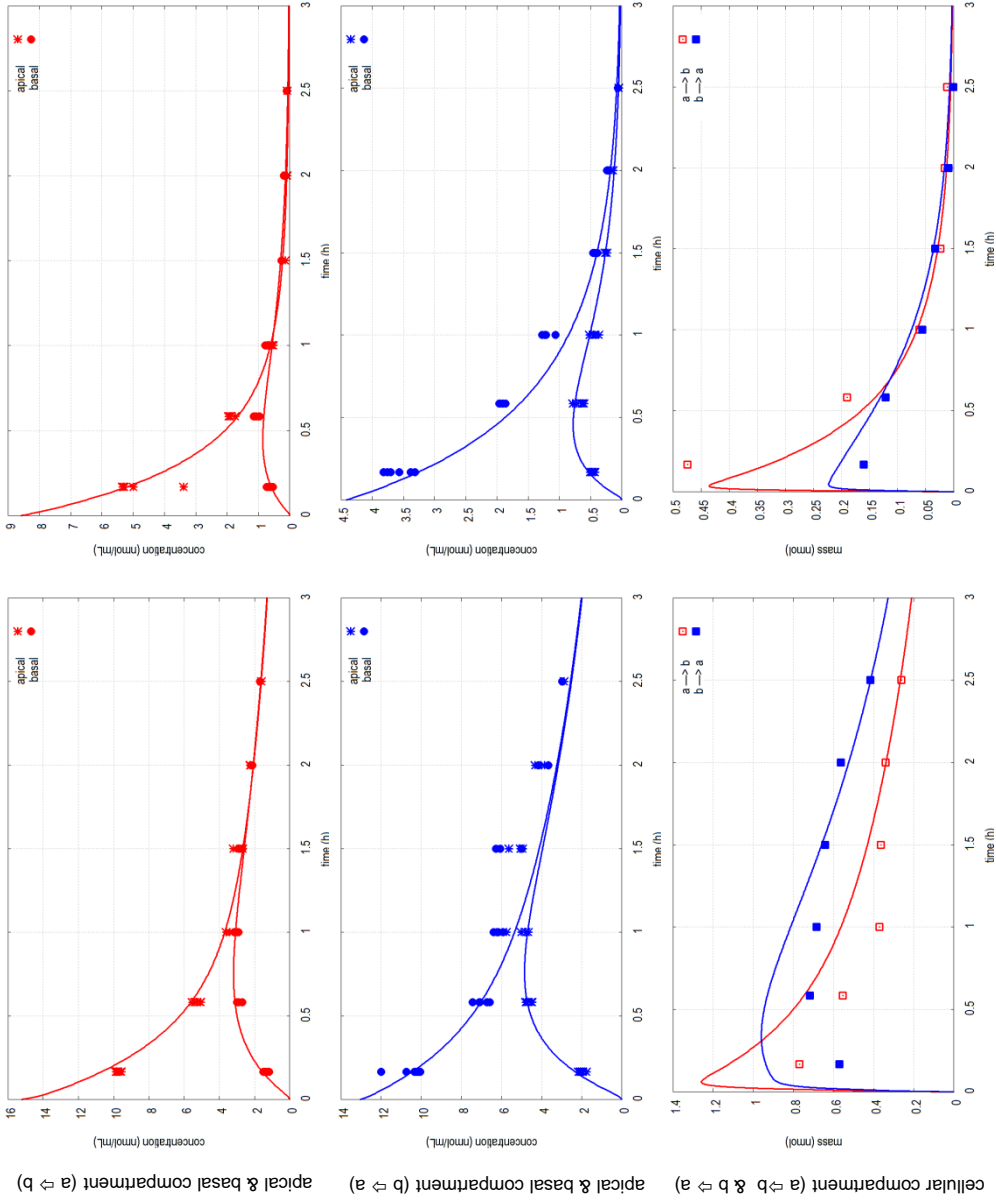


Nobilin concentration in presence of (left to right) verapamil, Ko143, and MK-571 in the apical-to-basal (top panels, red) and the basal-to-apical (middle panels, blue) transport direction in both compartments and nobilin mass in the cellular compartment (bottom panels) in both transport directions as a function of time. (●) apical concentration, (●) basal concentration, (□) mass in apical-to-basal transport direction (red), (■) mass in basal-to-apical transport direction (blue). Symbols represent measured data and lines fitted model curves.

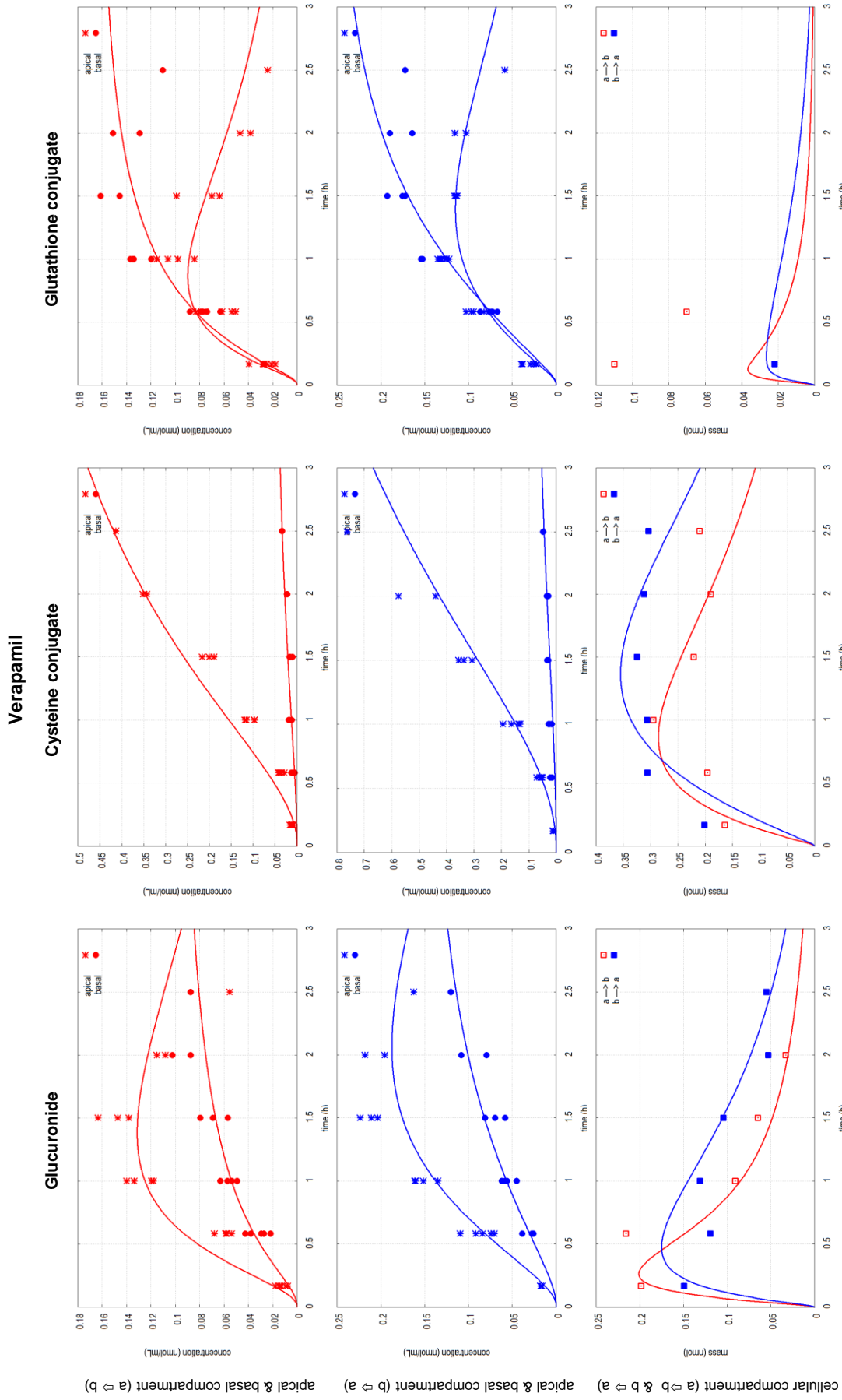
Nobilin

Verapamil/Ko143/MK-571

Leukotriene C4

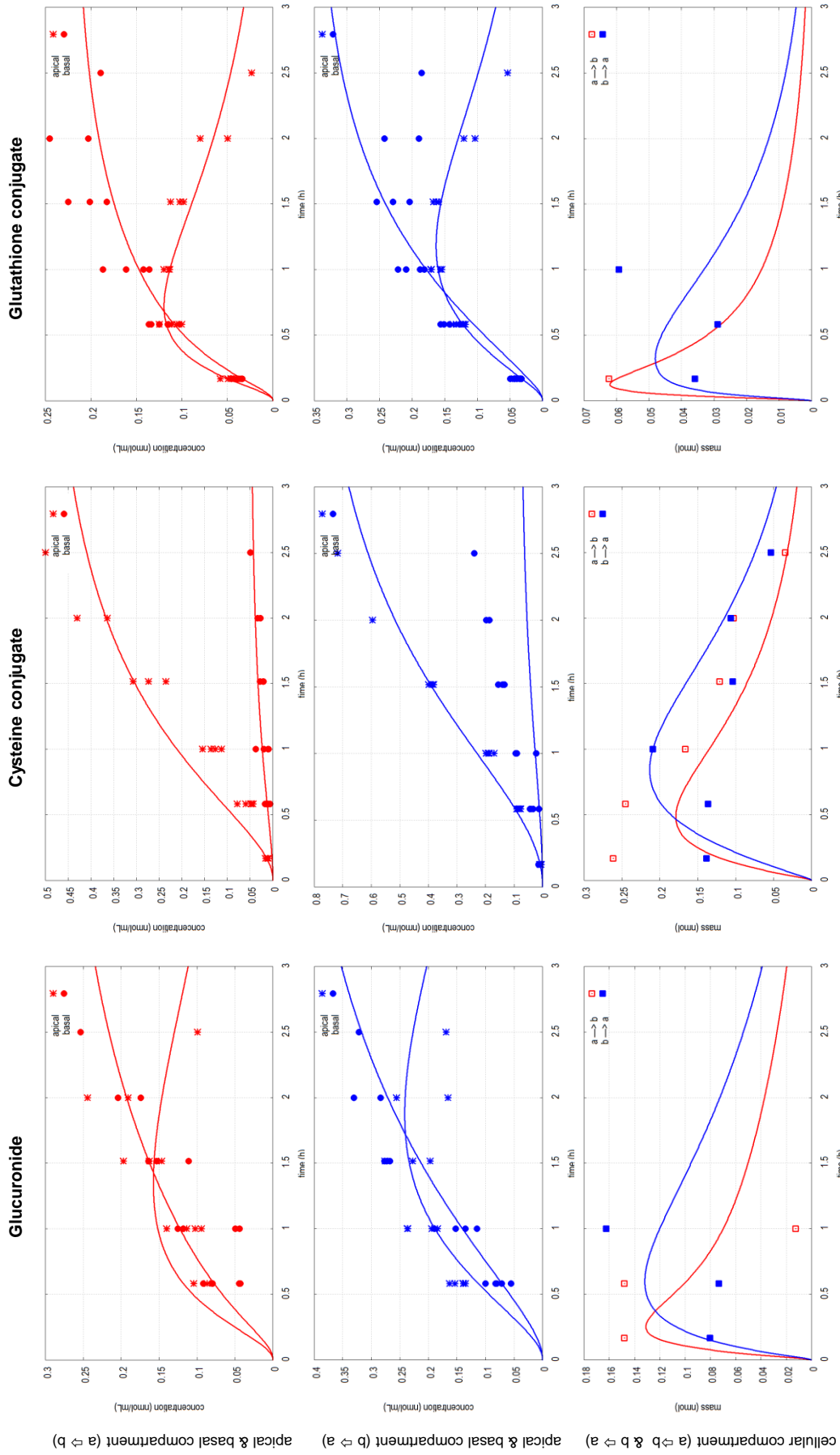


Nobilin concentration in presence of (left to right) verapamil/Ko143/MK-571 and leukotriene C4 in the apical-to-basal (top panels, red) and the basal-to-apical (middle panels, blue) transport direction in both compartments and nobilin mass in the cellular compartment (bottom panels) in both transport directions as a function of time. (●) apical concentration, (◼) basal concentration, (◻) mass in apical-to-basal transport direction (red), (◼) mass in basal-to-apical transport direction (blue). Symbols represent measured data and lines fitted model curves.

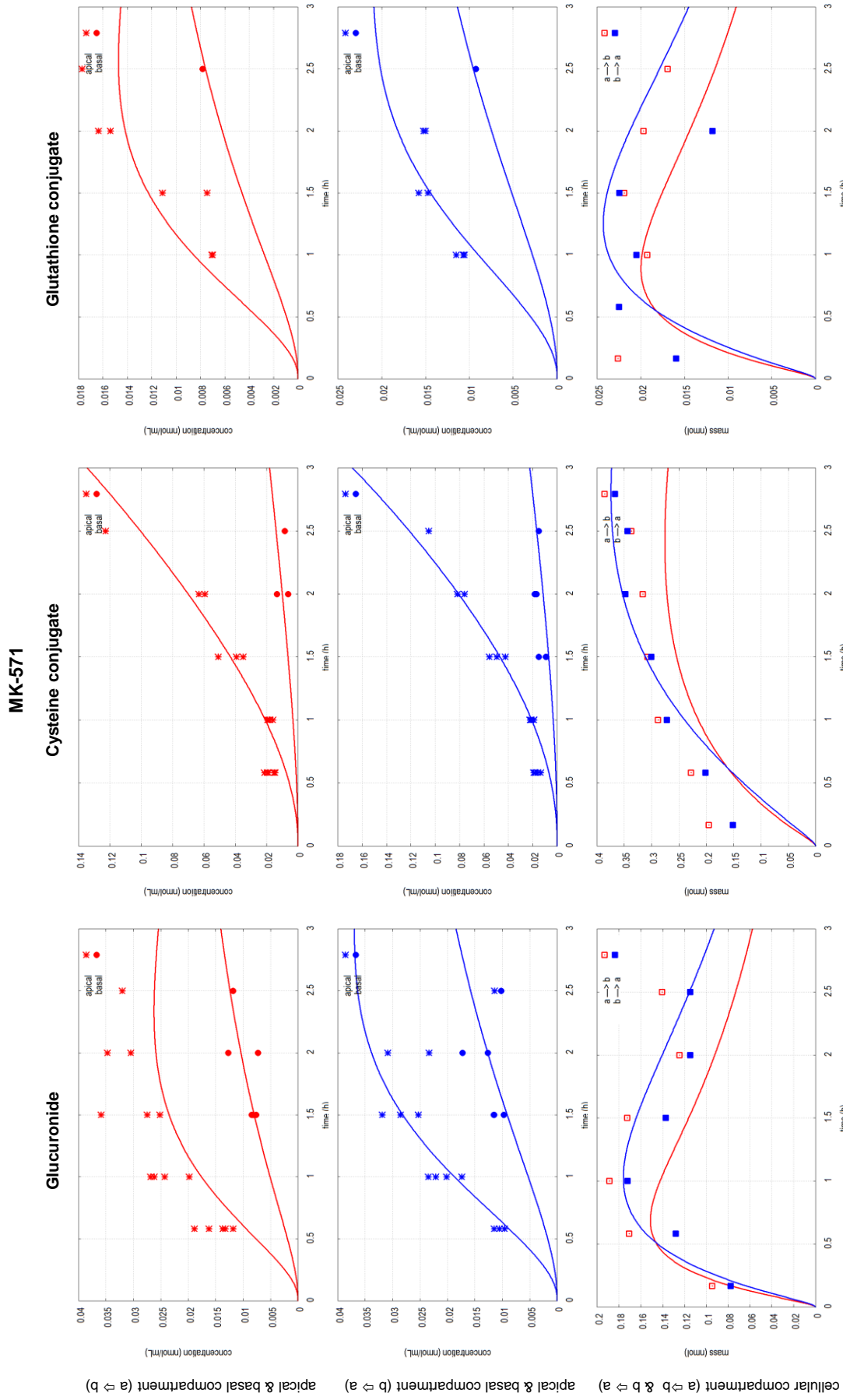


Concentration of (left to right) glucuronide, cysteine conjugate, and glutathione conjugate in the apical-to-basal (top panels, red) and the basal-to-apical (middle panels, blue) transport direction in both compartments and mass of (left to right) glucuronide, cysteine conjugate, and glutathione conjugate in the cellular compartment (bottom panels) in both transport directions as a function of time. (*) apical concentration, (●) mass in apical-to-basal transport direction (red), (■) mass in basal-to-apical transport direction (blue). Symbols represent measured data and lines represent fitted model curves.

Ko143

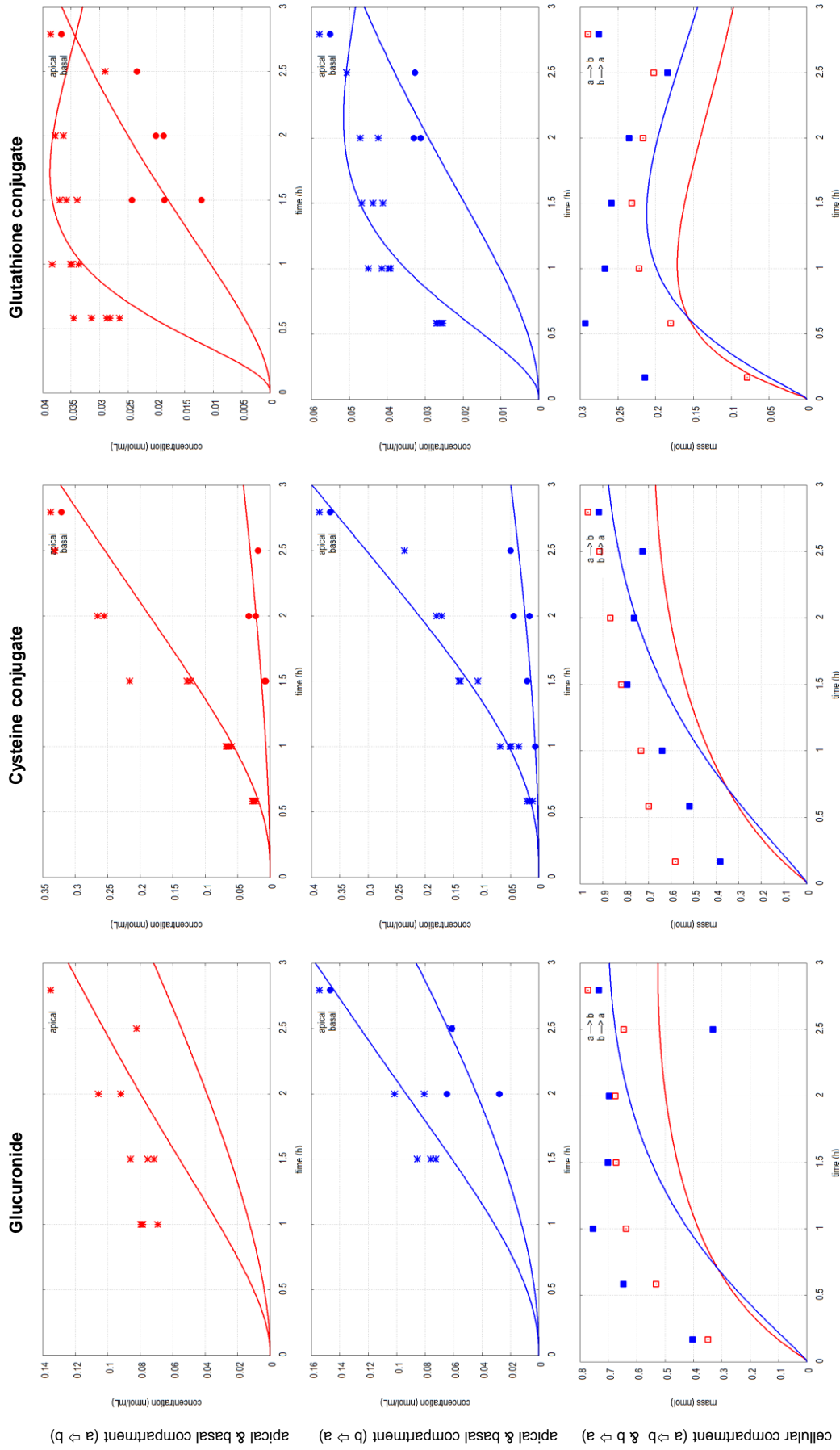


Concentration of (left to right) glucuronide, cysteine conjugate, and glutathione conjugate in presence of Ko143 in the apical-to-basal (top panels, red) and the basal-to-apical (middle panels, blue) transport direction in both compartments and mass of (left to right) glucuronide, cysteine conjugate, and glutathione conjugate in the cellular compartment (bottom panels) in both transport directions as a function of time. (*) apical concentration, (●) basal concentration, (□) mass in apical-to-basal transport direction (red), (■) mass in basal-to-apical transport direction (blue). Symbols represent measured data and lines fitted model curves.

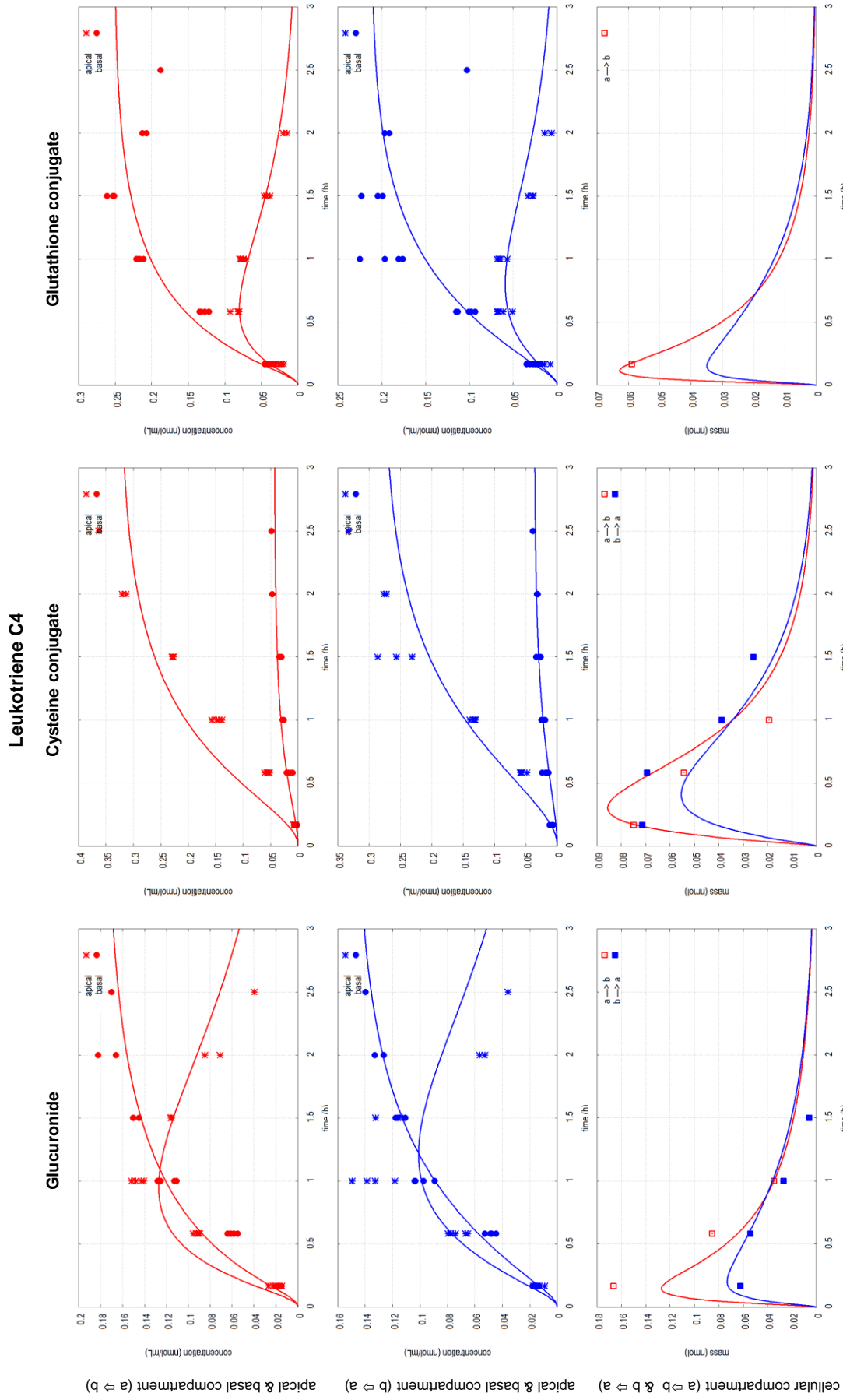


Concentration of (left to right) glucuronide, cysteine conjugate, and glutathione conjugate in presence of MK-571 in the apical-to-basal (top panels, red) and the basal-to-apical (middle panels, blue) transport direction in both compartments and mass of (left to right) glucuronide, cysteine conjugate, and glutathione conjugate in the cellular compartment (bottom panels) in both transport directions as a function of time. (*) apical concentration, (●) basal concentration, (□) mass in apical-to-basal transport direction (red), (■) mass in basal-to-apical transport direction (blue). Symbols represent measured data and lines fitted model curves.

Verapamil/Ko143/MK-571

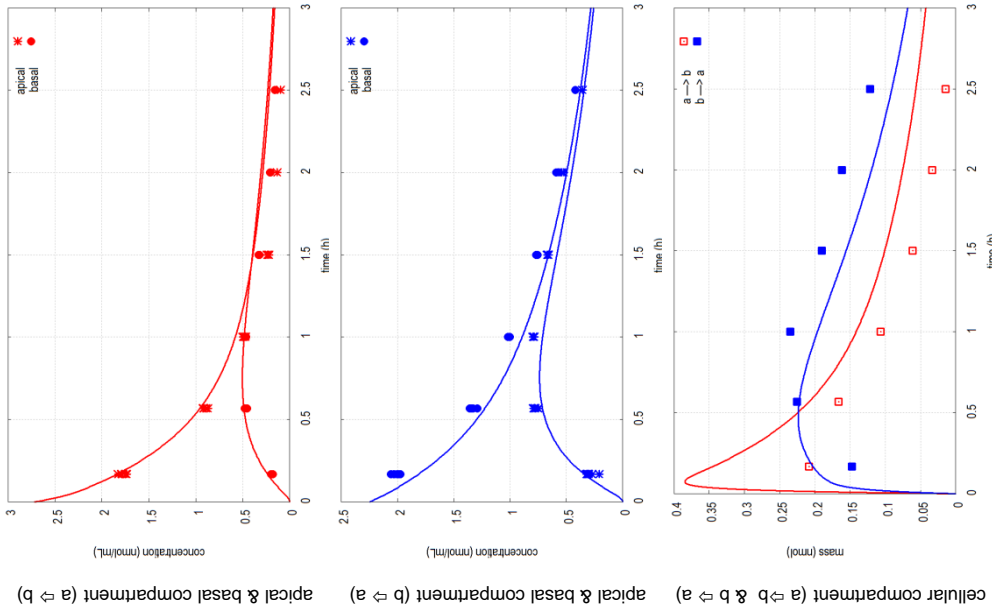


Concentration of (left to right) glucuronide, cysteine conjugate, and glutathione conjugate in presence of verapamil/Ko143/MK-571 in the apical-to-basal (top panels, red) and the basal-to-apical (middle panels, blue) transport direction in both compartments and mass of (left to right) glucuronide, cysteine conjugate, and glutathione conjugate in the cellular compartment (bottom panels) in both transport directions as a function of time. (*) apical concentration, (●) basal concentration, (□) mass in apical-to-basal transport direction (red), (■) mass in basal-to-apical transport direction (blue). Symbols represent measured data and lines fitted model curves.

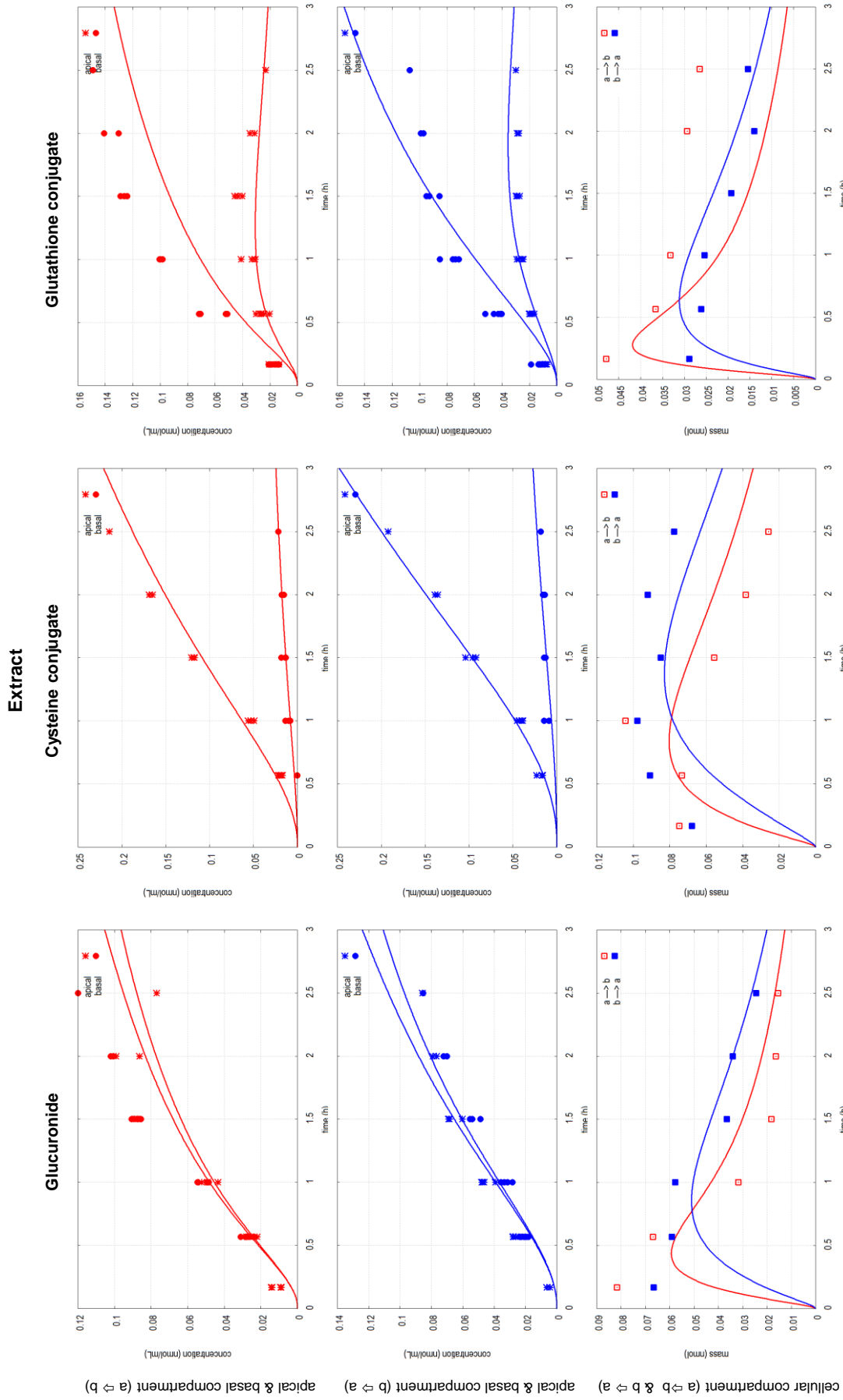


Concentration of (left to right) glucuronide, cysteine conjugate, and glutathione conjugate in presence of leukotriene C4 in the apical-to-basal (top panels, red) and the basal-to-apical (middle panels, blue) transport direction in both compartments and mass of (left to right) glucuronide, cysteine conjugate, and glutathione conjugate in the cellular compartment (bottom panels) in both transport directions as a function of time. (*) apical concentration, (●) basal concentration, (□) mass in apical-to-basal transport direction (red), (■) mass in basal-to-apical transport direction (blue). Symbols represent measured data and lines fitted model curves.

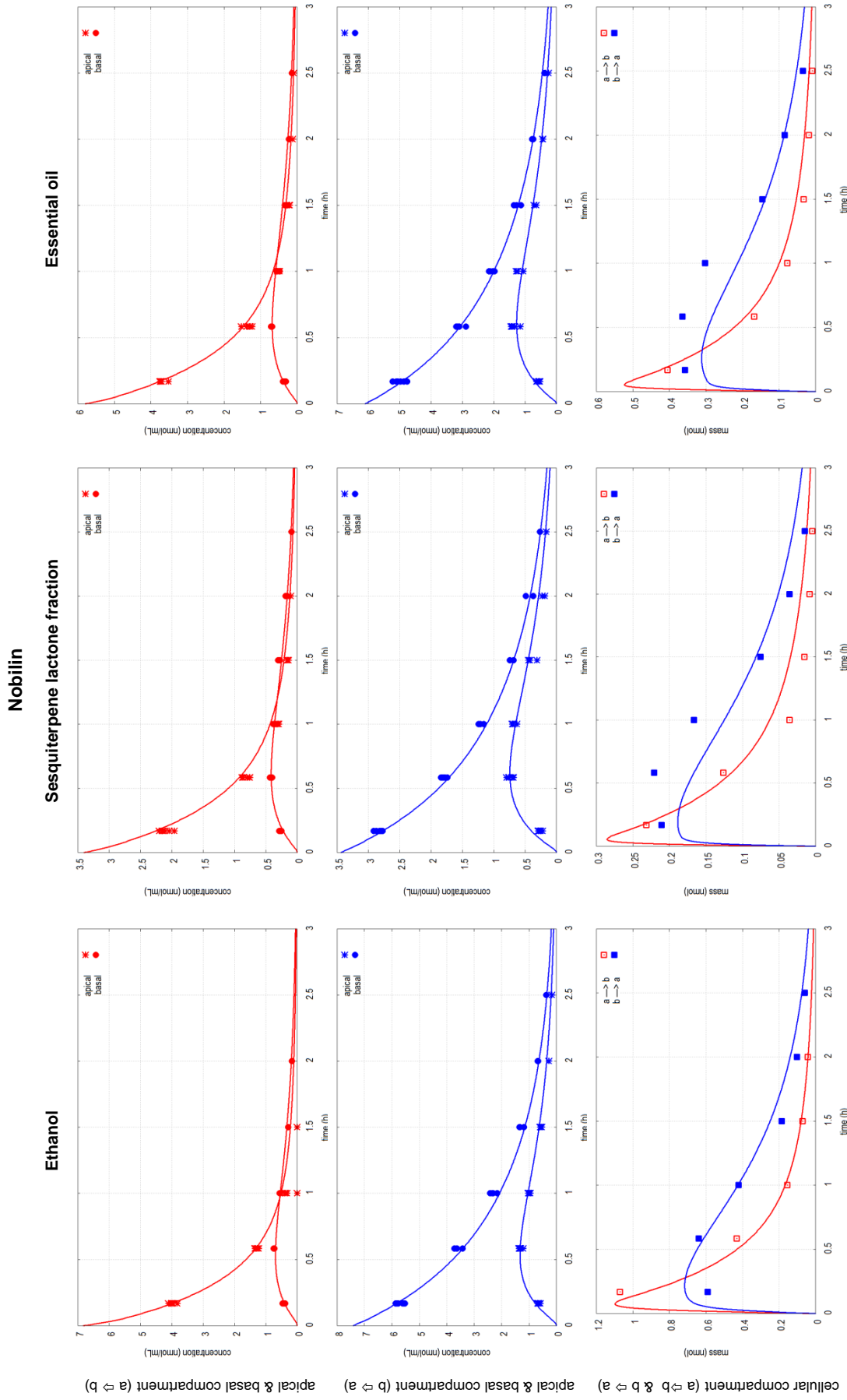
**Nobilin
Extrakt**



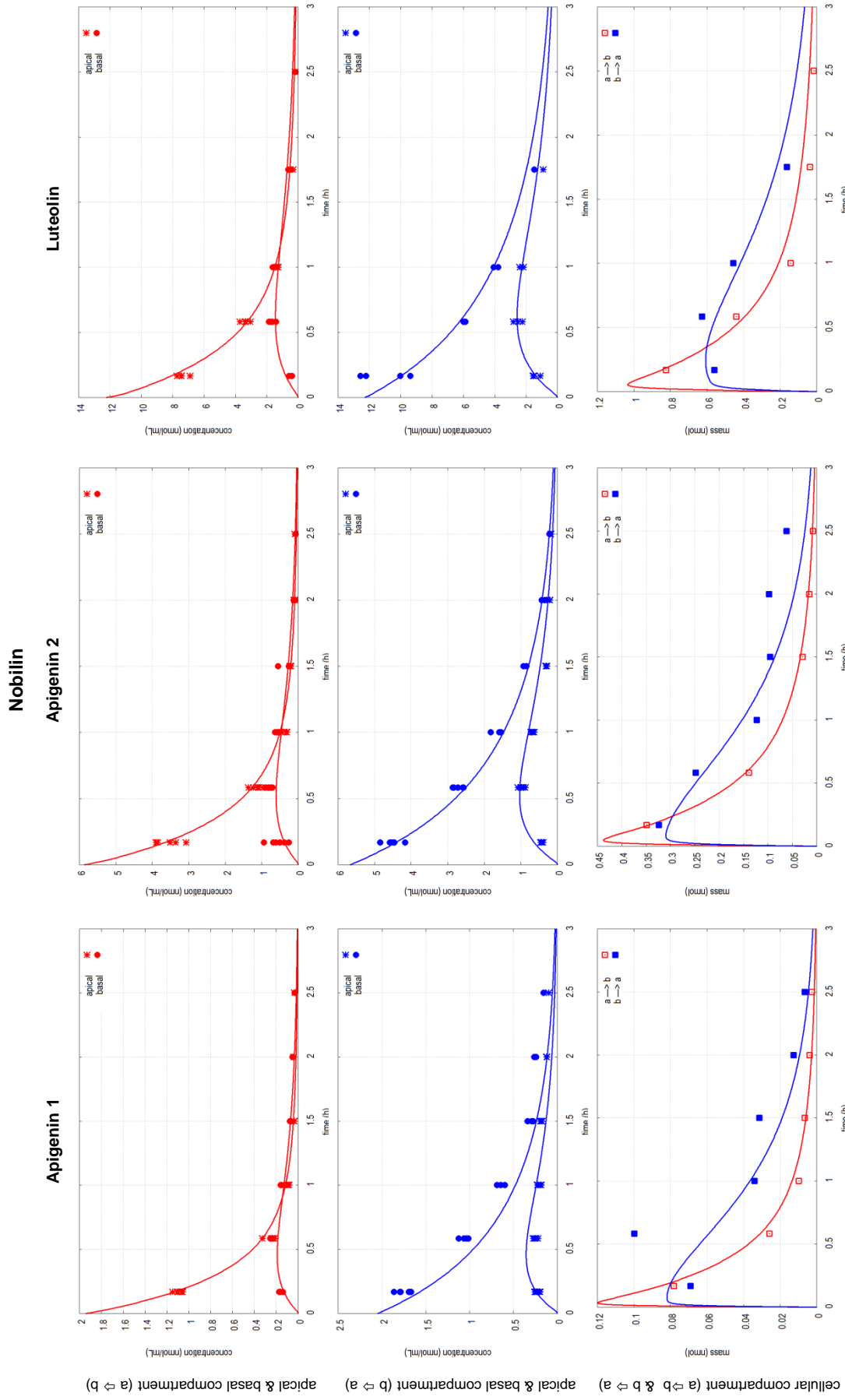
Nobilin concentration in presence of full extract in the apical-to-basal (top panels, red) and the basal-to-apical (middle panels, blue) transport direction in both compartments and nobilin mass in the cellular compartment (bottom panels) in both transport directions as a function of time. (*) apical concentration, (●) basal concentration, (□) mass in apical-to-basal transport direction (red), (■) mass in basal-to-apical transport direction (blue). Symbols represent measured data and lines fitted model curves.



Concentration of (left to right) glucuronide, cysteine conjugate, and glutathione conjugate in presence of full extract in the apical-to-basal (top panels, red) and the basal-to-apical (middle panels, blue) transport direction in both compartments and mass of (left to right) glucuronide, cysteine conjugate, and glutathione conjugate in the cellular compartment (bottom panels) in both transport directions as a function of time. (*) apical concentration, (●) basal concentration, (□) mass in apical-to-basal transport direction (red), (■) mass in basal-to-apical transport direction (blue). Symbols represent measured data and lines fitted model curves.



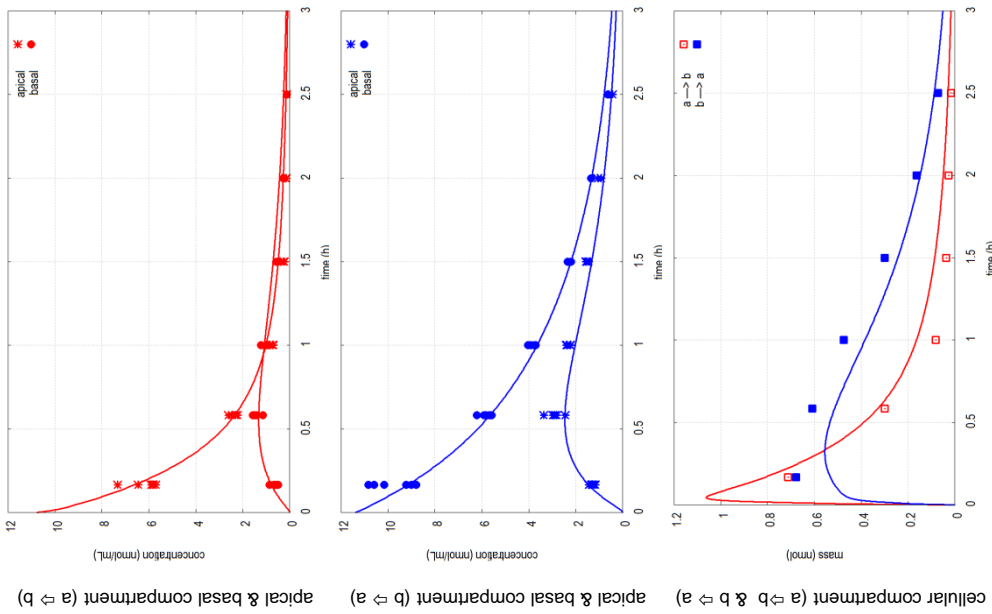
Nobilin concentration in presence of (left to right) ethanol, sesquiterpene lactone fraction, and essential oil in the apical-to-basal (top panels, red) and the basal-to-apical (middle panels, blue) transport direction in both compartments and nobilin mass in the cellular compartment (bottom panels) in both transport directions as a function of time. (●) apical concentration, (○) basal concentration, (■) mass in basal-to-apical transport direction (red), (□) mass in apical-to-basal transport direction (blue). Symbols represent measured data and lines fitted model curves.



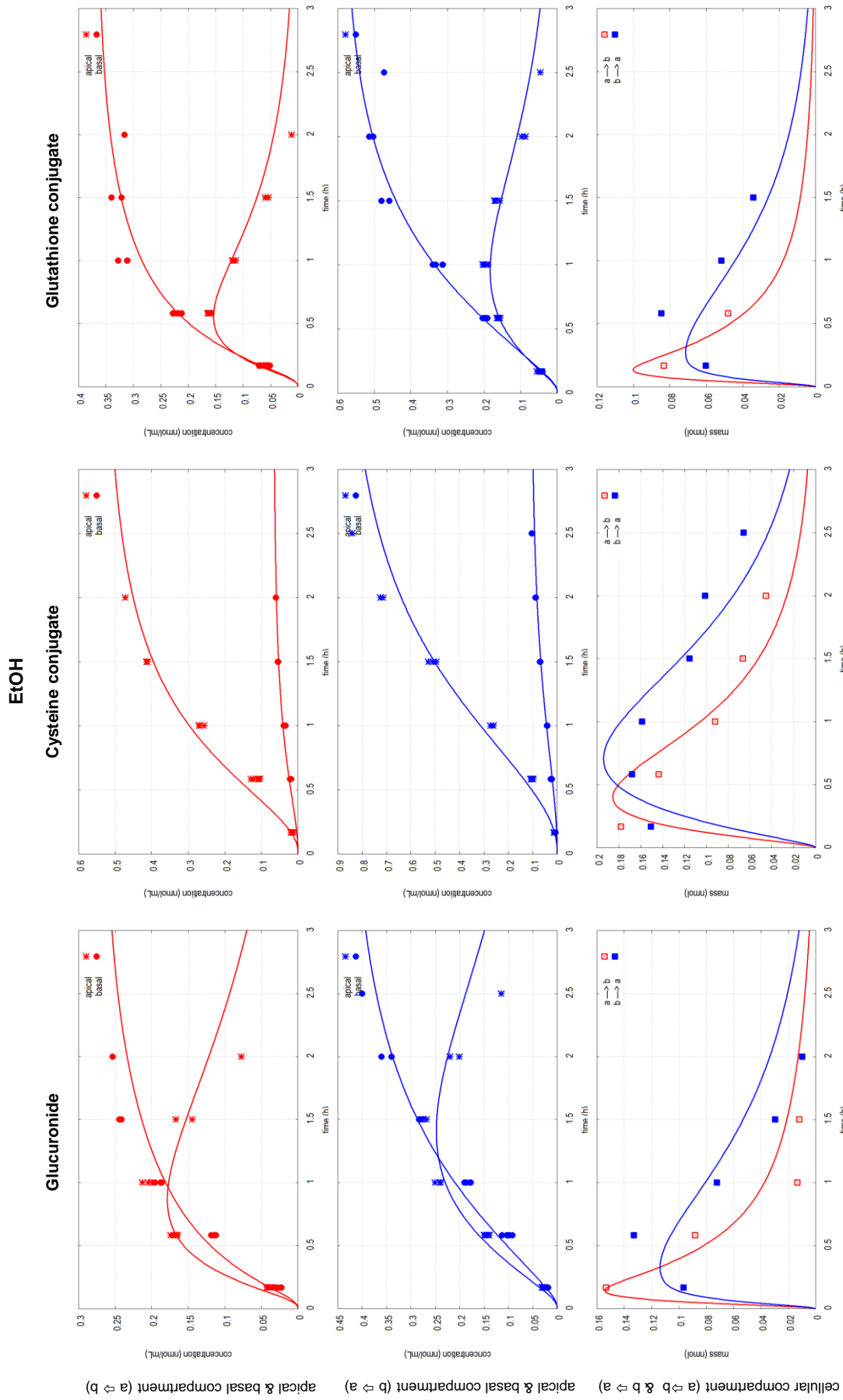
Nobilin concentration in presence of (left to right) apigenin 1, apigenin 2, and luteolin in the apical-to-basal (top panels, red) and the basal-to-apical (middle panels, blue) transport direction in both compartments and nobilin mass in the cellular compartment (bottom panels) in both transport directions as a function of time. (*) apical concentration, (●) basal concentration, (□) mass in apical-to-basal transport direction (red), (■) mass in basal-to-apical transport direction (blue). Symbols represent measured data and lines fitted model curves.

Nobilin

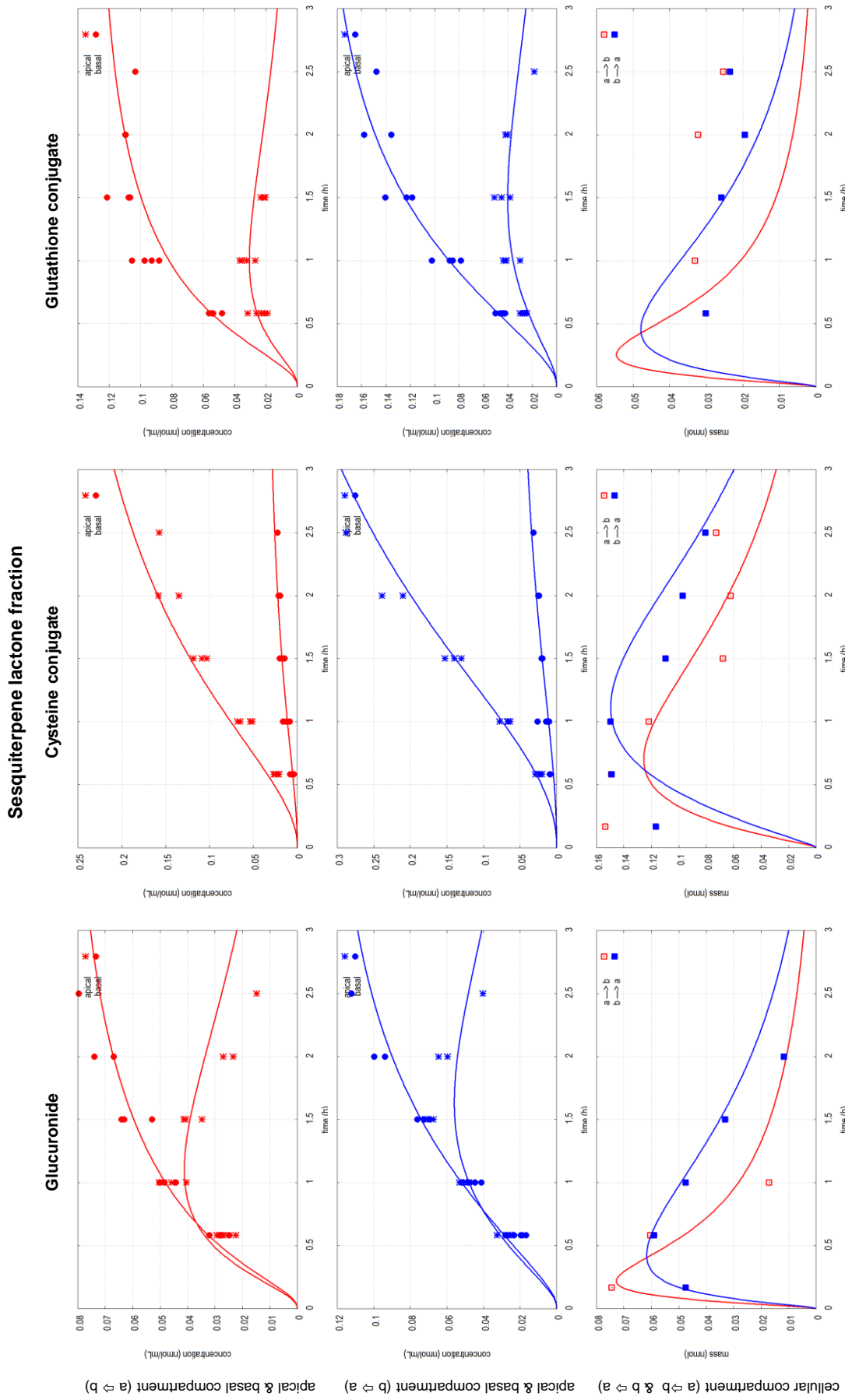
Apigenin 2/Luteolin



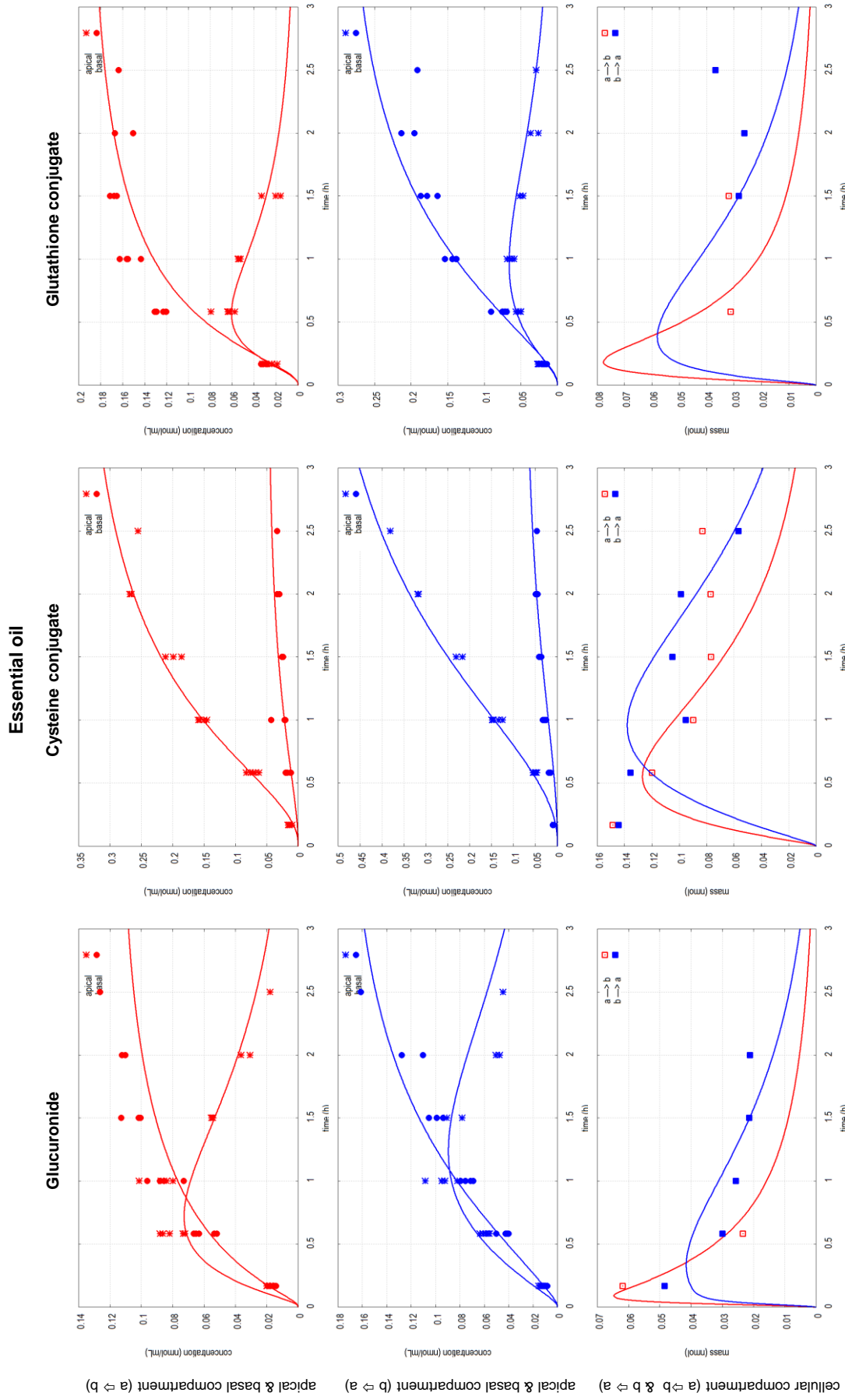
Nobilin concentration in presence of apigenin 2/luteolin in the apical-to-basal (top panels, red) and the basal-to-apical (middle panels, blue) transport direction in both compartments and nobilin mass in the cellular compartment (bottom panels) in both transport directions as a function of time. (*) apical concentration, (●) basal concentration, (□) mass in apical-to-basal transport direction (red), (■) mass in basal-to-apical transport direction (blue). Symbols represent measured data and lines fitted model curves.



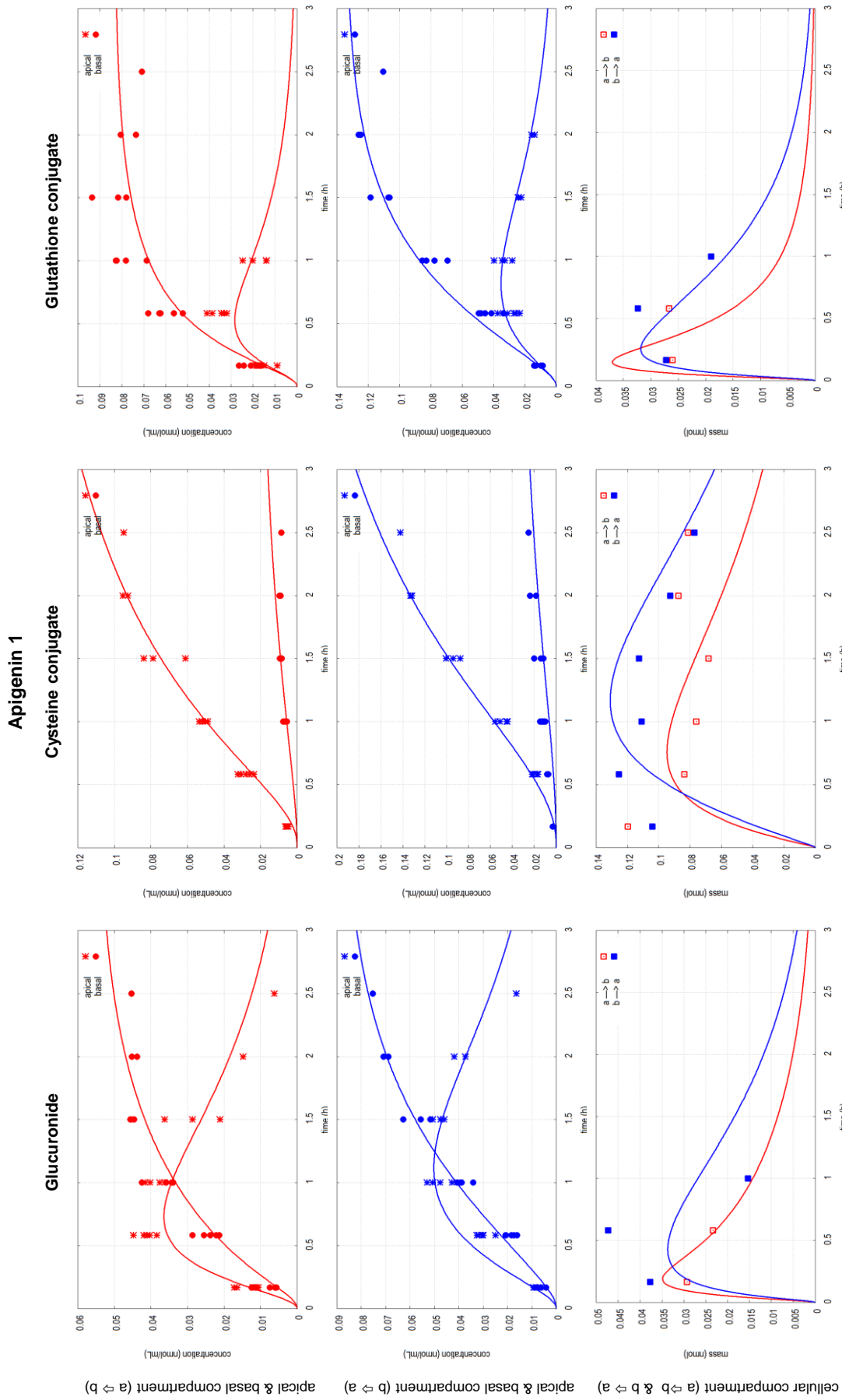
Concentration of (left to right) glucuronide, cysteine conjugate, and glutathione conjugate in presence of ethanol in the apical-to-basal (top panels, red) and the basal-to-apical (middle panels, blue) transport direction in both compartments and mass of (left to right) glucuronide, cysteine conjugate, and glutathione conjugate in the cellular compartment (bottom panels) in both transport directions as a function of time. (*) apical concentration, (●) basal concentration, (□) mass in apical-to-basal transport direction (red), (■) mass in basal-to-apical transport direction (blue). Symbols represent measured data and lines fitted model curves.



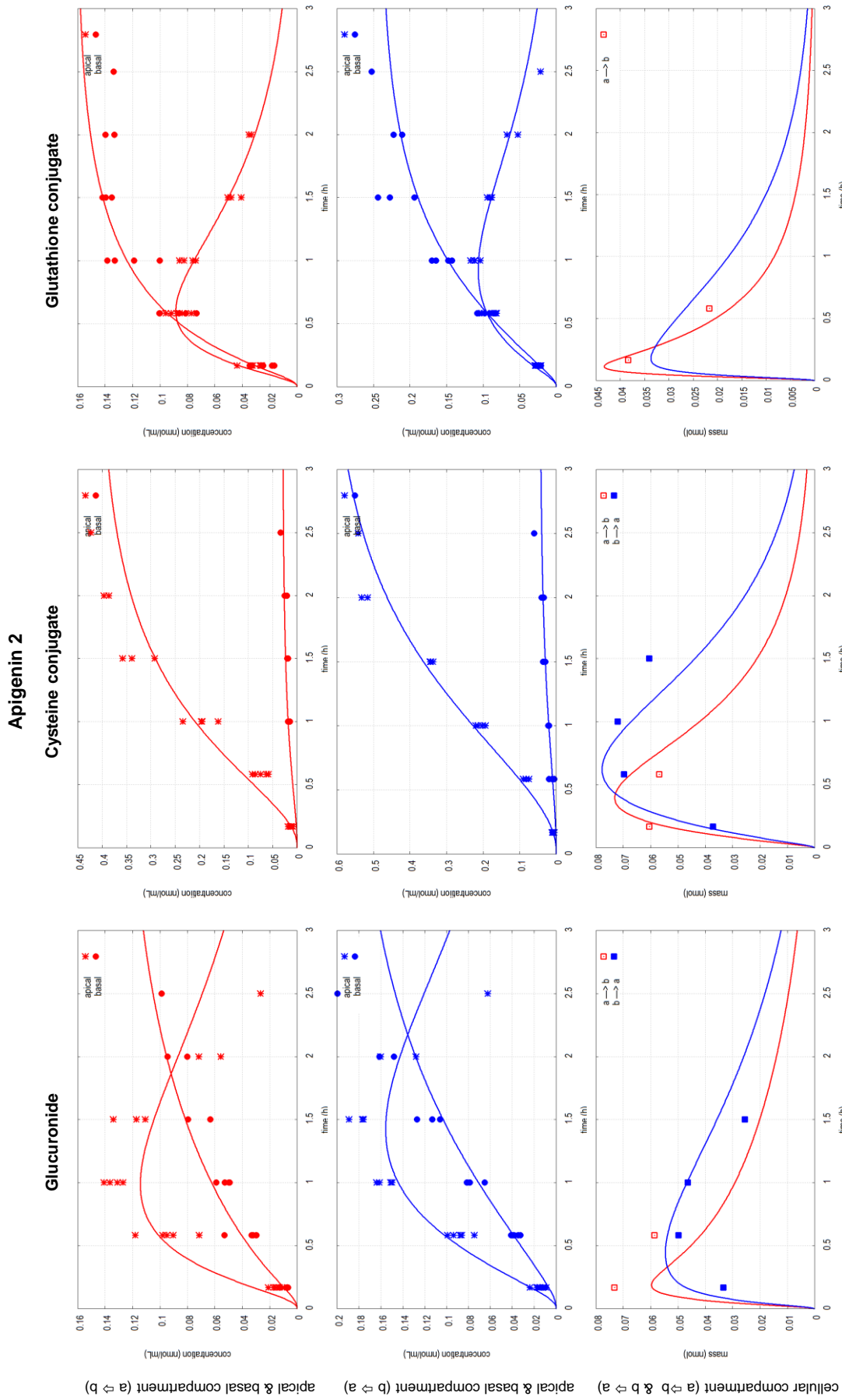
Concentration of (left to right) glucuronide, cysteine conjugate, and glutathione conjugate in presence of sesquiterpene lactone fraction in the apical-to-basal (top panels, red) and the basal-to-apical (middle panels, blue) transport direction in both compartments and mass of (left to right) glucuronide, cysteine conjugate, and glutathione conjugate in the cellular compartment (bottom panels) in both transport directions as a function of time. (*) apical concentration, (●) basal concentration, (□) mass in apical-to-basal transport direction (red), (■) mass in basal-to-apical transport direction (blue). Symbols represent measured data and lines fitted model curves.



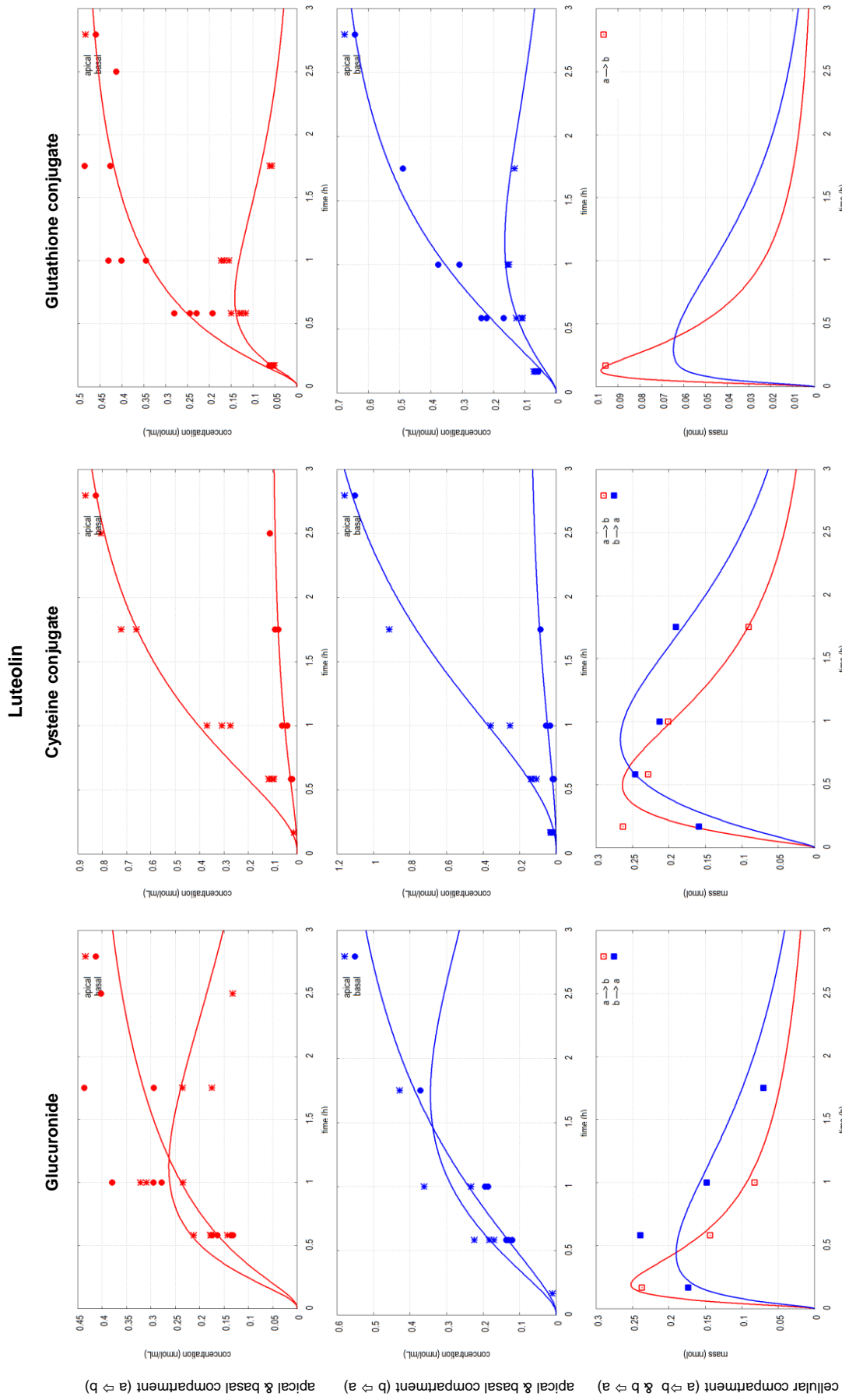
Concentration of (left to right) glucuronide, cysteine conjugate, and glutathione conjugate in presence of essential oil in the apical-to-basal (top panels, red) and the basal-to-apical (middle panels, blue) transport direction in both compartments and mass of (left to right) glucuronide, cysteine conjugate, and glutathione conjugate in the cellular compartment (bottom panels) in both transport directions as a function of time. (●) apical concentration, (●) basal concentration, (□) mass in apical-to-basal transport direction (red), (■) mass in basal-to-apical transport direction (blue). Symbols represent measured data and lines fitted model curves.



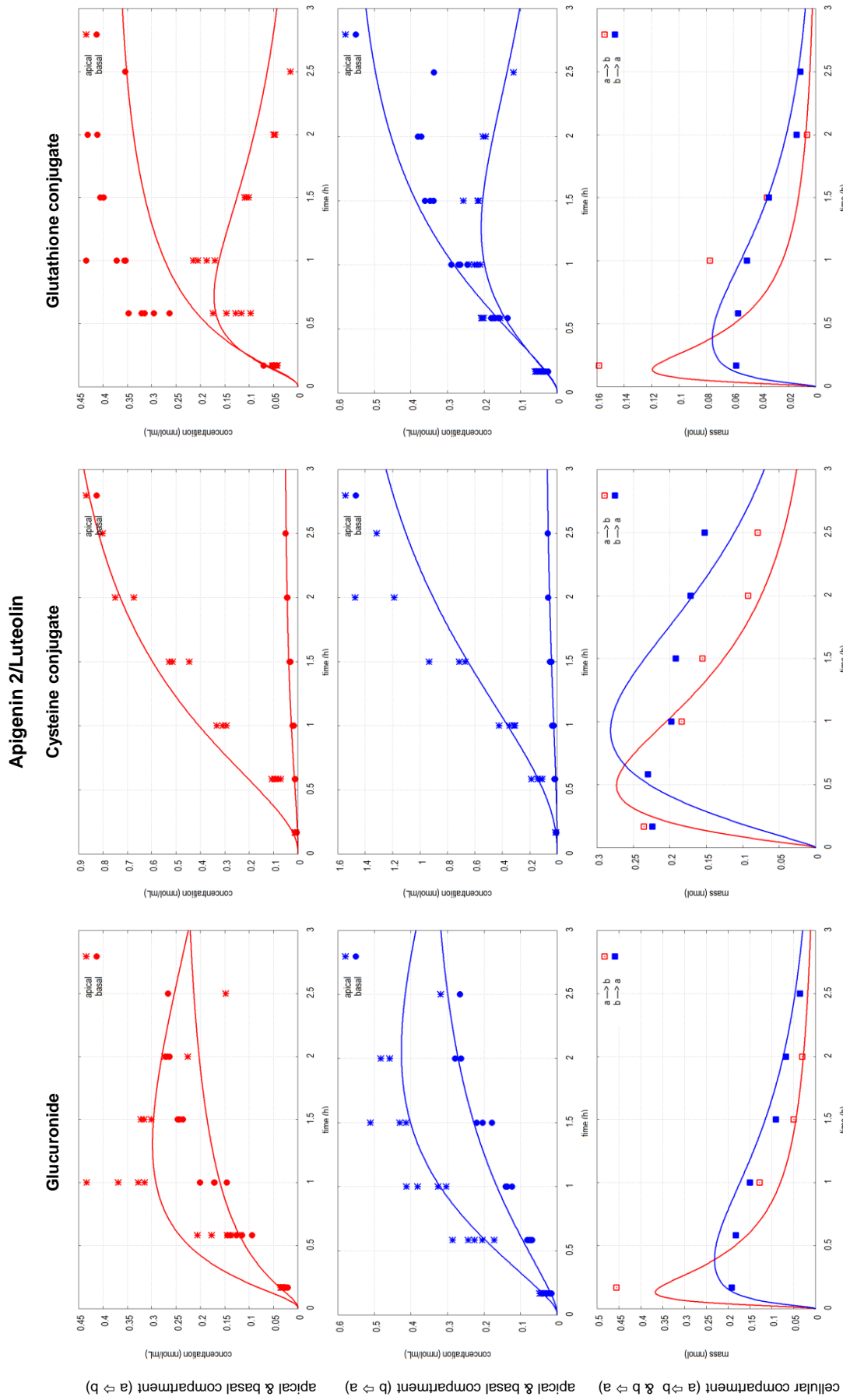
Concentration of (left to right) glucuronide, cysteine conjugate, and glutathione conjugate in presence of apigenin 1 in the apical-to-basal (top panels, red) and the basal-to-apical (middle panels, blue) transport direction in both compartments and mass of (left to right) glucuronide, cysteine conjugate, and glutathione conjugate in the cellular compartment (bottom panels) in both transport directions as a function of time. (*) apical concentration, (●) basal concentration, (□) mass in apical-to-basal transport direction (red), (■) mass in basal-to-apical transport direction (blue). Symbols represent measured data and lines fitted model curves.



Concentration of (left to right) glucuronide, cysteine conjugate, and glutathione conjugate in presence of apigenin 2 in the apical-to-basal (top panels, red) and the basal-to-apical (middle panels, blue) transport direction in both compartments and mass of (left to right) glucuronide, cysteine conjugate, and glutathione conjugate in the cellular compartment (bottom panels) in both transport directions as a function of time. (*) apical concentration, (●) basal concentration, (□) mass in apical-to-basal transport direction (red), (■) mass in basal-to-apical transport direction (blue). Symbols represent measured data and lines fitted model curves.



Concentration of (left to right) glucuronide, cysteine conjugate, and glutathione conjugate in presence of luteolin in the apical-to-basal (top panels, red) and the basal-to-apical (middle panels, blue) transport direction in both compartments and mass of (left to right) glucuronide, cysteine conjugate, and glutathione conjugate in the cellular compartment (bottom panels) in both transport directions as a function of time. (●) apical concentration, (○) basal concentration, (■) mass in apical-to-basal transport direction (red), (□) mass in basal-to-apical transport direction (blue). Symbols represent measured data and lines fitted model curves.



Concentration of (left to right) glucuronide, cysteine conjugate, and glutathione conjugate in presence of apigenin 2/luteolin in the apical-to-basal (top panels, red) and the basal-to-apical (middle panels, blue) transport direction in both compartments and mass of (left to right) glucuronide, cysteine conjugate, and glutathione conjugate in the cellular compartment (bottom panels) in both transport directions as a function of time. (*) apical concentration, (●) basal concentration, (□) mass in apical-to-basal transport direction (red), (■) mass in basal-to-apical transport direction (blue). Symbols represent measured data and lines fitted model curves.

4.8 REFERENCES

1. Custodio JM, Wu CY, Benet LZ 2008. Predicting drug disposition, absorption/elimination/transporter interplay and the role of food on drug absorption. *Advanced Drug Delivery Reviews* 60(6):717-733.
2. Suzuki H, Sugiyama Y 2000. Role of metabolic enzymes and efflux transporters in the absorption of drugs from the small intestine. *European Journal of Pharmaceutical Sciences* 12(1):3-12.
3. Jin J, Cai D, Bi H, Zhong G, Zeng H, Gu L, Huang Z, Huang M 2013. Comparative pharmacokinetics of paclitaxel after oral administration of *Taxus yunnanensis* extract and pure paclitaxel to rats. *Fitoterapia* 90:1-9.
4. Li N, Tsao R, Sui ZG, Ma JW, Liu ZQ, Liu ZY 2012. Intestinal transport of pure diester-type alkaloids from an aconite extract across the Caco-2 cell monolayer model. *Planta Medica* 78(7):692-697.
5. Fale PL, Ascensao L, Serralheiro MLM 2013. Effect of luteolin and apigenin on rosmarinic acid bioavailability in Caco-2 cell monolayers. *Food & Function* 4(3):426-431.
6. Zheng KYZ, Choi RCY, Guo AJY, Bi CWC, Zhu KY, Du CYQ, Zhang ZX, Lau DTW, Dong TTX, Tsim KWK 2012. The membrane permeability of Astragali radix-derived formononetin and calycosin is increased by *Angelicae sinensis* radix in Caco-2 cells: A synergistic action of an ancient herbal decoction Danggui Buxue Tang. *Journal of Pharmaceutical and Biomedical Analysis* 70:671-679.
7. Giacomini KM, Huang SM, Tweedie DJ, Benet LZ, Brouwer KLR, Chu XY, Dahlin A, Evers R, Fischer V, Hillgren KM, Hoffmaster KA, Ishikawa T, Keppler D, Kim RB, Lee CA, Niemi M, Polli JW, Sugiyama Y, Swaan PW, Ware JA, Wright SH, Yee SW, Zamek-Gliszczynski MJ, Zhang L, International T 2010. Membrane transporters in drug development. *Nature Reviews Drug Discovery* 9(3):215-236.
8. Pauli-Magnus C, von Richter O, Burk O, Ziegler A, Mettang T, Eichelbaum M, Fromm MF 2000. Characterization of the major metabolites of verapamil as substrates and inhibitors of P-glycoprotein. *Journal of Pharmacology and Experimental Therapeutics* 293(2):376-382.
9. Ming X, Knight BM, Thakker DR 2011. Vectorial transport of fexofenadine across Caco-2 cells: Involvement of apical uptake and basolateral efflux transporters. *Molecular Pharmaceutics* 8(5):1677-1686.
10. Estudante M, Morais JG, Soveral G, Benet LZ 2013. Intestinal drug transporters: An overview. *Advanced Drug Delivery Reviews* 64(10):1340-1356.
11. Gibbs JP, Yang JS, Slattery JT 1998. Comparison of human liver and small intestinal glutathione S-transferase-catalyzed busulfan conjugation in vitro. *Drug Metabolism and Disposition* 26(1):52-55.
12. Hu M, Chen J, Lin HM 2003. Metabolism of flavonoids via enteric recycling: Mechanistic studies of disposition of apigenin in the Caco-2 cell culture model. *Journal of Pharmacology and Experimental Therapeutics* 307(1):314-321.

13. Zhou SF, Wang LL, Di YM, Xue CC, Duan W, Li CG, Li Y 2008. Substrates and inhibitors of human multidrug resistance associated proteins and the implications in drug development. *Current Medicinal Chemistry* 15(20):1981-2039.
14. Jiang W, Xu BB, Wu BJ, Yu R, Hu M 2012. UDP-glucuronosyltransferase (UGT) 1A9-overexpressing HeLa cells is an appropriate tool to delineate the kinetic interplay between breast cancer resistance protein (BCRP) and UGT and to rapidly identify the glucuronide substrates of BCRP. *Drug Metabolism and Disposition* 40(2):336-345.
15. Cummins CL, Jacobsen W, Benet LZ 2002. Unmasking the dynamic interplay between intestinal P-glycoprotein and CYP3A4. *Journal of Pharmacology and Experimental Therapeutics* 300(3):1036-1045.
16. Cummins CL, Jacobsen W, Christians U, Benet LZ 2004. CYP3A4-transfected Caco-2 cells as a tool for understanding biochemical absorption barriers: Studies with sirolimus and midazolam. *Journal of Pharmacology and Experimental Therapeutics* 308(1):143-155.
17. Siissalo S, Heikkinen AT 2013. In vitro methods to study the interplay of drug metabolism and efflux in the intestine. *Current Drug Metabolism* 14(1):102-111.
18. Jeong EJ, Liu X, Jia XB, Chen J, Hu M 2005. Coupling of conjugating enzymes and efflux transporters: Impact on bioavailability and drug interactions. *Current Drug Metabolism* 6(5):455-468.
19. Artursson P, Borchardt RT 1997. Intestinal drug absorption and metabolism in cell cultures: Caco-2 and beyond. *Pharmaceutical Research* 14(12):1655-1658.
20. Hubatsch I, Ragnarsson EGE, Artursson P 2007. Determination of drug permeability and prediction of drug absorption in Caco-2 monolayers. *Nature Protocols* 2(9):2111-2119.
21. Sugano K, Kansy M, Artursson P, Avdeef A, Bendels S, Di L, Ecker GF, Faller B, Fischer H, Gerebtzoff G, Lennernaes H, Senner F 2010. Coexistence of passive and carrier-mediated processes in drug transport. *Nature Reviews Drug Discovery* 9(8):597-614.
22. Hayeshi R, Hilgendorf C, Artursson P, Augustijns P, Brodin B, Dehertogh P, Fisher K, Fossati L, Hovenkamp E, Korjamo T, Masungi C, Maubon N, Mols R, Mullertz A, Monkkonen J, O'Driscoll C, Oppers-Tiemissen HM, Ragnarsson EGE, Rooseboom M, Ungell AL 2008. Comparison of drug transporter gene expression and functionality in Caco-2 cells from 10 different laboratories. *European Journal of Pharmaceutical Sciences* 35(5):383-396.
23. Hilgendorf C, Ahlin G, Seithel A, Artursson P, Ungell AL, Karlsson J 2007. Expression of thirty-six drug transporter genes in human intestine, liver, kidney, and organotypic cell lines. *Drug Metabolism and Disposition* 35(8):1333-1340.
24. Prueksaritanont T, Gorham LM, Hochman JH, Tran LO, Vyas KP 1996. Comparative studies of drug-metabolizing enzymes in dog, monkey, and human small intestines, and in Caco-2 cells. *Drug Metabolism and Disposition* 24(6):634-642.

25. Englund G, Rorsman F, Ronnblom A, Karlbom U, Lazorova L, Grasjo J, Kindmark A, Artursson P 2006. Regional levels of drug transporters along the human intestinal tract: Co-expression of ABC and SLC transporters and comparison with Caco-2 cells. *European Journal of Pharmaceutical Sciences* 29(3-4):269-277.
26. Holub M, Samek Z 1977. Terpenes. CLXX. Isolation and structure of 3-epinobilin, 1,10-epoxynobilin and 3-dehydronobilin - other sesquiterpenic lactones from flowers of *Anthemis nobilis* L. revision of structure of nobilin and eucannabinolide. *Collection of Czechoslovak Chemical Communications* 42(3):1053-1064.
27. Otto I. 2007. *Chamaemelum nobilie* (L.) ALL. In Blaschek W, Ebel S, Hackenthal E, Holzgrabe U, Keller K, Reichling J, Schulz V, editors. *Hagers Enzyklopädie der Arzneistoffe und Drogen*, 6 ed., Stuttgart: Wissenschaftliche Verlagsgesellschaft mbh Stuttgart. p 298-308.
28. http://www.sigmaaldrich.com/etc/medialib/docs/Sigma/Product_Information_Sheet/1/d5030pis.Par.0001.File.tmp/d5030pis.pdf. (accessed on 2nd October 2013)
29. Kapitza SB, Michel BR, van Hoogevest P, Leigh MLS, Imanidis G 2007. Absorption of poorly water soluble drugs subject to apical efflux using phospholipids as solubilizers in the Caco-2 cell model. *European Journal of Pharmaceutics and Biopharmaceutics* 66(1):146-158.
30. Thormann U, De Mieri M, Verjee S, Neuburger M, Hamburger M, Imanidis G 2014. Mechanism of chemical degradation and determination of solubility by kinetic modeling of the highly unstable sesquiterpene lactone nobilin in different media. *Journal of Pharmaceutical Sciences* to be submitted.
31. Yumoto R, Murakami T, Nakamoto Y, Hasegawa R, Nagai J, Takano M 1999. Transport of rhodamine 123, a P-glycoprotein substrate, across rat intestine and Caco-2 cell monolayers in the presence of cytochrome P-450 3A-related compounds. *Journal of Pharmacology and Experimental Therapeutics* 289(1):149-155.
32. Wright JA, Haslam LS, Coleman T, Simmons NL 2011. Breast cancer resistance protein BCRP (ABCG2)-mediated transepithelial nitrofurantoin secretion and its regulation in human intestinal epithelial (Caco-2) layers. *European Journal of Pharmacology* 672(1-3):70-76.
33. Walgren RA, Karnaky KJ, Lindenmayer GE, Walle T 2000. Efflux of dietary flavonoid quercetin 4'-beta-glucoside across human intestinal Caco-2 cell monolayers by apical multidrug resistance-associated protein-2. *Journal of Pharmacology and Experimental Therapeutics* 294(3):830-836.
34. Shimoi K, Nakayama T. 2005. Glucuronidase deconjugation in inflammation. In Sies H, Parker L, editors. *Phase II conjugation enzymes and transport systems*, 1 ed., San Diego, New York, Berkeley, Boston, London, Sydney, Tokyo, Toronto: Academic Press. p 263-272.
35. Zhang Y, Wick DA, Haas AL, Seetharam B, Dahms NM 1995. Regulation of lysosomal and ubiquitin degradative pathways in differentiating human intestinal Caco-2 cells. *Biochimica Et Biophysica Acta-Molecular Cell Research* 1267(1):15-24.

36. Gietl Y, Vamvakas S, Anders MW 1991. Intestinal-absorption of S-(pentachlorobutadienyl)glutamine and S-(pentachlorobutadienyl)-L-cystiene, the glutathione and cysteine S-conjugates of hexachlorobuta-1,3-diene. *Drug Metabolism and Disposition* 19(3):703-707.
37. Korzekwa K, Nagar S 2013. Compartmental models for apical efflux by P-glycoprotein: Part 2—A theoretical study on transporter kinetic parameters. *Pharmaceutical Research* DOI 10.1007/s11095-013-1163-8.
38. Vertzoni M, Markopoulos C, Symillides M, Goumas C, Imanidis G, Reppas C 2012. Luminal lipid phases after administration of a triglyceride solution of danazol in the fed state and their contribution to the flux of danazol across Caco-2 cell monolayers. *Molecular Pharmaceutics* 9(5):1189-1198.
39. Markopoulos C, Thoenen F, Preisig D, Symillides M, Vertzoni M, Parrott N, Reppas C, Imanidis G 2013. Biorelevant media for transport experiments in the Caco-2 model to evaluate drug absorption in the fasted and fed state and their usefulness. *European Journal of Pharmaceutics and Biopharmaceutics* <http://dx.doi.org/10.1016/j.ejpb.2013.10.017>.
40. Thormann U, Imanidis G Influence of biorelevant media and lipid based formulations on the in vitro absorption and bioconversion of nobilin as pure compound in the Caco-2 model. in preparation.
41. Schittkowski K. 2003. Numerical data fitting in dynamical systems - A practical introduction with applications and software. 1 ed., Dordrecht, Boston: Kluwer Academic Publisher.
42. Advanced Chemistry Development (ACD/Labs) Software V11.02 (© 1994-2012 ACD/Labs) ed.
43. Lipinski CA, Lombardo F, Dominy BW, Feeney PJ 1997. Experimental and computational approaches to estimate solubility and permeability in drug discovery and development settings. *Advanced Drug Delivery Reviews* 23(1-3):3-25.
44. Amidon GL, Lennernas H, Shah VP, Crison JR 1995. A theoretical basis for a biopharmaceutic drug classification - the correlation of in-vitro drug product dissolution and in-vivo bioavailability. *Pharmaceutical Research* 12(3):413-420.
45. Khan SI, Abourashed EA, Khan IA, Walker LA 2003. Transport of parthenolide across human intestinal cells (Caco-2). *Planta Medica* 69(11):1009-1012.
46. Wu Q, Zhao B, Yang XW, Xu W, Zhang P, Zou L, Zhang LX 2010. Intestinal permeability of sesquiterpenes in the Caco-2 cell monolayer model. *Planta Medica* 76(4):319-324.
47. Augustijns P, Dhulst A, VanDaele J, Kinget R 1996. Transport of artemisinin and sodium artesunate in Caco-2 intestinal epithelial cells. *Journal of Pharmaceutical Sciences* 85(6):577-579.
48. Testa B, Krämer S. 2010. The biochemistry of drug metabolism: Conjugations, consequences of metabolism, influencing factors. 1 ed., Zürich, Weinheim: VHCA, WILEY-VCH.
49. Heilmann J, Wasescha MR, Schmidt TJ 2001. The influence of glutathione and cysteine levels on the cytotoxicity of helenanolide type sesquiterpene lactones against KB cells. *Bioorganic & Medicinal Chemistry* 9(8):2189-2194.

50. Wen J, You KR, Lee SY, Song CH, Kim DG 2002. Oxidative stress-mediated apoptosis - The anticancer effect of the sesquiterpene lactone parthenolide. *Journal of Biological Chemistry* 277(41):38954-38964.
51. Vellonen KS, Honkakoski P, Urtti A 2004. Substrates and inhibitors of efflux proteins interfere with the MTT assay in cells and may lead to underestimation of drug toxicity. *European Journal of Pharmaceutical Sciences* 23(2):181-188.
52. Loe DW, Deeley RG, Cole SPC 2000. Verapamil stimulates glutathione transport by the 190-kDa multidrug resistance protein 1 (MRP1). *Journal of Pharmacology and Experimental Therapeutics* 293(2):530-538.
53. Liu W, Feng Q, Li Y, Ye L, Hu M, Liu ZQ 2012. Coupling of UDP-glucuronosyltransferases and multidrug resistance-associated proteins is responsible for the intestinal disposition and poor bioavailability of emodin. *Toxicology and Applied Pharmacology* 265(3):316-324.
54. Jeong EJ, Lin HM, Hu M 2004. Disposition mechanisms of raloxifene in the human intestinal Caco-2 model. *Journal of Pharmacology and Experimental Therapeutics* 310(1):376-385.
55. Rothnie A, Conseil G, Lau AYT, Deeley RG, Cole SPC 2008. Mechanistic differences between GSH transport by multidrug resistance protein 1 (MRP1/ABCC1) and GSH modulation of MRP1-mediated transport. *Molecular Pharmacology* 74(6):1630-1640.
56. Fuchikami H, Satoh H, Tsujimoto M, Ohdo S, Ohtani H, Sawada Y 2006. Effects of herbal extracts on the function of human organic anion-transporting polypeptide OATP-B. *Drug Metabolism and Disposition* 34(4):577-582.
57. Mandery K, Bujok K, Schmidt I, Keiser M, Siegmund W, Balk B, Konig J, Fromm MF, Glaeser H 2010. Influence of the flavonoids apigenin, kaempferol, and quercetin on the function of organic anion transporting polypeptides 1A2 and 2B1. *Biochemical Pharmacology* 80(11):1746-1753.
58. Jiang W, Hu M 2012. Mutual interactions between flavonoids and enzymatic and transporter elements responsible for flavonoid disposition via phase II metabolic pathways. *Rsc Advances* 2(21):7948-7963.
59. Yoshida N, Koizumi M, Adachi I, Kawakami J 2006. Inhibition of P-glycoprotein-mediated transport by terpenoids contained in herbal medicines and natural products. *Food and Chemical Toxicology* 44(12):2033-2039.
60. Liang XL, Zhao LJ, Liao ZG, Zhao GW, Zhang J, Chao YC, Yang M, Yin RL 2012. Transport properties of puerarin and effect of *Radix angelicae dahuricae* extract on the transport of puerarin in Caco-2 cell model. *Journal of Ethnopharmacology* 144(3):677-682.
61. Dadkhah A, Allameh A, Khalafi H, Ashrafihelan J 2011. Inhibitory effects of dietary caraway essential oils on 1,2-dimethylhydrazine-induced colon carcinogenesis is mediated by liver xenobiotic metabolizing enzymes. *Nutrition and Cancer-an International Journal* 63(1):46-54.

62. Uchaipichat V, Mackenzie PI, Guo XH, Gardner-Stephen D, Galetin A, Houston JB, Miners JO 2004. Human UDP-glucuronosyltransferases: Isoform selectivity and kinetics of 4-methylumbelliferone and 1-naphthol glucuronidation, effects of organic solvents, and inhibition by diclofenac and probenecid. *Drug Metabolism and Disposition* 32(4):413-423.
63. Gyamfi MA, Wan YJY 2006. The effect of ethanol, ethanol metabolizing enzyme inhibitors, and Vitamin E on regulating glutathione, glutathione S-transferase, and S-adenosylmethionine in mouse primary hepatocyte. *Hepatology Research* 35(1):53-61.
64. Schutte ME, Boersma MG, Verhallen DAM, Groten JP, Rietjens I 2008. Effects of flavonoid mixtures on the transport of 2-amino-1-methyl-6-phenylimidazo 4,5-b pyridine (PhIP) through Caco-2 monolayers: An in vitro and kinetic modeling approach to predict the combined effects on transporter inhibition. *Food and Chemical Toxicology* 46(2):557-566.
65. Bousova I, Skalova L 2012. Inhibition and induction of glutathione S-transferases by flavonoids: Possible pharmacological and toxicological consequences. *Drug Metabolism Reviews* 44(4):267-286.
66. Tran VH, Marks D, Duke RK, Bebawy M, Duke CC, Roufogalis BD 2011. Modulation of P-glycoprotein-mediated anticancer drug accumulation, cytotoxicity, and ATPase activity by flavonoid interactions. *Nutrition and Cancer-an International Journal* 63(3):435-443.

Chapter 5

Influence of biorelevant media and lipid based formulations on the in vitro absorption and bioconversion of nobiletin as pure compound and as plant extract in the Caco-2 model

5.1 ABSTRACT

Nobiletin is a well permeable compound undergoing rapid chemical degradation and an even faster bioconversion to glucuronide, cysteine conjugate, and glutathione conjugate, which are asymmetrically transported out of the intestinal cell, resulting in a low in vitro absorption. The aim of this study was to investigate the effect of biorelevant media and lipid based formulations on intestinal relative fraction absorbed of nobiletin applied as a pure compound or as a full ethanolic extract of *Chamomillae romanae flos* considering chemical stability, bioconversion, and carrier mediated efflux of the conjugates. Fasted and fed state simulated intestinal fluid (FaSSIF-TM_{Caco} and FeSSIF-TM_{Caco}, respectively), and two self-emulsifying formulations, SMEDDS1 and SMEDDS2, were used. In vitro relative fraction absorbed was determined using the Caco-2 cell culture model and permeation and bioconversion parameters were deduced by means of kinetic multi-compartment modeling. FaSSIF-TM_{Caco} reduced apical efflux of all conjugates but did not affect nobiletin absorption while FeSSIF-TM_{Caco} increased absorption which was attributed to the increased chemical stability in the medium and decreased bioconversion while permeability coefficient was also decreased. SMEDDS1 increased and SMEDDS2 decreased relative fraction absorbed due to a decrease and an increase of bioconversion, respectively, although both formulations improved chemical stability and decreased permeability coefficient. The effect of FeSSIF-TM_{Caco}, SMEDDS1 and SMEDDS2 is consistent with an incorporation of nobiletin into colloidal lipid particles while FeSSIF-TM_{Caco}, SMEDDS1 appeared to inhibit and SMEDDS2 to promote enzymatic

Thormann U. et al. Influence of biorelevant media and lipid based formulations on the in vitro absorption and bioconversion of nobiletin as pure compound and as plant extract in the Caco-2 model. in preparation

reaction in the cell. In combination with the extract, no additional effect was observed although the extract alone markedly improved absorption. Formulation and transport media influence, therefore, in vitro absorption by changing bioconversion, chemical stability and permeation parameters.

5.2 INTRODUCTION

Chemical degradation, solubility, bioconversion by metabolizing enzymes, and membrane permeation by efflux and influx transporter proteins influence intestinal absorption. By targeting those properties of a compound absorption can be increased.¹⁻³

Stability and solubility in the gastrointestinal tract are influenced by the aqueous environment, a pH range from 1 to 8 and ingredients such as bile salts, phospholipids, digestive enzymes and lipolysis products.^{1,4} Bioavailability of the poorly soluble danazol, for example, was found to be increased by food whereas its solubility was increased by incorporating the drug into micelles of bile salts, phospholipids, and lipolysis products.⁵⁻⁸ Food effect has become the subject of a guidance for the industry issued by the FDA.⁹ Therefore, several attempts have been made to develop biorelevant media to simulate the conditions in the intestine in fasted and fed state.^{1,7,10-13} A quite good in vitro-in vivo correlation between in vivo bioavailability and in vitro dissolution was seen.^{7,11,12,14-18} Recently biorelevant transport media for in vitro absorption studies with the Caco-2 cell model simulating intestinal fluid in the fasted and the fed state, FaSSIF-TM_{Caco} and FeSSIF-TM_{Caco}, respectively, were developed.¹⁹

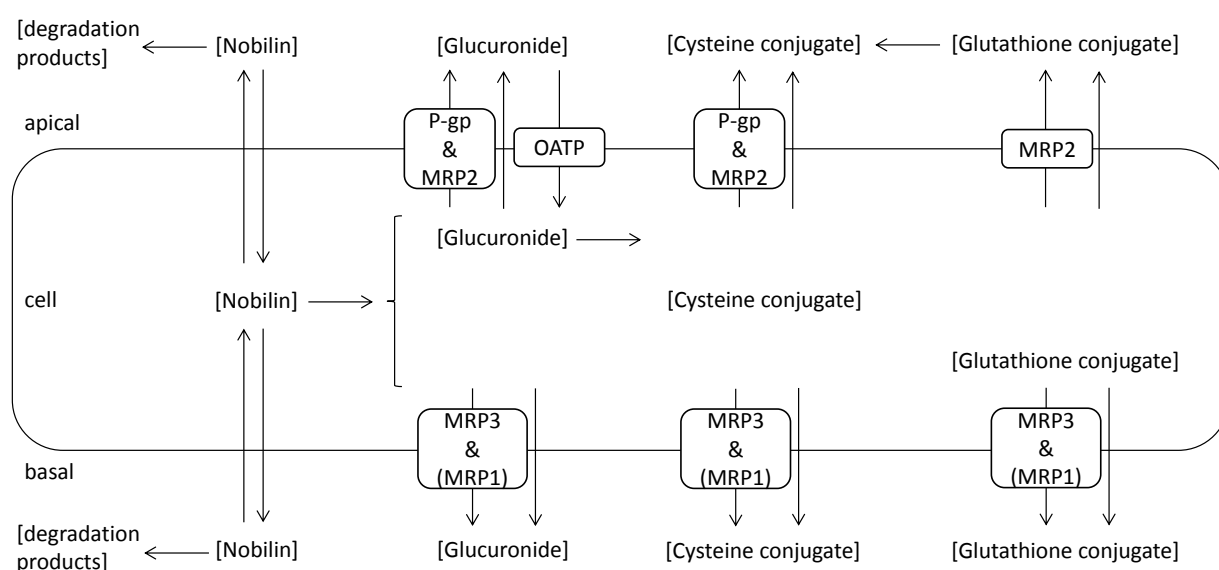
The approach of incorporating a drug into lipid particles is also attributed by lipid based formulations which were extensively discussed in recent years such as self-(micro)emulsifying drug delivery systems (S(M)EDDS).²⁰⁻²² This technique was applied to several poorly water soluble drugs like cyclosporine, for example, which is commercially available as a lipid based formulation (Neoral®)²³ or sirolimus by improving stability and solubility of the drug in presence of D- α -tocopheryl polyethylene glycol succinate micelles or SMEDDS.^{24,25}

Nobilin, a sesquiterpene lactone of the germacranolide type, is a marker compound isolated from *Chamomillae romanae flos*, the flowers of *Anthemis nobilis* L..²⁶ It is instable in an aqueous solution. Stability can be increased accompanied by an increased solubility by incorporating the compound into colloidal lipid particles of biorelevant media (FaSSIF-TM_{Caco} and FeSSIF-TM_{Caco}) and liposomal formulations with the same molar lipid content as FaSSIF-TM_{Caco} and FeSSIF-TM_{Caco} (Liposomes_{FaSSIF} and Liposomes_{FeSSIF}).²⁷ Previous Caco-2 studies showed that nobilin is a well permeable compound undergoing extensive intracellular bioconversion which results in poor in vitro absorption.²⁸ The three conjugation products glucuronide, cysteine conjugate, and glutathione conjugate were substrates of MRP2 (multidrug resistance protein, ABCC2), MRP3 (ABCC3), and possibly MRP1 (ABCC1). Glucuronide

and cysteine conjugate were also transported by P-gp (P-glycoprotein, ABCB1).²⁸ It was assumed that glucuronide was further a substrate of the influx carrier OATP (organic anion transporting polypeptide) and hydrolyzed in the cell by β -glucuronidase. Glutathione was proposed to be hydrolyzed in the apical compartment by γ -glutamyltranspeptidase and dipeptidase to the cysteine conjugate. Scheme 1 illustrates the diffusional and carrier mediated permeation, the intra- and extracellular bioconversion, and chemical degradation.²⁸ Absorption of nobiletin was increased on one hand by reducing efflux of the conjugation products which resulted in a diminished bioconversion and on the other hand by applying nobiletin as full extract of *Chamomillae romanae flos* which directly inhibited bioconversion and also indirectly by reducing efflux of the conjugation products.

Caco-2 cell culture model is routinely used to carry out in vitro study of intestinal absorption taking into consideration transporter proteins and metabolizing enzymes.²⁹⁻³² It is a well-established and well characterized model that shows a largely similar expression pattern of transporters and metabolizing enzymes as intestinal cells.³³⁻³⁵ In a study involving 10 different laboratories, Caco-2 cells were shown to well express the transporters P-gp, MRP2, MRP3, MRP1, and OATP and the phase II conjugating enzymes glutathione S-transferase and UDP-glucuronosyltransferase.³²

The first aim of this study was to investigate the effect of biorelevant media and lipid based formulation on nobiletin absorption taking into consideration chemical stability, bioconversion, and efflux of the conjugation products. The second aim was to study the effect of the extract in combination with biorelevant media and lipid based formulations on nobiletin absorption. The objective of this study was to first use stabilization as a physicochemical approach for absorption improvement that would then be investigated as a means to influence biochemical processes relevant for absorption.



Scheme 1: Transport of nobiletin and its conjugates by diffusional and/or carrier mediated permeation, nobiletin chemical degradation, and intra- and extracellular bioconversion.²⁸

5.3 MATERIALS AND METHODS

5.3.1 Chemicals

The human colon adenocarcinoma cell line Caco-2 was a gift of Prof. H. P. Hauri, Biocenter, University of Basel, and originated from the American Type Culture Collection (ATCC, Rockville, MD, USA). The Dulbecco's modified Eagle's medium (DMEM) (with L-glutamine, 4500 mg/L D-glucose, without sodium pyruvate), MEM non-essential amino acids solution (100×, without L-glutamine), L-glutamine 200 mM (100×), fetal bovine serum (FBS), Trypsin 0.5%-EDTA (10×) liquid, Dulbecco's phosphate buffered saline (with and without Ca^{2+} , Mg^{2+}) were all purchased from Gibco® Invitrogen corporation (Paisley, UK). The cell culture medium was supplemented with 10% (v/v) FBS, 1.8 mM L-glutamine, and 1% (v/v) MEM. Petri dishes (56.7 cm²) were purchased from Nunc A/S (Roskilde, Denmark) Petri dishes (21 cm²) and 6-well polycarbonate membrane transwell™ plates with an insert area of 4.7 cm² and 0.4 μm pore size were ordered from Costar (Corning Incorporated, Corning, NY, USA).

Nobilin, a sesquiterpene lactone with M_r 346 and the ethanolic extract of *Chamomillae romanae flos* (PhEur) were kindly provided by Alpinia Laudanum Institute of Phytopharmaceutical Sciences AG (ALIPS) (Walenstadt, Switzerland). Nobilin was purified from *Chamomillae romanae flos* (PhEur) as described before.²⁷ D-glucose, L-glutamine, 4-(2-Hydroxyethyl)piperazine-1-ethanesulfonic acid (HEPES), sodium chloride (NaCl), sodium hydroxide (NaOH), maleic acid, Tricaprylin, dimethyl sulfoxide (DMSO), Triton® X-100, Dulbecco's Modified Eagle's Medium (DMEM) base powder (without D-glucose, L-glutamine, phenol red, sodium pyruvate, and sodium bicarbonate),³⁶ sodium oleate were purchased from SIGMA-Aldrich Chemie GmbH (Buchs, Switzerland). Lipoid E PC S and Lipoid S 100 were kindly provided by Lipoid GmbH (Ludwigshafen, Germany). Glycerol monooleate was purchased from Danisco (Copenhagen, Denmark). Sodium taurocholate was bought from Prodotti Chimici e di Alimentari s. p. a. (Basaluzzo, Italy). Capmul MCM was purchased from Abitec Corporation (Columbus, OH, USA). Cremophor EL and Lutrol F 68 were kindly provided from BASF (Ludwigshafen, Germany). α-Tocopherol was purchased from Hänseler AG (Herisau, Switzerland).

Methanol and ethanol from J.T.Baker (Deventer, Nederland), sodium acetate and formic acid from SIGMA-Aldrich Chemie GmbH (Buchs, Switzerland) were of HPLC grade. Water was purified by reversed osmosis with the water purification system arium® 61215 of Sartorius (Goettingen, Germany).

5.3.2 Media

The three different TM_{Caco} (transport media) that are compatible with the Caco-2 cell line were described by Markopoulos et al.¹⁹ The compositions are shown in Table 1 (purely aqueous medium [aq-TM_{Caco}], fasted state simulated intestinal fluid [FaSSIF-TM_{Caco}] and fed state simulated intestinal fluid

[FeSSIF-TM_{Caco}]). The media contained DMEM base powder, L-glutamine, and D-glucose to support the viability of the cells.

The DMEM base powder was dissolved in autoclaved water. It was supplemented with D-glucose, L-glutamine, NaCl (aq-TM_{Caco}), and HEPES (aq-TM_{Caco}) or maleic acid (FaSSIF-TM_{Caco} and FeSSIF-TM_{Caco}). After adjusting the pH with sodium hydroxide and sterile filtration (Supor-200, 0.2 µm pore size, Pall Corporation, Port Washington, NY, USA) under aseptic conditions FaSSIF-TM_{Caco} and FeSSIF-TM_{Caco} were supplemented with sodium taurocholate, lecithin, glycerol monooleate (only FeSSIF-TM_{Caco}), and sodium oleate (only FeSSIF-TM_{Caco}). Lecithin and glycerol monooleate were added to the media separately as dichloromethane solution and the organic solvent was evaporated with a rotary evaporator (RE 120, Büchi, Flawil, Switzerland) at 40°C and 100 mbar.

Table 1: Composition of the three transport media.

	aq-TM _{Caco}	FaSSIF-TM _{Caco}	FeSSIF-TM _{Caco}
DMEM base powder [g/L] ^a	8.3	8.3	8.3
D-glucose [mM]	25	25	25
L-glutamine [mM]	6	6	6
NaCl [mM]	34	-	-
HEPES [mM]	19.98	-	-
Maleic acid [mM]	-	19.12	55.02
NaOH	qs	qs	qs
Sodium taurocholate [mM]	-	3	6.8
Lecithin (Lipoid E PC S) [mM]	-	0.2	6.8
Glycerol monooleate [mM]	-	-	3.4
Sodium oleate [mM]	-	-	0.8
pH	7.4	6.5	5.8
Osmolality [mOsm/kg]	350	320	390

^a contains amino acids, vitamins, electrolytes, trace elements³⁶; qs: sufficient

5.3.3 Liposomal formulations

Liposomes were prepared by the film method. Lipoid S 100 was dissolved in ethanol in a round bottomed flask and evaporated to dryness with a rotary evaporator at 40°C. The lipid film was suspended in tempered aq-TM_{Caco} (37°C) and extruded under nitrogen pressure of 8-9 bar through polycarbonate filters (Nucleopore track edge membrane filters, Whatman plc, Kent, UK) pore size 0.4 µm (3 times), 0.2 µm (5 times), and 0.1 µm (2 × 10 times).¹⁹ The two liposomal formulations in

aq-TM_{Caco} had the same lipid concentrations as FaSSIF-TM_{Caco} (3.2 mM) and FeSSIF-TM_{Caco} (17.8 mM) and were termed Liposomes_{FaSSIF} and Liposomes_{FeSSIF}, respectively.

5.3.4 Lipid based formulations

1) Formulation 1 (SMEDDS1)

The lipid phase consisted of Tricaprylin 35% (w/w) (triglyceride), Capmul MCM 18% (w/w) (mono- and diglyceride), Cremophor EL 37% (w/w) (emulsifier), and EtOH 10% (w/w). Nobiletin was dissolved in the EtOH of the lipid phase and added to that. Alternatively, the ethanolic plant extract was added to the lipid phase and EtOH was evaporated with a rotary evaporator (RE 120, Büchi, Flawil, Switzerland) at 40°C to the final content of 10% (w/w). The lipid phase was suspended in one third of tempered aq-TM_{Caco}, homogenized for 5 min at 15,000 rpm with a polytron homogenizer (Polytron PT 3000, Kinematica AG, Littau, Switzerland) and adjusted to 1:200 (w/v) with aq-TM_{Caco} to the final volume.

2) Formulation 2 (SMEDDS2)

The lipid phase containing Lutrol F 68 90% (w/w) and α -Tocopherol 10% (w/w) was melted in a water bath at 60°C. Ethanol containing nobiletin or the ethanolic plant extract was added and mixed with the lipid phase. Ethanol was evaporated to dryness with a rotary evaporator at 40°C. The lipid phase was suspended 1:200 (w/v) in tempered aq-TM_{Caco}. The described formulation is based on the patent WO 2007/104173.³⁷

5.3.5 Particle size measurement

The particle size of the mixed micelles of FaSSIF-TM_{Caco} and FeSSIF-TM_{Caco}, the two liposomal formulations (Liposomes_{FaSSIF} and Liposomes_{FeSSIF}), and lipid based formulations (SMEDDS1 and SMEDDS2) were measured by dynamic light scattering using a Zetasizer (Nano ZS, Malvern Instruments, Worcestershire, UK). The solutions were equilibrated at least 30 min at 37°C before measurement.

5.3.6 Kinetics of chemical degradation

Purified nobiletin was dissolved in DMSO at a concentration of 1 mg/mL and added to aq-TM_{Caco} to a starting concentration of 50 μ g/mL, and to the biorelevant media and liposomal formulations to a starting concentration of around 3 μ g/mL. The lipid based formulations were suspended 1:200 (w/v) in aq-TM_{Caco} as described above to a starting concentration of 2-5 μ g/mL nobiletin. The ethanolic plant extract was diluted 1:200 (v/v) with the media or the liposomal formulations and the lipid based formulations were suspended 1:200 (w/v) in aq-TM_{Caco} as described above to a starting concentration of

around 1-2 µg/mL nobilin. Degradation of nobilin was monitored in all preparations for 5-7 hours under magnetic stirring at 37°C.

The degradation process was described by pseudo first order kinetics:

$$C(t) = C(0) \cdot e^{-k_d t} \quad \text{Equation (1)}$$

where, C(t) is the measured concentration at a specific time point, C(0) is the concentration at time point 0, k_d is the degradation rate constant, and t is time. The degradation rate constant, k_d , was determined by fitting Equation (1) to the data.

5.3.7 Cell Culture

Caco-2 cells were cultivated in Petri dishes (56.7 cm²) using culture medium at 37°C in a water saturated atmosphere of 8% CO₂ (Sorvall Heraeus, Heracell, Kendro Laboratory Products, Zürich, Switzerland). The cells were passaged by treatment with a solution of 0.25% trypsin and 2.63 mM EDTA with a splitting ratio of 1:5-1:10 when the cell monolayer reached 70-90% confluence. Cells of passage numbers 60-65 were seeded at a density of 1.14×10^5 cells/cm² in 6-well transwell™ plates and incubated for 19-21 days. The medium was changed every other day.

5.3.8 TEER

The integrity of the Caco-2 cell monolayer in the transwell™ plates was ensured with TEER measurement before every permeation experiment. The monolayer was washed with pre-warmed (37°C) D-PBS (with Ca²⁺, Mg²⁺) (apical 3 mL and basal 4 mL). 1.6 mL of tempered aq-TM_{Caco} was added to the apical and 2.8 mL aq-TM_{Caco} to the basal compartment. The transwell™ plate was equilibrated for 60 min in the cell culture incubator and TEER was measured with an EVOM resistance meter (World Precision Instruments, Sarasota, FL, USA) equipped with an EndOhm-24SNAP chamber (World Precision Instruments, Sarasota, FL, USA) which was tempered at 37°C with 4.6 mL aq-TM_{Caco}. Caco-2 monolayers with TEER values above 470 Ω cm² were used for permeation experiments.

5.3.9 Permeation experiment

After the TEER measurement, the aq-TM_{Caco} was removed and the tempered nobilin containing aq-TM_{Caco} was added. Nobilin was dissolved in DMSO (1 mg/mL) and added to aq-TM_{Caco} (final DMSO concentration 0.3%) to a starting concentration of around 7 µM. To investigate the permeation in the apical-to-basal direction, 1.6 mL of the nobilin solution was added to the apical compartment and 2.8 mL of blank aq-TM_{Caco} to the basal compartment. For the basal-to-apical direction, 1.6 mL of blank

aq-TM_{Caco} was added to the apical and 2.8 mL of the nobilin solution to the basal compartment. One plate was used for each direction.

The biorelevant media, FaSSIF-TM_{Caco} and FeSSIF-TM_{Caco} were added to the apical compartment and the liposomal formulation with the corresponding amount of lipids to the basal compartment due to cytotoxic effects of the biorelevant media.¹⁹ Nobilin was added from the DMSO stock solution either to the biorelevant medium or to the liposomal formulation depending on the transport direction. The two lipid based formulations were suspended in aq-TM_{Caco} as described above and added to both compartments depending on the transport direction with nobilin or as placebo. The starting nobilin concentrations were around 7 µM.

The ethanolic extract of *Chamomillae romanae flos* was diluted 1:200 (v/v) with the media or the liposomal formulations yielding a nobilin concentration of approximately 3 µM. Extract was added to both formulations as described above and added to the plate depending on the transport direction to the apical or basal compartment with a starting nobilin concentration of 2 µM for SMEDDS1 and SMEDDS2(1), and 9 µM for SMEDDS2(2).

The transwell™ plate was shaken on an orbital shaker at 37°C in a water saturated atmosphere under an incubator hood with a stirring rate of 120 rpm (KS15, Edmund Bühler GmbH, Tübingen & Hechingen, Germany). Permeation of nobilin across the cell monolayer was monitored by drawing samples of 100 µL from both compartments after 10 min, 35 min, 1 h, 1.5 h, 2 h, and 2.5 h. One hundred µL of methanol was added and the samples were stored at 4°C. Under these conditions nobilin was chemically stable. Samples containing lipids were centrifuged for 30 min at 16,100 g and 4°C (5415R, Eppendorf AG, Hamburg, Germany) before HPLC measurement. At each time point one insert was removed and used for cell extraction.

5.3.10 Cell extraction

Both sides of the transwell™ were washed with 4°C cold D-PBS (without Ca²⁺ and Mg²⁺), the insert was transferred to a Petri dish (21 cm²), 750 µL of a 1% Triton® X-100 solution in aq-TM_{Caco} was added and the dish was shaken at 120 rpm on an orbital shaker for 15 min at 37°C under an incubator hood. The cells were scraped of the polycarbonate membrane using a cell scraper (BD Falcon, BD Biosciences Discovery Labware, Bedford, USA), transferred into a 1.5 mL tube (Eppendorf AG, Hamburg, Germany) and frozen at -80°C.

The sample was thawed within 3 min at 37°C under shaking with 1400 rpm (Thermomixer comfort, Eppendorf AG, Hamburg, Germany), 750 µL MeOH was added and kept on ice bath for 20 min. After shaking for 10 min at 37°C with 1400 rpm, the sample was centrifuged for 3 min at 16,100 g and 25°C (5415R, Eppendorf AG, Hamburg, Germany). The supernatant was transferred to a tube and stored at

4°C. The pellet was disintegrated in 750 μ L methanol with 6 pulses of an ultrasonic disintegrator (Branson Sonifier 250, Model 101-063-197, Branson Ultrasonics Corporation, Danbury, CT, USA, instrument settings: output control 2, duty cycle 30%), shaken for 5 min on the thermomixer (37°C and 1400 rpm) and centrifuged at 16,100 g and 25°C for 3 min. After repeating the pellet disintegration once, the methanolic supernatants were united and the methanol was evaporated under nitrogen flow. The residue was taken up with the methanol-water supernatant of the first extraction. The sample was shaken on the thermomixer at 1400 rpm and 37°C for 3 min and centrifuged for 25 min at 16,100 g and 25°C before HPLC analysis.

5.3.11 HPLC

Nobilin and its conjugates were analysed by HPLC-UV-MS of Agilent series 1200 equipped with a degaser G1379B, a binary pump G1312A, an autosampler G1367B, a thermostat G1330B, a column oven G1316A, a variable wavelength detector G1314B and a single quadrupole MS detector G6130A. A C-18 reversed phase column (Agilent Eclipse XBD-C18, 5 μ m, 2 \times 125 mm) and mobile phase consisting of (A) water with 0.1% (v/v) formic acid and 0.05 mM sodium acetate and (B) methanol with 0.1% (v/v) formic acid and 0.05 mM sodium acetate were used. The composition of the mobile phase was varied in a gradient mode: 0 min A:B 50:50, 0-18 min linear change to A:B 10:90, 18-22 min A:B 10:90, 22-23 min linear change to A:B 50:50, and 23-28 min A:B 50:50 (all samples apart from SMEDDS1) or 0 min A:B 35:65, 0-18 min linear change to A:B 10:90, 18-22 min A:B 10:90, 22-23 min linear change to A:B 35:65, and 23-28 min A:B 35:65 (samples with SMEDDS1) with a flow rate of 0.25 mL/min and a runtime of 28 minutes. The samples were cooled in the autosampler to 4°C and the column was heated to 40°C (all samples apart from SMEDDS1) or 20°C (samples with SMEDDS1). The ions were generated by atmospheric pressure electrospray ionisation and the MS detector was run in scan mode (m/z 100 - 1000, for all samples) and SIM mode (for samples of the cell extraction) at positive polarity with capillary voltage 4000 V, fragmentor 160 V, drying gas flow 10 L/min, drying gas temperature 350°C and nebulizer pressure 20 psig. Nobilin was detected at 218 nm in UV and at m/z 369, and 716 in MS corresponding to the sodium adduct of nobilin and the sodium adduct of the dimer of nobilin, respectively. The glucuronide was detected at m/z 525, the glutathione conjugate at m/z 654, and the cysteine conjugate at m/z 468 corresponding to their protonated forms. The conjugates were quantified with the calibration curve of nobilin. The LOQ of nobilin for an injection volume of 100 μ L was 0.02 μ g/mL in the UV and 0.004 and 0.0001 μ g/mL in MS scan and SIM mode, respectively. Linearity was fulfilled in UV for concentrations up to 100 μ g/mL and in MS (scan and SIM mode) up to 1 μ g/mL. Standard deviation of measured concentrations of the calibration curve in UV and MS (scan and SIM mode) was at maximum 10%.

5.3.12 Kinetic modeling

To describe the processes taking place in the course of nobiletin absorption in the Caco-2 model and comprising diffusional, intracellular bioconversion, and chemical degradation, a kinetic model was developed taking into account that:

1. Nobiletin permeates the cell membrane by diffusion.
2. Nobiletin is chemically degraded in aqueous solution following first order kinetics.²⁷
3. Three conjugation products of nobiletin, i.e., glucuronide, cysteine conjugate and glutathione conjugate are formed in the cells.²⁸

For the proposed model the following assumptions were made:

1. Conjugation reactions and the degradation of glucuronide and glutathione conjugates obey first order kinetics.
2. Permeability coefficient (diffusional) of nobiletin is different for the apical and the basal membrane because of the difference between the two membranes.

A system of differential equations was established describing the change of concentration of nobiletin as a function of time in the apical, the cellular, and the basal compartments for apical-to-basal and basal-to-apical transport taking into consideration chemical degradation, bioconversion, and diffusional permeation as shown in Scheme 1. Similar models were described by this group previously.^{5,19,28,38}

The system of equations is given below:

apical to basal (index ab):

$$\frac{dCA_{ab}}{dt} = -P_a \cdot (CA_{ab} - K_{a/c} \cdot CC_{ab}) \cdot \frac{S}{VA} - k_d \cdot CA_{ab} \quad \text{Equation (2)}$$

$$\frac{dCB_{ab}}{dt} = P_b \cdot (K_{a/c} \cdot CC_{ab} - u \cdot CB_{ab}) \cdot \frac{S}{VB} - k_d \cdot CB_{ab} \quad \text{Equation (3)}$$

$$\begin{aligned} \frac{dCC_{ab}}{dt} = & P_a \cdot (CA_{ab} - K_{a/c} \cdot CC_{ab}) \cdot \frac{S}{VC} - P_b \cdot (K_{a/c} \cdot CC_{ab} - u \cdot CB_{ab}) \cdot \frac{S}{VC} \\ & - k_{dc} \cdot CC_{ab} \end{aligned} \quad \text{Equation (4)}$$

basal to apical (index ba):

$$\frac{dCA_{ba}}{dt} = P_a \cdot (K_{a/c} \cdot CC_{ba} - CA_{ba}) \cdot \frac{S}{VA} - k_d \cdot CA_{ba} \quad \text{Equation (5)}$$

$$\frac{dCB_{ba}}{dt} = -P_b \cdot (u \cdot CB_{ba} - K_{a/c} \cdot CC_{ba}) \cdot \frac{S}{VB} - k_d \cdot CB_{ba} \quad \text{Equation (6)}$$

$$\begin{aligned} \frac{dCC_{ba}}{dt} = & -P_a \cdot (K_{a/c} \cdot CC_{ba} - CA_{ba}) \cdot \frac{S}{VC} + P_b \cdot (u \cdot CB_{ba} - K_{a/c} \cdot CC_{ba}) \cdot \frac{S}{VC} \\ & - k_{dc} \cdot CC_{ba} \end{aligned} \quad \text{Equation (7)}$$

where, CA, CB, and CC are concentration of nobilin in the apical, basal, and cellular compartments, respectively, P_a and P_b are permeability coefficient of the apical and the basal membranes, respectively, K_{a/c} is the partition coefficient between apical and cellular compartment, u is the partition coefficient between the apical and the basal compartment, k_d is the chemical degradation rate constant, k_{dc} is the total conjugation rate constant in the cell, VA, VB, and VC are volume of the apical, basal, and cellular compartments, respectively, S is the surface area (4.7 cm²), and t is time. The cellular volume was 0.0094 mL calculated with a monolayer thickness of 20 μm.

A combined permeability coefficient, P, applying to both membranes was calculated from P_a and P_b by Equation (8) and the standard error with Equation (9).

$$P = \frac{2P_a P_b}{P_a + P_b} \quad \text{Equation (8)}$$

$$SE = \sqrt{\frac{4}{(P_a + P_b)^4} \cdot (P_b^4 \cdot (SE)_a^2 + P_a^4 \cdot (SE)_b^2)} \quad \text{Equation (9)}$$

The extent of in vitro absorption was introduced to quantify the maximal amount of intact nobilin appearing in the basal compartment and was expressed as the relative fraction absorbed given by Equation (10). The denominator of Equation (10) gives the amount of nobilin in the basal compartment at equilibrium when neither chemical degradation nor bioconversion takes place and was defined as 100% in vitro absorption.

$$F_a = \frac{\int_0^{t_{max}} P_b \cdot (K_{a/c} \cdot CC_{ab} - u \cdot CB_{ab}) \cdot S \, dt}{\int_0^{t_{max}^0} P_b \cdot (K_{a/c} \cdot CC_{ab}^0 - u \cdot CB_{ab}^0) \cdot S \, dt} \quad \text{Equation (10)}$$

where, F_a is the relative fraction absorbed, CB_{ab}⁰ and CC_{ab}⁰ is concentration in the basal and cellular compartment, respectively, when neither chemical degradation nor bioconversion take place, and t_{max} and t_{max}⁰ is the time at which maximum absorption is observed. CB_{ab}⁰ and CC_{ab}⁰ were simulated using the determined values of P_b and K_{a/c}.

The system of differential equations (2) through (7) was numerically solved and simultaneously fitted to experimental concentration or mass data of nobilin and its three conjugation products in all three compartments in both transport directions using the EASY-FIT® software.³⁹ From the least square

regression analysis, values of the permeability coefficients, partition coefficients ($K_{a/c}$ and u), and total conjugation rate constant which were treated as adjustable parameters were deduced.

The reduction of the volume in the apical and basal compartment because of sampling was described by the following empirical equations.

$$VA = 1.6241 - 0.341t + 0.0821t^2 - 0.0148t^3 \quad \text{Equation (11)}$$

$$VB = 2.8241 - 0.341t + 0.0821t^2 - 0.0148t^3 \quad \text{Equation (12)}$$

Significance test was carried out based on the incidence of overlap of the confidence intervals at the $p = 0.01$ level of two estimated values of a parameter from different experimental sets. In addition, the relation

$$F = \frac{(\text{value}(\alpha) - \text{value}(\beta))^2}{(SE)_\alpha^2 + (SE)_\beta^2} \quad \text{Equation (13)}$$

was used where, $\text{value}(\alpha)$ and $\text{value}(\beta)$ are two values of a parameter and $(SE)_\alpha$ and $(SE)_\beta$ are the corresponding standard errors of the estimates. Significance was determined by comparing F with the critical value $F_{0.01[1,df]}$, where df is degrees of freedom of residuals for which $df = 8$ was used. An agreement between the two tests was required for declaring statistical significance of the difference between two values of a parameter; this agreement was observed in the vast majority of cases. The significant tests of the chemical degradation rate constant, k_d , deduced using Equation (1) was also carried out with Equation (13) and df between 3 and 7 depending on the number of measurements.

5.4 RESULTS

5.4.1 Stability study

The estimated parameter values of nobilin and nobilin as plant extract in presence of different media, liposomes, and lipid based formulations are shown in Table 2. The degradation rate constant of nobilin in aq-TM_{Caco} was $1.17 \times 10^{-4} \text{ s}^{-1}$. It was decreased by FaSSIF-TM_{Caco}, FeSSIF-TM_{Caco}, Liposomes_{FaSSIF}, Liposomes_{FeSSIF}, SMEDDS1, and SMEDDS2 1.3-, 8-, 8.7-, 44.8-, 5.3-, and 2.1-fold, respectively. Similar results were obtained for nobilin as a full extract in presence of different media, liposomes, and lipid based formulations.

Table 2: Degradation constant of nobilin (pure compound) and nobilin as a full extract in different media, liposomes, and lipid based formulations.

	pure compound	extract	particle size [nm] (pure compound)	total lipid conc. [mg/mL]
	$k_d \text{ [s}^{-1}\text{]}$	$k_d \text{ [s}^{-1}\text{]}$		
aq-TM _{Caco}	1.17×10^{-4}	1.08×10^{-4}	-	-
FaSSIF-TM _{Caco}	9.02×10^{-5}	7.85×10^{-5}	83.2	1.76
FeSSIF-TM _{Caco}	1.46×10^{-5}	2.33×10^{-5}	68.8	10.39
Liposomes _{FaSSIF}	1.34×10^{-5}	1.66×10^{-5}	120.7	2.37
Liposomes _{FeSSIF}	2.61×10^{-6}	2.36×10^{-6}	124.9	13.2
SMEDDS1	2.22×10^{-5}	2.47×10^{-5}	79.7	5
SMEDDS2	5.65×10^{-5}	5.29×10^{-5}	28.3	5

5.4.2 Influence of media on the transport of nobilin and its conjugates

Figure 1 shows the result of nobilin in the media in the Caco-2 permeation experiment. Drawn lines were obtained by fitting the model to the experimental data of nobilin. A rapid permeation of nobilin in aq-TM_{Caco} from the donor into the cells and onward in the receiver compartment was observed. Nobilin concentration decreased quickly in all three compartments and reached near zero concentrations after 2.5 hours. Same observations were reported before.²⁸ Concentration-time profiles were different in presence of FaSSIF-TM_{Caco}. The concentration in the basal compartment was higher than in the apical compartment. The permeation was slower in FeSSIF-TM_{Caco} and concentrations were equal in the apical and basal compartments in the apical-to-basal transport direction and a higher concentration in the basal compartment than in the apical compartment in the basal-to-apical transport direction whereas the intracellular amount was increased after 2.5 h. Fitted curves are in good agreement with the data.

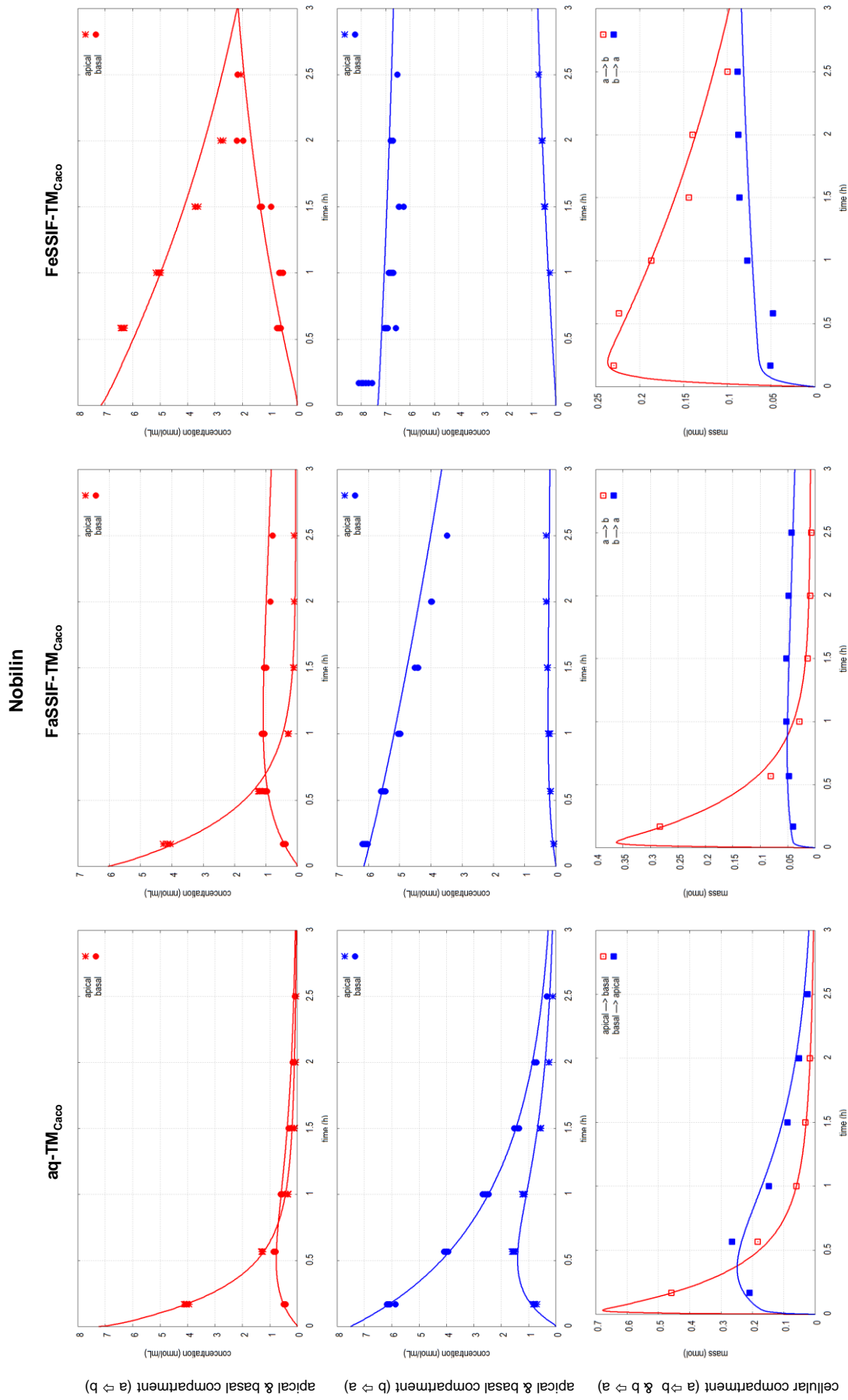


Figure 1: Nobilin concentration in (left to right) aq-TM_{Caco}, FaSSIF-TM_{Caco}, and FeSSIF-TM_{Caco} in the apical-to-basal (top panels, red) and the basal-to-apical (middle panels, blue) transport direction in both compartments and nobilin mass in the cellular compartment (bottom panels) in both transport directions as a function of time. (●) apical concentration, (●) basal concentration, (□) mass in apical-to-basal transport direction (red), (■) mass in basal-to-apical transport direction (blue). Symbols represent measured data and lines fitted model curves.

The estimated parameter values of nobiletin in the media are shown in Figure 2. Nobiletin in aq-TM_{Caco} had a quite large permeability coefficient (2.69×10^{-4} cm/s) and a partition coefficient $K_{a/c}$ of 0.057.

FaSSIF-TM_{Caco} did not have an effect on the permeability coefficient or the partition coefficient $K_{a/c}$ whereas FeSSIF-TM_{Caco} decreased the former 5-fold and increased the latter almost 2-fold. The partition coefficient u in the experiment with FaSSIF-TM_{Caco} was slightly smaller than the one with FeSSIF-TM_{Caco}. The conjugation rate constant was considerably larger than the chemical degradation rate constant of nobiletin in aq-TM_{Caco}. FaSSIF-TM_{Caco} did not have an effect on the total conjugation rate constant whereas this constant was not statistically different from zero in presence of FeSSIF-TM_{Caco}. The relative fraction absorbed of nobiletin in aq-TM_{Caco} was 37% and in FaSSIF-TM_{Caco} 38%. FeSSIF-TM_{Caco} increased it to 96%.

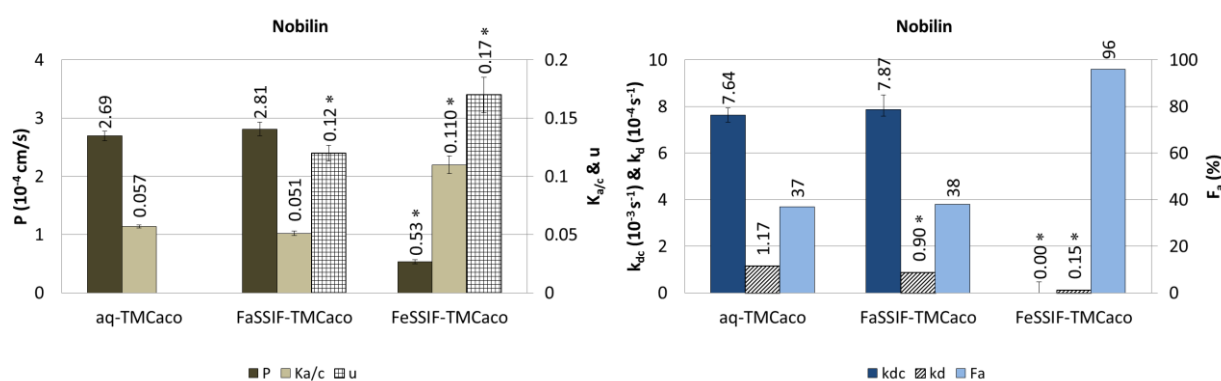


Figure 2: Deduced values (columns) and standard errors (bars) of permeability coefficient P , partition coefficient $K_{a/c}$, partition coefficient u (dark, light, and crosshatched columns, respectively, on left panel), total conjugation rate constant k_{dc} , chemical degradation rate constant k_d , and relative fraction absorbed F_a (dark, diagonally hatched, and light columns, respectively, on right panel) of nobiletin from model fitting in different media. * $p < 0.01$.

Figure 3 and Figure 4 show the results of the three conjugation products of nobiletin in aq-TM_{Caco} and FaSSIF-TM_{Caco}, respectively, in the Caco-2 permeation experiment. Rather large concentrations / amounts of all three conjugation products were detected in aq-TM_{Caco} (Figure 3). The concentration of glucuronide in the apical solution increased in the beginning and later decreased while concentration in the basal solution steadily increased over time. As a result, apical concentration was at early time points greater and at later times lower than the basal concentration. This was true for both transport directions. The concentration-time profiles of the cysteine conjugate were rather different. Apical and basal concentrations increased constantly with time but the former was considerably greater than the latter throughout the experiment in both transport directions. Glutathione conjugate concentration pattern, finally, was similar to that of glucuronide, apical concentrations, however, briefly increased and then rapidly declined while basal concentrations steadily increased reaching a large difference to the apical ones. The amount of all conjugates in the cell increased at first and then decreased to very low levels over time in both transport directions. These results demonstrate that transport of the conjugates out of the cell was highly asymmetric which was reported before.²⁸

In presence of FaSSIF-TM_{Caco} (Figure 4) concentration of glucuronide steadily increased in the apical and basal compartment over time whereas the latter was considerably greater than the former in both transport direction. Also a constant increase of cysteine conjugate and glutathione conjugate in the basal compartment was observed but none of these conjugates were detected in the apical compartment in both transport direction. After 2.5 h all three conjugates were still present in the cells. Cell extraction was carried out at the end of the experiment as described elsewhere.¹⁹ In presence of FeSSIF-TM_{Caco} no conjugates were detected in all three compartments.

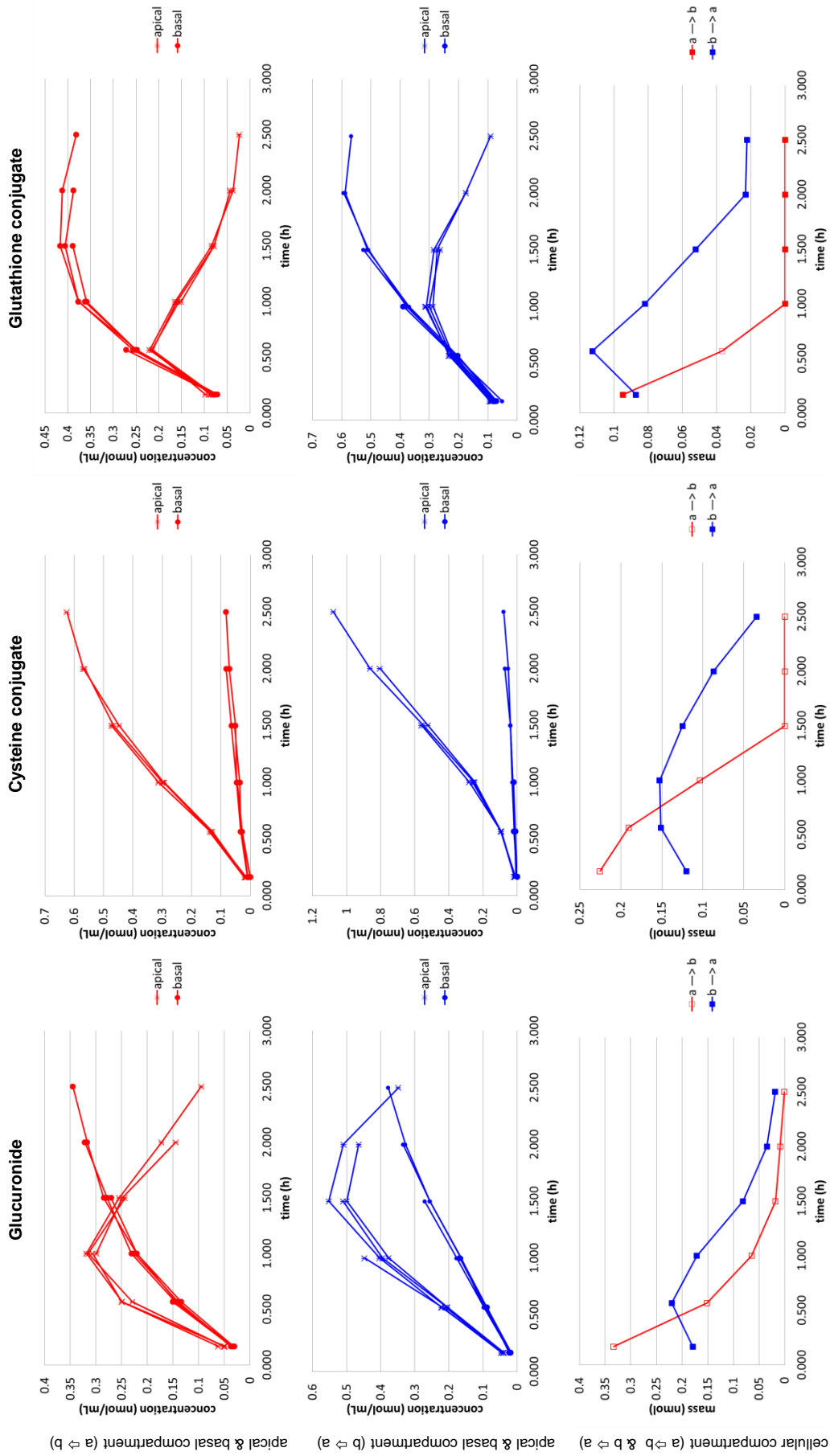


Figure 3: Concentration of (left to right) glucuronide, cysteine conjugate, and glutathione conjugate in aq-TM_{Caco} in the apical-to-basal (top panels, red) and the basal-to-apical (middle panels, blue) transport direction in both compartments and mass of (left to right) glucuronide, cysteine conjugate, and glutathione conjugate in the cellular compartment (bottom panels) in both transport directions as a function of time. (*) apical concentration, (●) basal concentration, (□) mass in apical-to-basal transport direction (red), (■) mass in basal-to-apical transport direction (blue). Symbols represent measured data.

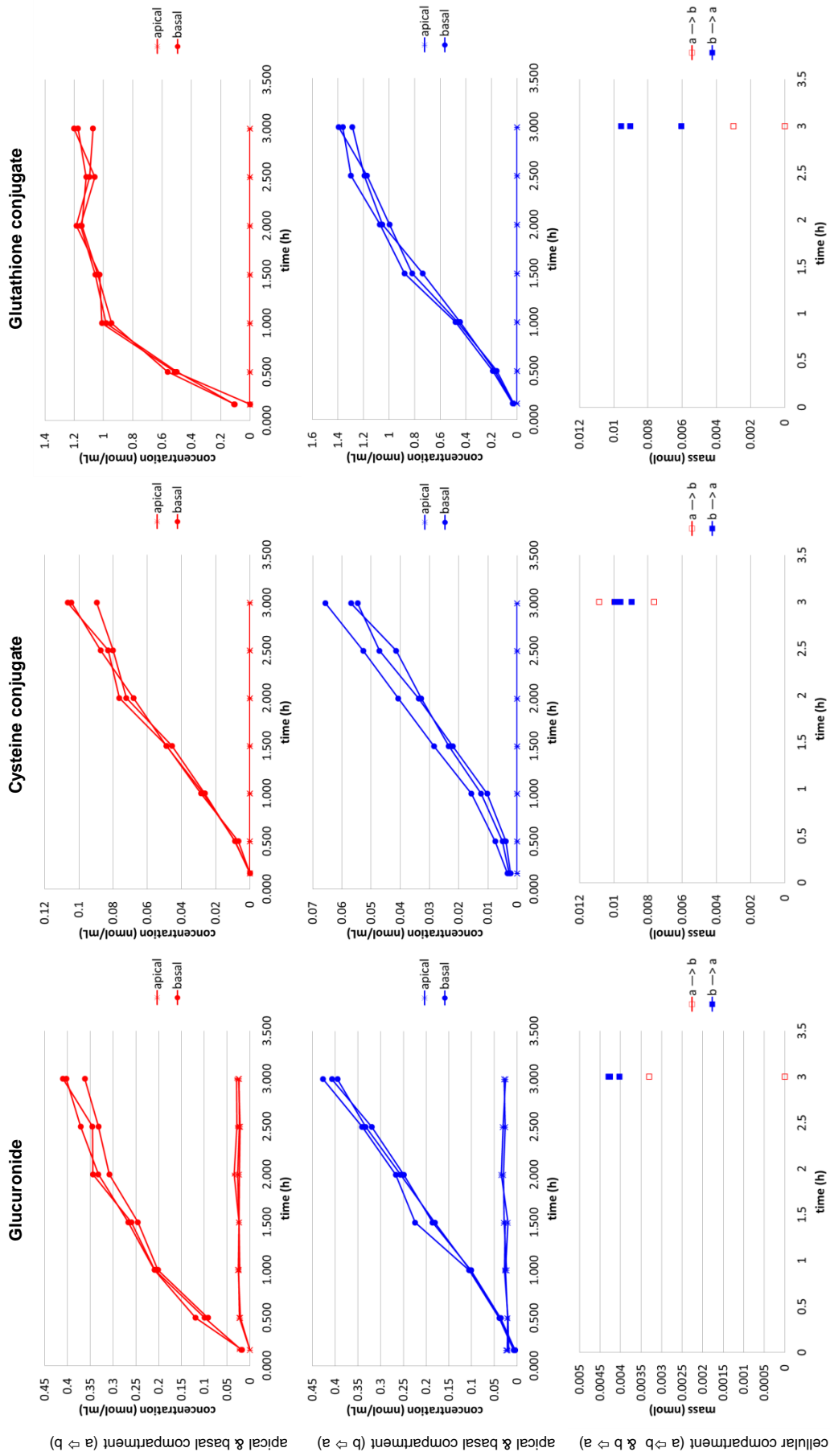


Figure 4: Concentration of (left to right) glucuronide, cysteine conjugate, and glutathione conjugate in FaSSIF-TM_{Caco} in the apical-to-basal (top panels, red) and the basal-to-apical (middle panels, blue) transport direction in both compartments and mass of (left to right) glucuronide, cysteine conjugate, and glutathione conjugate in the cellular compartment (bottom panels) in both transport directions as a function of time. (*) apical concentration, (●) basal concentration, (◐) mass in apical-to-basal transport direction (red), (◑) mass in basal-to-apical transport direction (blue). Symbols represent measured data.

5.4.3 Influence of SMEDDS on the transport of nobilin and its conjugates

Figure 5 shows the result of nobilin in presence of the lipid based formulations in the Caco-2 permeation experiment. Drawn lines were obtained by fitting the model to the experimental data of nobilin. Slow permeation of nobilin in presence of SMEDDS1 from the donor into the cells and onward in the receiver compartment was observed whereas nobilin was detected in all three compartments after 2.5 h in both transport directions. A slightly slower permeation of nobilin was observed in presence of SMEDDS2 compared to no formulation (Figure 1). Rapid decline of the nobilin concentration in all three compartments was found which reached near zero after 2.5 h in both transport directions. Fitted curves are in good agreement with the data.

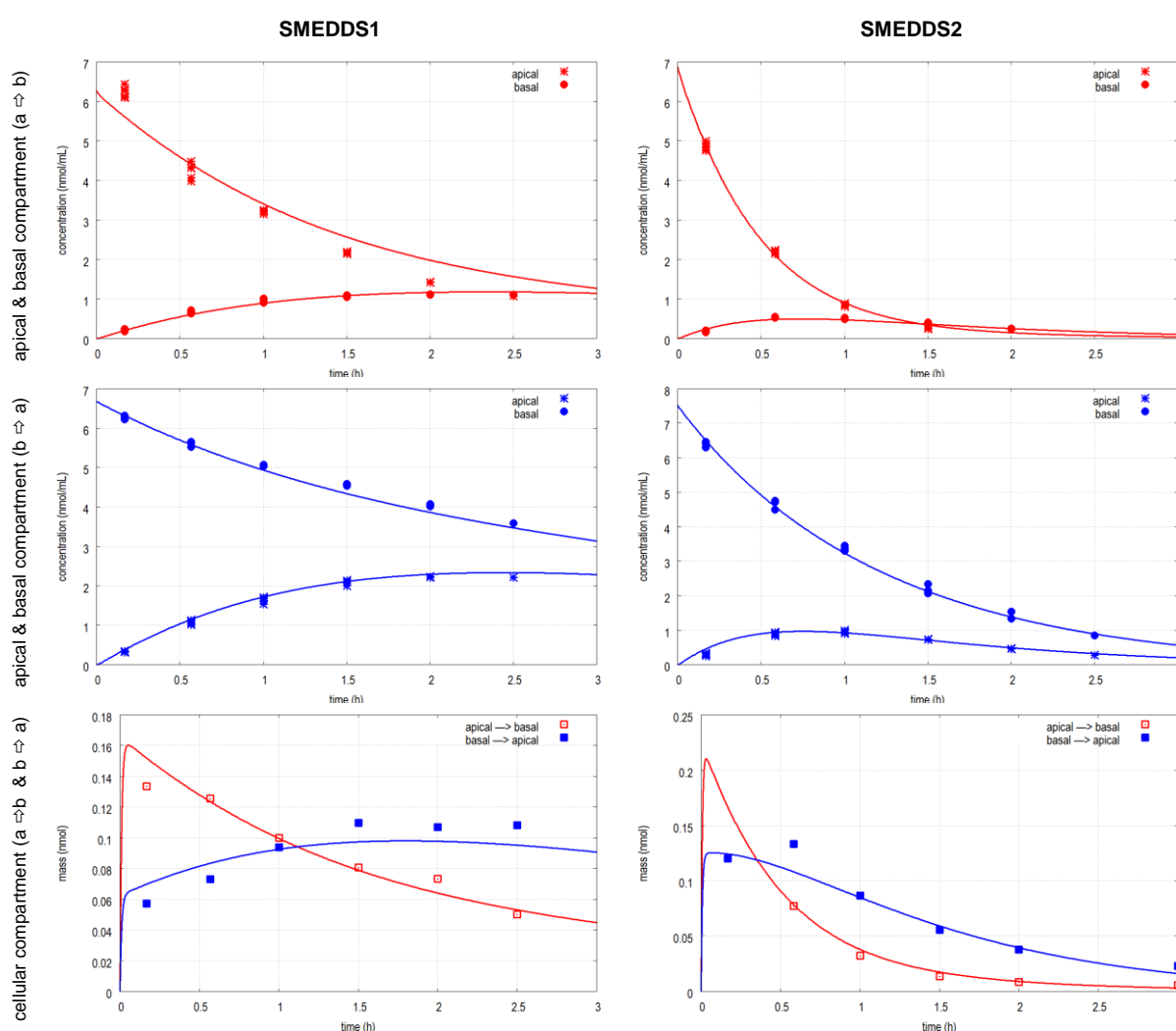


Figure 5: Nobilin concentration in presence of (left to right) SMEDDS1 and SMEDDS2 in the apical-to-basal (top panels, red) and the basal-to-apical (middle panels, blue) transport direction in both compartments and nobilin mass in the cellular compartment (bottom panels) in both transport directions as a function of time. (*) apical concentration, (●) basal concentration, (□) mass in apical-to-basal transport direction (red), (■) mass in basal-to-apical transport direction (blue). Symbols represent measured data and lines fitted model curves.

The estimated parameter values of nobiletin in presence of SMEDDS are shown in Figure 6. SMEDDS1 and SMEDDS2 decreased the permeability coefficient 3.4- and 1.5-fold, respectively, whereas the partition coefficient $K_{a/c}$ was increased by SMEDDS1 and SMEDDS2 4.2- and 1.7-fold, respectively. The total conjugation rate constant was decreased by SMEDDS1 3.2-fold and was increased by SMEDDS2 2.3-fold which was accompanied by an increased and reduced relative fraction absorbed of 70% and 24%, respectively.

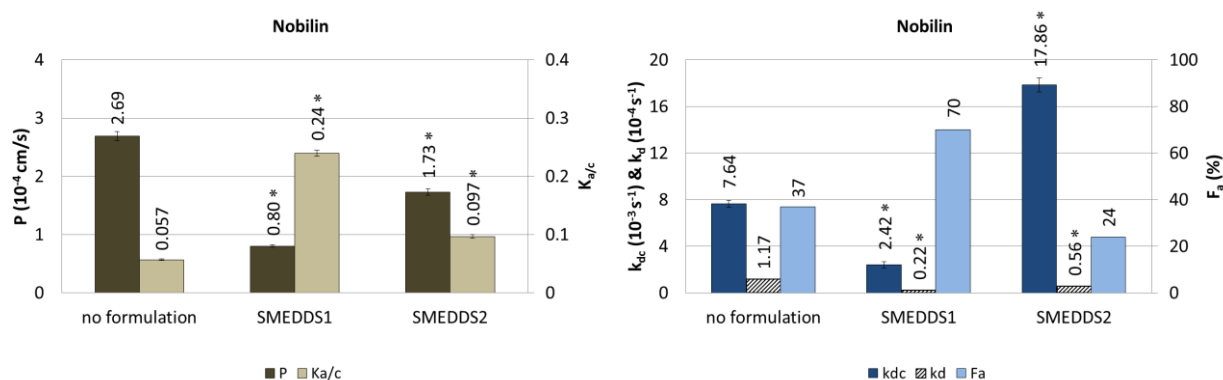


Figure 6: Deduced values (columns) and standard errors (bars) of permeability coefficient P , partition coefficient $K_{a/c}$, partition coefficient u (dark and light columns, respectively, on left panel), total conjugation rate constant k_{dc} , chemical degradation rate constant k_d , and relative fraction absorbed F_a (dark, diagonally hatched, and light columns, respectively, on right panel) of nobiletin from model fitting in the presence of SMEDDS (lipid based formulations). * $p < 0.01$.

Figure 7 shows the results of the three conjugation products of nobiletin in presence of SMEDDS2 in the Caco-2 permeation experiment. The concentration-time profiles of the conjugates in presence of SMEDDS2 were similar to those with no formulation in both transport directions (Figure 3). Rapid increase of glucuronide concentration followed by a decline was observed in the apical compartment whereas the concentration steadily increased in the basal compartment over time, resulting in a higher concentration in the basal than in the apical compartment. Concentration of cysteine conjugate constantly increased in both compartments, although, remarkably faster in the apical than in the basal compartment. Glutathione conjugate concentration increased in the apical and basal compartment, however, it decreased in the apical compartment over time which resulted in a higher concentration in the basal than in the apical compartment after 2.5 h. The amount of conjugates in the cells declined during the experiment. The concentration-time profiles of the conjugates in presence of SMEDDS1 are not shown (see appendix). Almost no conjugates were detected apart from a slow increase of concentration of glucuronide and cysteine conjugate in the apical compartment.

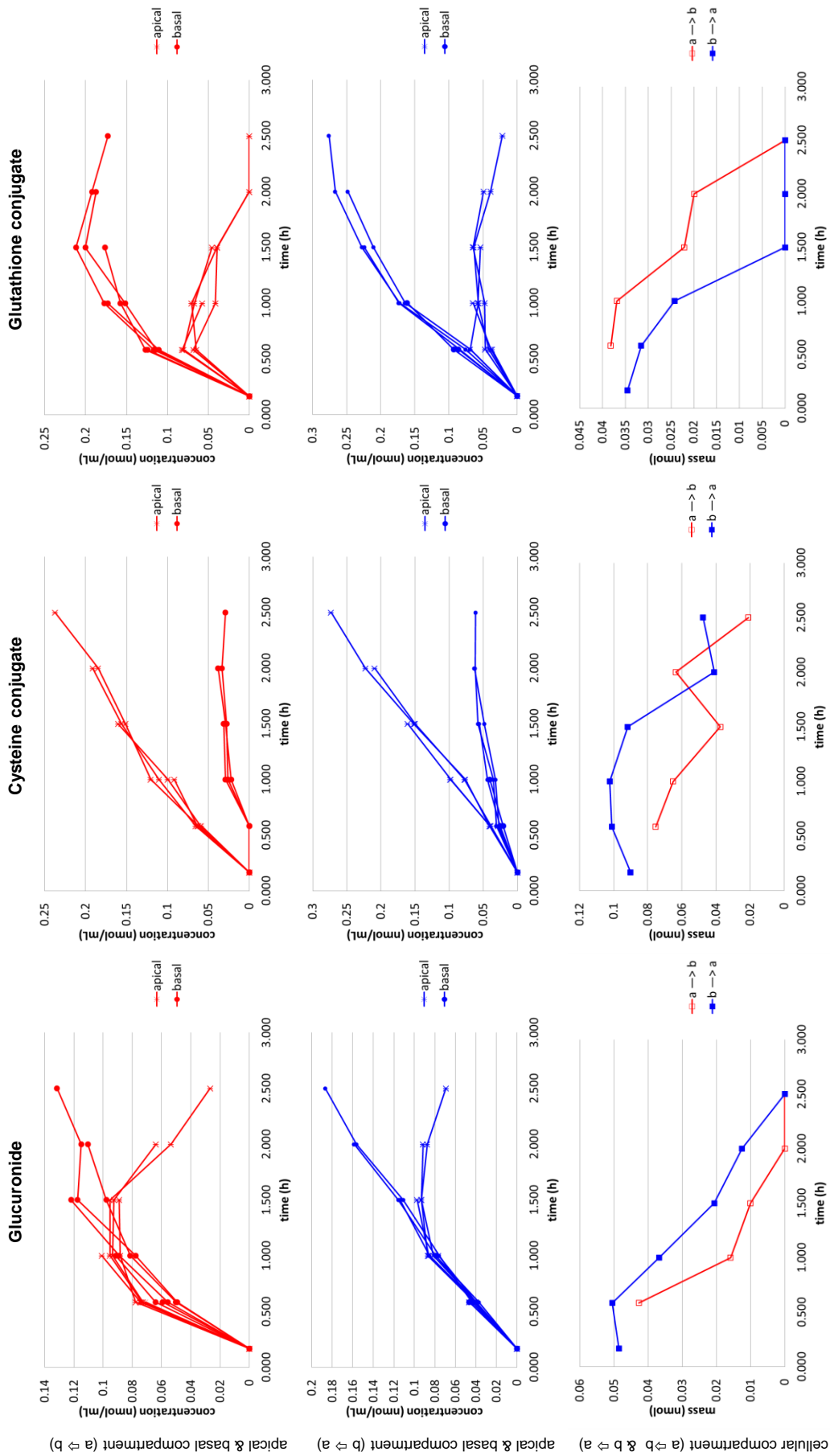


Figure 7: Concentration of (left to right) glucuronide, cysteine conjugate, and glutathione conjugate in presence of SMEDDS2 in the apical-to-basal (top panels, red) and the basal-to-apical (middle panels, blue) transport direction in both compartments and mass of (left to right) glucuronide, cysteine conjugate, and glutathione conjugate in the cellular compartment (bottom panels) in both transport directions as a function of time. (* apical concentration, (●) mass in apical-to-basal transport direction (red), (■) mass in basal-to-apical transport direction (blue). Symbols represent measured data.

5.4.4 Influence of biorelevant media and SMEDDS on transport of nobiletin and its conjugates in full extract

The estimated parameter values of nobiletin applied as full plant extract and in the presence of different media and lipid based formulations are shown in Figure 8. Concentration-time profiles are not shown (see appendix). The full extract did not have an effect on the permeability coefficient whereas a significant reduction of the partition coefficient was observed. The extract reduced the total conjugation rate constant almost 10-fold and increased the relative fraction absorbed from 37% to 72%. For the combination of the full extract with biorelevant media or lipid based formulations the following results were obtained: FeSSIF-TM_{Caco}, SMEDDS1, SMEDDS2(1), and SMEDDS2(2) decreased the permeability coefficient 3.8-, 3.6-, 1.5-, and 1.5-fold, respectively, accompanied by a 3-, 3.8-, 1.7-, 1.5-fold increased partition coefficient $K_{a/c}$, respectively. A significant reduction of the partition coefficient $K_{a/c}$ was obtained in the presence of FaSSIF-TM_{Caco}. The partition coefficient u was 0.14 and 0.37 of FaSSIF-TM_{Caco} and FeSSIF-TM_{Caco}, respectively. FaSSIF-TM_{Caco}, FeSSIF-TM_{Caco}, SMEDDS1, and SMEDDS2(1) reduced the total conjugation rate constant 5.8-, 3.6-, 6.9-, and 1.7-fold respectively, and it was abolished in presence of SMEDDS2(2). The relative fraction absorbed was increased by the biorelevant media and the lipid based formulations.

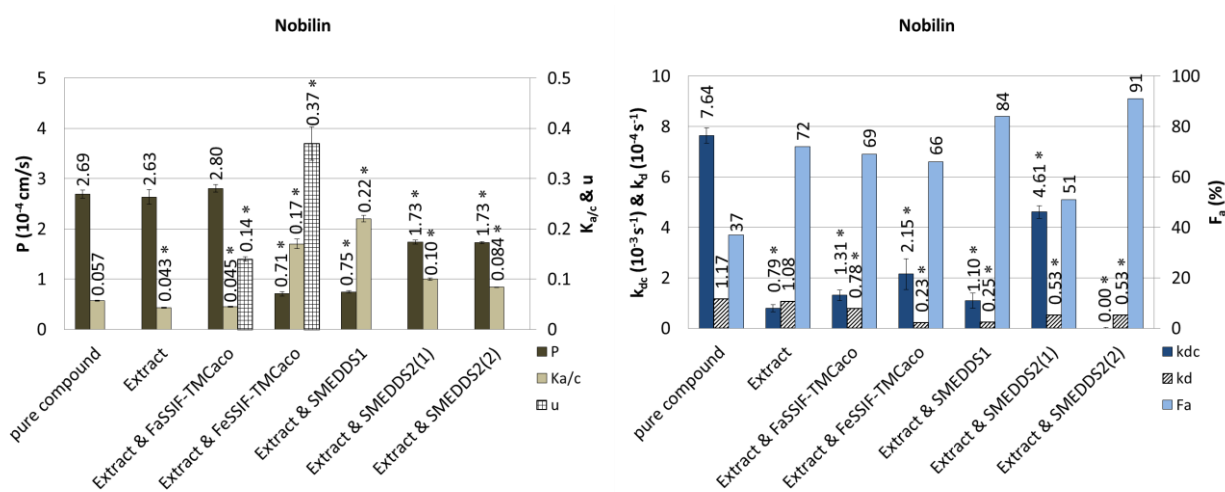


Figure 8: Deduced values (columns) and standard errors (bars) of permeability coefficient P , partition coefficient $K_{a/c}$, partition coefficient u (dark, light, and crosshatched columns, respectively, on left panel), total conjugation rate constant k_{dc} , chemical degradation rate constant k_d , and relative fraction absorbed F_a (dark, diagonally hatched, and light columns, respectively, on right panel) of nobiletin applied as a full extract from model fitting in different media and in presence of SMEDDS (lipid based formulations). * $p < 0.01$.

The results of the three conjugates of nobiletin applied as a full extract in aq-TM_{Caco}, FaSSIF-TM_{Caco}, and in presence of SMEDDS2(1) and SMEDDS2(2) in the Caco-2 permeation experiment are shown in Figure 9, Figure 10, Figure 11, and Figure 12 respectively. Concentrations of glucuronide increased in the apical and basal compartment simultaneously and were more or less the same after 2.5 h in the presence of

the full extract (Figure 9). The concentration of cysteine conjugate rose in the apical and basal compartment over time whereas it was higher in the apical compartment after 2.5 h. The concentration-time profiles of glutathione conjugates show that the concentration in the apical compartment increased and declined during the experiment whereas it increased in the basal compartment which resulted in a higher concentration in the basal than in the apical compartment at the end of the experiment. The amount of conjugates in the cells diminished over time and a slight accumulation of cysteine conjugate was observed. These observations were made for both transport directions.

Full extract & FaSSIF-TM_{Caco} increased the concentration of all three conjugates in the apical compartment whereas only a slight increase of glucuronide concentration was observed in the basal compartment in both transport directions (Figure 10). No conjugates were found in the cells. In presence of full extract & FeSSIF-TM_{Caco} no conjugates were detected in all three compartments in both transport directions.

Full extract & SMEDDS2(1) increased the concentration of glucuronide and glutathione conjugate in the apical and basal compartment whereas it was higher in the basal compartment after 2.5 h (Figure 11). The concentration of cysteine conjugate was increased in the apical compartment in both transport directions.

Full extract & SMEDDS2(2) increased the concentration of glucuronide in the apical and basal compartment simultaneously which resulted in an equal concentration in both compartments (Figure 12). The concentrations of cysteine conjugate and glutathione conjugate rose in the apical and basal compartments over time whereas only a small concentration of cysteine conjugate was measured at time point 2.5 h in the basal compartment in both transport directions. No conjugates were detected in the cellular compartment.

In combination with SMEDDS1 a low concentration of cysteine conjugate was found only in the apical compartments in both transport directions, therefore, the concentration-time profiles are not shown (see appendix).

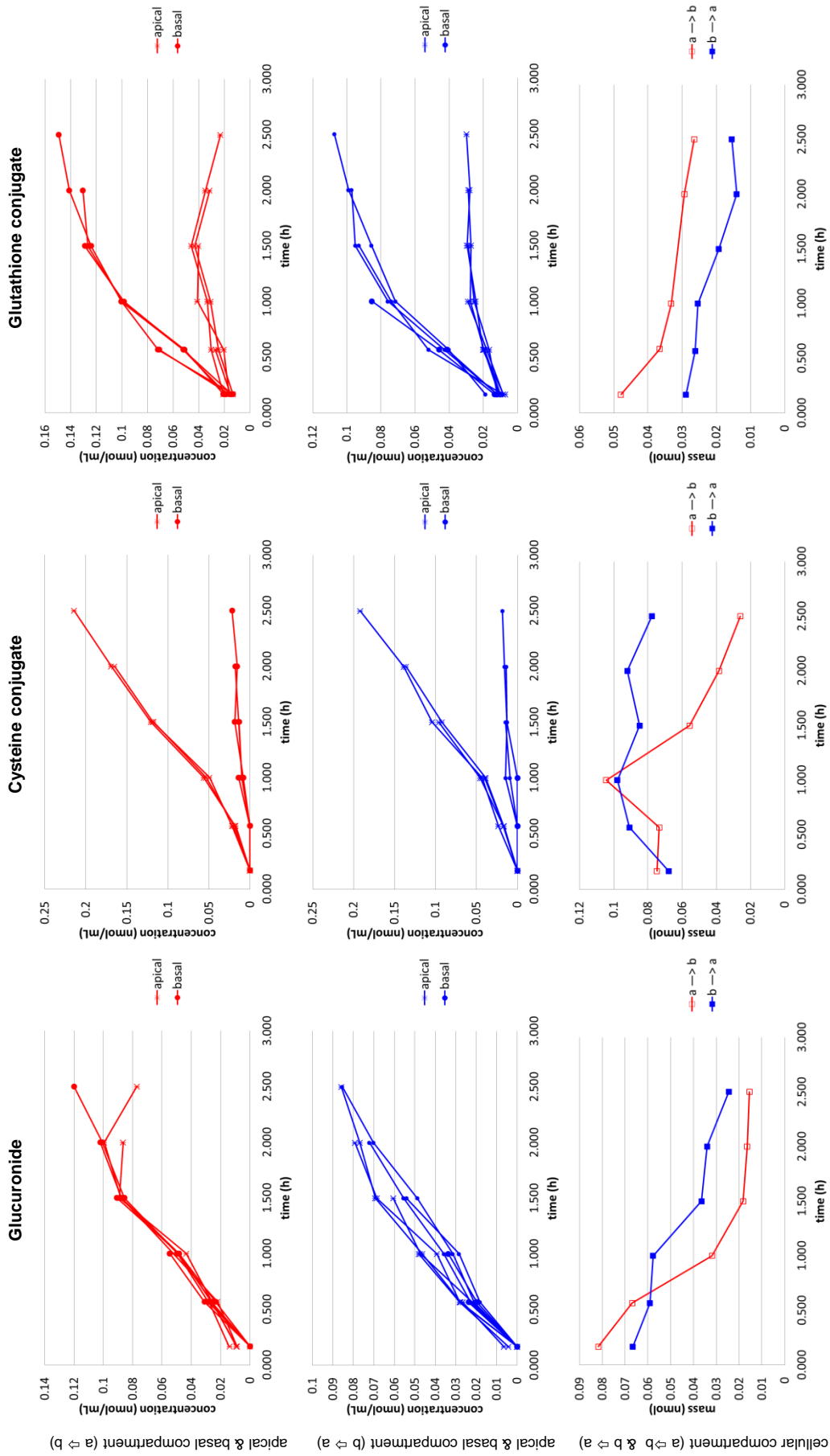


Figure 9: Concentration of (left to right) glucuronide, cysteine conjugate, and glutathione conjugate in presence of the extract in the apical-to-basal (top panels, red) and the basal-to-apical (middle panels, blue) transport direction in both compartments and mass of (left to right) glucuronide, cysteine conjugate, and glutathione conjugate in the cellular compartment (bottom panels) in both transport directions as a function of time. (* apical concentration, (●) mass in apical-to-basal transport direction (red), (■) mass in basal-to-apical transport direction (blue). Symbols represent measured data.

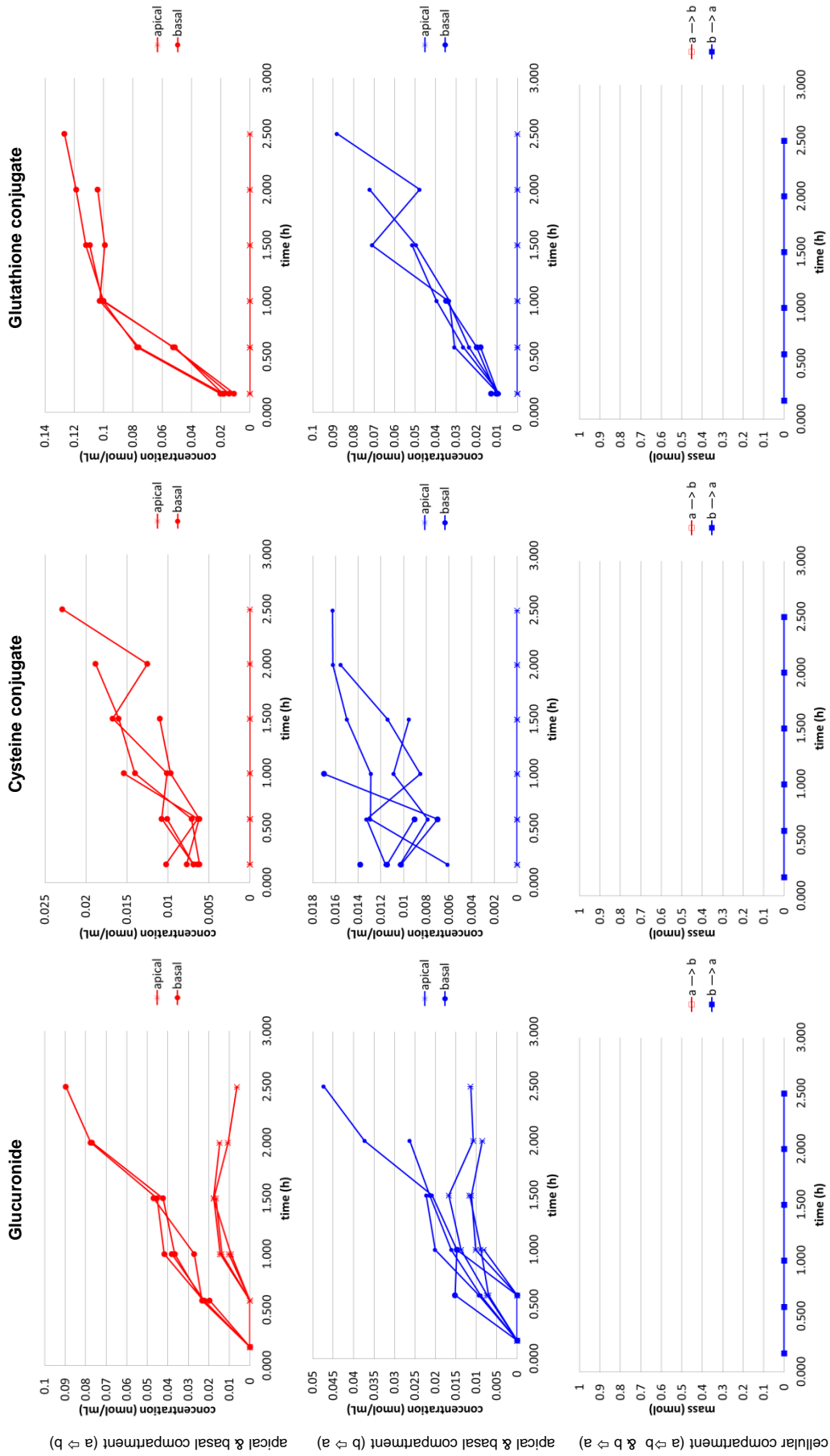


Figure 10: Concentration of (left to right) glucuronide, cysteine conjugate, and glutathione conjugate in presence of the extract & FASSIF-TM_{Caco} in the apical-to-basal (top panels, red) and the basal-to-apical (middle panels, blue) transport direction in both compartments and mass of (left to right) glucuronide, cysteine conjugate, and glutathione conjugate in the cellular compartment (bottom panels) in both transport directions as a function of time. (*) apical concentration, (●) basal concentration, (□) mass in apical-to-basal transport direction (red), (■) mass in basal-to-apical transport direction (blue). Symbols represent measured data.

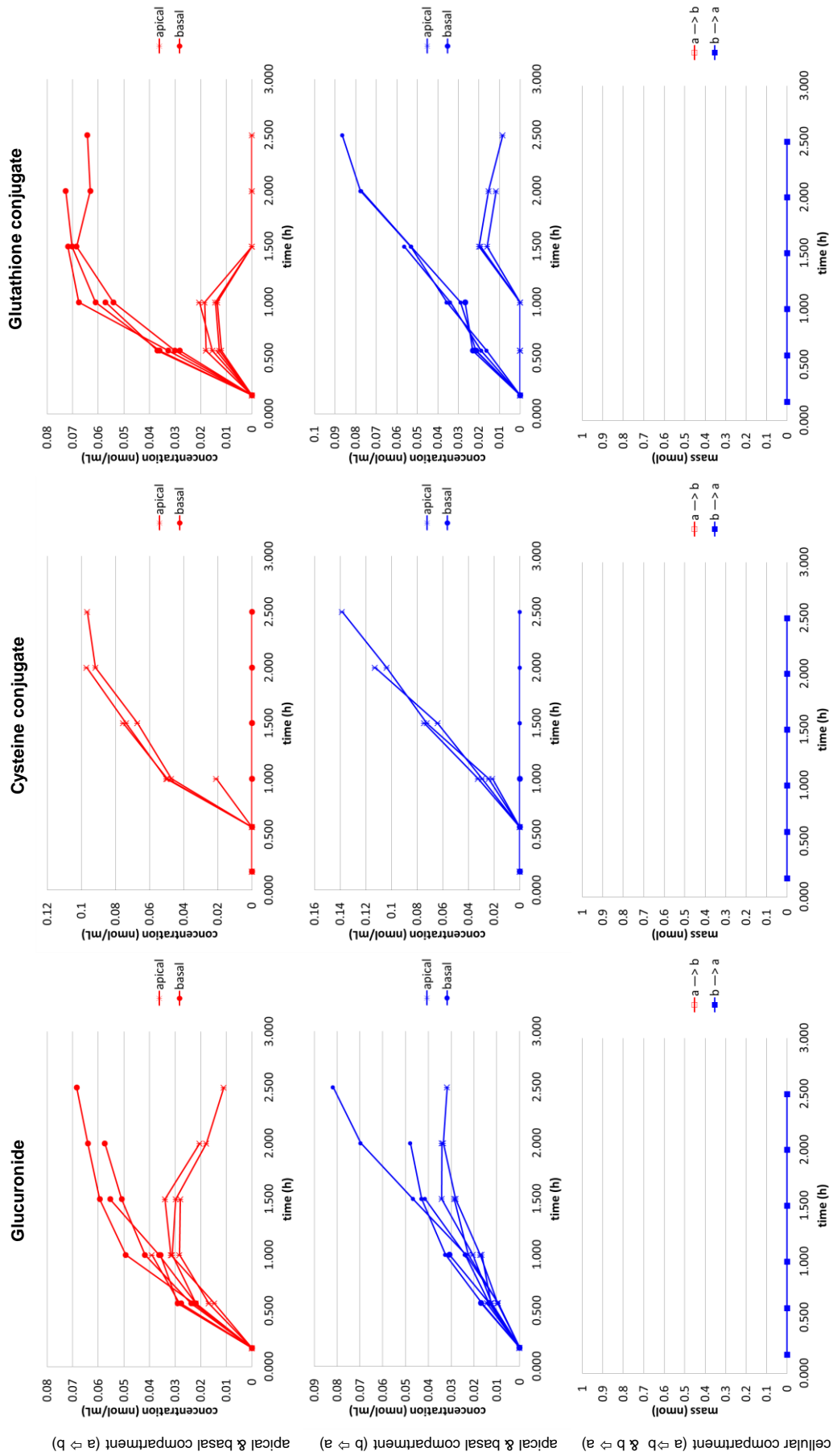


Figure 11: Concentration of (left to right) glucuronide, cysteine conjugate, and glutathione conjugate in presence of the extract & SMEDDS2(1) in the apical-to-basal (top panels, red) and the basal-to-apical (middle panels, blue) transport direction in both compartments and mass of (left to right) glucuronide, cysteine conjugate, and glutathione conjugate in the cellular compartment (bottom panels) in both transport directions as a function of time. (*) apical concentration, (●) basal concentration, (◐) mass in apical-to-basal transport direction (red), (◑) mass in basal-to-apical transport direction (blue). Symbols represent measured data.

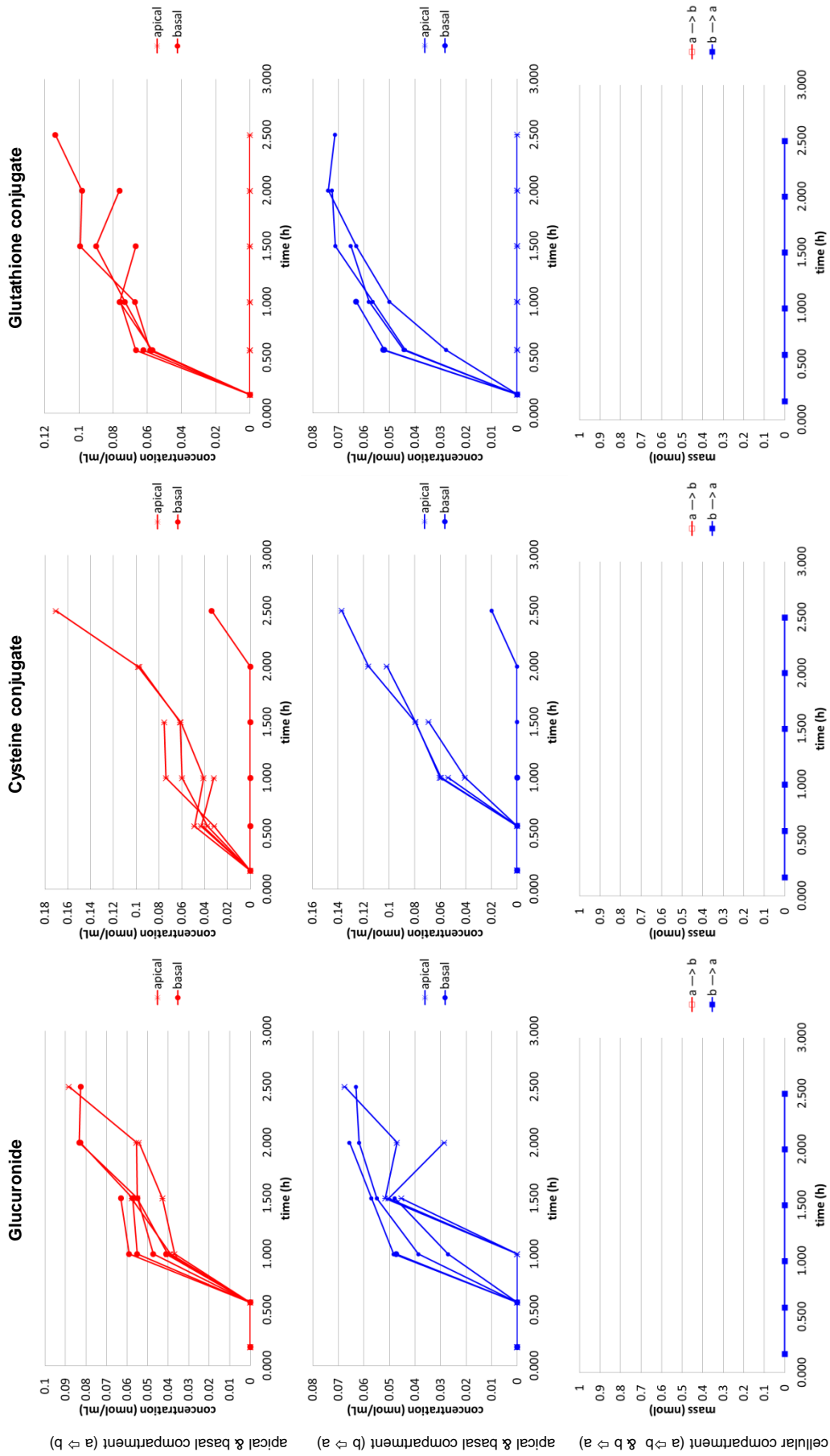


Figure 12: Concentration of (left to right) glucuronide, cysteine conjugate, and glutathione conjugate in presence of the extract & SMEDDS2(2) in the apical-to-basal (top panels, red) and the basal-to-apical (middle panels, blue) transport direction in both compartments and mass of (left to right) glucuronide, cysteine conjugate, and glutathione conjugate in the cellular compartment (bottom panels) in both transport directions as a function of time. (*) apical concentration, (●) basal concentration, (■) mass in apical-to-basal transport direction (red), (■) mass in basal-to-apical transport direction (blue). Symbols represent measured data.

5.5 DISCUSSION

Nobilin is a well permeable but highly instable compound undergoing chemical degradation and extensive bioconversion resulting in a low relative fraction absorbed of 37% in the Caco-2 model which was already reported before.²⁸ A previous study showed that stability and solubility of nobilin can be increased by the incorporation of the compound into colloidal lipid particles of biorelevant media and liposomes that protects it from degradation in water.²⁷ This study confirms this observation with lipid based formulations. Chemical stability of nobilin in an aqueous solution in the presence of colloidal lipid particles was significantly improved in the following rank order: Liposomes_{FeSSIF} > Liposomes_{FaSSIF} ≥ FeSSIF-TM_{Caco} > SMEDDS1 > SMEDDS2 > FaSSIF-TM_{Caco}. Intracellular bioconversion of nobilin to the three conjugation products glucuronide, cysteine conjugate, and glutathione conjugate was reported to be almost 10-fold faster than the chemical degradation.²⁸ These conjugation products exhibited asymmetrical transport out of the cells. The same study showed that the three conjugates were substrates of MRP2 at the apical membrane, and MRP3 and possibly MRP1 at the basal membrane. Glucuronide and cysteine conjugate were also shown to be transported by P-gp at the apical membrane. The decline of glucuronide concentration in the apical compartment (Figure 3) was assumed to be due to the carrier mediated influx by OATP at the apical membrane and hydrolysis reaction by β -glucuronidase in the cell. The reduction of glutathione conjugate concentration in the apical compartment (Figure 3) was attributed to the brush border membrane enzymes γ -glutamyltranspeptidase and dipeptidase to the cysteine conjugate.²⁸ The full mechanism is shown in Scheme 1 and explains the concentration-time profiles in Figure 3. It was proposed that the chemical degradation and mainly the more rapid bioconversion in the cell were responsible for the poor in vitro absorption of nobilin.^{27,28}

The biorelevant medium FaSSIF-TM_{Caco} did not have an effect on the relative fraction absorbed of nobilin whereas FeSSIF-TM_{Caco} increased it from 37% to 96%. FaSSIF-TM_{Caco} did not have an effect on the estimated values of permeability coefficient, partition coefficient $K_{a/c}$, and the total conjugation rate constant. The partition coefficient u was 0.14 which indicated that nobilin is better soluble in Liposomes_{FaSSIF} than in FaSSIF-TM_{Caco}. This observation is consistent with the previously reported higher solubility of nobilin in Liposomes_{FaSSIF} than in FaSSIF-TM_{Caco}.²⁷ The increased solubility and also the improved stability in Liposomes_{FaSSIF} caused a higher concentration in the basal compartment than in the apical compartment at the end of the experiment (Figure 1). Interestingly, the concentration-time profiles of the conjugates showed that FaSSIF-TM_{Caco} nearly abolished the apical efflux of all conjugates. It was reported that FaSSIF can inhibit apical efflux of P-gp substrates such as digoxin, cyclosporine A, doxorubicin, and etoposide.⁴⁰⁻⁴³ As a result no conversion of glutathione conjugate to cysteine conjugate took place in the apical compartment while the amount of glutathione conjugate in the basal

compartment was strongly increased (Figure 4). The overall reduced apical efflux did not affect the conjugation rate constant in the cell which shows that no interplay between transporter and bioconversion was elicited by FaSSIF-TM_{Caco}.

FeSSIF-TM_{Caco} increased the partition coefficient $K_{a/c}$ accompanied by a decreased permeability coefficient which were consistent with the decreased amount of nobiletin in the cells (Figure 1). The reduced permeability coefficient in presence of biorelevant media was reported to be a result of incorporation of a compound into colloidal lipid particles.⁴¹⁻⁴⁴ The relationship between the partition coefficient $K_{a/c}$ and the permeability coefficient was discussed before where an increase in lipid content of the media resulted in a decreased permeability coefficient and simultaneously increased partition coefficient $K_{a/c}$.¹⁹ The partition coefficient u was slightly larger for FeSSIF-TM_{Caco} than in the experiment with FaSSIF-TM_{Caco}. Also, indicating that nobiletin is better soluble in Liposomes_{FeSSIF} than in FeSSIF-TM_{Caco}.²⁷ The increased partition coefficient $K_{a/c}$ was also accompanied by a markedly decreased chemical degradation rate constant which further confirms the high affinity of nobiletin to the colloidal lipid particles as discussed before.²⁷ The abolished bioconversion of nobiletin was in agreement with the results that no conjugates were detected in presence of FeSSIF-TM_{Caco}. FeSSIF-TM_{Caco} was suggested to be compatible with the Caco-2 cells for three hours.¹⁹ Even though no loss of membrane integrity and no cytotoxic effect in the MTT assay was reported over 300 min of incubation, the LDH assay showed cytotoxicity of 10% over the first 180 min and 20% over 300 min.¹⁹ This observation does not exclude a reduced metabolism due to some adverse on enzymes of the cells.

Hence, FaSSIF-TM_{Caco} diminished apical efflux of the conjugates which did not result in reduced bioconversion and therefore no interplay between transporter and conjugation reactions and no increase of absorption was observed. FeSSIF-TM_{Caco} increased stability in the medium and reduced bioconversion, causing an increased relative fraction absorbed.

The two lipid based formulations showed an opposite effect on absorption of nobiletin. SMEDDS1 increased the relative fraction absorbed from 37% to 70% and SMEDDS2 decreased it to 24%. The colloidal lipid particles of SMEDDS1 increased the partition coefficient $K_{a/c}$ and reduced the permeability coefficient as well as chemical degradation. These observations are related to the high affinity of nobiletin to the lipid particles in analogy to FeSSIF-TM_{Caco}. Additionally the increased concentration in the apical and basal compartments and reduced amount of nobiletin in the cells was because of the increased $K_{a/c}$ compared to aq-TM_{Caco} (Figure 5). Bioconversion was reduced by SMEDDS1 which is consistent with the considerably low concentrations of conjugates in all three compartments (not shown, see appendix). Only low concentrations of glucuronide and cysteine conjugates were detected in the apical compartment whereas SMEDDS1 completely abolished the formation of glutathione conjugates. It is well known that surfactants such as Cremophor EL have an inhibitory effect on cell enzymes.⁴⁵⁻⁴⁸

SMEDDS2 increased the partition coefficient $K_{a/c}$ accompanied by a reduction of the permeability coefficient and the degradation rate constant as discussed above for SMEDDS1. However, bioconversion of nobilin was increased which is currently not understood. A biological effect of the antioxidant α -Tocopherol may play a role by counteracting the known prooxidative activity of sesquiterpene lactones such as nobilin which might be responsible for reduction of metabolic activity of the cells.^{49,50} Although, Lutrol F 68 and α -Tocopherol were reported to inhibit P-gp and the later also MRP2,^{46,51,52} no reduction of the efflux was observed in this study (Figure 7). The concentration-time profiles of the conjugates were similar to those with no formulation (Figure 3).

Finally, the lipid based formulation SMEDDS1 improved the relative fraction absorbed of nobilin. This effect was attributed to the increased chemical stability and more important to the reduced bioconversion of nobilin in presence of SMEDDS1. SMEDDS2 reduced chemical degradation but not bioconversion and therefore no increase in absorption was observed.

The full extract increased the relative fraction absorbed to 72%. It did not have an influence on the chemical degradation rate constant whereas the conjugation rate constant was markedly decreased.²⁸ This effect was reported to be due to a direct inhibitory effect of the extract on the conjugation reactions and to a lesser extend also on efflux carriers which resulted in a decreased bioconversion because of the interplay between transporter and conjugation reactions. Additionally, the extract was assumed to inhibit influx by OATP as indicated by the parallel increase of glucuronide concentration in the apical and basal compartment (Figure 9).²⁸

Biorelevant media or lipid based formulations had the same effect on the chemical degradation rate constant, the partition coefficient $K_{a/c}$, and the permeability coefficient when used with the extract as with pure nobilin. The combination of the extract with the media and the formulations produced the same effect on the bioconversion rate constant as the extract or the media and formulations alone, however, possible interactions between them were not further investigated. Interestingly, the increase of bioconversion elicited by SMEDDS2 was dependent on the concentration of the extract. At low extract concentration (SMEDDS2(1)) the bioconversion rate constant was smaller compared to the one of nobilin in aq-TM_{Caco} but it was larger than the one in presence of the extract (Figure 8). This observation suggests a competing effect of the extract and the formulation. At 3-fold higher extract concentration (SMEDDS2(2)) the effect of the extract dominated and the bioconversion was abolished which resulted in a larger relative fraction absorbed. The concentration-time profiles of the conjugates show the same effects of FaSSIF-TM_{Caco}, FeSSIF-TM_{Caco}, and SMEDDS1 on the efflux and formation of the conjugates as discussed above for pure nobilin. In presence of SMEDDS2 the competing effect of the extract and the formulation was also seen in the concentration-time profiles of the conjugates. While

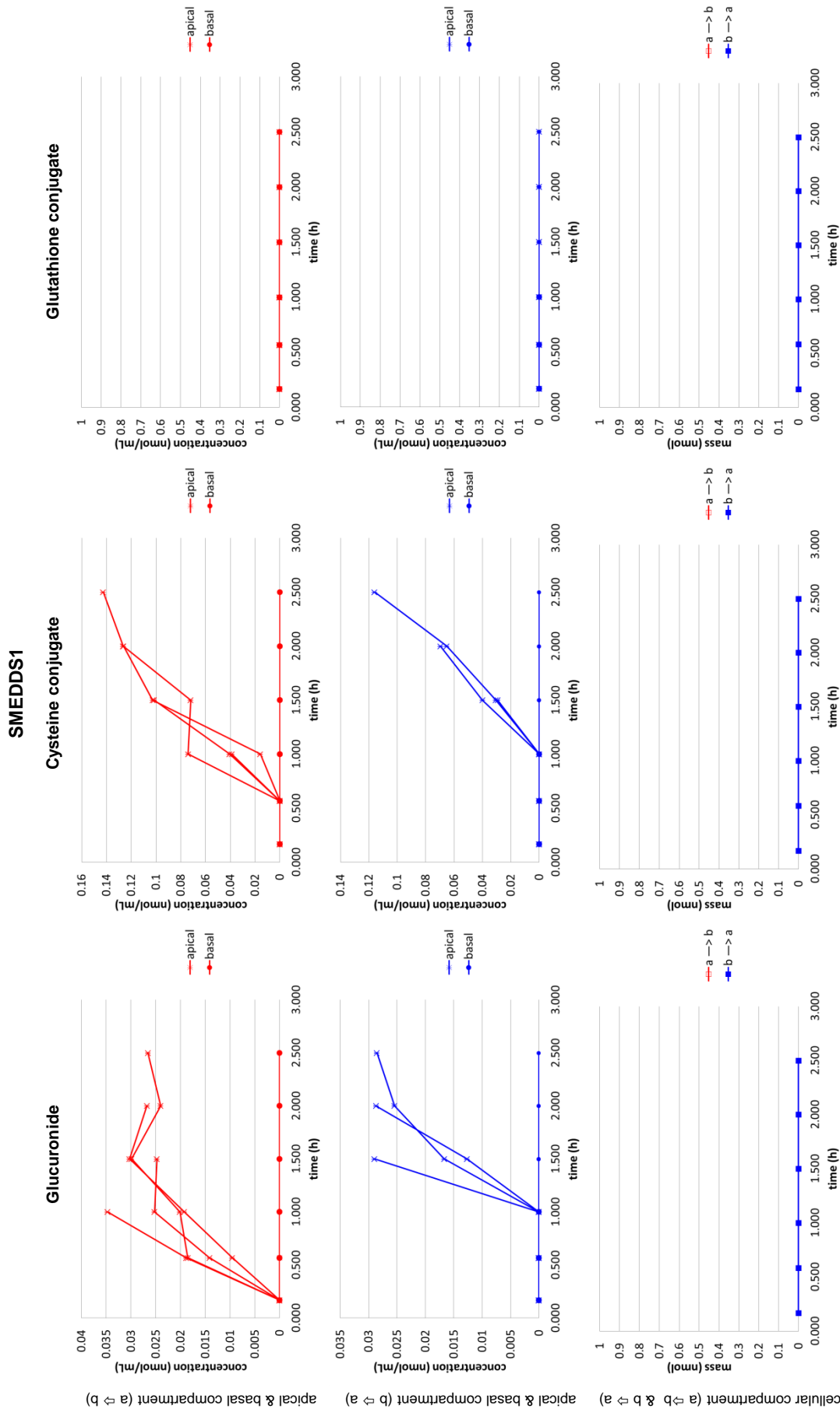
those in presence of SMEDDS2(1) were similar to those with SMEDDS2 with pure nobilin, the SMEDDS2(2) resembled the extract in aq-TM_{Caco}.

5.6 CONCLUSION

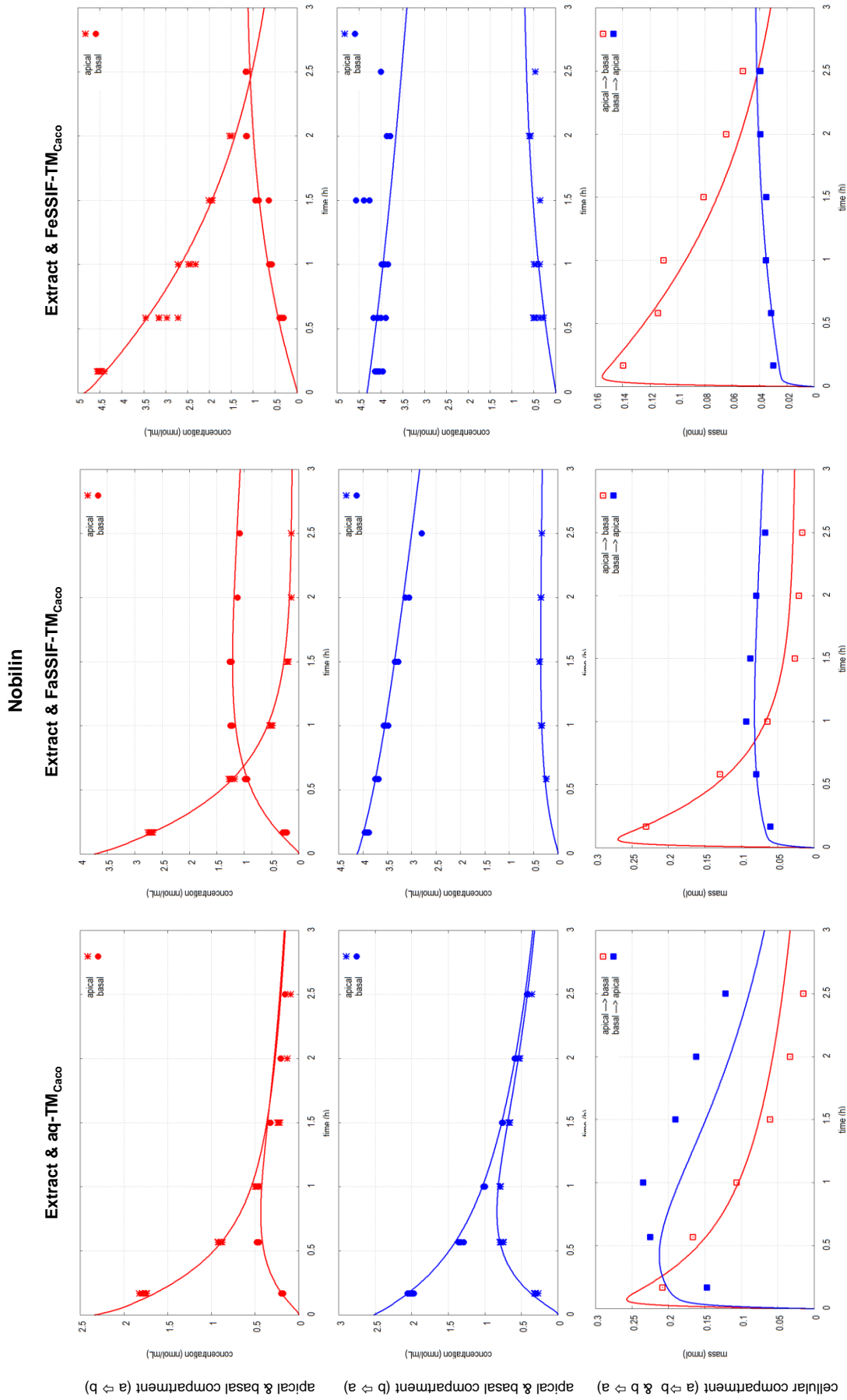
FaSSIF-TM_{Caco} reduced the apical efflux of the three conjugates glucuronide, cysteine conjugate, and glutathione conjugate which did not result in a decreased bioconversion due to transporter conjugation reaction interplay and did not increase nobilin absorption. Also the lipid based formulation SMEDDS2 did not have an improving effect on absorption even though chemical stability was increased.

FeSSIF-TM_{Caco} and SMEDDS1 increased chemical stability, reduced bioconversion accompanied by an increased absorption. An inhibitory effect on cell enzymes was assumed to be a reason for the decreased bioconversion. In combination with the full extract of *Chamomillae romanae flos* no additive effect of the extract on chemical stability, bioconversion, and on absorption was observed.

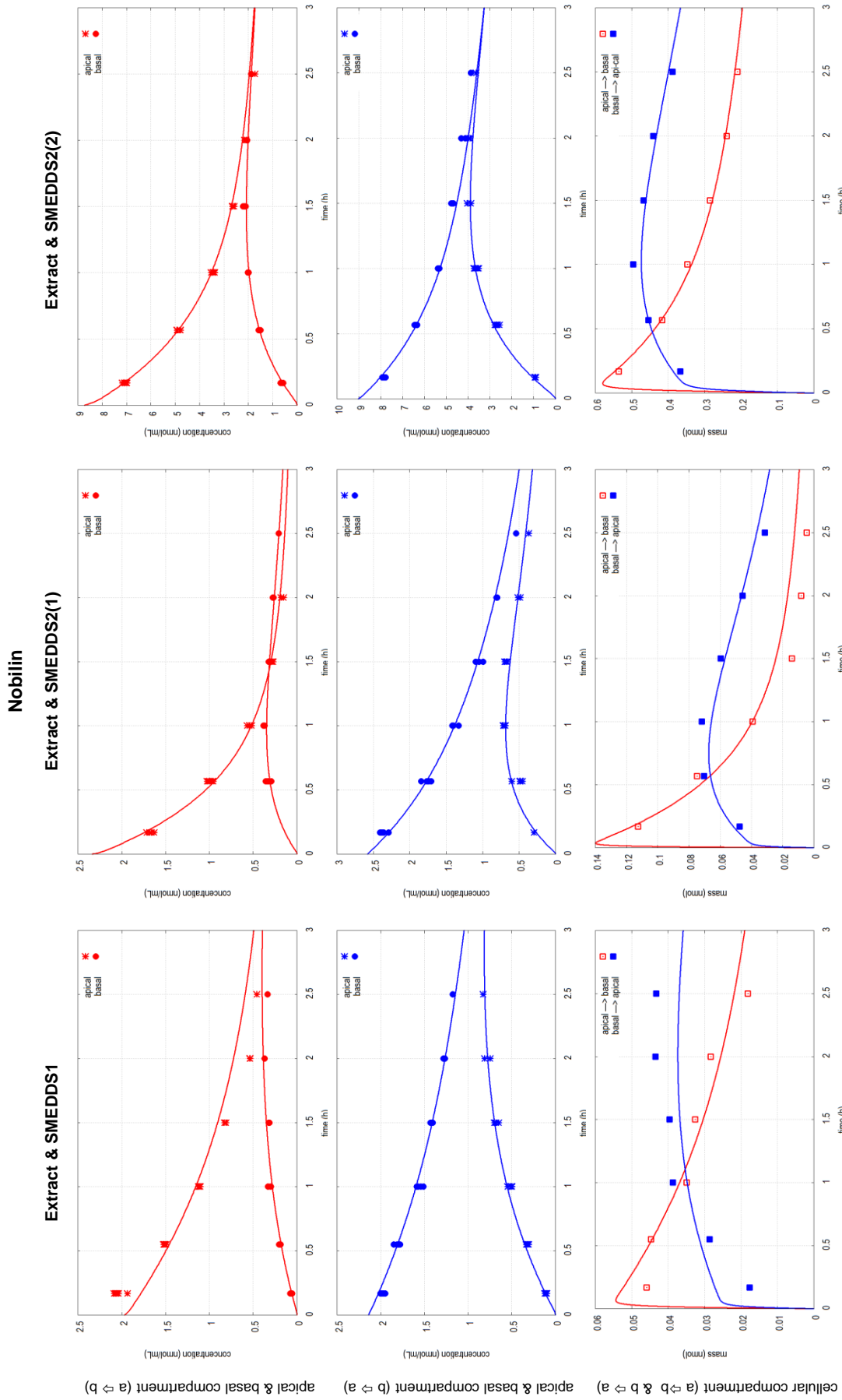
5.7 APPENDIX



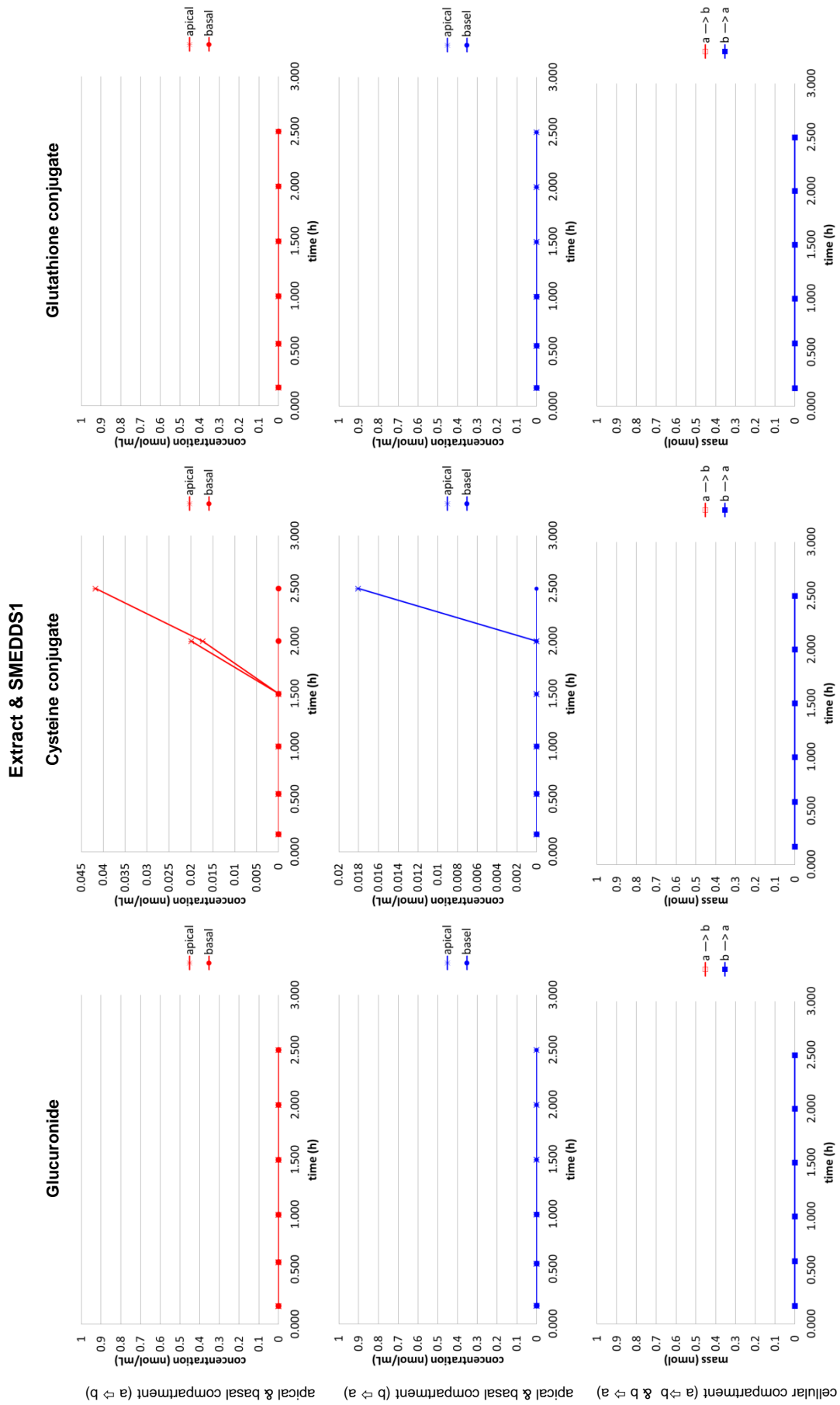
Concentration of (left to right) glucuronide, cysteine conjugate, and glutathione conjugate in presence of SMEDDS1 in the apical-to-basal (top panels, red) and the basal-to-apical (middle panels, blue) transport direction in both compartments and mass of (left to right) glucuronide, cysteine conjugate, and glutathione conjugate in the cellular compartment (bottom panels) in both transport directions as a function of time. (*) apical concentration, (●) basal concentration, (□) mass in apical-to-basal transport direction (red), (■) mass in basal-to-apical transport direction (blue). Symbols represent measured data.



Nobilin concentration in the presence of the (left to right) extract & aq-TM_{Caco}, extract & FaSSIF-TM_{Caco}, and extract & FeSSIF-TM_{Caco} in the apical-to-basal (top panels, red) and the basal-to-apical (middle panels, blue) transport direction in both compartments and nobilin mass in the cellular compartment (bottom panels) in both transport directions as a function of time. (●) apical concentration, (●) basal concentration, (■) mass in apical-to-basal transport direction (red), (■) mass in basal-to-apical transport direction (blue). Symbols represent measured data and lines fitted model curves.



Nobilin concentration in presence of (left to right) the extract & SMEDDS1, extract & SMEDDS2(1), and extract & SMEDDS2(2) in the apical-to-basal (top panels, red) and the basal-to-apical (middle panels, blue) transport direction in both compartments and nobilin mass in the cellular compartment (bottom panels) in both transport directions as a function of time. (*) apical concentration, (●) basal concentration, (■) mass in apical-to-basal transport direction (red), (■) mass in basal-to-apical transport direction (blue). Symbols represent measured data and lines fitted model curves.



Concentration of (left to right) glucuronide, cysteine conjugate, and glutathione conjugate in presence of the extract & SMEDDS1 in the apical-to-basal (top panels, red) and the basal-to-apical (middle panels, blue) transport direction in both compartments and mass of (left to right) glucuronide, cysteine conjugate, and glutathione conjugate in the cellular compartment (bottom panels) in both transport directions as a function of time. (*) apical concentration, (●) mass in apical-to-basal transport direction (red), (■) mass in basal-to-apical transport direction (blue). Symbols represent measured data.

5.8 REFERENCES

1. Dressman JB, Amidon GL, Reppas C, Shah VP 1998. Dissolution testing as a prognostic tool for oral drug absorption: Immediate release dosage forms. *Pharmaceutical Research* 15(1):11-22.
2. Custodio JM, Wu CY, Benet LZ 2008. Predicting drug disposition, absorption/elimination/transporter interplay and the role of food on drug absorption. *Advanced Drug Delivery Reviews* 60(6):717-733.
3. Suzuki H, Sugiyama Y 2000. Role of metabolic enzymes and efflux transporters in the absorption of drugs from the small intestine. *European Journal of Pharmaceutical Sciences* 12(1):3-12.
4. Diakidou A, Vertzoni M, Goumas K, Soderlind E, Abrahamsson B, Dressman J, Reppas C 2009. Characterization of the contents of ascending colon to which drugs are exposed after oral administration to healthy adults. *Pharmaceutical Research* 26(9):2141-2151.
5. Vertzoni M, Markopoulos C, Symillides M, Goumas C, Imanidis G, Reppas C 2012. Luminal lipid phases after administration of a triglyceride solution of danazol in the fed state and their contribution to the flux of danazol across Caco-2 cell monolayers. *Molecular Pharmaceutics* 9(5):1189-1198.
6. Charman WN, Rogge MC, Boddy AW, Berger BM 1993. Effect of food and a monoglyceride emulsion formulation on danazol bioavailability. *Journal of Clinical Pharmacology* 33(4):381-386.
7. Sunesen VH, Pedersen BL, Kristensen HG, Mullertz A 2005. In vivo in vitro correlations for a poorly soluble drug, danazol, using the flow-through dissolution method with biorelevant dissolution media. *European Journal of Pharmaceutical Sciences* 24(4):305-313.
8. Bakatselou V, Oppenheim RC, Dressman JB 1991. Solubilization and wetting effects of bile-salts on the dissolution of steroids. *Pharmaceutical Research* 8(12):1461-1469.
9. FDA. 2002. Guidance for industry: Food-effect bioavailability and fed bioequivalence studies. Rockville, MD, USA: Food and Drug Administration. http://www.fda.gov/downloads/regulatory_information/guidances/ucm126833.pdf.
10. Galia E, Nicolaides E, Horter D, Lobenberg R, Reppas C, Dressman JB 1998. Evaluation of various dissolution media for predicting in vivo performance of class I and II drugs. *Pharmaceutical Research* 15(5):698-705.
11. Wei H, Lobenberg R 2006. Biorelevant dissolution media as a predictive tool for glyburide a class II drug. *European Journal of Pharmaceutical Sciences* 29(1):45-52.
12. Parojcic J, Duric J, Jovanovic M, Ibric S, Jovanovic D 2004. Influence of dissolution media composition on drug release and in-vitro/in-vivo correlation for paracetamol matrix tablets prepared with novel carbomer polymers. *Journal of Pharmacy and Pharmacology* 56(6):735-741.
13. Vertzoni M, Fotaki N, Kostewicz E, Stippler E, Leuner C, Nicolaides E, Dressman J, Reppas C 2004. Dissolution media simulating the intraluminal composition of the small intestine: Physiological issues and practical aspects. *Journal of Pharmacy and Pharmacology* 56(4):453-462.

14. Nicolaidis E, Galia E, Efthymiopoulos C, Dressman JB, Reppas C 1999. Forecasting the in vivo performance of four low solubility drugs from their in vitro dissolution data. *Pharmaceutical Research* 16(12):1876-1882.
15. Kambayashi A, Dressman JB 2013. An in vitro-in silico-in vivo approach to predicting the oral pharmacokinetic profile of salts of weak acids: Case example dantrolene. *European Journal of Pharmaceutics and Biopharmaceutics* 84(1):200-207.
16. Dressman JB, Reppas C 2000. In vitro-in vivo correlations for lipophilic, poorly water-soluble drugs. *European Journal of Pharmaceutical Sciences* 11:S73-S80.
17. Nicolaidis E, Symillides M, Dressman JB, Reppas C 2001. Biorelevant dissolution testing to predict the plasma profile of lipophilic drugs after oral administration. *Pharmaceutical Research* 18(3):380-388.
18. Schamp K, Schreder SA, Dressman J 2006. Development of an in vitro/in vivo correlation for lipid formulations of EMD 50733, a poorly soluble, lipophilic drug substance. *European Journal of Pharmaceutics and Biopharmaceutics* 62(3):227-234.
19. Markopoulos C, Thoenen F, Preisig D, Symillides M, Vertzoni M, Parrott N, Reppas C, Imanidis G 2013. Biorelevant media for transport experiments in the Caco-2 model to evaluate drug absorption in the fasted and fed state and their usefulness. *European Journal of Pharmaceutics and Biopharmaceutics* <http://dx.doi.org/10.1016/j.ejpb.2013.10.017>.
20. Humberstone AJ, Charman WN 1997. Lipid-based vehicles for the oral delivery of poorly water soluble drugs. *Advanced Drug Delivery Reviews* 25(1):103-128.
21. Gershanik T, Benita S 2000. Self-dispersing lipid formulations for improving oral absorption of lipophilic drugs. *European Journal of Pharmaceutics and Biopharmaceutics* 50(1):179-188.
22. Gursoy RN, Benita S 2004. Self-emulsifying drug delivery systems (SEDDS) for improved oral delivery of lipophilic drugs. *Biomedicine & Pharmacotherapy* 58(3):173-182.
23. Dunn CJ, Wagstaff AJ, Perry CM, Plosker GL, Goa KL 2001. Cyclosporin - An updated review of the pharmacokinetic properties, clinical efficacy and tolerability of a microemulsion-based formulation (Neoral®)¹ in organ transplantation. *Drugs* 61(13):1957-2016.
24. Sun MH, Si LQ, Zhai XZ, Fan ZZ, Ma YM, Zhang R, Yang XL 2011. The influence of co-solvents on the stability and bioavailability of rapamycin formulated in self-microemulsifying drug delivery systems. *Drug Development and Industrial Pharmacy* 37(8):986-994.
25. Kim MS, Kim JS, Cho WK, Hwang SJ 2013. Enhanced solubility and oral absorption of sirolimus using D-alpha-tocopheryl polyethylene glycol succinate micelles. *Artificial Cells Nanomedicine and Biotechnology* 41(2):85-91.
26. Holub M, Samek Z 1977. Terpenes. CLXX. Isolation and structure of 3-epinobilin, 1,10-epoxynobilin and 3-dehydronobilin - other sesquiterpenic lactones from flowers of *Anthemis nobilis* L.

- revision of structure of nobilin and eucannabinolide. Collection of Czechoslovak Chemical Communications 42(3):1053-1064.
27. Thormann U, De Mieri M, Verjee S, Neuburger M, Hamburger M, Imanidis G 2014. Mechanism of chemical degradation and determination of solubility by kinetic modeling of the highly unstable sesquiterpene lactone nobilin in different media. Journal of Pharmaceutical Sciences to be submitted.
28. Thormann U, Hänggi R, Imanidis G 2014. Transport of nobilin conjugation products and the use of the extract of Chamomillae romanae flos influence absorption of nobilin in the Caco-2 model. Pharmaceutical Research to be submitted.
29. Artursson P, Borchardt RT 1997. Intestinal drug absorption and metabolism in cell cultures: Caco-2 and beyond. Pharmaceutical Research 14(12):1655-1658.
30. Hubatsch I, Ragnarsson EGE, Artursson P 2007. Determination of drug permeability and prediction of drug absorption in Caco-2 monolayers. Nature Protocols 2(9):2111-2119.
31. Sugano K, Kansy M, Artursson P, Avdeef A, Bendels S, Di L, Ecker GF, Faller B, Fischer H, Gerebtzoff G, Lennernaes H, Senner F 2010. Coexistence of passive and carrier-mediated processes in drug transport. Nature Reviews Drug Discovery 9(8):597-614.
32. Hayeshi R, Hilgendorf C, Artursson P, Augustijns P, Brodin B, Dehertogh P, Fisher K, Fossati L, Hovenkamp E, Korjamo T, Masungi C, Maubon N, Mols R, Mullertz A, Monkkonen J, O'Driscoll C, Oppers-Tiemissen HM, Ragnarsson EGE, Rooseboom M, Ungell AL 2008. Comparison of drug transporter gene expression and functionality in Caco-2 cells from 10 different laboratories. European Journal of Pharmaceutical Sciences 35(5):383-396.
33. Hilgendorf C, Ahlin G, Seithel A, Artursson P, Ungell AL, Karlsson J 2007. Expression of thirty-six drug transporter genes in human intestine, liver, kidney, and organotypic cell lines. Drug Metabolism and Disposition 35(8):1333-1340.
34. Prueksaritanont T, Gorham LM, Hochman JH, Tran LO, Vyas KP 1996. Comparative studies of drug-metabolizing enzymes in dog, monkey, and human small intestines, and in Caco-2 cells. Drug Metabolism and Disposition 24(6):634-642.
35. Englund G, Rorsman F, Ronnblom A, Karlbom U, Lazorova L, Grasjo J, Kindmark A, Artursson P 2006. Regional levels of drug transporters along the human intestinal tract: Co-expression of ABC and SLC transporters and comparison with Caco-2 cells. European Journal of Pharmaceutical Sciences 29(3-4):269-277.
36. http://www.sigmaaldrich.com/etc/medialib/docs/Sigma/Product_Information_Sheet/1/d5030pis.Par.0001.File.tmp/d5030pis.pdf. (accessed on 2nd October 2013)
37. Strobel H. 2007. Method for solubilizing, dispersing, and stabilizing materials, products manufactured according to said method, and use thereof. A61K 9/16 (2006.01), A01N 25/04 (2006.01),

- A61K 38/28 (2006.01), A61K 8/67 (2006.01), A61K 8/90 (2006.01), A61K 8/98 (2006.01) ed.: LABOSWISS AG [CH], STROBEL HANSPETER [CH]. p 1-40.
38. Kapitza SB, Michel BR, van Hoogevest P, Leigh MLS, Imanidis G 2007. Absorption of poorly water soluble drugs subject to apical efflux using phospholipids as solubilizers in the Caco-2 cell model. *European Journal of Pharmaceutics and Biopharmaceutics* 66(1):146-158.
39. Schittkowski K. 2003. Numerical data fitting in dynamical systems - A practical introduction with applications and software. 1 ed., Dordrecht, Boston: Kluwer Academic Publisher.
40. Ingels F, Deferme S, Destexhe E, Oth M, Van den Mooter G, Augustijns P 2002. Simulated intestinal fluid as transport medium in the Caco-2 cell culture model. *International Journal of Pharmaceutics* 232(1-2):183-192.
41. Ingels F, Beck B, Oth M, Augustijns P 2004. Effect of simulated intestinal fluid on drug permeability estimation across Caco-2 monolayers. *International Journal of Pharmaceutics* 274(1-2):221-232.
42. Fossati L, Dechaume R, Hardillier E, Chevillon D, Prevost C, Bolze S, Maubon N 2008. Use of simulated intestinal fluid for Caco-2 permeability assay of lipophilic drugs. *International Journal of Pharmaceutics* 360(1-2):148-155.
43. Lind ML, Jacobsen J, Holm R, Mullertz A 2007. Development of simulated intestinal fluids containing nutrients as transport media in the Caco-2 cell culture model: Assessment of cell viability, monolayer integrity and transport of a poorly aqueous soluble drug and a substrate of efflux mechanisms. *European Journal of Pharmaceutical Sciences* 32(4-5):261-270.
44. Patel N, Forbes B, Eskola S, Murray J 2006. Use of simulated intestinal fluids with Caco-2 cells in rat ileum. *Drug Development and Industrial Pharmacy* 32(2):151-161.
45. Kiss L, Walter FR, Bocsik A, Veszeka S, Oszvari B, Puskas LG, Szabo-Revesz P, Deli MA 2013. Kinetic analysis of the toxicity of pharmaceutical excipients cremophor EL and RH40 on endothelial and epithelial cells. *Journal of Pharmaceutical Sciences* 102(4):1173-1181.
46. Li L, Yi T, Lam CWK 2013. Interactions between human multidrug resistance related protein (MRP2; ABCC2) and excipients commonly used in self-emulsifying drug delivery systems (SEDDS). *International Journal of Pharmaceutics* 447(1-2):192-198.
47. Ren XH, Mao XL, Cao L, Xue KW, Si LQ, Qiu J, Schimmer AD, Li G 2009. Nonionic surfactants, are strong inhibitors of cytochrome P450 3A biotransformation activity in vitro and in vivo. *European Journal of Pharmaceutical Sciences* 36(4-5):401-411.
48. Mountfield RJ, Senepin S, Schleimer M, Walter I, Bittner B 2000. Potential inhibitory effects of formulation ingredients on intestinal cytochrome P450. *International Journal of Pharmaceutics* 211(1-2):89-92.

49. Wen J, You KR, Lee SY, Song CH, Kim DG 2002. Oxidative stress-mediated apoptosis - The anticancer effect of the sesquiterpene lactone parthenolide. *Journal of Biological Chemistry* 277(41):38954-38964.
50. Singh M, Kumar D, Yusuf MA, Sardar M, Sarin NB 2013. Effects of wild-type and alpha-tocopherol-enriched transgenic *Brassica juncea* on the components of xenobiotic metabolism, antioxidant status, and oxidative stress in the liver of mice. *Transgenic Research* 22(4):813-822.
51. Huang JG, Si LQ, Jiang LL, Fan ZZ, Qiu J, Li G 2008. Effect of pluronic F68 block copolymer on P-glycoprotein transport and CYP3A4 metabolism. *International Journal of Pharmaceutics* 356(1-2):351-353.
52. Tang JL, Fu Q, Wang YJ, Racette K, Wang D, Liu F 2013. Vitamin E reverses multidrug resistance in vitro and in vivo. *Cancer Letters* 336(1):149-157.

List of Abbreviations

Ac-5-ASA	N-acetyl 5-aminosalicylic acid
aq-TM_{Caco}	aqueous transport medium
ABC	ATP-binding cassette
ASBT	ileal apical sodium/bile acid co-transporter
ATCC	American Type Culture Collection
BCRP	breast cancer resistance protein
BCS	biopharmaceutics classification system
Caco-2	colon adenocarcinoma cells
CAS	Cemical Abstract Service
CES	carboxylesterase
c-Myb	transcription factor
COMT	catechol- <i>O</i> -methyltransferase
CYP	cytochrome P450
DMEM	Dulbecco's modified Eagle's medium
DMSO	dimethyl sulfoxide
D-PBS	Dulbecco's phosphate-buffered saline
EDTA	ethylenediaminetetraacetic acid
EGCG	epigallocatechin gallate
EtOH	ethanol
FaSSIF-TM_{Caco}	fasted state simulated intestinal fluid
FBS	fetal bovine serum
FDA	Food and Drug Administration
FeSSIF-TM_{Caco}	fed state simulated intestinal fluid
GLUT	facilitated glucose transporter
GOF	goodness of fit
GSH	glutathione
GST	glutathione S-transferase
HeLa	cervical carcinoma cells
HEPES	4-(2-hydroxyethyl)piperazine-1-ethanesulfonic acid
HPLC	high pressure liquid chromatography

HPT	human peptide transporter
hTAS2R46	bitter taste receptor
IBAT	ileal sodium/bile acid co-transporter
KB	nasopharynx carcinoma cells
LDH	lactose dehydrogenase
LOQ	limit of quantification
LPH	lactase phloridizin hydrolase
MCT	monocarboxylic acid transporter
MDCK	Madin-Darby canine kidney (renal tubular cells)
MDR	multidrug resistance
MEM	minimum essential medium
MeOH	methanol
MPLC	medium pressure liquid chromatography
MRP	multidrug resistance protein
MS	mass spectrometry
MTT	3-(4,5-dimethylthiazol-2-yl)-2,5-diphenyl tetrazolium bromide
NaCl	sodium chloride
NaOH	sodium hydroxide
OATP	organic anion transporting polypeptide
OCT	organic cation transporter
OSTα-OSTβ	heteromeric organic solute transporter
PAPS	3'-phosphoadenylyl sulfate or 3'-phosphoadenosine 5'posphosulfate
PEPT	peptide transporter
P-gp	P-glycoprotein
PhEur	European pharmacopoeia
PhIP	2-amino-1-methyl-6-phenylimidazol[3,4-b]pyridine
SGLT	sodium-dependent glucose transporter
SIM	selected ion monitoring
SLC	solute carrier
S(M)EDDS	self-(micro)emulsifying drug delivery system
SULT	sulfotransferase
TEER	trans epithelial electrical resistance
TM_{Caco}	aqueous transport medium
UDPGA	uridin-5'-diphospho- α -D-glucuronic acid
UGT	UDP-glucuronosyltransferase

List of Symbols

<i>a</i>	coefficient
<i>ab</i>	apical-to-basal transport direction
<i>clogK_{o/w}</i>	logarithm of the calculated partition coefficient between octanol and water (Chapter 4)
<i>clogP</i>	logarithm of the calculated partition coefficient between octanol and water (Chapter 2 and 3)
<i>ba</i>	basal-to-apical transport direction
<i>d</i>	particle diameter
<i>df</i>	degrees of freedom
<i>h</i>	thickness of diffusion boundary layer
<i>k₁</i>	chemical degradation rate constant of nobiletin to degradation product 1
<i>k₂</i>	chemical degradation rate constant of nobiletin to degradation product 2
<i>k₃</i>	chemical degradation rate constant of nobiletin to degradation product 3
<i>k₄</i>	chemical degradation rate constant of nobiletin to degradation product 4
<i>k₅</i>	chemical degradation rate constant of nobiletin to degradation product 5
<i>k_d</i>	chemical degradation rate constant of nobiletin
<i>k_{d1}</i>	hydrolysis rate constant of glucuronide
<i>k_{d3}</i>	hydrolysis rate constant of glutathione conjugate
<i>k_{dc}</i>	total conjugation rate constant
<i>k_{dc1}</i>	conjugation rate constant of nobiletin to glucuronide
<i>k_{dc2}</i>	conjugation rate constant of nobiletin to cysteine conjugate
<i>k_{dc3}</i>	conjugation rate constant of nobiletin to glutathione conjugate
<i>k_{dcr}</i>	parameter (introduced to establish mass balance)
<i>k_r</i>	parameter (introduced to establish mass balance)
<i>k_s</i>	degradation rate constant (solubility study)
<i>m</i>	dissolved mass
<i>m_{degr}</i>	mass of degraded compound
<i>m_{init}</i>	initial mass of solid material
<i>m_{solid}</i>	mass of solid material
<i>n</i>	fraction of particle size distribution
<i>p</i>	significance level
<i>t</i>	time

$t_{1/2}$	half-life
t_{max}	time at which maximum absorption is observed
t_{max}^o	time at which maximum absorption is observed when neither chemical degradation nor bioconversion take place
u	partition coefficient between the apical and basal compartment
v_{a1}	carrier mediated transport rate constant of glucuronide (apical efflux)
v_{aa1}	carrier mediated transport rate constant of glucuronide (apical influx)
v_{a2}	carrier mediated transport rate constant of cysteine conjugate (apical efflux)
v_{a3}	carrier mediated transport rate constant of glutathione conjugate (apical efflux)
v_{b1}	carrier mediated transport rate constant of glucuronide (basal efflux)
v_{b2}	carrier mediated transport rate constant of cysteine conjugate (basal efflux)
v_{b3}	carrier mediated transport rate constant of glutathione conjugate (basal efflux)
$value(\alpha)$	value of a parameter
$value(\beta)$	value of a parameter
x	order of reaction kinetics (Chapter 3)
x	inverse fraction of glutathione conjugate that is metabolized to cysteine conj. (Chapter 4)
A	surface area
$A1$	area of the degradation product 1 peak of the UV-chromatogram
$A2$	area of the degradation product 2 peak of the UV-chromatogram
$A3$	area of the degradation product 3 peak of the UV-chromatogram
$A4$	area of the degradation product 4 peak of the UV-chromatogram
$A5$	area of the degradation product 5 peak of the UV-chromatogram
AN	area of the nobilin peak of the UV-chromatogram
Ar	introduced to establish mass balance
AQ	absorptive quotient
C	concentration
C_0	initial concentration (Chapter 2)
$C(0)$	concentration at time point 0 (Chapter 5)
CA	concentration of nobilin in the apical compartment
CB	concentration of nobilin in the basal compartment
CB_{ab}^o	concentration in the basal compartment when neither chemical degradation nor bioconversion take place
CC	concentration of nobilin in the cellular compartment

CC_{ab}^o	concentration in the cellular compartment when neither chemical degradation nor bioconversion take place
C_s	solubility
D	diffusion coefficient
ER	efflux ratio
F	critical value of F-distribution
F_a	relative fraction absorbed
J	flux
M_r	molecular weight
P	combined permeability coefficient (nobilin)
P_1	permeability coefficient (glucuronide)
P_2	permeability coefficient (cysteine conjugate)
P_3	permeability coefficient (glutathione conjugate)
P_a	permeability coefficient of the apical membrane (nobilin)
P_{app}	apparent permeability coefficient
$P_{app,AB}$	apparent permeability coefficient for the apical-to-basal transport direction
$P_{app,BA}$	apparent permeability coefficient for the basal-to-apical transport direction
P_b	permeability coefficient of the basal membranes (nobilin)
$P_{PD,AB}$	apparent permeability coefficient for the apical-to-basal transport direction in the presence of an inhibitor
$K_{a/c}$	partition coefficient between the apical and the cellular compartment
$MA1$	concentration of glucuronide in the apical compartment
$MA2$	concentration of cysteine conjugate in the apical compartment
$MA3$	concentration of glutathione conjugate in the apical compartment
$MB1$	concentration of glucuronide in the basal compartment
$MB2$	concentration of cysteine conjugate in the basal compartment
$MB3$	concentration of glutathione conjugate in the basal compartment
$MC1$	concentration of glucuronide in the cellular compartment
$MC2$	concentration of cysteine conjugate in the cellular compartment
$MC3$	concentration of glutathione conjugate in the cellular compartment
S	surface area
$(SE)_a$	standard error of P_a
$(SE)_b$	standard error of P_b
$(SE)_\alpha$	standard error of an estimate
$(SE)_\beta$	standard error of an estimate

V	volume of the solution
VA	volume of the apical compartment
VB	volume of the basal compartment
VC	volume of the cellular compartment
X	measured mass
ρ	density
Γ	shape factor

List of Figures

Chapter 2

- 1 Relative transporter gene expression levels of ABC and SLC transporters in 16 day old Caco-2 cells, human tissues isolated from jejunum mucosa.....21
- 2 *Anthemis nobilis* L. and dried flowers of *Anthemis nobilis* L. (*Chamomillae romanae flos*).....31
- 3 Chemical structure of nobiletin with absolute configuration.....33

Chapter 3

- 1 Chemical structure of nobiletin and UV-chromatograms of nobiletin and its degradation products at time zero and 7 h 13 min in purified water at 37°C.....63
- 2 X-ray structure of degradation product 1.....64
- 3 Measured concentrations of nobiletin and fitted curves at different pH values as a function of time..68
- 4 Peak area of UV chromatograms of nobiletin and its degradation products in purified water as a function of time.....69
- 5 Concentration of dissolved nobiletin as a function of time and fitted model curves in solubility measurements in different vehicles.....71
- 6 Particle size distribution of purified nobiletin.....72
- 7 Proposed degradation mechanism of nobiletin.....73

Chapter 4

- 1 MS-chromatograms of the apical and basal compartment for the transport direction apical-to-basal and basal-to-apical. Chromatograms with the nobiletin peak represent the time point 10 min and the chromatograms with m/z 525, 468, and 654 represent the time point 2.5 h.....95
- 2 Nobiletin concentration in the apical-to-basal and the basal-to-apical transport direction in both compartments and nobiletin mass in the cellular compartment in both transport directions as a function of time.....96
- 3 Concentration of glucuronide, cysteine conjugate, and glutathione conjugate in the apical-to-basal and the basal-to-apical transport direction in both compartments and mass of glucuronide, cysteine

	conjugate, and glutathione conjugate in the cellular compartment in both transport directions as a function of time.....	97
4	Deduced values and standard errors of permeability coefficient P , partition coefficient $K_{a/c}$, total conjugation rate constant k_{dc} , and relative fraction absorbed F_a of nobiletin from model fitting in the presence of inhibitors.....	100
5	Deduced values and standard errors of carrier mediated apical efflux rate v_{ar} , carrier mediated apical influx rate v_{aa} , carrier mediated basal efflux rate v_b , conjugation rate constant k_{dc} , and hydrolysis rate constant of glucuronide and glutathione conjugate k_d of the three conjugates from model fitting in the presence of inhibitors.....	101
6	Deduced values and standard errors of permeability coefficient P , partition coefficient $K_{a/c}$, total conjugation rate constant k_{dc} , and relative fraction absorbed F_a of nobiletin from model fitting in the presence of full extract and ingredients of the extract.....	102
7	Deduced values and standard errors of carrier mediated apical efflux rate v_{ar} , carrier mediated apical influx rate v_{aa} , carrier mediated basal efflux rate v_b , conjugation rate constant k_{dc} , and hydrolysis rate constant of glucuronide and glutathione conjugate k_d of the three conjugates from model fitting in the presence of the full extract and ingredients of the extract.....	103
8	Chemical structure of nobiletin with absolute configuration.....	104
Appendix (Chapter 4):		
	Nobiletin concentration in presence of verapamil, Ko143, and MK-571 in the apical-to-basal and the basal-to-apical transport direction in both compartments and nobiletin mass in the cellular compartment in both transport directions as a function of time.....	110
	Nobiletin concentration in presence of verapamil/Ko143/MK-571 and leukotriene C4 in the apical-to-basal and the basal-to-apical transport direction in both compartments and nobiletin mass in the cellular compartment in both transport directions as a function of time.....	111
	Concentration of glucuronide, cysteine conjugate, and glutathione conjugate in presence of verapamil in the apical-to-basal and the basal-to-apical transport direction in both compartments and mass of glucuronide, cysteine conjugate, and glutathione conjugate in the cellular compartment in both transport directions as a function of time.....	112
	Concentration of glucuronide, cysteine conjugate, and glutathione conjugate in presence of Ko143 in the apical-to-basal and the basal-to-apical transport direction in both compartments and mass of glucuronide, cysteine conjugate, and glutathione conjugate in the cellular compartment in both transport directions as a function of time.....	113

Concentration of glucuronide, cysteine conjugate, and glutathione conjugate in presence of MK-571 in the apical-to-basal and the basal-to-apical transport direction in both compartments and mass of glucuronide, cysteine conjugate, and glutathione conjugate in the cellular compartment in both transport directions as a function of time.....	114
Concentration of glucuronide, cysteine conjugate, and glutathione conjugate in presence of verapamil/Ko143/MK-571 in the apical-to-basal and the basal-to-apical transport direction in both compartments and mass of glucuronide, cysteine conjugate, and glutathione conjugate in the cellular compartment in both transport directions as a function of time.....	115
Concentration of glucuronide, cysteine conjugate, and glutathione conjugate in presence of leukotriene C4 in the apical-to-basal and the basal-to-apical transport direction in both compartments and mass of glucuronide, cysteine conjugate, and glutathione conjugate in the cellular compartment in both transport directions as a function of time.....	116
Nobilin concentration in presence of full extract in the apical-to-basal and the basal-to-apical transport direction in both compartments and nobilin mass in the cellular compartment in both transport directions as a function of time.....	117
Concentration of glucuronide, cysteine conjugate, and glutathione conjugate in presence of full extract in the apical-to-basal and the basal-to-apical transport direction in both compartments and mass of glucuronide, cysteine conjugate, and glutathione conjugate in the cellular compartment in both transport directions as a function of time.....	118
Nobilin concentration in presence of ethanol, sesquiterpene lactone fraction, and essential oil in the apical-to-basal and the basal-to-apical transport direction in both compartments and nobilin mass in the cellular compartment in both transport directions as a function of time.....	119
Nobilin concentration in presence of apigenin 1, apigenin 2, and luteolin in the apical-to-basal and the basal-to-apical transport direction in both compartments and nobilin mass in the cellular compartment in both transport directions as a function of time.....	120
Nobilin concentration in presence of apigenin 2/luteolin in the apical-to-basal and the basal-to-apical transport direction in both compartments and nobilin mass in the cellular compartment in both transport directions as a function of time.....	121
Concentration of glucuronide, cysteine conjugate, and glutathione conjugate in presence of ethanol in the apical-to-basal and the basal-to-apical transport direction in both compartments and mass of glucuronide, cysteine conjugate, and glutathione conjugate in the cellular compartment in both transport directions as a function of time.....	122

Concentration of glucuronide, cysteine conjugate, and glutathione conjugate in presence of sesquiterpene lactone fraction in the apical-to-basal and the basal-to-apical transport direction in both compartments and mass of glucuronide, cysteine conjugate, and glutathione conjugate in the cellular compartment in both transport directions as a function of time.....	123
Concentration of glucuronide, cysteine conjugate, and glutathione conjugate in presence of essential oil in the apical-to-basal and the basal-to-apical transport direction in both compartments and mass of glucuronide, cysteine conjugate, and glutathione conjugate in the cellular compartment in both transport directions as a function of time.....	124
Concentration of glucuronide, cysteine conjugate, and glutathione conjugate in presence of apigenin 1 in the apical-to-basal and the basal-to-apical transport direction in both compartments and mass of glucuronide, cysteine conjugate, and glutathione conjugate in the cellular compartment in both transport directions as a function of time.....	125
Concentration of glucuronide, cysteine conjugate, and glutathione conjugate in presence of apigenin 2 in the apical-to-basal and the basal-to-apical transport direction in both compartments and mass of glucuronide, cysteine conjugate, and glutathione conjugate in the cellular compartment in both transport directions as a function of time.....	126
Concentration of glucuronide, cysteine conjugate, and glutathione conjugate in presence of luteolin in the apical-to-basal and the basal-to-apical transport direction in both compartments and mass of glucuronide, cysteine conjugate, and glutathione conjugate in the cellular compartment in both transport directions as a function of time.....	127
Concentration of glucuronide, cysteine conjugate, and glutathione conjugate in presence of apigenin 2/luteolin in the apical-to-basal and the basal-to-apical transport direction in both compartments and mass of glucuronide, cysteine conjugate, and glutathione conjugate in the cellular compartment in both transport directions as a function of time.....	128

Chapter 5

1 Nobilin concentration in aq-TM _{Caco} , FaSSIF-TM _{Caco} , and FeSSIF-TM _{Caco} in the apical-to-basal and the basal-to-apical transport direction in both compartments and nobilin mass in the cellular compartment in both transport directions as a function of time.....	148
2 Deduced values and standard errors of permeability coefficient P, partition coefficient $K_{a/c}$, partition coefficient u, total conjugation rate constant k_{dc} , chemical degradation rate constant k_d , and relative fraction absorbed F_a of nobilin from model fitting in different media.....	149

-
- 3 Concentration of glucuronide, cysteine conjugate, and glutathione conjugate in aq-TM_{Caco} in the apical-to-basal and the basal-to-apical transport direction in both compartments and mass of glucuronide, cysteine conjugate, and glutathione conjugate in the cellular compartment in both transport directions as a function of time..... 151
 - 4 Concentration of glucuronide, cysteine conjugate, and glutathione conjugate in FaSSIF-TM_{Caco} in the apical-to-basal and the basal-to-apical transport direction in both compartments and mass of glucuronide, cysteine conjugate, and glutathione conjugate in the cellular compartment in both transport directions as a function of time..... 152
 - 5 Nobiletin concentration in presence of SMEDDS1 and SMEDDS2 in the apical-to-basal and the basal-to-apical transport direction in both compartments and nobiletin mass in the cellular compartment in both transport directions as a function of time..... 153
 - 6 Deduced values and standard errors of permeability coefficient P , partition coefficient $K_{a/c}$, partition coefficient u , total conjugation rate constant k_{dc} , chemical degradation rate constant k_d , and relative fraction absorbed F_a of nobiletin from model fitting in the presence of SMEDDS..... 154
 - 7 Concentration of glucuronide, cysteine conjugate, and glutathione conjugate in presence of SMEDDS2 in the apical-to-basal and the basal-to-apical transport direction in both compartments and mass of glucuronide, cysteine conjugate, and glutathione conjugate in the cellular compartment in both transport directions as a function of time..... 155
 - 8 Deduced values and standard errors of permeability coefficient P , partition coefficient $K_{a/c}$, partition coefficient u , total conjugation rate constant k_{dc} , chemical degradation rate constant k_d , and relative fraction absorbed F_a of nobiletin applied as a full extract from model fitting in different media and in presence of SMEDDS..... 156
 - 9 Concentration of glucuronide, cysteine conjugate, and glutathione conjugate in presence of the extract in the apical-to-basal and the basal-to-apical transport direction in both compartments and mass of glucuronide, cysteine conjugate, and glutathione conjugate in the cellular compartment in both transport directions as a function of time..... 158
 - 10 Concentration of glucuronide, cysteine conjugate, and glutathione conjugate in presence of the extract & FaSSIF-TM_{Caco} in the apical-to-basal and the basal-to-apical transport direction in both compartments and mass of glucuronide, cysteine conjugate, and glutathione conjugate in the cellular compartment in both transport directions as a function of time..... 159
 - 11 Concentration of glucuronide, cysteine conjugate, and glutathione conjugate in presence of the extract & SMEDDS2(1) in the apical-to-basal and the basal-to-apical transport direction in both

compartments and mass of glucuronide, cysteine conjugate, and glutathione conjugate in the cellular compartment in both transport directions as a function of time.....	160
12 Concentration of glucuronide, cysteine conjugate, and glutathione conjugate in presence of the extract & SMEDDS2(2) in the apical-to-basal and the basal-to-apical transport direction in both compartments and mass of glucuronide, cysteine conjugate, and glutathione conjugate in the cellular compartment in both transport directions as a function of time.....	161
Appendix (Chapter 5):	
Concentration of glucuronide, cysteine conjugate, and glutathione conjugate in presence of SMEDDS1 in the apical-to-basal and the basal-to-apical transport direction in both compartments and mass of glucuronide, cysteine conjugate, and glutathione conjugate in the cellular compartment in both transport directions as a function of time.....	166
Nobilin concentration in presence of the extract & aq-TM _{Caco} , extract & FaSSIF-TM _{Caco} , and extract & FeSSIF-TM _{Caco} in the apical-to-basal and the basal-to-apical transport direction in both compartments and nobilin mass in the cellular compartment in both transport directions as a function of time.....	167
Nobilin concentration in presence of the extract & SMEDDS1, extract & SMEDDS2(1), and extract & SMEDDS2(2) in the apical-to-basal and the basal-to-apical transport direction in both compartments and nobilin mass in the cellular compartment in both transport directions as a function of time.....	168
Concentration of glucuronide, cysteine conjugate, and glutathione conjugate in presence of the extract & SMEDDS1 in the apical-to-basal and the basal-to-apical transport direction in both compartments and mass of glucuronide, cysteine conjugate, and glutathione conjugate in the cellular compartment in both transport directions as a function of time.....	169

List of Schemes

Chapter 2

- 1 Transporters of the intestinal epithelia are P-gp, BCRP, MRP2, MRP3, one or more members of the organic anion transporting polypeptide (OATP) family, PEPT1, ASBT, MCT1, OCT1, and the heteromeric organic solute transporter (OST α -OST β).....20
- 2 Unidirectional single barrier model and compartment modeling.....22
- 3 Parallel interplay and concatenated interplay.....30

Chapter 4

- 1 Transport of nobilin and its conjugates.90

Chapter 5

- 1 Transport of nobilin and its conjugates by diffusional and/or carrier mediated permeation, nobilin chemical degradation, and intra- and extracellular bioconversion.....137

List of Tables

Chapter 2

1	Influence of plant extracts on absorption of phytopharmaceutical compounds in the Caco-2 model.....	15
2	Influence of plant ingredients on absorption of phytopharmaceutical compounds in the Caco-2 model.....	18
3	Substrates of carrier mediated transport, investigated in the Caco-2 model.	24
4	Reported studies of metabolism in Caco-2 cells.....	29
5	Chemical composition of <i>Chamomillae romanae flos</i>	32

Chapter 3

1	Composition of the three transport media.....	57
2	¹ H spectroscopic data (CD ₃ OD, 500.13 MHz) for degradation products 1-5.....	66
3	¹³ C spectroscopic data (CD ₃ OD, hsqc/hmbc, 500.13 MHz) for degradation product 1-5.....	67
4	Degradation rate constant and half-life of purified nobilin in water and maleate buffer.....	68
5	Kinetic constants of nobilin degradation and formation of degradation products in purified water.....	69
6	Degradation constant and order of reaction kinetics in different vehicles.....	70
7	Proportion of degradation products formed in different vehicles.....	70
8	Solubility of purified nobilin in different vehicles.....	72

Chapter 4

1	Kinetic parameter values of nobilin and its conjugates.....	99
---	---	----

Chapter 5

1	Composition of the three transport media.....	139
2	Degradation constant of nobilin (pure compound) and nobilin as a full extract in different media, liposomes, and lipid based formulations.....	147